

VOL. 644 NO. 2 AUGUST 6, 1993

THIS ISSUE COMPLETES VOL. 644

JOURNAL OF

CHROMATOGRAPHY

INCLUDING ELECTROPHORESIS AND OTHER SEPARATION METHODS

EDITORS

U.A.Th. Brinkman (Amsterdam)
 R.W. Giese (Boston, MA)
 J.K. Haken (Kensington, N.S.W.)
 K. Macek (Prague)
 L.R. Snyder (Orinda, CA)

EDITORS, SYMPOSIUM VOLUMES,

E. Heftmann (Orinda, CA), Z. Deyl (Prague)

EDITORIAL BOARD

D.W. Armstrong (Rolla, MO)
 W.A. Aue (Halifax)
 P. Boček (Brno)
 A.A. Boulton (Saskatoon)
 P.W. Carr (Minneapolis, MN)
 N.H.C. Cooke (San Ramon, CA)
 V.A. Davankov (Moscow)
 Z. Deyl (Prague)
 S. Dilli (Kensington, N.S.W.)
 H. Engelhardt (Saarbrücken)
 F. Erni (Basle)
 M.B. Evans (Hatfield)
 J.L. Glajch (N. Billerica, MA)
 G.A. Guiochon (Knoxville, TN)
 P.R. Haddad (Hobart, Tasmania)
 I.M. Hais (Hradec Králové)
 W.S. Hancock (San Francisco, CA)
 S. Hjerten (Uppsala)
 S. Honda (Higashi-Osaka)
 Cs. Horváth (New Haven, CT)
 J.F.K. Huber (Vienna)
 K.P. Hupe (Waldbronn)
 T.W. Hutchens (Houston, TX)
 J. Janák (Brno)
 P. Jandera (Pardubice)
 B.L. Karger (Boston, MA)
 J.J. Kirkland (Newport, DE)
 E. sz. Kováts (Lausanne)
 A.J.P. Martin (Cambridge)
 L.W. McLaughlin (Chestnut Hill, MA)
 E.D. Morgan (Keele)
 J.D. Pearson (Kalamazoo, MI)
 H. Poppe (Amsterdam)
 F.E. Regnier (West Lafayette, IN)
 P.G. Righetti (Milan)
 P. Schoenmakers (Eindhoven)
 R. Schwarzenbach (Dübendorf)
 R.E. Shoup (West Lafayette, IN)
 R.P. Singhal (Wichita, KS)
 A.M. Siouffi (Marseille)
 D.J. Strydom (Boston, MA)
 N. Tanaka (Kyoto)
 S. Terabe (Hyogo)
 K.K. Unger (Mainz)
 R. Verpoorte (Leiden)
 Gy. Vigh (College Station, TX)
 J.T. Watson (East Lansing, MI)
 B.D. Westerlund (Uppsala)

EDITORS, BIBLIOGRAPHY SECTION

Z. Deyl (Prague), J. Janák (Brno), V. Schwartz (Prague)

ELSEVIER

JOURNAL OF CHROMATOGRAPHY

INCLUDING ELECTROPHORESIS AND OTHER SEPARATION METHODS

Scope. The *Journal of Chromatography* publishes papers on all aspects of **chromatography, electrophoresis** and related methods. Contributions consist mainly of research papers dealing with chromatographic theory, instrumental developments and their applications. The section *Biomedical Applications*, which is under separate editorship, deals with the following aspects: developments in and applications of chromatographic and electrophoretic techniques related to clinical diagnosis or alterations during medical treatment; screening and profiling of body fluids or tissues related to the analysis of active substances and to metabolic disorders; drug level monitoring and pharmacokinetic studies; clinical toxicology; forensic medicine; veterinary medicine; occupational medicine; results from basic medical research with direct consequences in clinical practice. In *Symposium volumes*, which are under separate editorship, proceedings of symposia on chromatography, electrophoresis and related methods are published.

Submission of Papers. The preferred medium of submission is on disk with accompanying manuscript (see *Electronic manuscripts* in the Instructions to Authors, which can be obtained from the publisher, Elsevier Science Publishers B.V., P.O. Box 330, 1000 AH Amsterdam, Netherlands). Manuscripts (in English; four copies are required) should be submitted to: Editorial Office of *Journal of Chromatography*, P.O. Box 681, 1000 AR Amsterdam, Netherlands, Telefax (+31-20) 5862 304, or to: The Editor of *Journal of Chromatography, Biomedical Applications*, P.O. Box 681, 1000 AR Amsterdam, Netherlands. Review articles are invited or proposed in writing to the Editors who welcome suggestions for subjects. An outline of the proposed review should first be forwarded to the Editors for preliminary discussion prior to preparation. Submission of an article is understood to imply that the article is original and unpublished and is not being considered for publication elsewhere. For copyright regulations, see below.

Publication. The *Journal of Chromatography* (incl. *Biomedical Applications*) has 40 volumes in 1993. The subscription prices for 1993 are:

J. Chromatogr. (incl. *Cum. Indexes, Vols. 601-650*) + *Biomed. Appl.* (Vols. 612-651):

Dfl. 8520.00 plus Dfl. 1320.00 (p.p.h.) (total ca. US\$ 5466.75)

J. Chromatogr. (incl. *Cum Indexes, Vols. 601-650*) only (Vols. 623-651):

Dfl. 7047.00 plus Dfl. 957.00 (p.p.h.) (total ca. US\$ 4446.75)

Biomed. Appl. only (Vols. 612-622):

Dfl. 2783.00 plus Dfl. 363.00 (p.p.h.) (total ca. US\$ 1747.75).

Subscription Orders. The Dutch guilder price is definitive. The US\$ price is subject to exchange-rate fluctuations and is given as a guide. Subscriptions are accepted on a prepaid basis only, unless different terms have been previously agreed upon. Subscriptions orders can be entered only by calendar year (Jan.-Dec.) and should be sent to Elsevier Science Publishers, Journal Department, P.O. Box 211, 1000 AE Amsterdam, Netherlands, Tel. (+31-20) 5803 642, Telefax (+31-20) 5803 598, or to your usual subscription agent. Postage and handling charges include surface delivery except to the following countries where air delivery via SAL (Surface Air Lift) mail is ensured: Argentina, Australia, Brazil, Canada, China, Hong Kong, India, Israel, Japan*, Malaysia, Mexico, New Zealand, Pakistan, Singapore, South Africa, South Korea, Taiwan, Thailand, USA. *For Japan air delivery (SAL) requires 25% additional charge of the normal postage and handling charge. For all other countries airmail rates are available upon request. Claims for missing issues must be made within six months of our publication (mailing) date, otherwise such claims cannot be honoured free of charge. Back volumes of the *Journal of Chromatography* (Vols. 1-611) are available at Dfl. 230.00 (plus postage). Customers in the USA and Canada wishing information on this and other Elsevier journals, please contact Journal Information Center, Elsevier Science Publishing Co. Inc., 655 Avenue of the Americas, New York, NY 10010, USA, Tel. (+1-212) 633 3750, Telefax (+1-212) 633 3764.

Abstracts/Contents Lists published in Analytical Abstracts, Biochemical Abstracts, Biological Abstracts, Chemical Abstracts, Chemical Titles, Chromatography Abstracts, Current Awareness in Biological Sciences (CABS), Current Contents/Life Sciences, Current Contents/Physical, Chemical & Earth Sciences, Deep-Sea Research/Part B: Oceanographic Literature Review, Excerpta Medica, Index Medicus, Mass Spectrometry Bulletin, PASCAL-CNRS, Referativnyi Zhurnal, Research Alert and Science Citation Index.

US Mailing Notice. *Journal of Chromatography* (ISSN 0021-9673) is published weekly (total 52 issues) by Elsevier Science Publishers (Sara Burgerhartstraat 25, P.O. Box 211, 1000 AE Amsterdam, Netherlands). Annual subscription price in the USA US\$ 4446.75 (subject to change), including air speed delivery. Second class postage paid at Jamaica, NY 11431. **USA POSTMASTERS:** Send address changes to *Journal of Chromatography*, Publications Expediting, Inc., 200 Meacham Avenue, Elmont, NY 11003. Airfreight and mailing in the USA by Publications Expediting.

See inside back cover for Publication Schedule, Information for Authors and information on Advertisements.

© 1993 ELSEVIER SCIENCE PUBLISHERS B.V. All rights reserved.

0021-9673/93/\$06.00

No part of this publication may be reproduced, stored in a retrieval system or transmitted in any form or by any means, electronic, mechanical, photocopying, recording or otherwise, without the prior written permission of the publisher, Elsevier Science Publishers B.V., Copyright and Permissions Department, P.O. Box 521, 1000 AM Amsterdam, Netherlands.

Upon acceptance of an article by the journal, the author(s) will be asked to transfer copyright of the article to the publisher. The transfer will ensure the widest possible dissemination of information.

Special regulations for readers in the USA. This journal has been registered with the Copyright Clearance Center, Inc. Consent is given for copying of articles for personal or internal use, or for the personal use of specific clients. This consent is given on the condition that the copier pays through the Center the per-copy fee stated in the code on the first page of each article for copying beyond that permitted by Sections 107 or 108 of the US Copyright Law. The appropriate fee should be forwarded with a copy of the first page of the article to the Copyright Clearance Center, Inc., 27 Congress Street, Salem, MA 01970, USA. If no code appears in an article, the author has not given broad consent to copy and permission to copy must be obtained directly from the author. All articles published prior to 1980 may be copied for a per-copy fee of US\$ 2.25, also payable through the Center. This consent does not extend to other kinds of copying, such as for general distribution, resale, advertising and promotion purposes, or for creating new collective works. Special written permission must be obtained from the publisher for such copying.

No responsibility is assumed by the Publisher for any injury and/or damage to persons or property as a matter of products liability, negligence or otherwise, or from any use or operation of any methods, products, instructions or ideas contained in the materials herein. Because of rapid advances in the medical sciences, the Publisher recommends that independent verification of diagnoses and drug dosages should be made.

Although all advertising material is expected to conform to ethical (medical) standards, inclusion in this publication does not constitute a guarantee or endorsement of the quality or value of such product or of the claims made of it by its manufacturer.

This issue is printed on acid-free paper.

CONTENTS

(Abstracts/Contents Lists published in Analytical Abstracts, Biochemical Abstracts, Biological Abstracts, Chemical Abstracts, Chemical Titles, Chromatography Abstracts, Current Awareness in Biological Sciences (CABS), Current Contents/Life Sciences, Current Contents/Physical, Chemical & Earth Sciences, Deep-Sea Research/Part B: Oceanographic Literature Review, Excerpta Medica, Index Medicus, Mass Spectrometry Bulletin, PASCAL-CNRS, Referativnyi Zhurnal, Research Alert and Science Citation Index)

REGULAR PAPERS

Column Liquid Chromatography

- Studies on a new cross-axis coil planet centrifuge for performing counter-current chromatography. I. Design of the apparatus, retention of the stationary phase, and efficiency in the separation of proteins with polymer phase systems by K. Shinomiya, J.-M. Menet, H.M. Fales and Y. Ito (Bethesda, MD, USA) (Received March 30th, 1993) . . . 215
- Studies on a new cross-axis coil planet centrifuge for performing counter-current chromatography. II. Path and acceleration of coils and comparison with type J coil planet centrifuge by J.-M. Menet and Y. Ito (Bethesda, MD, USA) (Received March 30th, 1993) . . . 231
- Studies on new cross-axis coil planet centrifuge for performing counter-current chromatography. III. Speculations on the hydrodynamic mechanism in stationary phase retention by J.-M. Menet, K. Shinomiya and Y. Ito (Bethesda, MD, USA) (Received March 30th, 1993) . . . 239
- Rapid group-type analysis of crude oils using high-performance liquid chromatography and gas chromatography by M.S. Akhlaq (Clausthal-Zellerfeld, Germany) (Received February 11th, 1993) . . . 253
- Reversed-phase high-performance liquid chromatography and chemometrics, a combined investigation tool for complex phytochemical problems by C. Baiocchi, E. Marengo, G. Saini, M.A. Roggero and D. Giacosa (Turin, Italy) (Received April 13th, 1993) 259
- Retention behaviour of aromatic sulphonic acids in reversed-phase ion-pair liquid chromatography with methanol and acetonitrile as organic modifiers by H. Zou, Y. Zhang, M. Hong and P. Lu (Dalian, China) (Received April 8th, 1993) . . . 269
- High-performance liquid chromatographic separation of enantiomeric amino acids on bis[carbamoyl(alkyl)methylamino]-6-chloro-s-triazine-derived chiral stationary phases by J.-Y. Lin and M.-H. Yang (Taipei, Taiwan) (Received April 15th, 1993) . . . 277
- Observation of a conformational effect in peptide molecule by reversed-phase high-performance liquid chromatography by M. Lebl (Tucson, AZ, USA) (Received February 23rd, 1993) . . . 285
- Interaction of catechol-2,3-dioxygenase of *Pseudomonas putida* with immobilized histidine and histamine by K. Haupt and M.A. Vijayalakshmi (Compiègne, France) (Received March 26th, 1993) . . . 289
- Efficient separation of natural ribonucleotides by low-pressure anion-exchange chromatography by T. Cihlář and I. Rosenberg (Prague, Czech Republic) (Received January 18th, 1993) . . . 299
- Coupled-column reversed-phase liquid chromatography-UV analyser for the determination of polar pesticides in water by E.A. Hogendoorn (Bilthoven, Netherlands), U.A.Th. Brinkman (Amsterdam, Netherlands) and P. van Zoonen (Bilthoven, Netherlands) (Received April 8th, 1993) . . . 307
- Direct column liquid chromatographic enantiomer separation of the coumarin anticoagulants phenprocoumon, warfarin, acenocoumarol and metabolites on an α_1 -acid glycoprotein chiral stationary phase by J.X. de Vries and E. Schmitz-Kummer (Heidelberg, Germany) (Received April 15th, 1993) . . . 315
- Analysis of paralytic shellfish poisoning toxins by automated pre-column oxidation and microcolumn liquid chromatography with fluorescence detection by M. Janeček and M.A. Quilliam (Halifax, Canada) and J.F. Lawrence (Ottawa, Canada) (Received April 19th, 1993) . . . 321
- Ultratrace anion analysis of high-purity water. A column comparison by M.W. Martin and R.A. Giacofei (Rochester, NY, USA) (Received April 5th, 1993) . . . 333

(Continued overleaf)

ห้องสมุดสารเคมีวิทยาศาสตร์บริการ

- 7 ก.ย. 2536

Contents (continued)

Evaluation of ion-exchange chromatography for nitrate determination in wastewaters
by S. Bignami, M.L. Daví, C. Milan, M. Moretti and F. Navarra (Ferrara, Italy) (Received April 3rd, 1993) . . . 341

Determination of nitrate in surface waters by ion-exchange chromatography after oxidation of total organic nitrogen to nitrate
by M.L. Daví, S. Bignami, C. Milan, M. Liboni and M.G. Malfatto (Ferrara, Italy) (Received April 3rd, 1993) 345

Gas Chromatography

Alkali flame ionization detector for gas chromatography using an alkali salt aerosol as the enhancement source
by E.D. Conte and E.F. Barry (Lowell, MA, USA) (Received April 6th, 1993) 349

Determination of polar pesticides by phase-transfer catalysed derivatization and negative-ion chemical ionization gas chromatography-mass spectrometry
by H.D. Meiring, G. den Engelsman and A.P.J.M. de Jong (Bilthoven, Netherlands) (Received February 18th, 1993) 357

On-line combination of automated micro liquid-liquid extraction and capillary gas chromatography for the determination of pesticides in water
by G.R. van der Hoff and R.A. Baumann (Bilthoven, Netherlands), U.A.Th. Brinkman (Amsterdam, Netherlands) and P. van Zoonen (Bilthoven, Netherlands) (Received April 12th, 1993) 367

Gas chromatographic-mass spectrometric determination of halogenated acetic acids in water after direct derivatization
by H. Ozawa (Ibaraki, Japan) (Received April 19th, 1993) 375

Determination of furan-based amines in reaction mixtures by gas chromatography
by M.S. Holfinger, A.H. Conner and C.G. Hill, Jr. (Madison, WI, USA) (Received March 4th, 1993) 383

Electrophoresis

Determination of ionic species formed during growth of *Escherichia coli* by capillary isotachopheresis
by K. Futschik, M. Ammann, S. Bachmayer and E. Kenndler (Vienna, Austria) (Received April 21st, 1993) . . . 389

SHORT COMMUNICATIONS

Column Liquid Chromatography

High-performance liquid chromatographic separation of fullerenes (C₆₀ and C₇₀) using chemically bonded γ -cyclodextrin as stationary phase
by K. Cabrera, G. Wieland and M. Schäfer (Darmstadt, Germany) (Received April 22nd, 1993) 396

Determination of isocyanuric acid and its chlorinated derivatives in swimming pool waters by ion chromatography
by J.K. Debowski and F.A. Gerber (Modderfontein, South Africa) (Received April 21st, 1993) 400

High-performance liquid chromatographic determination of the major saponin from *Opilia celtidifolia* Guill. Perr.
by F. Crespin, E. Ollivier, R. Elias, C. Maillard and G. Balansard (Marseille, France) (Received April 13th, 1993) 404

Electrophoresis

Isotachopheretic separation of polyols in boric acid solutions
by S.P. Atamas and G.V. Troitsky (Simferopol, Ukraine) (Received February 16th, 1993) 407

Separation of D-galactonic and D-gluconic acids by capillary zone electrophoresis
by A. Bergholdt, J. Overgaard and A. Colding (Lyngby, Denmark) and R.B. Frederiksen (Hedehusene, Denmark) (Received April 15th, 1993) 412

BOOK REVIEW

Advances in Chromatography (by J.C. Giddings, E. Grushka, J. Cazes and P.R. Brown), reviewed by P. Jandera (Czech Republic) 416

AUTHOR INDEX 418

ERRATUM 420

**FOR ADVERTISING
INFORMATION
PLEASE CONTACT OUR
ADVERTISING
REPRESENTATIVES**

USA/CANADA

Weston Media Associates

Mr. Daniel S. Lipner
P.O. Box 1110, GREENS FARMS, CT 06436-1110
Tel: (203) 261-2500, Fax: (203) 261-0101

GREAT BRITAIN

T.G. Scott & Son Ltd.

Tim Blake/Vanessa Bird
Portland House, 21 Narborough Road
COSBY, Leicestershire LE9 5TA
Tel: (0533) 753-333, Fax: (0533) 750-522

JAPAN

ESP - Tokyo Branch

Mr. S. Onoda
20-12 Yushima, 3 chome, Bunkyo-Ku
TOKYO 113
Tel: (03) 3836 0810, Fax: (03) 3839-4344
Telex: 02657617



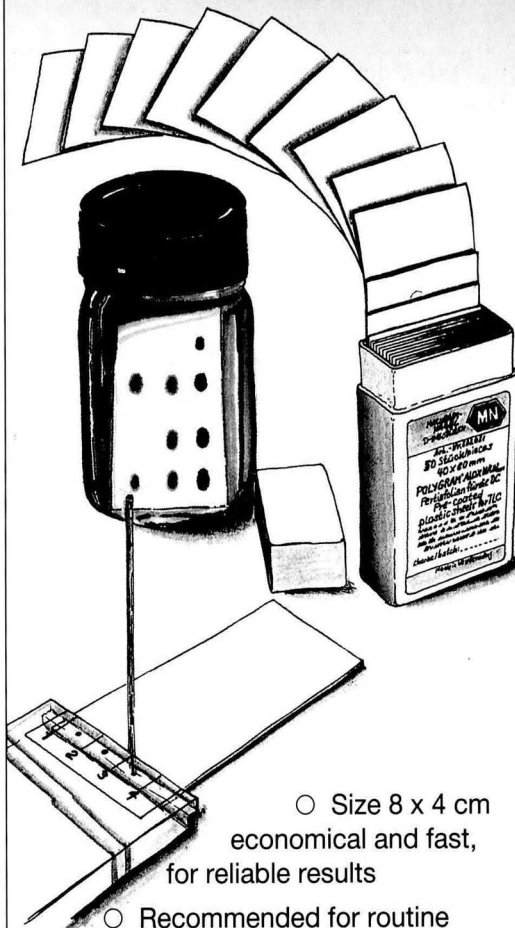
REST OF WORLD

**ELSEVIER
SCIENCE
PUBLISHERS**

Ms. W. van Cattenburch
Advertising Department
P.O. Box 211, 1000 AE AMSTERDAM,
The Netherlands
Tel: (20) 515.3220/21/22, Telex: 16479 els vi nl
Fax: (20) 683.3041

**Rapid low cost
analyses!**

**Thin Layer Chromatography
with economy size sheets**



- Size 8 x 4 cm
economical and fast,
for reliable results
- Recommended for routine
analyses and in production control
- Economy size sheets are available
as POLYGRAM® or ALUGRAM®
(polyester resp. aluminium supports)
coated with silica, cellulose and
aluminium oxide.

Please ask for further information about our TLC plates and sheets.

MACHEREY-NAGEL



MACHEREY-NAGEL GmbH & Co. KG · P.O. Box 10 1352 · D-52348 Düren
Germany · Tel. (02421) 698-0 · Telex 833893 mana d · Fax (02421) 62054
Switzerland: MACHEREY-NAGEL AG · CH-4702 Oensingen · Tel. (062) 762066
France: MACHEREY-NAGEL S.a.r.l. · F-67038 Strasbourg Cedex · Tel. 88.76.53.34

Jork, Funk, Fischer, Wimmer
Thin-Layer Chromatography:
Reagents and Detection Methods
Volume 1b

Physical and Chemical Detection Methods:
Activation Reactions, Reagent Series, Reagents II

1993. Ca XIV, 450 pages with ca 150 figures,
more than 30 in color and ca 20 tables. Flexicover.
DM 178.00. ISBN 3-527-28205-X

From reviews on 'Thin-Layer Chromatography:
Reagents and Detection Methods, Volume 1a':

'This book forms part of what will...be one of the
most important contributions to the literature of thin-
layer chromatography...if I were contemplating the
purchase of only one book on TLC this year, it would
be this one.' (*Journal of Planar Chromatography*)

To order please contact your bookseller or:

VCH, P.O. Box 10 11 61, D-69451 Weinheim,
Telefax (0) 62 01 - 80 61 84

VCH, Hardstrasse 10, P.O. Box, CH-4020 Basel

VCH, 8 Wellington Court, Cambridge CB1 1HZ, UK

VCH, 220 East 23rd Street,

New York, NY 10010-4606, USA

(toll free: 1-800-367-8249)

VCH, Eikow Building,

10-9 Hongo 1-chome, Bunkyo-ku, Tokyo 113



006

**PLEASE
MENTION
THIS
JOURNAL
WHEN
ANSWERING
ADVER-
TISEMENTS**

USE THIS ADVERTISING SPACE FOR YOUR NEXT RECRUITMENT SEARCH!

This Elsevier Science Publication
presents the latest and most
authoritative selection of articles in
this field.

For this reason, the contents of this
journal are avidly and intensely read
by qualified people who **want** and
need to keep informed of the latest
scientific and technological
information.

For these reasons, companies desiring
to hire qualified personnel will find
this journal to be a clear channel of
communication to a significant group
of specialists in this field. In addition,
your advertisement will gain the
benefit of the authority and stature
which this journal enjoys its readers.

Call for advertising rates.

Professional typesetting now available
at our editorial facilities.

USA/CANADA
WESTON MEDIA ASS.
Dan Lipner
(203) 261.2500 (fax: 261.0101)

GREAT BRITAIN
TG SCOTT & SON LTD.
Tim Blake
(0533) 753.333 (fax: 750.522)

JAPAN
ELSEVIER SCIENCE PUBLISHERS
Mr. S. Onoda
(03) 3836.0810 (fax: 3839.4344)

REST OF WORLD
ELSEVIER SCIENCE PUBLISHERS
Willeke van Cattenburch
(20) 515.3220 (fax: 6833041)

Studies on a new cross-axis coil planet centrifuge for performing counter-current chromatography

I. Design of the apparatus, retention of the stationary phase, and efficiency in the separation of proteins with polymer phase systems

Kazufusa Shinomiya[☆], Jean-Michel Menet^{☆☆}, Henry M. Fales and Yoichiro Ito^{*}

Laboratory of Biophysical Chemistry, National Heart, Lung, and Blood Institute, National Institutes of Health, Building 10, Room 7N322, Bethesda, MD 20892 (USA)

(First received November 24th, 1992; revised manuscript received March 30th, 1993)

ABSTRACT

An improved model of the cross-axis synchronous flow-through coil planet centrifuge has been designed in light of previous studies. The apparatus has a versatile feature in that both analytical and preparative columns can be accommodated in both off-center and central positions. Each has merit in separations.

Retention of stationary phase was examined with various two-phase solvent systems used for the separation of biopolymers. Both analytical and preparative columns showed satisfactory retention of the stationary phase under optimum conditions. The apparatus was evaluated in separation of a set of protein samples using a polyethylene glycol–potassium phosphate biphasic system. In both types of columns all proteins were resolved with partition efficiencies of 260 to 670 theoretical plates. Further studies indicated that the relatively low partition efficiency of proteins is mainly attributed to their high molecular mass or molecular heterogeneity within each species rather than due to the high viscosity of the polymer phase system.

INTRODUCTION

Counter-current chromatography (CCC) has been increasingly used for the separation and purification of various natural and synthetic products and biological samples [1,2]. In the

past, development of CCC technology has been focussed mainly on improvement of the retention of stationary phase, peak resolution and separation times using organic–aqueous two-phase solvent systems. Among various CCC models developed, the high-speed CCC centrifuge has proven most useful since it provides advantages in peak resolution and separation times in addition to durability and stability of the instrument [3]. On the other hand, the apparatus shows poor retention of the stationary phase when using the aqueous–aqueous polymer phase systems [4] so useful for the separation of macromolecules. This problem is apparently caused by violent mixing of the two phases that tends to

* Corresponding author.

[☆] Visiting Scientist from College of Pharmacy, Nihon University, 7-7-1, Narashinodai, Funabashi-shi, Chiba 274, Japan.

^{☆☆} Guest scientist from Laboratoire de Chimie Analytique, Ecole Supérieure de Physique et de Chimie Industrielles de Paris, 10 Rue Vauquelin, 75231 Paris Cedex 05, France.

produce emulsification; the result is loss of stationary phase from the column.

The cross-axis coil planet centrifuge (CPC) introduced in the mid-1980s has a unique mode of planetary motion such that the column holder rotates about its horizontal axis while revolving around the vertical axis of the centrifuge [5,6]. This motion allows much better retention of the stationary phase. The apparatus has been successfully used for preparative-scale separations of natural and synthetic products [7].

Recent studies have shown that retention of the stationary phase in the cross-axis CPC can be further improved by shifting the column holder laterally along the rotary shaft. In this position, the column is subjected to a strong lateral centrifugal force component that acts across the diameter of the tube to suppress emulsification. The proper combination of coil orientation and elution mode provides satisfactory retention of the stationary phase for viscous, low-interfacial-tension solvent systems [8].

Using aqueous–aqueous polymer phase systems, a standard mixture of stable proteins [9], lipoproteins [10] and recombinant enzymes from *Escherichia coli* lysate [11] have been separated using the type-XLL cross-axis CPC with a 10-cm revolution radius equipped with a pair of multi-layer coils at an off-center position 20 cm from

the mid point of the rotary shaft. In this work it was found that the ratio between the revolution radius (X) and the lateral deviation (L) of the column is an important parameter in retention of the stationary phase. In general, an increase in ratio L/X resulted in higher retention of stationary phase by reducing the phase mixing effect.

The present paper describes the design and performance of a new cross-axis CPC which can accommodate a pair of column holders in two different positions, the off-center position ($L/X = 1.5$) or the central position ($X = 0$). The apparatus was evaluated for retention of the stationary phase of four solvent systems each providing a specific merit on the separation of macromolecules as shown in Table I. Under the optimized conditions for polyethylene glycol–phosphate two-phase system (solvent 2), the partition efficiency was measured in the separation of a set of stable proteins using both analytical and preparative coiled columns.

EXPERIMENTAL

Apparatus

The cross-axis synchronous flow-through CPC used in the present studies was designed in our laboratory and constructed at the NIH machine shop. Both analytical and preparative columns

TABLE I
FOUR TYPICAL SOLVENT SYSTEMS FOR PARTITION OF MACROMOLECULES

HPC = Hexadecylpyridinium chloride; PEG = polyethylene glycol.

No.	Solvent systems	Target samples	Characteristic features
1	<i>n</i> -Butanol– 0.13 M NaCl (1:1) containing 1.5% (w/v) HPC	Polysaccharides: chondroitin sulfate, heparin, hyaluronic acid	No other efficient solvent system available
2	12.5% (w/w) PEG 1000, 12.5% (w/w) K ₂ HPO ₄	Proteins	High retention, good efficiency
3	4.4% (w/w) PEG 8000, 7.0% (w/w) dextran T500	Proteins	High solubility for proteins
4	4.0% (w/w) PEG 8000, 5.0% (w/w) dextran T500	Nucleic acids, cell particles	Physiological pH and osmotic pressure for cell separation

can be accommodated in two different positions, off-center ($X - 1.5L$) and central (L) locations. Each position has its own merit on the separation of macromolecules with aqueous–aqueous polymer phase systems.

Fig. 1 illustrates the design of the apparatus. The motor (not shown in the diagram) drives the central shaft and the rotary frame around the central axis of the centrifuge. The rotary frame consists of two pairs of side-plates: a pair of inner side-plates is bridged by a pair of horizontal plates at the upper and lower edges. These rigidly support the outer side-plates with a set of links. Column holders and counter-rotating tube holders are mounted between the inner and outer side-plates in two different positions on each side of the rotary frame, *i.e.*, an off-center position ($X - 1.5L$ position) as shown in Fig. 1 and a central position (L position). The planetary motion of the column holder is provided by a set of miter gears and countershafts as follows: a stationary miter gear (45°) is rigidly mounted coaxially around the central shaft on the bottom plate of the centrifuge. This stationary gear is engaged to an identical gear affixed at the proximal end of the countershaft radially mounted on each side of the rotary frame. The above engagement produces synchronous rotation of the countershaft on the rotating rotary frame. This motion is further conveyed to each column holder by coupling a pair of identical pulleys, one on the distal end of the countershaft and the other on the column holder shaft using a toothed belt.

In order to prevent the flow tubes from being twisted, a pair of counter-rotating tube holders is placed one on each side of the rotary frame. The plastic gear (10 cm in pitch diameter) mounted on each tube holder is engaged to an identical gear affixed on the neighboring column holder so that the tube holder synchronously rotates with the column holder in the opposite direction. The positions of the column holder and the tube holder are easily interchanged by loosening the screws on each bearing block from the rotary frame: When the column holder is mounted at the off-center position (as shown in Fig. 1), the tube holder is placed at the central position and *vice versa*. The layout of the flow tubes shown in

Fig. 1B connects the pair of separation columns in series and permits continuous elution through the running columns without the use of a rotary seal device. Each flow tube is lubricated with grease and individually protected with a short sheath of Tygon tubing at each projecting hole to prevent direct contact with the metal parts.

The apparatus measures 60 cm wide, 60 cm long and 34 cm in height. The speed of the apparatus is regulated up to 1000 rpm by a speed control unit (Bodine Electric, Chicago, IL, USA). In the earlier model of the cross-axis CPC a set of metal gears produced noise and vibration. This problem has been largely eliminated by replacing the miter gears with plastic gears and restricting the up-and-down movement of the centrifuge shaft with shims. Consequently, the noise level of the present apparatus became acceptable, provided that the applied speed is away from the resonance points ranging between 650 and 700 rpm.

Preparation of coiled columns

The measurement of stationary phase retention in the preparative columns was performed using short coils of 2.6 mm I.D. polytetrafluoroethylene (PTFE) tubing (Zeus Industrial Products, Raritan, NJ, USA). Two columns were prepared by winding the tubing directly around the holders of 5- and 10-cm hub diameters forming a single-layer coil with a total capacity of 19.8 ml and 41.0 ml, respectively. Both right-handed and left-handed coils were used. Each coiled column was firmly affixed on the holder with several pieces of fiber-glass reinforced adhesive tape. Each end of the column was connected to a 0.85 mm I.D. PTFE flow tube by inserting a series of smaller-diameter PTFE tubing into one another.

The protein separations were performed by three types of coiled columns shown in Fig. 2. Column I is a preparative-scale multilayer coil which consists entirely of left-handed coils of 2.6 mm I.D. PTFE tubing measuring 5 to 10 cm in diameter. Each multilayer coil was prepared by winding a single piece of PTFE tubing directly onto the holder hub making a tightly packed coil between the pair of flanges spaced 7.6 cm apart. After completing each coiled layer, the whole

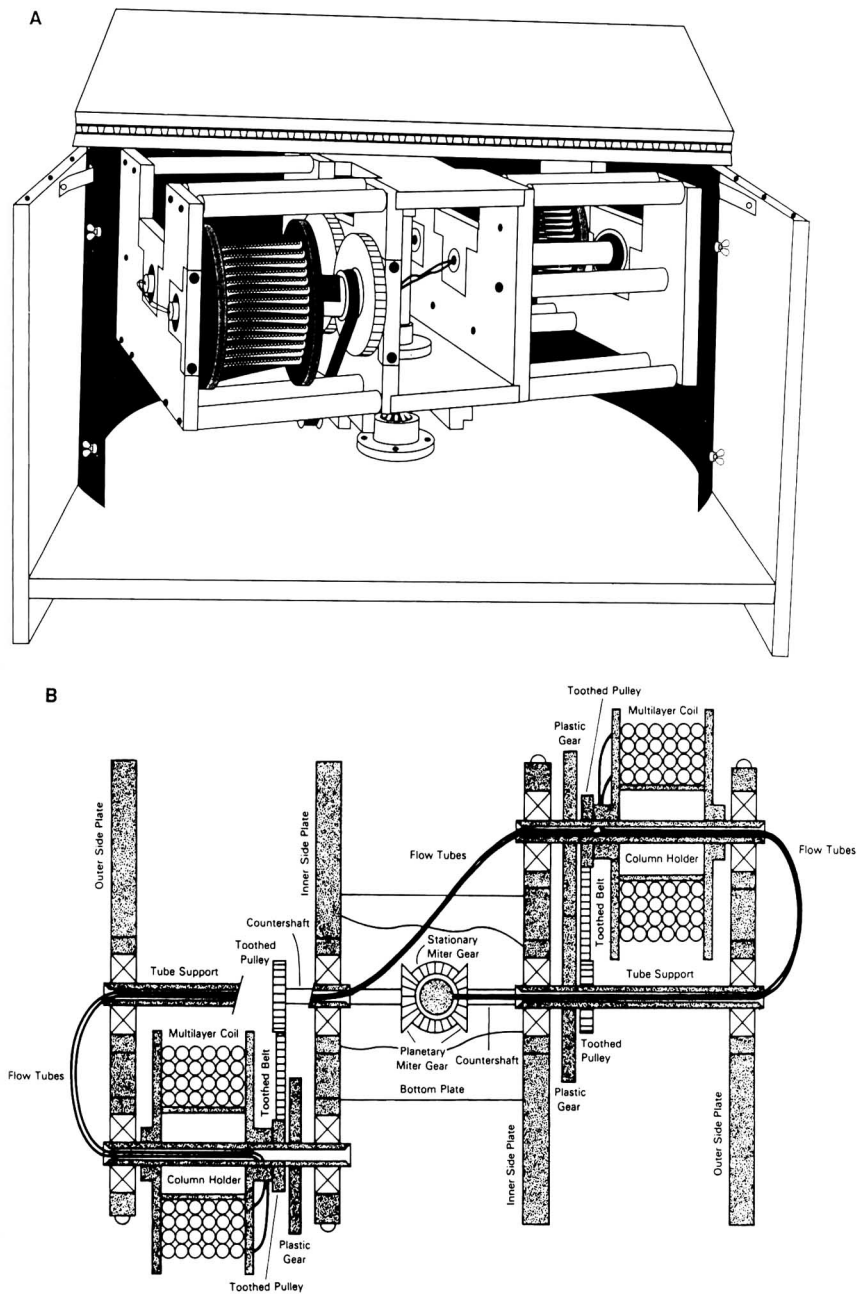


Fig. 1. Design of the apparatus. (A) Front view; (B) horizontal cross-sectional view through the axis of the column holder.

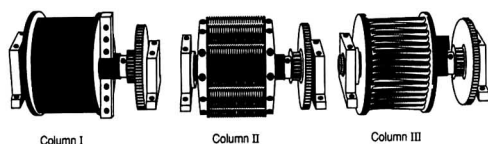


Fig. 2. Three coiled columns used for protein separations. I = Preparative multilayer coil; II = analytical eccentric coil assembly (2.0 cm core diameter); III = analytical eccentric coil assembly (5 mm core).

layer was wrapped with a piece of adhesive tape and the tubing was directly returned to the original side to start the next layer by winding the tube over the interconnection tube. In order to prevent excessive distortion of the coiled column, interconnection tubes were evenly distributed around the holder with minimum overlapping. Two identical multilayer coils were connected in series to make up a total capacity of 575 ml. Columns II and III are the eccentric coil assemblies for analytical separations. Column II consists of 8 column units each prepared by winding a 0.85 mm I.D. PTFE tube onto a 7.6 cm long, 2 cm diameter stainless-steel core forming left-handed coils. Column III consists of 32 units which are similarly prepared by winding a 0.85 mm I.D. PTFE tube onto a 7.6 cm long, 5 mm diameter nylon pipe making tight left-handed coils. In each analytical column assembly, the set of coil units is symmetrically arranged around the holder in parallel to and at the same distance (5 cm in column II and 4 cm for column III) from the holder axis. Each pair of the coil assemblies is connected in series. The total column capacities of these analytical columns are 35.4 ml for column II and 34.0 ml for column III.

Reagents

n-Butanol was chromatographic grade and purchased from Burdick & Jackson (Muskegon, MI, USA). Polyethylene glycol (PEG) 1000 (M_r 1000), PEG 8000 (M_r 8000), cytochrome *c* (horse heart), myoglobin (horse heart), ovalbumin (chicken egg), hemoglobin (bovine), serum albumin (human and bovine) and 1-hexadecylpyridinium chloride were purchased from Sigma (St. Louis, MO, USA); dibasic potassium phosphate and sodium chloride from J.T. Baker (Phillipsburg, NJ, USA); potassium dichromate

from Fisher Scientific (Fair Lawn, NJ, USA); fumaric acid and maleic acid from Chem Service (West Chester, PA, USA) and dextran T500 (M_r 500 000) from Pharmacia (Sollentuna, Sweden). All reagents are of reagent grade.

Preparation of two-phase solvent systems and sample solutions

The composition of the four pairs of two-phase solvent systems used in the present studies are shown in Table I. Each solvent mixture was thoroughly equilibrated in a separatory funnel at room temperature and the two phases separated after the clear two phases has been formed.

Samples were prepared by dissolving a mixture of cytochrome *c* (horse heart), myoglobin (horse heart), ovalbumin (chicken egg) and hemoglobin (bovine) in about equal volumes of the upper and lower phases of the two-phase solvent system.

Measurement of retention of stationary phase

A series of experiments was performed to measure the volume of the stationary phase retained in the column using single-layer coils of 2.6 mm I.D. PTFE tube mounted on the holders with 5 cm and 10 cm diameter.

In each measurement, the entire column including the space in the flow tubes was filled with the stationary phase. Then, the apparatus was rotated at the desired speed while the mobile phase was pumped into the column at a given flow-rate using a metering pump (Milton Roy Minipump, UDC, FL, USA). The effluent from the outlet of the column was collected in a graduated cylinder to measure the volume of the stationary phase eluted from the column as well as the total elution volume. The experiment was continued until the total elution volume exceeded the capacity of the column. During the experiment, the temperature inside the centrifuge was controlled within $28 \pm 2^\circ\text{C}$ by placing a dry ice bag over the top plate of the centrifuge. After the run was terminated, the column contents were emptied into a graduated cylinder by connecting the inlet of the column to a nitrogen line (*ca.* 80 p.s.i.; 1 p.s.i. = 6894.76 Pa). Then the column was washed with *ca.* 100 ml of

distilled water and flushed with the stationary phase to be used for the next experiment.

The measurements of the stationary phase retention were performed with four different solvent systems at the maximum revolution speed of 800 rpm and at a flow-rate of 3.0 ml/min. The retention of each solvent system was measured under eight different experimental conditions, *i.e.*, all possible combinations of the direction of revolution (P_I = counterclockwise; P_{II} = clockwise), the head–tail elution mode (H = head to tail; T = tail to head), and inward–outward elution mode (I = inward; O = outward). The inward–outward refers to the direction of the elution along the holder axis: “inward” is from the peripheral toward the promixal against the action of the centrifugal force field and “outward” is in the opposite direction. These studies required the use of both right-handed and left-handed coils. The eight elution modes at the off-center position ($X - 1.5L$) are summarized in Table II. The elution modes applied to the central position (L) are similarly defined by modifying the orbit of the column rotation in P_I and P_{II} shown in Table II.

After choosing the experimental conditions

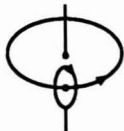
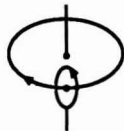
producing the highest retention of stationary phase in each handedness of the coil, the retention of the stationary phase was further studied under both reduced speeds (600, 400 and 200 rpm at a fixed flow-rate of 2.0 ml/min) and flow-rates (2.0, 1.0 and 0.5 ml/min at a fixed 800 rpm of revolution). Retention data for each mobile phase from each solvent system are summarized in a diagram (Figs. 3 and 4) where the percentage retention of the stationary phase is plotted against either the applied revolution speeds or flow-rates.

Similar experiments were performed to measure the retention of the stationary phase in the analytical columns (column II).

CCC separation of proteins

A set of stable proteins, including cytochrome *c*, myoglobin, ovalbumin and hemoglobin, was selected as test samples in the present study. Using a two-phase solvent system composed of 12.5% (w/w) PEG and 12.5% (w/w) dibasic potassium phosphate in distilled water, the partition efficiency of both analytical and preparative columns was evaluated at the two different column positions.

TABLE II
EIGHT DIFFERENT ELUTION MODES AT OFF-CENTER COIL POSITION ($X - 1.5L$)

Planetary motion	Head–tail elution mode	Inward–outward elution mode (handedness of coil) ^a	Combined elution mode ^b
P_I 	Head → tail	Inward (R)	P_I -H-I
	Head → tail	Outward (L)	P_I -H-O
	Tail → head	Inward (L)	P_I -T-I
	Tail → head	Outward (R)	P_I -T-O
P_{II} 	Head → tail	Inward (L)	P_{II} -H-I
	Head → tail	Outward (R)	P_{II} -H-O
	Tail → head	Inward (R)	P_{II} -T-I
	Tail → head	outward (L)	P_{II} -T-O

^a R = Right-handed; L = left-handed.

^b H = head → tail; T = tail → head; I = inward; O = outward.

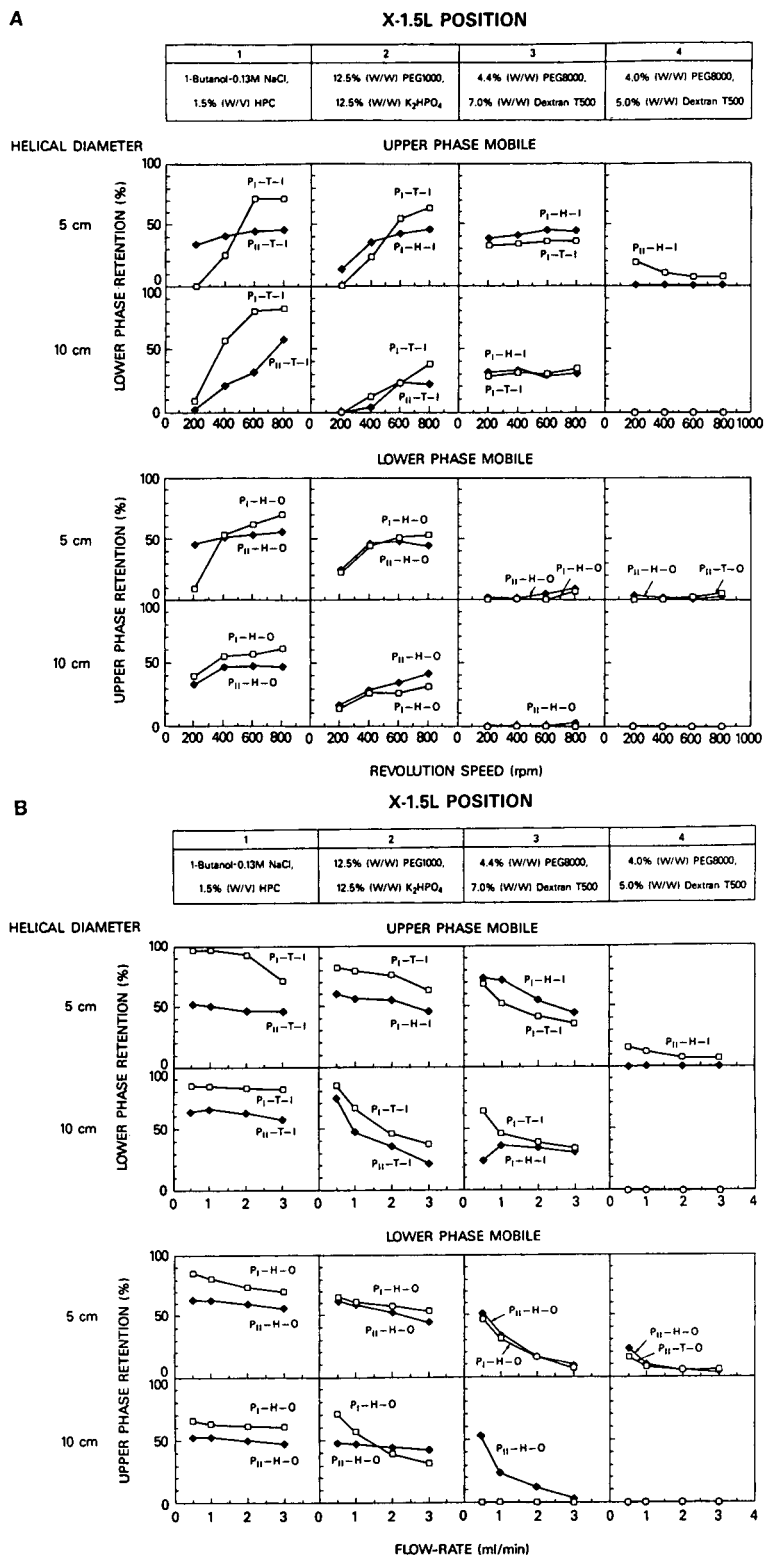


Fig. 3. Phase retention diagrams obtained from the coaxial single-layer coils (2.6 mm I.D.) at the off-center ($X - 1.5L$) position. (A) Effects of revolution on the retention of stationary phase; (B) effects of flow-rate on the retention of stationary phase.

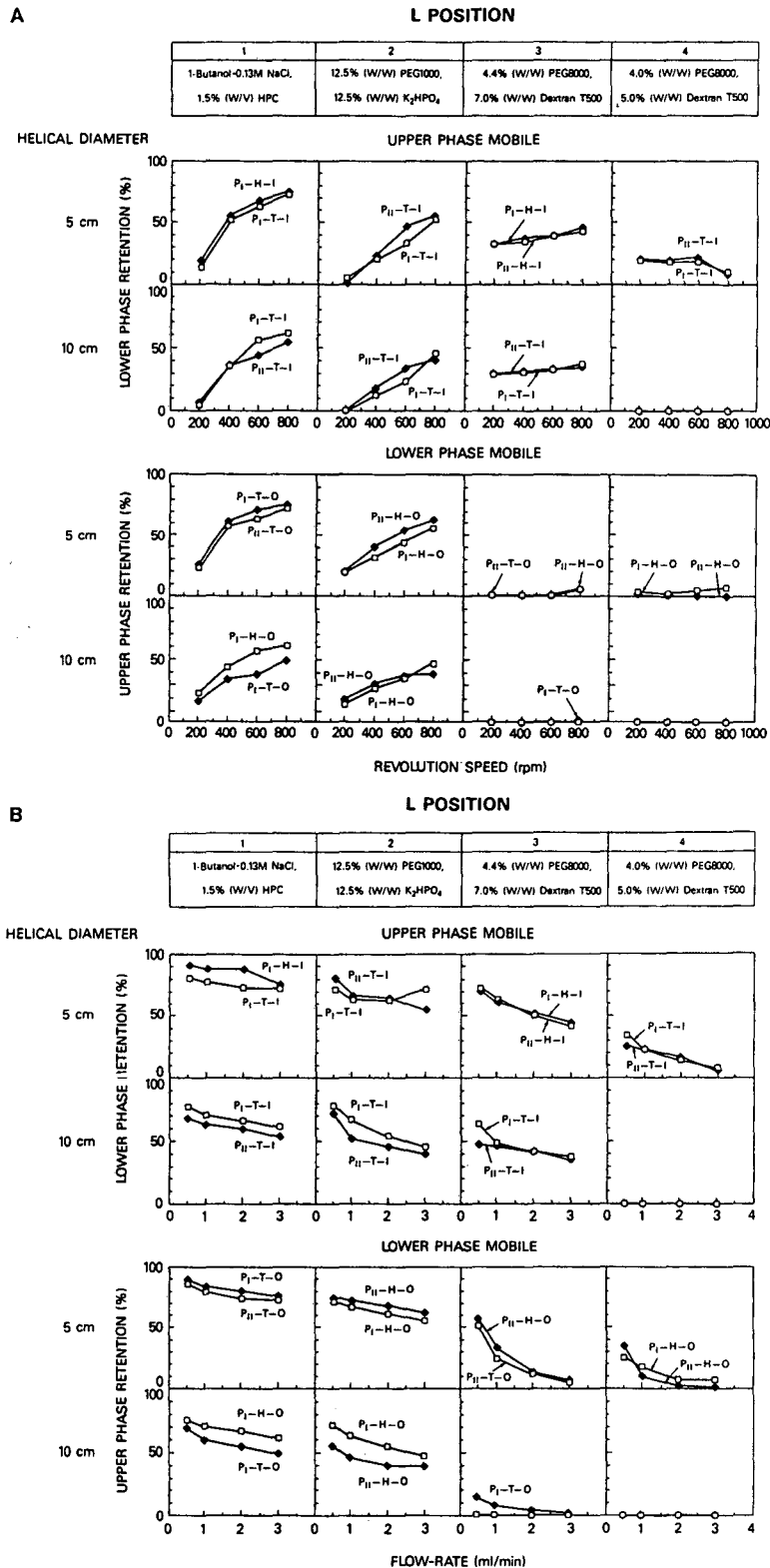


Fig. 4. Phase retention diagrams obtained from the coaxial single-layer coils (2.6 mm I.D.) at the central (*L*) position. (A) Effects of revolution on the retention of stationary phase; (B) effects of flow-rate on the retention of stationary phase.

For each separation, the coil was first completely filled with the PEG-rich upper stationary phase and an appropriate amount of the sample solution was charged into the column through the sample port. Then, the phosphate-rich lower mobile phase was pumped into the column at the optimum flow-rate (2.0 ml/min for column I and 0.2 ml/min for columns II and III), while the apparatus was rotated at a revolution speed of 800 rpm. The effluent from the outlet of the column was continuously monitored with an LKB (Stockholm/Bromma, Sweden) Uvicord S at 280 nm and collected into test tubes (4 ml per tube for column I and 0.4 ml/tube for columns II and III) using an LKB Ultrac fraction collector.

Since the direct tracing of the elution profile by the uv monitor was often disturbed by carryover of the stationary phase, each collected fraction was manually analyzed with a Zeiss (Hanover, PA, USA) PM6 spectrophotometer at 280 nm.

Evaluation of partition efficiency

The partition efficiencies of separations can be computed from the chromatogram and expressed in terms of both the theoretical plate number (N) and peak resolution (R_s). Both values are based on the assumption that each peak represents the distribution of a single component. Among the four proteins in the sample mixture, ovalbumin produced an extremely broad peak which gave low partition efficiencies in both theoretical plate number and peak resolution. We later found that the ovalbumin used in the present studies produced two distinct bands in sodium dodecyl sulfate–polyacrylamide gel electrophoresis. Because of the heterogeneity of the ovalbumin (third peak), the partition efficiencies in the present studies are exclusively expressed as the theoretical plate number of the second peak (myoglobin), since the first peak (cytochrome *c*) is eluted close to the solvent front while the fourth peak (hemoglobin) is excessively retained in the column.

The theoretical plate number of the second peak was calculated from the conventional equation:

$$N = (4R/W)^2 \quad (1)$$

where R denotes the retention volume or time of the peak maximum and W the peak width expressed by the same unit as R .

RESULTS AND DISCUSSION

Studies on stationary phase retention

Fig. 3A illustrates a set of phase retention diagrams for four different solvent systems at the off-center position ($X - 1.5L$ position) obtained by varying the revolution speed at a given flow-rate of 3 ml/min. In this diagram, the upper panel shows the retention of the lower stationary phase obtained by eluting with the upper mobile phase and the lower panel, the retention of the upper stationary phase by eluting with the lower phase. In each panel, the retention diagrams in the first row were obtained from the coil mounted on the 5-cm diameter holder and those in the second row, from the coil mounted on the 10-cm diameter holder. Each diagram contains two best retention curves, one obtained from the right-handed coil and the other from the left-handed coil, each being selected among four possible combinations of the elution modes. In general, retention of over 50% produces an excellent result but 30% retention is considered satisfactory if carryover of the stationary phase is minimum.

The overall results of the experiments indicate that the stationary phase retention is improved by increasing the revolution speed up to the maximum of 800 rpm. The butanol solvent system (solvent 1) shows the highest retention where the head–tail elution mode plays a significant role in stationary phase retention. In the aqueous–aqueous polymer phase systems (solvents 2–4), the inward–outward elution mode plays the most important role in the retention of the stationary phase. The best retention is always achieved by eluting the upper phase inward or the lower phase outward through the coil. Different from the previous results with the X-LL cross-axis CPC [8], the left-handed coil (white square) yields only slightly higher retention of the stationary phase than the right-handed coil (black square) in the 5-cm helical diameter coil.

Among three polymer two-phase systems the PEG–phosphate system (solvent 2) produces the highest retention especially in the 5-cm helical diameter coil. This may be attributed to the physical properties of the PEG–phosphate system characterized by its relatively lower viscosity and greater differences in density and surface tension between the upper and lower phases. In the PEG–dextran systems (solvents 3 and 4) the retention of the lower phase (upper phase mobile) is always greater than that of the upper phase (lower phase mobile). This may be due to an extremely high viscosity of the lower dextran phase. In general the use of the less viscous phase as the mobile phase produces better retention of the stationary phase. This tendency is more pronounced in a small-bore analytical coil as described later.

Fig. 3B illustrates the retention diagrams for the same set of solvent systems at the off-center position ($X - 1.5L$ position) obtained by varying the flow-rate from 0.5 to 3.0 ml/min at 800 rpm. Among the two retention curves drawn in each diagram, one was obtained from the right-handed coil (black square) and the other from the left-handed coil (white square). The results indicate that the retention of the stationary phase is maximum at the lowest flow-rate of 0.5 ml/min and decreases rather sharply with the increased flow rate of the mobile phase. At a low flow-rate of 0.5 ml/min, the retention of the viscous PEG–dextran phase (solvent 3) is improved over 50% of the total column capacity.

The similar sets of the phase retention diagrams for the central column position (L position) are illustrated in Figs. 4A and 4B. The results indicate that the coil mounted in the central position yields slightly higher retention of the stationary phase than the coil mounted in the off-center position. In the central coil position, the retention of the stationary phase is almost entirely governed by the inward–outward elution mode in all solvent systems including the butanol–aqueous solvent system (solvent 1) while other parameters such as direction of the revolution and head–tail elution mode only play a minor role in retention.

The retention of the stationary phase in the analytical coil (column II consisting of three coil

units) was also studied with the PEG–phosphate systems (solvent 2) and PEG–dextran system (solvent 3). The results are summarized in Fig. 5A and B where four retention curves obtained from different elution modes are shown in each diagram. Different from the results obtained with the preparative coil, all elution modes produce similar retention patterns that are very sensitive to the flow-rate at a low range between 0 to 0.2 ml/min. The PEG–phosphate system (solvent 2) produces substantially higher retention than the PEG–dextran system (solvent 3) reaching 50% level at a low flow-rate of 0.1 ml/min. In both solvent systems, the use of the

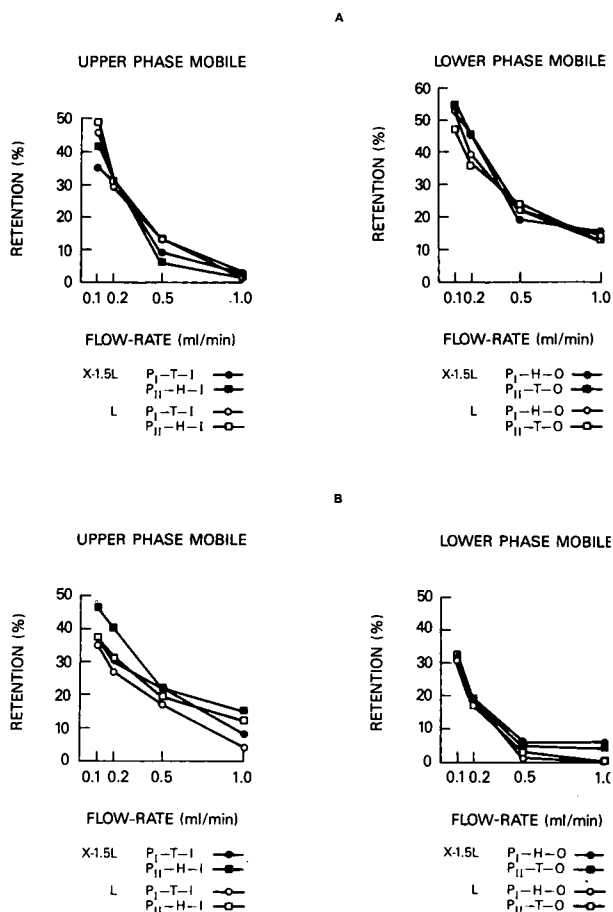


Fig. 5. Phase retention diagrams obtained from the analytical eccentric coil assembly (0.85 mm I.D. and 2 cm core diameter). (A) Effects of flow-rate on retention of 12.5% (w/w) PEG 1000, 12.5% (w/w) dibasic potassium phosphate; (B) effects of flow-rate on retention of 4.4% (w/w) PEG 8000, 7.0% (w/w) dextran T500.

less viscous phase favours the retention of the stationary phase, and this effect is clearly seen in the PEG–dextran solvent system (solvent 3) where the lower dextran phase has extremely high viscosity close to 100 cP.

Separation of proteins with polymer phase systems

The performance of the present apparatus was evaluated in the separation of a set of four stable proteins using both preparative multilayer coils (column I) and analytical composite coil assemblies (columns II and III) each at the off-center and central positions. A series of experimental runs was performed with an aqueous two-phase solvent system composed of 12.5% (w/w) PEG 1000 and 12.5% (w/w) dibasic potassium phosphate using a phosphate-rich lower phase as the mobile phase.

Fig. 6 shows preparative separations of the standard protein mixture by the present apparatus equipped with a pair of multilayer coils (column I) with a total capacity of 575 ml. The separations were performed at 800 rpm and a flow-rate of 1.0 ml/min with the column held at the off-center position (A) and the central position (B). Cytochrome *c* and myoglobin were well separated at both column positions while myoglobin and ovalbumin were only partially resolved. The partition efficiencies computed from the second peak (myoglobin) are 202 theoretical plates (TP) for the column mounted at the off-center position (Fig. 6A) and 169 TP for the same column mounted at the central position (Fig. 6B). The difference in TP between the two coil positions indicates that the off-center position yields slightly higher partition efficiencies than the central position for the polymer phase system used in the present study. This may be mainly due to an efficient phase mixing produced by the strong rotating centrifugal force component acting on the off-center position (see Part II [12]). Although the central coil position produces less efficient separation compared with the off-center coil position, it provides the advantage of retaining a greater amount of the stationary phase in the column that allows application of higher flow-rates of mobile phase to shortening elution times without appreciable loss

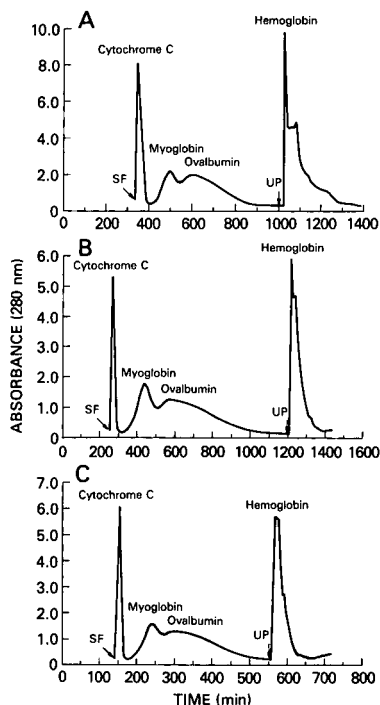


Fig. 6. Protein separations obtained from the preparative multilayer coils (column I) (A) at the off-center ($X - 1.5L$) position at 1 ml/min; (B) at the central (L) position at 1 ml/min; and (C) at the central (L) position at 2 ml/min. Other experimental conditions were as follows: solvent system, 12.5% (w/w) PEG 1000–12.5% (w/w) dibasic potassium phosphate; mobile phase, lower phase; revolution: 800 rpm. SF = Solvent front; UP = the column was eluted with the upper phase in the opposite direction.

in peak resolution. This effect was demonstrated by increasing and flow-rate to 2 ml/min in the central coil position but under the otherwise identical experimental conditions (Fig. 6C). In the chromatogram obtained at a higher flow-rate, the theoretical plates calculated from the myoglobin peak dropped to 104 TP while the peak resolution between the cytochrome *c* and myoglobin peaks was unaltered.

Protein separations obtained by the analytical columns (column II in Fig. 2) are shown in Fig. 7. All separations were performed at 800 rpm and at a flow-rate of 0.2 ml/min. Among three chromatograms, chromatogram A was obtained from 27 mg of the protein mixture and chromatogram B from an increased sample size of 44 mg both using the column mounted at the off-center position. The partition efficiencies com-

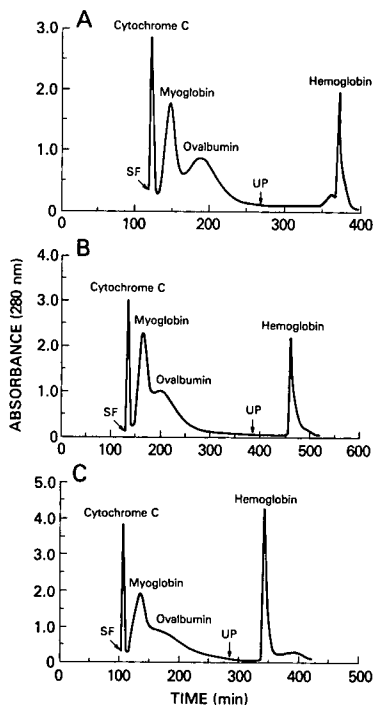


Fig. 7. Protein separations obtained from the analytical coil assembly (column II). (A) A 27-mg amount of sample mixture at the off-center ($X-1.5L$) position; (B) 44 mg sample mixture at the off-center position; (C) 44 mg sample mixture at the central (L) position. Other experimental conditions were as follows: solvent system, 12.5% (w/w) PEG 1000–12.5% (w/w) dibasic potassium phosphate; mobile phase, lower phase; flow-rate, 0.2 ml/min; revolution: 800 rpm. SF = Solvent front; UP = the column was eluted with the upper phase in the opposite direction.

puted from the myoglobin peak are 670 TP for chromatogram A and 505 TP for chromatogram B. Chromatogram C was obtained from 44 mg of the protein mixture using the same column mounted at the central position (L position). In this case, the partition efficiencies measured from the second myoglobin peak is reduced to 228 TP.

The performance of the two analytical columns (columns II and III in Fig. 2) was compared by separations of 44 mg protein mixture at the off-center column position. Separations were performed under the optimum experimental conditions for each column. The result indicates that the chromatogram (Fig. 8B) obtained from the 5-mm-core-diameter analytical column (column III) gives substantially higher

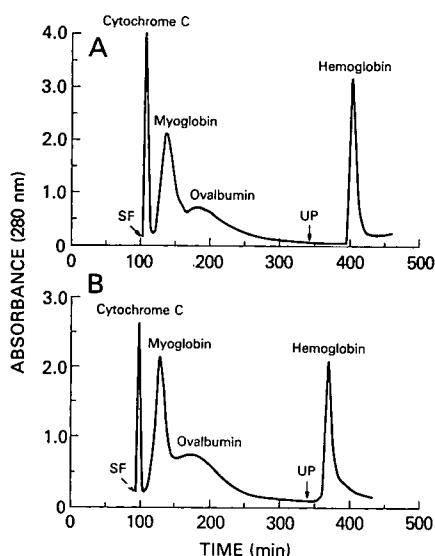


Fig. 8. Protein separations obtained from the analytical coil assemblies: (A) column II and (B) column III (see Fig. 2). Other experimental conditions were as follows: solvent system, 12.5% (w/w) PEG 1000–12.5% (w/w) dibasic potassium phosphate; mobile phase, lower phase; flow-rate, 0.2 ml/min; sample size, 44 mg; revolution, 800 rpm. SF = Solvent front; UP = the column was eluted with the upper phase in the opposite direction.

partition efficiencies of 402 TP for the myoglobin peak compared to 260 TP for the same peak in the chromatogram (Fig. 8A) obtained from the 2-cm-core-diameter analytical column (column II). This result indicates that the smaller diameter core produces a higher efficiency for a given length of tubing.

Comparative studies on partition efficiency

Partition efficiencies of protein separations in the polymer phase systems ranged from 100 to 200 TP which are considerably lower than those obtained from separations of small molecules in organic–aqueous biphasic systems. For example, a preparative column with a 570-ml capacity yielded 160 TP that correspond to 50 cm/TP (length of the column required to produce one TP) in protein separation whereas a similar column produced a much higher efficiency of 5 cm/TP in dinitrophenyl amino acid separations with chloroform–acetic acid–0.1 M HCl (2:2:1) [13]. The low partition efficiency in the protein separation may be attributed to high viscosity of

the polymer phase system and/or some particular nature inherent to the protein molecule. Further studies have been conducted to investigate the cause of low partition efficiencies in protein separation.

Using an analytical column (column III), a series of experiments was performed to measure partition efficiencies of various samples, including both low- and high-molecular-mass compounds, with the same polymer phase system under the identical experimental conditions. Since the TP values calculated from the same chromatogram tend to decrease with increased retention time of the solute, fair comparison of the partition efficiencies should be made from the samples with similar retention times. Therefore, we have selected a set of samples with similar partition coefficient values listed in Table III. It should be noted here that the majority of low molecular weight compounds distribute unilaterally in the PEG-rich upper phase and, therefore, the choice of the sample is extremely limited.

Fig. 9 illustrates analytical chromatograms of potassium dichromate (A), maleic acid (B) and fumaric acid (C) obtained with the polymer phase system composed of 12.5% (w/w) PEG 1000 and 12.5% (w/w) dibasic potassium phosphate in distilled water. Separations were performed at a flow-rate of 0.2 ml/min at 800 rpm.

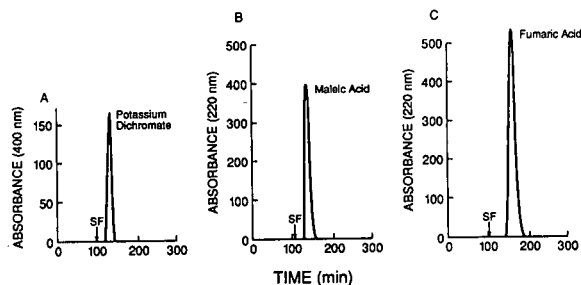


Fig. 9. Chromatograms of potassium dichromate (A), maleic acid (B) and fumaric acid (C) obtained from the analytical coil. Experimental conditions were as follows: solvent system, 12.5% (w/w) PEG 1000–12.5% (w/w) dibasic potassium phosphate; mobile phase, lower phase; flow-rate, 0.2 ml/min; sample size, 20 mg; revolution, 800 rpm. SF = solvent front.

Both potassium dichromate (M_r 294.22) and maleic acid (M_r 116.07) yield high TP values of 1340 and 1156, respectively. Fumaric acid, an isomer of maleic acid, gives a considerably lower TP value of 484, apparently due to the longer retention time resulting from its high K value (see Table III).

Fig. 10 shows a set of chromatograms of protein samples obtained from the same polymer phase system under the identical experimental conditions. Among those, ovalbumin (A), bovine albumin (C), and human albumin (D) have K values similar to that of fumaric acid whereas myoglobin (B) has K value close to those of

TABLE III
SUMMARY OF PARTITION STUDIES

All data were obtained from the analytical column (column III) and the solvent system composed of 12.5% (w/w) PEG 1000 and 12.5% (w/w) dibasic potassium phosphate in distilled water.

Compounds	M_r	Mol. vol. (10^3 \AA^3)	K (C_U/C_L) ^b	Retention time (min)	TP
Potassium dichromate	294.22	0.342	0.62	128	1340
Maleic acid	116.07	0.512	0.78	136	1156
Fumaric acid	116.07	0.512	1.37	154	484
Myoglobin	18 800	48.4 [6]	0.76	128	253
Ovalbumin	45 000	102 [7]	1.38	164	41 ^a
Human albumin	68 000	180 [8]	1.66	158	119
Bovine albumin	68 000	180 [8]	1.75	160	92

^a This low TP value is due to the presence of an impurity which was detected by gel electrophoresis (see text).

^b C_U = Solute concentration in upper phase; C_L = solute concentration in lower phase.

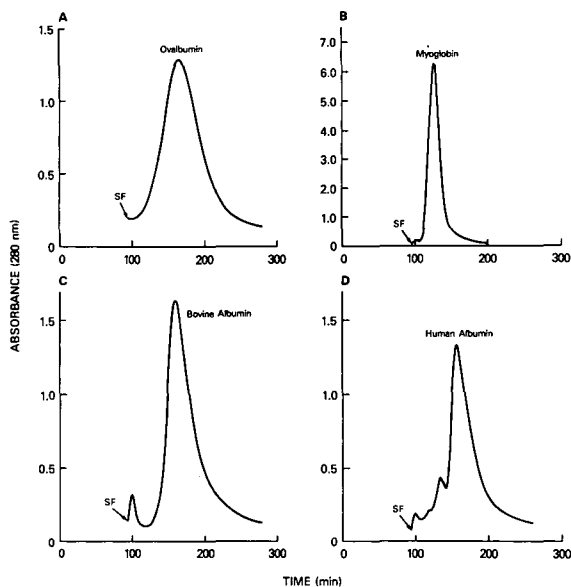


Fig. 10. Chromatograms of ovalbumin (A), myoglobin (B), bovine serum albumin (C) and human serum albumin (D) obtained from the analytical coil. Experimental conditions: solvent system, 12.5% (w/w) PEG 1000–12.5% (w/w) dibasic potassium phosphate; mobile phase, lower phase; flow-rate, 0.2 ml/min; sample size, 30 mg; revolution, 800 rpm. SF = Solvent front.

potassium dichromate and maleic acid (see Table III).

All protein samples yielded substantially lower TP values compared with those obtained from the low-molecular-mass compounds. Among these four proteins, myoglobin with a low K value (similar to that of maleic acid) produced the best TP value of 253, while other proteins with high K values (similar to that of fumaric acid) showed much lower TP values of 41 for ovalbumin (A), 92 for bovine albumin (C), and 119 for human albumin (D). The extremely low TP value of ovalbumin suggested a heterogeneous nature of the sample. This possibility was supported by the analysis of the original sample with sodium dodecyl sulfate gel electrophoresis that revealed two distinct bands at a calibration point corresponding to M_r 44 000. Further studies are being carried out to determine these two products.

The overall results of the present studies indicate that the low partition efficiency in protein separation is not primarily caused by the

high viscosity of the polymer phase system but more likely due to the high molecular mass and/or some heterogeneity of the proteins.

CONCLUSIONS

The results of the present studies indicate that the new cross-axis CPC can be used for separation of proteins at both analytical and preparative scales. As briefly mentioned earlier, the four different two-phase solvent systems examined each provide a specific merit for separation of the biopolymers (Table I). Thus, solvent 1 (*n*-butanol–aqueous solution containing NaCl and hexadecylpyridinium chloride) has been effectively applied to the separation of mucopolysaccharides including heparin and chondroitin sulfate [14]. Because the hexadecylpyridinium chloride in the solvent system acts as a surfactant, the high-speed CCC centrifuge based on the type J planetary motion fails to retain a satisfactory amount of the stationary phase in the column, while the present apparatus produces excellent retention of the stationary phase.

Solvent 2 (PEG–potassium phosphate) systems have been most effectively used for separation of proteins [9–11]. In this polymer phase system, the low-molecular-mass compounds are generally partitioned unilaterally in the upper phase regardless of the pH and the polymer composition whereas the partition coefficients of the proteins are broadly adjusted by pH and the polymer composition.

Solvent 3 (7% PEG 8000 and 4.4% dextran T500) systems form two phases by themselves without an addition of salts. Although the systems have high viscosity and require an application of lower flow-rate of the mobile phase, it can be effectively used for separation of proteins and other macromolecules that tend to be salted-out by a high salt concentration of the PEG–phosphate systems (solvent 2).

Solvent 4 (4% PEG 8000 and 5% dextran T500) systems have a low interfacial tension and small difference in density between the upper and lower phases. This particular physical properties of the solvent system cause emulsification resulting in low retention of the stationary phases in the present apparatus. However, this

polymer phase system can be applied to separation of cell particles by adjusting the osmotic pressure and pH to meet the physiological requirements of the live cells. Since cell particles are mainly partitioned between the upper phase and the interface between the two phases, a large amount of the stationary phase is not required for the partition of cells. In this case, phase emulsification may give a beneficial effect for cell partitioning by providing a large interfacial surface. Therefore, the present apparatus also has a potential in cell partitioning with the polymer phase systems.

ACKNOWLEDGEMENT

The authors are deeply indebted to Mr. Jimmie L. Slemp of the Department of Engineering and Research Services, the National Institutes of Health for fabrication of the apparatus.

REFERENCES

- 1 N.B. Mandava and Y. Ito (Editors), *Countercurrent Chromatography: Theory and Practice*, Marcel Dekker, New York, 1988.

- 2 W.D. Conway, *Countercurrent Chromatography — Apparatus, Theory and Applications*, VCH, New York, 1990.
- 3 Y. Ito, *CRC Crit. Rev. Anal. Chem.*, 17 (1986) 65.
- 4 P.Å. Albertsson, *Partition of Cell Particles and Macromolecules*, Wiley-Interscience, New York, 1986.
- 5 Y. Ito, *Sep. Sci. Tech.*, 22 (1987) 1971.
- 6 Y. Ito, *Sep. Sci. Tech.*, 22 (1987) 1989.
- 7 T.-Y. Zhang, Y.-W. Lee, Q.C. Fang, R. Xiao and Y. Ito, *J. Chromatogr.*, 454 (1988) 185.
- 8 Y. Ito, E. Kitazume and J.L. Slemp, *J. Chromatogr.*, 538 (1991) 81.
- 9 Y. Shibusawa and Y. Ito, *J. Chromatogr.*, 550 (1991) 695.
- 10 Y. Shibusawa, Y. Ito, K. Ikewaki, D.J. Rader and H.B. Brewer, Jr., *J. Chromatogr.*, 596 (1992) 118.
- 11 Y.-W. Lee, Y. Shibusawa, F.T. Chen, J. Myers, J.M. Schooler and Y. Ito, *J. Liq. Chromatogr.*, 15 (1992) 2831.
- 12 J.-M. Menet and Y. Ito, *J. Chromatogr.*, 644 (1993) 231.
- 13 Y. Ito and T.-Y. Zhang, *J. Chromatogr.*, 449 (1988) 153.
- 14 E. Hurst, Y.P.J. Sheng and Y. Ito, *Anal. Biochem.*, 85 (1978) 230.

Studies on a new cross-axis coil planet centrifuge for performing counter-current chromatography

II. Path and acceleration of coils and comparison with type J coil planet centrifuge

Jean-Michel Menet[☆] and Yoichiro Ito^{*}

Laboratory of Biophysical Chemistry, National Heart, Lung, and Blood Institute, National Institutes of Health, Building 10, Room 7N322, Bethesda, MD 20892 (USA)

(First received November 24th, 1992; revised manuscript received March 30th, 1993)

ABSTRACT

A comprehensive approach is introduced using parametric equations to describe the motion induced by type J and cross-axis type coil planet centrifuges. The plots of a line parallel to the coil axis are given. The centrifugal forces are then analyzed in two ways. Three-dimensional graphs show their geometry and the relative intensity of the lateral component is compared to that of the perpendicular component. This allowed a better understanding of the differences in paths and acceleration fields induced by the two types of counter-current chromatography devices.

INTRODUCTION

Type J [1] and cross-axis type [2] coil planet centrifuges (CPCs) induce motions that are best studied using parametric equations. Since the global motions are separated, they allow a better comprehension of the resulting path. The parametric equations for the motion of a point belonging to the column are given as well as those for its acceleration. The β parameter [3], the ratio of the coil radius to the radius of rotation for the coil holder, is then introduced for both units. The path of a line, parallel to the

axis of the coil, is shown for type J CPC and cross-axis CPC equipped with coils in various positions. The plots allow examination of the influence of β on the shape of the paths.

Two procedures are applied to study the accelerations. First, the use of parametric definitions provides simple plots of their three-dimensional geometry. Alternatively perpendicular and lateral components of the total acceleration are considered relative to the axis of the tube.

Both procedures show the complexity of the acceleration field for type J CPC and the important role of the lateral component of the acceleration. The L position (central position of the coil) on the cross-axis CPC shows a simpler acceleration field while the lateral component remains small compared to the perpendicular acceleration. The $X - 1.5L$ position (off-center position) on the cross-axis CPC involves a quite complex acceleration field, leading to a particu-

* Corresponding author.

[☆] Guest scientist from Laboratoire de Chimie Analytique, Ecole Supérieure de Physique et de Chimie Industrielles de Paris, 10 Rue Vauquelin, 75231 Paris Cedex 05, France.

larly important lateral component of the total acceleration.

APPARATUS

Two classical CPCs are studied using our theoretical investigations. One is a Type J CPC from P.C. Inc. (Potomac, MD, USA). Its planetary motion has been widely described in the literature [1].

The other one is the fifth cross-axis prototype; its mechanical principle has been described in Part I [4]. The coil is made of a thin polytetrafluoroethylene (PTFE) tube wound directly onto a cylinder, whose axis is horizontal. This column is mounted in a holder, turning around the central (vertical) axis of the apparatus. Coils of two diameters were used. The holder was designed to accommodate the column in a central position (its axis cuts off the central axis of the CPC), named L , or the off-center position, named $X - 1.5L$.

The main geometrical characteristics of the two devices are gathered in Table I.

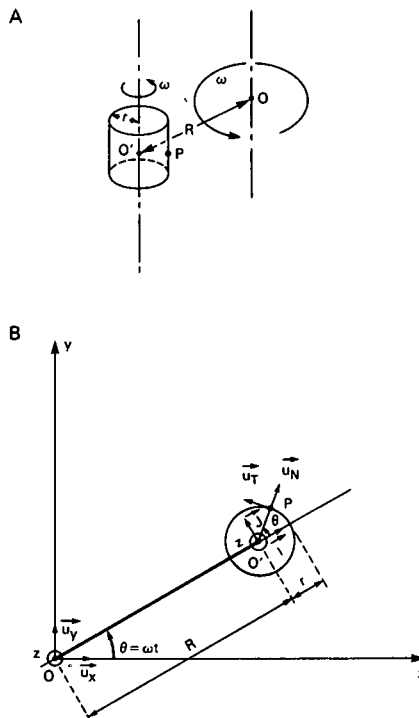


Fig. 1. Type J motion. (A) Principle; (B) mathematical study.

TABLE I

GEOMETRICAL CHARACTERISTICS AND MAXIMUM CENTRIFUGAL FORCE INTENSITIES FOR TWO COUNTER-CURRENT CHROMATOGRAPHY (CCC) DEVICES: TYPE J CPC UNIT AND CROSS-AXIS PROTOTYPE

n.d. = Not defined.

CCC device	Type J CCC	Cross-axis CCC			
		L position		$X - 1.5L$ position	
r (mm)	$58.0 < r < 87.0$	27.5	50.0	27.5	50.0
R (mm)	101.5	0	0	104	104
L (mm)	n.d.	168.6	168.6	168.6	168.6
β	$0.55 < \beta < 0.77$	0.16	0.30	0.26	0.48
θ_0 (°)	n.d.	0	0	31.7	31.7
ω (rpm)	750	800	800	800	800
Maximum number of gravities obtained	280	160	195	180	250

THEORY

All the calculations for the type J CPC have previously been made for the path and acceleration [5]. However, the goal here is to separate the global motion into elementary motions in order to provide better understanding of the results. These procedures are applied below to type J CPC, yielding the results previously computed and the same technique is also applied to the cross-axis type CPC.

Type J synchronous coil planet centrifuge

Analysis of the path. The motion can be studied with a three-dimensional coordinate system $O; \vec{u}_x, \vec{u}_y, \vec{u}_z$ named (R) . This system is considered as the motionless reference system. Another coordinate system $O'; \vec{I}, \vec{J}, \vec{u}_z$ named (R') is also introduced. O' is a point undergoing a circular motion around the z axis with radius R at a constant angular velocity ω . The principle of type J motion is explained in Fig. 1A and all the notations used for the mathematical studies are shown in Fig. 1B. The circular motion of O' is described in the (R) system by the parametric equations:

$$\vec{OO}' = \begin{pmatrix} R \cos(\omega t) & \vec{u}_x \\ R \sin(\omega t) & \vec{u}_y \\ 0 & \vec{u}_z \end{pmatrix} \quad (1)$$

Let us consider an arbitrary point P, belonging to the column. Its motion in the (R') system is a circle of radius r , in the $O'; \vec{I}, \vec{J}$ plane, with an ω angular velocity around the z axis. The parametric equations are:

$$\vec{O'P} = \begin{pmatrix} r \cos(\omega t) & \vec{I} \\ r \sin(\omega t) & \vec{J} \\ 0 & \vec{u}_z \end{pmatrix} \quad (2)$$

Then these equations are given in the (R) system:

$$\vec{OP} = \begin{pmatrix} R \cos(\omega t) + r \cos(2\omega t) & \vec{u}_x \\ R \sin(\omega t) + r \sin(2\omega t) & \vec{u}_y \\ 0 & \vec{u}_z \end{pmatrix} \quad (3)$$

The β ratio, equal to r/R , is introduced, leading to

$$\vec{OP} = R \begin{pmatrix} \cos(\omega t) + \beta \cos(2\omega t) & \vec{u}_x \\ \sin(\omega t) + \beta \sin(2\omega t) & \vec{u}_y \\ 0 & \vec{u}_z \end{pmatrix} \quad (4)$$

Analysis of the acceleration. The acceleration, defined in the (R) system by:

$$\vec{a}(P) = \frac{d^2 \vec{OP}}{dt^2} \quad (5)$$

is then written in the (R) coordinate system:

$$\vec{a}(P) = -R\omega^2 \begin{pmatrix} \cos(\omega t) + 4\beta \cos(2\omega t) & \vec{u}_x \\ \sin(\omega t) + 4\beta \sin(2\omega t) & \vec{u}_y \\ 0 & \vec{u}_z \end{pmatrix} \quad (6)$$

Cross-axis synchronous coil planet centrifuge

Analysis of the path. Two coordinate systems are used. $O; \vec{u}_x, \vec{u}_y, \vec{u}_z$ named (R) and $O'; \vec{I}, \vec{J}, \vec{u}_z$

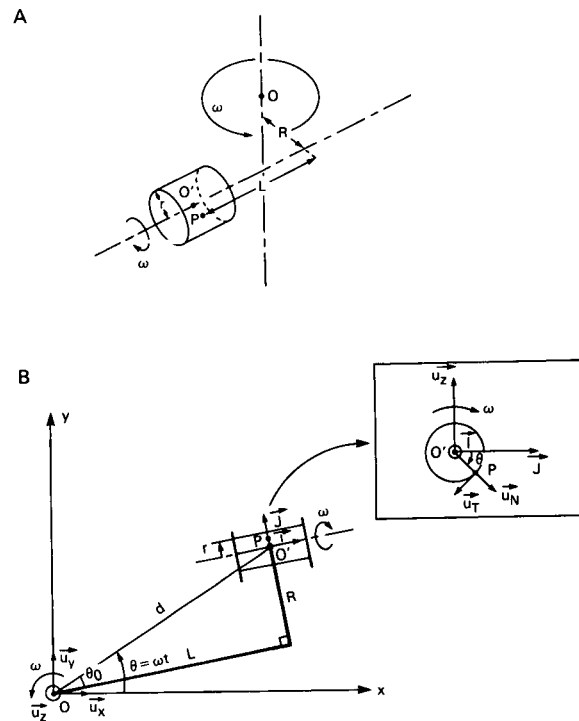


Fig. 2. Cross-axis type motion. (A) Principle; (B) mathematical study.

named (R') were previously defined. O' is a point undergoing a circular motion around the z axis with radius d at a constant angular velocity ω . The principle of cross-axis type motion is explained in Fig. 2A. Fig. 2B gives all the notations used for the following studies. The length d is computed as $d = \sqrt{R^2 + L^2}$ and angle θ_0 is defined by $\tan \theta_0 = R/L$. The circular motion of O' is described in the (R) system by the parametric equations:

$$\vec{OO'} = \begin{pmatrix} d \cos(\omega t) & \vec{u}_x \\ d \sin(\omega t) & \vec{u}_y \\ 0 & \vec{u}_z \end{pmatrix} \quad (7)$$

Let us consider an arbitrary point P, belonging to the column. Its motion in the (R') system is a circle of radius r , in the $O'; \vec{J}, \vec{K}$ plane, with an ω angular velocity around the $O'; \vec{I}$ axis. The parametric equations are:

$$\vec{O'P} = \begin{pmatrix} 0 & \vec{I} \\ r \cos(\omega t) & \vec{J} \\ -r \sin(\omega t) & \vec{u}_z \end{pmatrix} \quad (8)$$

Then these equations are given in the (R) system:

$$\vec{OP} = \begin{pmatrix} d \cos(\omega t) - r \cos(\omega t) \sin(\omega t - \theta_0) & \vec{u}_x \\ d \sin(\omega t) + r \cos(\omega t) \cos(\omega t - \theta_0) & \vec{u}_y \\ -r \sin(\omega t) & \vec{u}_z \end{pmatrix} \quad (9)$$

Analysis of the acceleration. Using the relation 5 in the (R) system, the acceleration is written:

$$\vec{a}(P) = -\omega^2 \begin{pmatrix} d \cos(\omega t) - 2r \sin(2\omega t - \theta_0) & \vec{u}_x \\ d \sin(\omega t) + 2r \cos(2\omega t - \theta_0) & \vec{u}_y \\ -r \sin(\omega t) & \vec{u}_z \end{pmatrix} \quad (10)$$

TABLE II

PARAMETRIC EQUATIONS DESCRIBING THE POSITION OF A POINT BELONGING TO THE COLUMN AND ITS ACCELERATION FOR TYPE J AND CROSS-AXIS CPCs

β is defined as $\beta = r/R$, except for the L -position for which $\beta = r/L$.

	Column position	\vec{OP}	$\vec{a}(P)$
Type J CPC	Not defined	$R \begin{pmatrix} \cos(\omega t) + \beta \cos(2\omega t) \\ \sin(\omega t) + \beta \sin(2\omega t) \\ 0 \end{pmatrix}$	$-R\omega^2 \begin{pmatrix} \cos(\omega t) + 4\beta \cos(2\omega t) \\ \sin(\omega t) + 4\beta \sin(2\omega t) \\ 0 \end{pmatrix}$
	L	$L \begin{pmatrix} \cos(\omega t) - \beta \sin(\omega t) \cos(\omega t) \\ \sin(\omega t) + \beta \cos^2(\omega t) \\ -\beta \sin(\omega t) \end{pmatrix}$	$-L\omega^2 \begin{pmatrix} \cos(\omega t) - 2\beta \sin(2\omega t) \\ \sin(\omega t) + 2\beta \cos(2\omega t) \\ -\beta \sin(\omega t) \end{pmatrix}$
Cross-axis CPC	$X-LL$	$\frac{L}{2} \begin{pmatrix} \sqrt{5} \cos(\omega t) - \beta \sin(\omega t - \theta_0) \cos(\omega t) \\ \sqrt{5} \sin(\omega t) + \beta \cos(\omega t) \cos(\omega t - \theta_0) \\ -\beta \sin(\omega t) \end{pmatrix}$	$\frac{-L\omega^2}{2} \begin{pmatrix} \sqrt{5} \cos(\omega t) - 2\beta \sin(2\omega t - \theta_0) \\ \sqrt{5} \sin(\omega t) + 2\beta \cos(2\omega t - \theta_0) \\ -\beta \sin(\omega t) \end{pmatrix}$
	$X-L$	$L \begin{pmatrix} \sqrt{2} \cos(\omega t) - \beta \sin(\omega t - \pi/4) \cos(\omega t) \\ \sqrt{2} \sin(\omega t) + \beta \cos(\omega t) \cos(\omega t - \pi/4) \\ -\beta \sin(\omega t) \end{pmatrix}$	$-L\omega^2 \begin{pmatrix} \sqrt{2} \cos(\omega t) - 2\beta \sin(2\omega t - \pi/4) \\ \sqrt{2} \sin(\omega t) + 2\beta \cos(2\omega t - \pi/4) \\ -\beta \sin(\omega t) \end{pmatrix}$
	General	$\begin{pmatrix} d \cos(\omega t) - r \cos(\omega t) \sin(\omega t - \theta_0) \\ d \sin(\omega t) + r \cos(\omega t) \cos(\omega t - \theta_0) \\ -r \sin(\omega t) \end{pmatrix}$	$-\omega^2 \begin{pmatrix} d \cos(\omega t) - 2r \sin(2\omega t - \theta_0) \\ d \sin(\omega t) + 2r \cos(2\omega t - \theta_0) \\ -r \sin(\omega t) \end{pmatrix}$

Three positions of the coil were then studied. The notations were defined by Ito [6]. The L position corresponds to $R = 0$, leading to $d = L$ and $\theta_0 = 0$. The $X - L$ position corresponds to $R = L$, leading to $d = \sqrt{2}R$ and $\theta_0 = \pi/4$. The $X - LL$ position is defined by $L = 2R$ and leads to $d = \sqrt{5}R$ and θ_0 defined by $\tan \theta_0 = 1/2$. Table II gathers all the parametric equations for type J CPC and cross-axis CPC involving a coil in three different positions, L , $X - L$ and $X - LL$. Type J equations were previously given in formulas 4 and 6, and general equations for cross-axis type were also obtained in formulas 9 and 10. The equations for the L , $X - L$ and $X - LL$ positions are derived from the general ones, using their geometric characteristics.

RESULTS AND DISCUSSION

All the equations given in Table II allow three-dimensional plots of paths of points or accelerations. In order to better understand the motions induced by the two CPCs, we studied the paths of a line drawn on the coil, parallel to the axis of the latter. The accelerations of one point were also studied.

Analysis of the path

All the equations given in Table II involve the β ratio as a key parameter. Selected values were then used to plot the paths for a line drawn along the axis of the coil, for type J CPC and cross-axis type CPC, with a coil in L , $X - L$ or $X - LL$ position. The shapes of the paths are all shown in Fig. 3. The individual paths of five points were plotted, allowing display of the path of the interconnecting straight line parallel to the axis of the coil.

For type J CPC, the shapes of the path are greatly dependent on β [7]. They are only two-dimensional, in the xy plane. For small β ($\beta < 0.25$), the path is quite circular, but slightly flattened. For $\beta = 0.25$, the shape becomes cycloidal. For $0.25 < \beta < 0.5$, the cycloidal path is more pronounced. β values greater than 0.5 involve an inner loop, whose size increases with β .

The shapes for the three positions L , $X - L$ and $X - LL$ of the cross-axis CPC are very

similar. All are three-dimensional. For small β values ($\beta < 0.4$), the shape is again simple resembling a circle, with a small component on the vertical axis Oz . As the β value increases ($0.4 \leq \beta \leq 0.5$), a deformation occurs near the Oy axis, and at larger β values, this deformation evolves from a “drop” of the path near the Oy axis to a loop. The latter is shown for each of the three positions when the radius of the coil is twice the radius R .

These studies can be applied to the two CPCs described in part Apparatus. The type J device involves β values greater than 0.5; consequently, the path always shows a loop. The cross-axis prototype shows more simple paths, quite circular with a small component on the vertical axis. No loop intervenes as the radii of the coils are small compared to the R radius.

Analysis of the acceleration

The following explanations refer to the force field which is opposite to the acceleration field. Two different studies were carried out. First, the geometric characteristics of the centrifugal force fields were considered. The influence of the β ratio has revealed to be important for the force field created by the type J motion [8]. Therefore, five plots are shown in Fig. 4, drawn in the xy plane. For $\beta = 0.1$, the shape of the path is quite circular, and the corresponding force field is similar to that obtained with a completely circular motion. The direction of the force is almost perpendicular to the path and the variations in intensity are small. Where $\beta = 0.2$, a modification is seen near the Ox axis: the relative intensity of the lateral component of the centrifugal force field increases while the total intensity of this latter greatly diminishes. For $\beta = 0.25$, the total intensity becomes equal to 0 on the Ox axis. For higher β values, the centrifugal force field never cancels, but the relative intensity of the lateral force becomes very important near the loop. The influence of β for the centrifugal force field created by the cross-axis CPC is less important than for the type J CPC. Four plots are given in Fig. 5. Fig. 5A corresponds to the L position of the coil with $\beta = 0.5$ and two plots are necessary to represent the force field, since it is three-dimensional. The

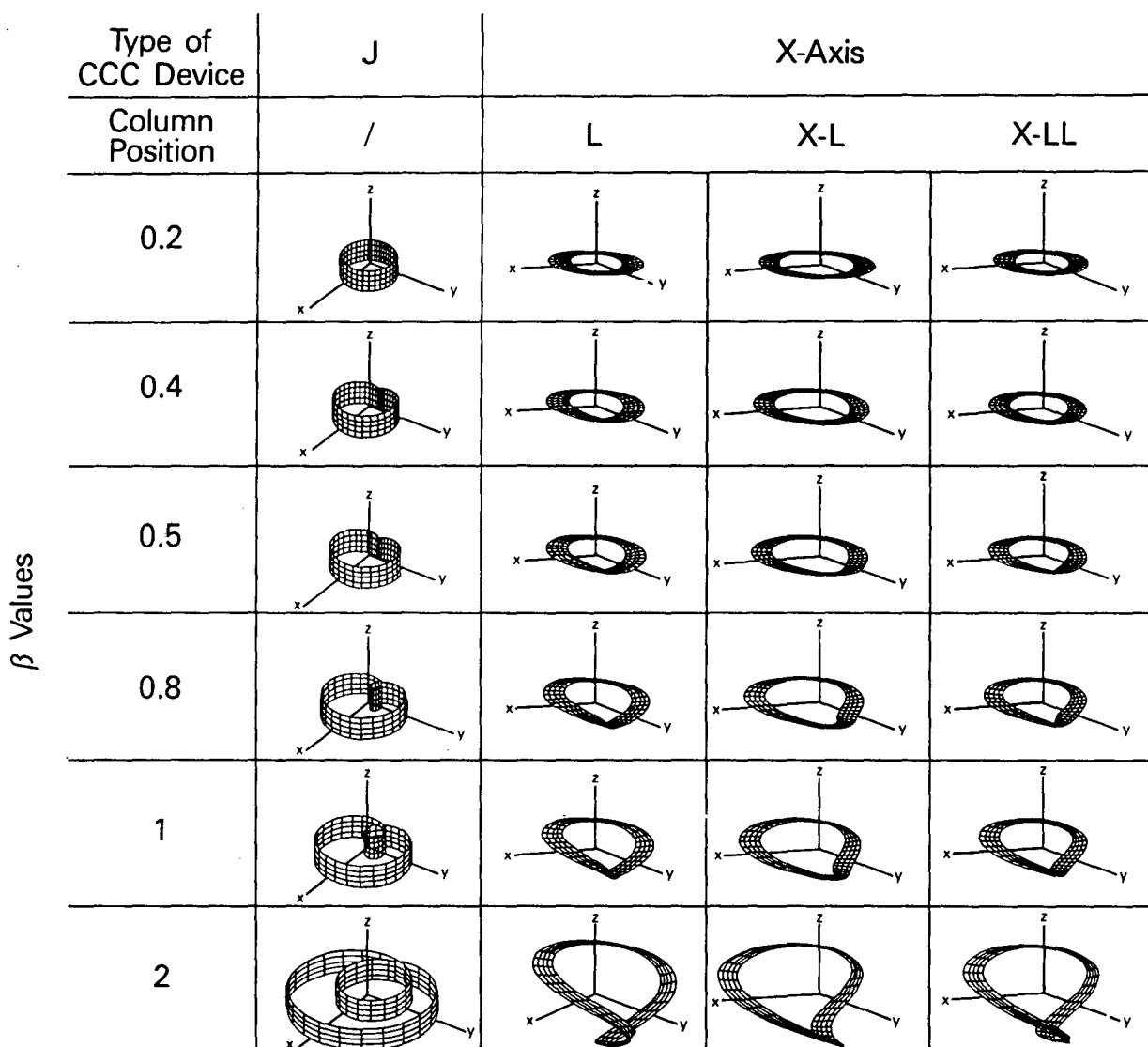


Fig. 3. Paths of a line drawn along the axis of the coil belonging to a type J CPC or a cross-axis (X-axis) CPC; influence of the β ratio and of the position of the coil for a cross-axis CPC.

centrifugal field in the xy plane (Fig. 5A, 1) is similar to that obtained with type J motion for $\beta = 0.25$, but it never cancels completely. Its projection in the xz plane is shown in Fig. 5A, 2. Fig. 5B refers to the $X-L$ position of the coil with $\beta = 0.5$. The projections in the xy and xz planes are given in Fig. 5B, 1 and 2. The geometry of the centrifugal force field appears similar to that for the L position of the coil, as

the axis of symmetry in the xy plane is no longer Oy but a line defined by the θ_0 angle.

The second set of studies was done to examine the influence of the total centrifugal acceleration by analyzing its tangential (lateral) and normal (perpendicular) components. For both CPCs, the direction perpendicular to the tube is given by vector $\vec{O'P}$ (see Figs. 1 and 2). The corre-

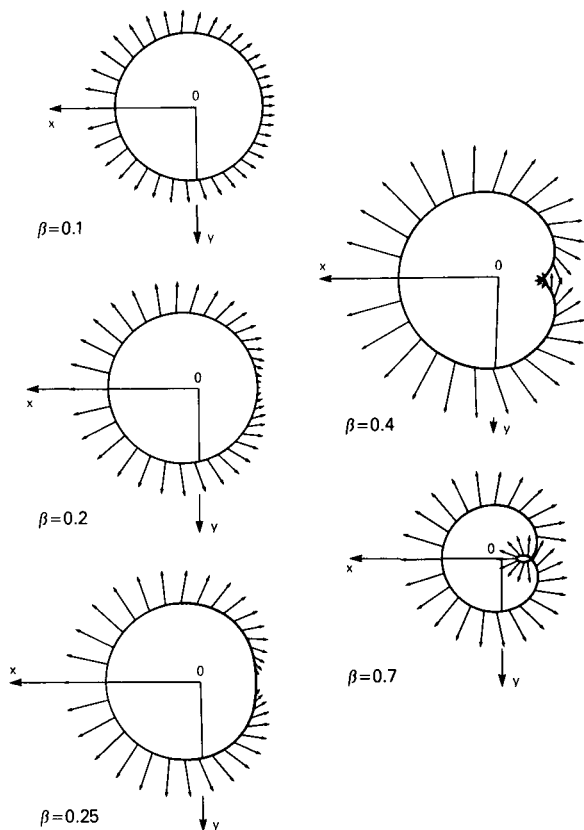


Fig. 4. Type J CCC unit: relative magnitude and direction of the centrifugal force field at various angles along the path of a point. Influence of β .

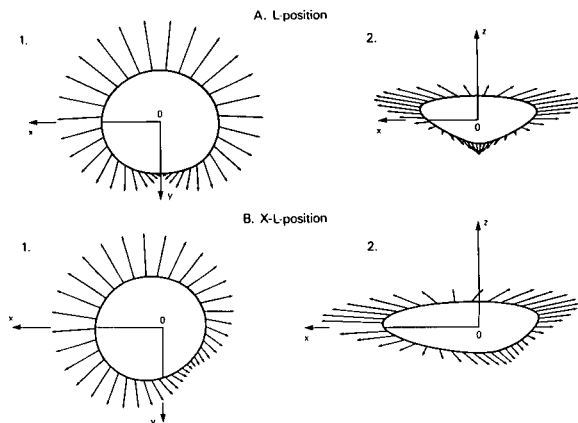


Fig. 5. Cross-axis CCC unit: relative magnitude and direction of the centrifugal force field at various angles along the path of a point. (A) L Position; (B) X-L position.

responding normalized vectors \vec{u}_T and \vec{u}_N are computed in the (R') coordinate system. For type J CPC, using the acceleration of point P, $\vec{a}(P)$, given in formula 6 and rewritten in the (R') system, its tangential component a_T and normal component a_N are computed as:

$$\begin{cases} a_T = \vec{a}(P) \cdot \vec{u}_T = R\omega^2 \sin(\omega t) \\ a_N = \vec{a}(P) \cdot \vec{u}_N = -R\omega^2 [\cos(\omega t) + 4\beta] \end{cases} \quad (11)$$

For the type J apparatus (P.C. Inc.), $\beta > 0.25$; consequently, the term $\cos(\omega t) + 4\beta$ remains always positive. The normal component of the acceleration is thus always directed toward the interior of the coil. Except for two angular positions, which lead to $\sin(\omega t) = 0$, a lateral component is involved but is always smaller than a_T . The maximum relative intensity of the lateral acceleration is obtained when $\sin(\omega t) = 1$, resulting in $a_T/a_N = 1/4\beta$. Using the smaller β values of the type J CPC, this ratio is equal to 0.45, which indicates the tangential acceleration represents up to 45% of the normal acceleration. For the first half of the path ($0 < \theta < 180^\circ$), \vec{u}_T and the lateral force have opposite directions, although for the second half of the path ($180 < \theta < 360^\circ$), their directions are the same. The influence of that change of direction is more important for $\theta \approx 180^\circ$ because the normal force is smaller than that corresponding to $\theta \approx 0^\circ$, thus increasing the relative importance of the tangential force. This could be related to the settling zone around $\theta = 0^\circ$ and the mixing zone around $\theta = 180^\circ$, as described by Conway and Ito from stroboscopic observations [9].

The same studies apply to the cross-axis prototype. Using the acceleration of point P, $\vec{a}(P)$, given in formula 10 and rewritten in the (R') system, its tangential component a_T , normal component a_N and component a_I on the $O'I$ axis are computed as:

$$\begin{cases} a_I = \vec{a}(P) \cdot \vec{I} = -L\omega^2 + 2r\omega^2 \sin(\omega t) \\ a_T = \vec{a}(P) \cdot \vec{u}_T = \omega^2 \sin(\omega t) [R + r \cos(\omega t)] \\ a_N = \vec{a}(P) \cdot \vec{u}_N = -r\omega^2 - \cos(\omega t)\omega^2 [R + r \cos(\omega t)] \end{cases} \quad (12)$$

These expressions can be simplified for the L position and lead to:

$$\begin{cases} a_I = r\omega^2 \left[2 \sin(\omega t) - \frac{L}{r} \right] \\ a_T = r\omega^2 \sin(\omega t) \cos(\omega t) \\ a_N = -r\omega^2 \left[\cos^2(\omega t) + 1 \right] \end{cases} \quad (13)$$

In that case, it is easy to study the relative intensities of the three components of the total acceleration. The geometrical dimensions of the cross-axis prototype with a coil in the L position (see Table I) are introduced in formula 13. Examination of the ratio $a_T/(\sqrt{a_I^2 + a_N^2})$ demonstrates that the tangential component represents up to 16.5% of the total normal component for the larger radius ($r = 50.0$ mm); it can represent up to 9% for the smaller radius ($r = 27.5$ mm). Consequently, the total centrifugal force acting on the fluids inside the tube involves three forces: two are perpendicular to the tube, directed toward the outside; the third is parallel to the axis of the tube, acting with a small intensity (a maximum 16.5% of the gathered two perpendicular forces for the 50.0 mm coil radius) and changing direction four times during one turn of the central axis of the device. Whereas type J CPC involves a maximum 280 g centrifugal force and a lateral force representing up to 45% of the perpendicular force, the lateral force for the cross-axis prototype using a coil in the L position is three times smaller and the maximum centrifugal force is 195 g. The position $X - 1.5L$ was also studied as the geometrical characteristics of the cross-axis prototype (given in Table I) are introduced in formula 12. Whatever the radius of the coil may be (2.75 cm or 5.0 cm), a_I is always negative, a_T has the sign of $\sin(\omega t)$ and a_N is positive or negative. Analysis of the ratio $a_T/(\sqrt{a_I^2 + a_N^2})$ allowed estimation of the relative intensity of the lateral force compared to the centrifugal force exerted perpendicularly to the axis of the tube. For the small radius ($r = 2.75$ cm), the maximum for the ratio is 0.9 and the larger radius ($r = 5.0$ cm) can lead to 1.25.

CONCLUSIONS

The results demonstrate that the two CCC types create different force fields. The type J

CPC induces a loop for β larger than 0.25, leading to a specific force field. The intensity of the lateral component of the acceleration may represent one half of the component perpendicular to the axis of the tube. For the cross-axis CPC, the positions of the coil lead to similar paths but different acceleration characteristics. The L position induces mainly an acceleration perpendicular to the tube, with a small lateral component representing a maximum of one sixth of the total intensity of the forces perpendicular to the tube. The $X - 1.5L$ position greatly increases the role of the lateral force, whose intensity can be larger than that of the total perpendicular centrifugal force.

Further investigations will be necessary to correlate these acceleration studies with the observed retention of the stationary phase related to the position of the coil and the direction of elution or the elution mode. The use of four two-phase solvent systems and statistical analysis should help in this goal. In the following article (Part III [10]), retention data of the four two-solvent systems are analysed by reference to these studies.

REFERENCES

- 1 Y. Ito, in N.B. Mandava and Y. Ito (Editors), *Counter-current Chromatography—Theory and Practice*, Marcel Dekker, New York, 1988, Ch. 3, p. 422.
- 2 Y. Ito, *Sep. Sci. Technol.*, 22 (1987) 1971.
- 3 Y. Ito, in N.B. Mandava and Y. Ito (Editors), *Counter-current Chromatography—Theory and Practice*, Marcel Dekker, New York, 1988, Ch. 3, p. 333.
- 4 K. Shinomiya, J.-M. Menet, H.M. Fales and Y. Ito, *J. Chromatogr.*, 644 (1993) 215.
- 5 W.D. Conway, *Countercurrent Chromatography—Apparatus, Theory and Applications*, VCH, New York, 1990, pp. 128-136.
- 6 Y. Ito, E. Kitazume, M. Bhatnagar and F. Trimble, *J. Chromatogr.*, 538 (1991) 59.
- 7 W.D. Conway, *Countercurrent Chromatography—Apparatus, Theory and Applications*, VCH, New York, 1990, p. 130.
- 8 W.D. Conway, *Countercurrent Chromatography—Apparatus, Theory and Applications*, VCH, New York, 1990, p. 135.
- 9 W.D. Conway and Y. Ito, presented at the *Pittsburgh Conference, Atlantic City, NJ, March 1984*.
- 10 J.-M. Menet, K. Shinomiya and Y. Ito, *J. Chromatogr.*, 644 (1993) 239.

Studies on new cross-axis coil planet centrifuge for performing counter-current chromatography

III. Speculations on the hydrodynamic mechanism in stationary phase retention

Jean-Michel Menet^{*}, Kazufusa Shinomiya^{**} and Yoichiro Ito^{*}

Laboratory of Biophysical Chemistry, National Heart, Lung, and Blood Institute, National Institutes of Health, Building 10, Room 7N322, Bethesda, MD 20892 (USA)

(First received November 24th, 1992; revised manuscript received March 30th, 1993)

ABSTRACT

Retention of the stationary phases of one organic–aqueous solvent system and three aqueous–aqueous polymer solvent systems was investigated on a cross-axis coil planet centrifuge. A graphic statistical treatment of all the data highlighted the prevailing effect of the inward–outward elution mode. A simplified model was proposed and studies on the paths and accelerations of cross-axis devices described in the previous paper provided explanations about the observed hydrodynamic behaviors.

INTRODUCTION

A series of experiments has been performed on the latest version of the cross-axis coil planet centrifuge (CPC) to measure retention of its stationary phase; those were described in Part I [1]. The results were obtained with one organic–aqueous and three aqueous–aqueous polymer two-phase solvent systems using a preparative single layer column. When the coil is mounted in the L position, retention of the stationary phase

was found to be almost entirely governed by the inward–outward elution mode. The lighter mobile phase had to be eluted in the inward mode while the heavier mobile phase requires the use of the outward mode. When using the $X - 1.5L$ position, such results apply to the three aqueous–aqueous polymer systems. The organic–aqueous system was also found to be dependent on the head–tail elution mode. Moreover the coil mounted in the L position produced a slightly higher retention of stationary phase than that used in the $X - 1.5L$ position.

In this Part, statistics based on graphic studies are used to separate and evaluate the effects produced by each factor, *i.e.*, head–tail elution mode, inward–outward elution mode, direction of rotation and coil diameter. An explanation on the great influence of the inward–outward elution mode is given. Then the studies of Part II [2] are used to provide further explanations of the experimental observations.

* Corresponding author.

** Guest scientist from Laboratoire de Chimie Analytique, Ecole Supérieure de Physique et de Chimie Industrielles de Paris, 10 Rue Vauquelin, 75231 Paris Cedex 05, France.

** Visiting scientist from The College of Pharmacy, Nihon University, 7-7-1, Narashinodai, Funabashi-shi, Chiba 274, Japan.

ANALYSIS OF PHASE RETENTION DATA

As described in Part I [1], the cross-axis coil planet centrifuge allows use of 5.5 cm and 10 cm diameter columns in the L or $X-1.5L$ positions. Table I (5.5 cm diameter) and Table II (10 cm diameter) list all the results for the L position, as Table III (5.5 cm diameter) and Table IV (10 cm diameter) for the $X-1.5L$ position. Each table shows the retention percentage of stationary phase inside the apparatus for four two-phase solvent systems with both upper and lower phases used as mobile phase. All the measurements were made with the short pre-

parative columns (one layer, 5.5 and 10 cm hub diameter for 19.8 ml and 41.0 ml internal volumes) described in part I [1] and a 3 ml/min flow-rate at 800 rpm. With a fixed mobile phase, eight retention data are shown. They are expressed from three factors: the direction of planetary motion (P_I and P_{II} , as shown at the bottom of Table I); the head-tail elution mode (H = head-to-tail; T = tail-to-head); and the direction of elution along the axis of the column (I = inward; O = outward). These data are arranged from top to bottom in decreasing of phase retention. The measurements obtained with left-handed coils are shaded in the four tables.

TABLE I

RETENTION (%) OF STATIONARY PHASE IN 5.5-cm HELICAL DIAMETER COIL, L POSITION

Mobile phase	Solvent system ^a							
	1: 1-Butanol- 0.13 M NaCl (1:1) containing 1.5% (w/v) HPC		2: PEG 1000 12.5%, K ₂ HPO ₄ 12.5%		3: PEG 8000 4.4%, dextran T500 7.0%		4: PEG 8000 4.0%, dextran T500 5.0%	
	Condition ^b	%	Condition	%	Condition	%	Condition	%
Upper	P_I -H-I	74.7	P_{II} -T-I	55.6	P_I -H-I	46.0	P_I -T-I	9.3
	P_{II} -T-I	74.2	P_I -H-I	53.0	P_{II} -T-I	43.4	P_{II} -H-I	8.8
	P_I -T-I	72.6	P_I -T-I	52.1	P_{II} -H-I	42.3	P_{II} -T-I	7.4
	P_{II} -H-I	63.3	P_{II} -H-I	40.9	P_I -T-I	40.0	P_I -H-I	3.6
	P_I -H-O	6.0	P_{II} -H-O	2.0	P_I -H-O	9.9	P_I -H-O	0
	P_{II} -H-O	0	P_I -H-O	0	P_{II} -H-O	9.5	P_{II} -H-O	0
	P_I -T-O	0	P_I -T-O	0	P_I -T-O	1.8	P_I -T-O	0
	P_{II} -T-O	0	P_{II} -T-O	0	P_{II} -T-O	0.5	P_{II} -T-O	0
Lower	P_I -T-O	75.8	P_{II} -H-O	62.1	P_{II} -H-O	8.4	P_I -H-O	6.8
	P_{II} -H-O	74.2	P_I -T-O	61.1	P_{II} -T-O	7.9	P_{II} -H-O	1.0
	P_{II} -T-O	72.6	P_I -H-O	55.8	P_I -H-O	6.1	P_{II} -T-O	0
	P_I -H-O	72.1	P_{II} -T-O	52.1	P_I -T-O	5.5	P_I -T-O	0
	P_I -T-I	4.2	P_I -T-I	7.4	P_{II} -H-I	1.9	P_{II} -H-I	0
	P_{II} -T-I	3.0	P_{II} -H-I	3.7	P_I -T-I	0	P_I -T-I	0
	P_{II} -H-I	1.9	P_{II} -T-I	3.0	P_{II} -T-I	0	P_{II} -T-I	0
	P_I -H-I	1.5	P_I -H-I	1.5	P_I -H-I	0	P_I -H-I	0

^a Composition indicated in % (w/w) except the first one v/v; HPC = 1-hexadecylpyridinium chloride.

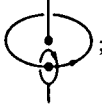
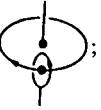
^b P_I = Planetary motion ; P_{II} = planetary motion ; H = head to tail; T = tail to head; I = inward elution, O = outward elution; plain background = right-handed coil; shaded background = left-handed coil.

TABLE II
RETENTION (%) OF STATIONARY PHASE IN 10.0-cm HELICAL DIAMETER COIL, *L* POSITION

Mobile phase	Solvent system ^a							
	1: 1-Butanol– 0.13 M NaCl (1:1) containing 1.5% (w/v) HPC		2: PEG 1000 12.5%, K ₂ HPO ₄ 12.5%		3: PEG 8000 4.4%, dextran T500 7.0%		4: PEG 8000 4.0%, dextran T500 5.0%	
	Condition ^b	%	Condition	%	Condition	%	Condition	%
Upper	P _I -T-I	61.0	P _I -T-I	45.4	P _I -T-I	37.1	P _I -T-I	0
	P _{II} -H-I	56.1	P _{II} -T-I	40.0	P _{II} -T-I	35.1	P _I -T-I	0
	P _{II} -T-I	53.7	P _I -H-I	35.6	P _{II} -H-I	34.1	P _{II} -H-I	0
	P _I -H-I	50.0	P _{II} -H-I	29.8	P _I -H-I	29.8	P _I -H-I	0
	P _{II} -H-O	13.9	P _I -T-O	11.7	P _I -T-O	21.5	P _I -T-O	0
	P _I -H-O	7.8	P _{II} -H-O	4.9	P _{II} -T-O	20.7	P _{II} -T-O	0
	P _I -T-O	6.3	P _{II} -T-O	2.4	P _I -H-O	14.6	P _I -H-O	0
	P _{II} -T-O	0	P _I -H-O	0	P _{II} -H-O	12.2	P _{II} -H-O	0
Lower	P _I -H-O	61.0	P _I -H-O	46.8	P _I -T-O	1.5	P _I -T-O	0
	P _{II} -T-O	59.8	P _{II} -H-O	39.0	P _I -H-I	0.7	P _I -H-I	0
	P _I -T-O	48.8	P _{II} -T-O	38.3	P _{II} -T-O	0	P _{II} -T-O	0
	P _{II} -H-O	48.3	P _I -T-O	36.6	P _I -H-O	0	P _I -H-O	0
	P _{II} -T-I	13.2	P _I -H-I	9.8	P _I -T-I	0	P _I -T-I	0
	P _I -T-I	9.0	P _{II} -T-I	8.5	P _{II} -H-I	0	P _{II} -H-I	0
	P _I -H-I	7.3	P _I -H-I	7.3	P _{II} -H-O	0	P _{II} -H-O	0
	P _{II} -H-I	3.7	P _{II} -T-I	6.1	P _{II} -T-I	0	P _{II} -T-I	0

^{a,b} See footnotes in Table I.

The overall results show that the eight experimental conditions combined with the choice of mobile phase and the four two-phase solvent systems lead to different values for the retention of stationary phase. It is difficult to give a direct interpretation of all these results. Consequently, statistical methods were applied to assess the influence of each of the three factors (P_I – P_{II} , H–T or I–O) along with the diameter of the column (5.5 cm or 10 cm), the choice of mobile phase (lighter or heavier) and the position of the column (*L* or *X*–1.5*L*).

Two statistical methods have been applied to the measurements of retention of stationary phase. One is called “experimental design” [3] and allows an accurate estimation of the influence of each factor along with the possible interactions between these factors. The other method is based on graphic interpretations and was previously introduced by Ito [4]. Thus, the

retention of stationary phase is plotted as one parameter is changed between the horizontal axis and the vertical axis. This is done for four factors: the planetary motion P_{II} vs. P_I (Figs. 1 and 2 for the *L* and *X*–1.5*L* positions), the tail-to-head vs. the head-to-tail elution mode (Figs. 3 and 4 for the *L* and *X*–1.5*L* positions), the outward vs. the inward elution mode (Figs. 5 and 6 for the *L* and *X*–1.5*L* positions) and the 10.0 cm vs. the 5.5 cm diameter (Fig. 7 for *L* and *X*–1.5*L* positions). Each figure includes a set of four graphs showing the retention of stationary phase in both 5.5 cm (A) and 10.0 cm (B) diameter columns with the upper (left) or the lower (right) phase used as the mobile phase, except for Fig. 7 involving four graphs with a mobile phase either heavier or lighter on both *L* and *X*–1.5*L* positions.

Each graph is separated in four squares by thin horizontal and vertical lines. The upper right

TABLE III
RETENTION (%) OF STATIONARY PHASE IN 5.5-cm HELICAL DIAMETER COIL, X – 1.5L POSITION

Mobile phase	Solvent system ^a							
	1: 1-Butanol– 0.13 M NaCl (1:1) containing 1.5% (w/v) HPC		2: PEG 1000 12.5%, K ₂ HPO ₄ 12.5%		3: PEG 8000 4.4%, dextran T500 7.0%		4: PEG 8000 4.0%, dextran T500 5.0%	
	Condition ^b	%	Condition	%	Condition	%	Condition	%
Upper	P _I -T-I	85.0	P _I -T-I	38.7	P _I -H-I	44.4	P _{II} -H-I	6.5
	P _{II} -T-I	74.7	P _{II} -H-I	36.0	P _I -T-I	35.3	P _I -T-I	2.8
	P _I -H-I	48.9	P _I -H-I	29.9	P _{II} -H-I	32.6	P _I -H-I	0
	P _{II} -H-I	45.8	P _{II} -T-I	20.1	P _{II} -T-I	32.3	P _{II} -T-I	0
	P _I -H-O	29.4	P _{II} -T-O	2.0	P _I -H-O	20.0	P _{II} -H-O	0
	P _{II} -H-O	26.2	P _I -H-O	1.6	P _{II} -H-O	14.1	P _{II} -H-O	0
	P _{II} -T-O	0	P _{II} -H-O	0.7	P _{II} -T-O	11.6	P _{II} -T-O	0
	P _I -T-O	0	P _I -T-O	0	P _I -T-O	0	P _I -T-O	0
Lower	P _I -H-O	60.8	P _I -H-O	55.0	P _{II} -H-O	8.0	P _{II} -T-O	4.7
	P _{II} -H-O	55.3	P _{II} -T-O	54.5	P _I -H-O	6.0	P _{II} -H-O	2.0
	P _I -H-I	40.3	P _I -T-O	24.4	P _{II} -T-O	2.8	P _I -H-O	0.9
	P _{II} -T-O	28.5	P _{II} -H-O	24.4	P _{II} -H-I	0	P _{II} -H-I	0.5
	P _{II} -H-I	26.8	P _I -T-I	3.7	P _I -T-I	0	P _I -T-I	0
	P _I -T-O	5.3	P _{II} -H-I	3.0	P _I -T-O	0	P _I -T-O	0
	P _I -T-I	2.0	P _{II} -T-I	1.4	P _I -H-I	0	P _I -H-I	0
	P _{II} -T-I	1.7	P _I -H-I	1.0	P _{II} -T-I	0	P _{II} -T-I	0

^{a,b} See footnotes in Table I.

square indicates a satisfactory retention of stationary phase for the two values of the studied parameter. The most important information is provided by the thick diagonal line that separates the diagram into two triangles. The data points located on or near the diagonal line indicate the studied effect has no influence on the retention of the stationary phase. The deviation of the point from that diagonal line indicates an effect of the studied parameter, whose relative magnitude is shown by the distance between the point and the diagonal line. Each graph contains 16 points corresponding to the four solvent systems and the four combinations between the two remaining factors. The points are numbered from 1 to 4 to show the solvent system used (see tables for identification).

Fig. 1A consists in a pair of graphs showing the retention of stationary phase with a column in the *L* position for P_{II} vs. P_I, for the upper (left) and the lower (right) phases used as mobile phase. Each point is displayed as a specific symbol, *i.e.*, open circle for the head-to-tail elution mode and solid circle for the tail-to-head mode with arrows indicating the inward elution mode if directed toward the right and the outward mode if directed toward the left. All the points are very close to the diagonal line with either the upper or the lower phase as a mobile phase. It demonstrates the direction of planetary motion P_I or P_{II} has little effect on the retention of stationary phase with the 5.5 cm diameter column. Fig. 1B also shows that no effect appears with the 10.0-cm diameter column as all

TABLE IV

RETENTION (%) OF STATIONARY PHASE IN 10.0-cm HELICAL DIAMETER COIL, X – 1.5L POSITION

Mobile phase	Solvent system ^a							
	1: 1-Butanol– 0.13 M NaCl (1:1) containing 1.5% (w/v) HPC		2: PEG 1000 12.5%, K ₂ HPO ₄ 12.5%		3: PEG 8000 4.4%, dextran T500 7.0%		4: PEG 8000 4.0%, dextran T500 5.0%	
	Condition ^b	%	Condition	%	Condition	%	Condition	%
Upper	P _I -T-I	81.7	P _I -T-I	37.3	P _I -T-I	34.1	P _I -T-I	0
	P _{II} -T-I	57.1	P _{II} -T-I	21.5	P _I -H-I	30.2	P _I -H-I	0
	P _{II} -H-I	40.2	P _{II} -H-O	14.1	P _{II} -T-I	20.5	P _{II} -T-I	0
	P _I -H-I	37.1	P _I -H-I	12.2	P _I -T-O	19.8	P _I -T-O	0
	P _{II} -H-O	26.8	P _I -T-O	11.7	P _{II} -T-O	14.1	P _{II} -T-O	0
	P _I -H-O	18.3	P _{II} -H-I	4.9	P _I -H-O	9.8	P _I -H-O	0
	P _I -T-O	4.9	P _I -H-O	0	P _{II} -H-I	8.5	P _{II} -H-I	0
	P _{II} -T-O	0	P _{II} -T-O	0	P _{II} -H-O	2.4	P _{II} -H-O	0
	Lower	P _I -H-O	60.5	P _{II} -H-O	41.5	P _{II} -H-O	3.4	P _{II} -H-O
P _{II} -H-O		46.8	P _I -H-O	31.2	P _I -H-O	0	P _I -H-O	0
P _I -H-I		44.9	P _I -H-I	28.3	P _I -H-I	0	P _I -H-I	0
P _{II} -T-O		30.5	P _I -T-O	19.5	P _I -T-O	0	P _I -T-O	0
P _{II} -H-I		20.7	P _{II} -H-I	8.8	P _{II} -H-I	0	P _{II} -H-I	0
P _I -T-O		6.3	P _{II} -T-I	3.9	P _{II} -T-I	0	P _{II} -T-I	0
P _{II} -T-I		3.7	P _{II} -T-O	3.4	P _{II} -T-O	0	P _{II} -T-O	0
P _I -T-I		2.4	P _I -T-I	0	P _I -T-I	0	P _I -T-I	0

^{a,b} See footnotes in Table I.

the points stay as close as they were for the smaller diameter. Fig. 2A shows the same lack of effect, except for the 1-butanol–0.13 M NaCl_{aq} (+HPC) system. Its retention of stationary phase is enhanced by the combination of the P_I planetary motion and the tail-to-head elution mode with the a mobile upper phase or the P_{II} planetary motion and the tail-to-head elution mode with a mobile lower phase, whatever the diameter may be. No effect is involved in the head-to-tail elution mode with the 5.5 cm diameter column, whereas the P_{II}-H (upper phase mobile) and P_I-H (lower phase mobile) combinations increase the retention of stationary phase with the 10.0 cm diameter.

All the points in Fig. 3A and B are close to the diagonal line. The head-to-tail or tail-to-head elution modes consequently have no effect on the retention of stationary phase with a column in the L position. Neither does Fig. 4A charac-

terize a real effect of the (H) or (T) elution modes. However, Fig. 4B illustrates a general effect of the head-to-tail or tail-to-head elution mode. With few exceptions, the combinations of upper phase mobile/tail-to-head and lower phase mobile/head-to-tail lead to the best retention of stationary phase in a 10.0-cm diameter column in the X – 1.5L position.

Fig. 5A and B show a strong effect of the inward/outward elution mode. All the points are located either below the diagonal line if the upper phase is mobile and above, if the lower phase is mobile. This indicates that for both diameters the best retention of stationary phase is obtained with the upper phase used as the mobile phase with the inward mode or the mobile lower phase with the outward mode. The same effects are shown on Fig. 6A and B. They are weaker compared to that shown for the L position. The stationary phase retention is thus

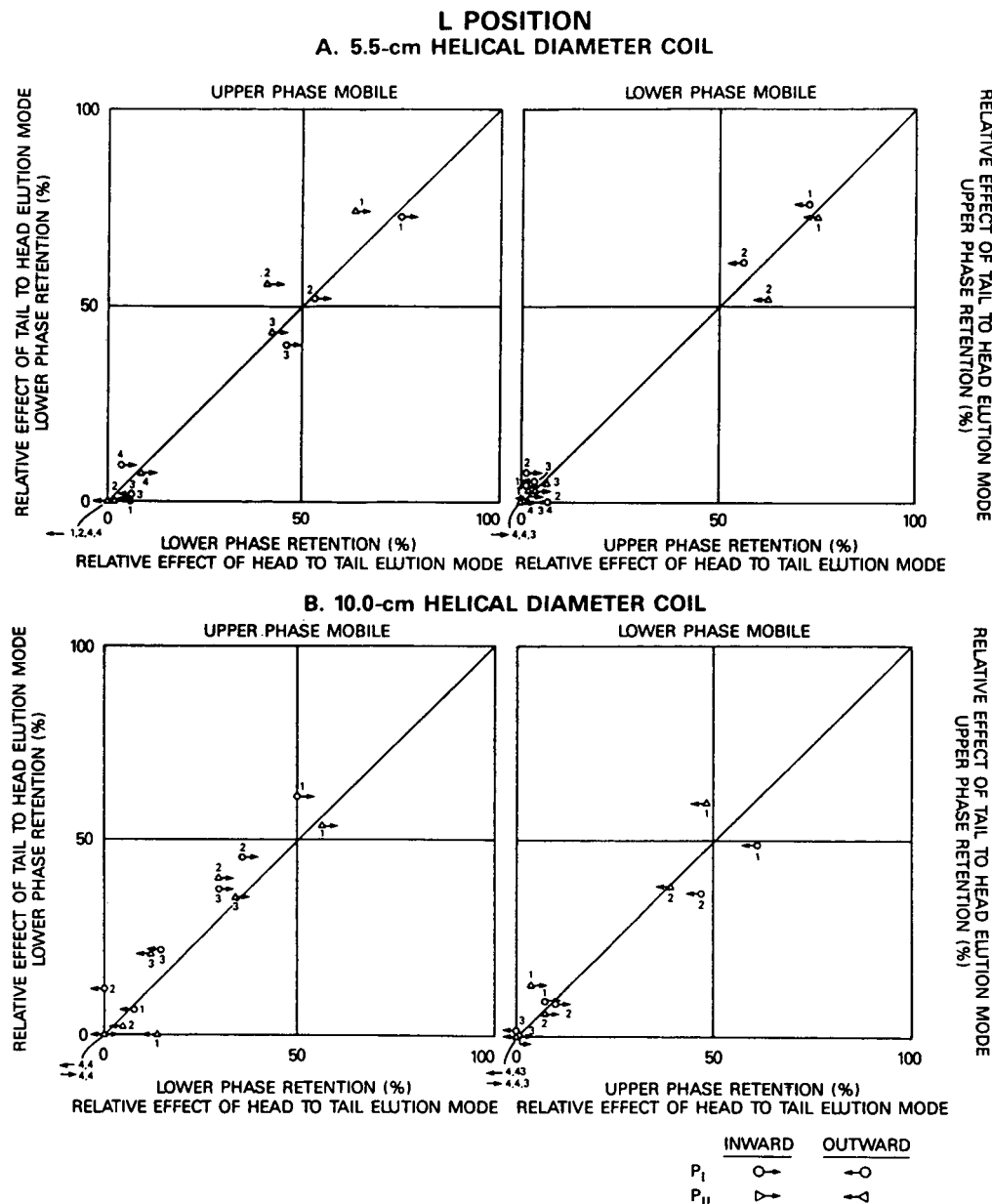


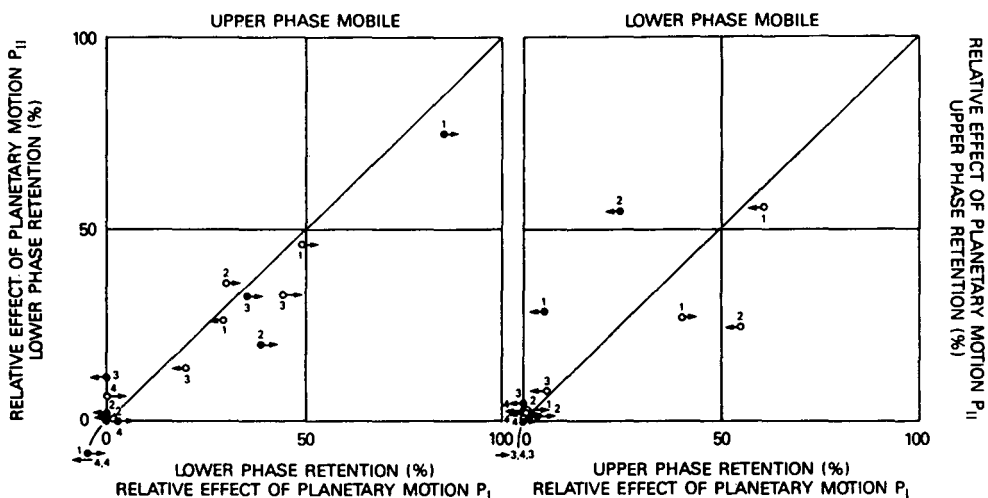
Fig. 1. *L* position: effects of planetary motion P_I and P_{II} on the retention of the stationary phase. (A) 5.5-cm helical diameter coil; (B) 10.0-cm helical diameter; left: upper phase mobile; right: lower phase mobile.

enhanced by the combinations of upper phase mobile/inward mode and lower phase mobile/outward mode, whatever the position and the diameter of the column.

Fig. 7 illustrates the influence of the column diameter. All the points with a retention of stationary phase higher than 20% are located

below the diagonal line for both upper and lower phases as mobile. The 5.5 cm diameter consequently enhances the retention of stationary phase for both *L* and $X - 1.5L$ positions. When the upper phase is chosen as mobile with the *L* position, the data points corresponding to at least 20% of retention have the arrows directed

X-1.5L POSITION
A. 5.5-cm HELICAL DIAMETER COIL



B. 10.0-cm HELICAL DIAMETER COIL

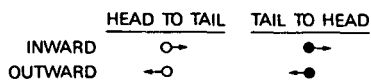
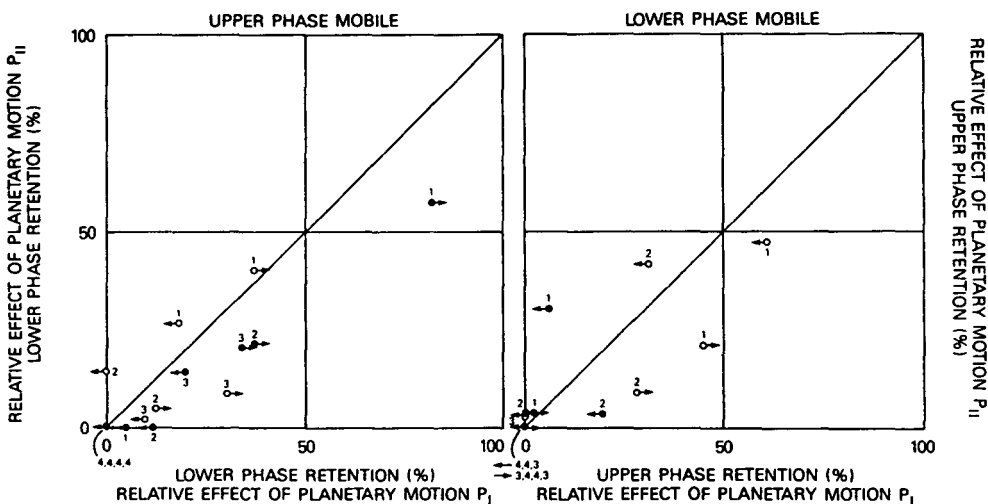


Fig. 2. $X-1.5L$ position: effects of planetary motion P_1 and P_{11} on the retention of the stationary phase. (A) 5.5-cm helical diameter coil; (B) 10.0-cm helical diameter; left: upper phase mobile; right: lower phase mobile.

toward the right. Sufficient retention of stationary lower phase is thus achieved with the inward elution mode, while the use of stationary upper phase profits by the outward elution mode. These observations are correlated with the conclusions derived from Fig. 5 illustrating the effects of the inward–outward elution mode. The

data points corresponding to the $X-1.5L$ position do not all show the same arrow direction, pointing out the weaker effect of the inward–outward elution mode for this position.

The above analysis shows the relative importance of all the factors studied and their possible interactions. The inward–outward factor is the

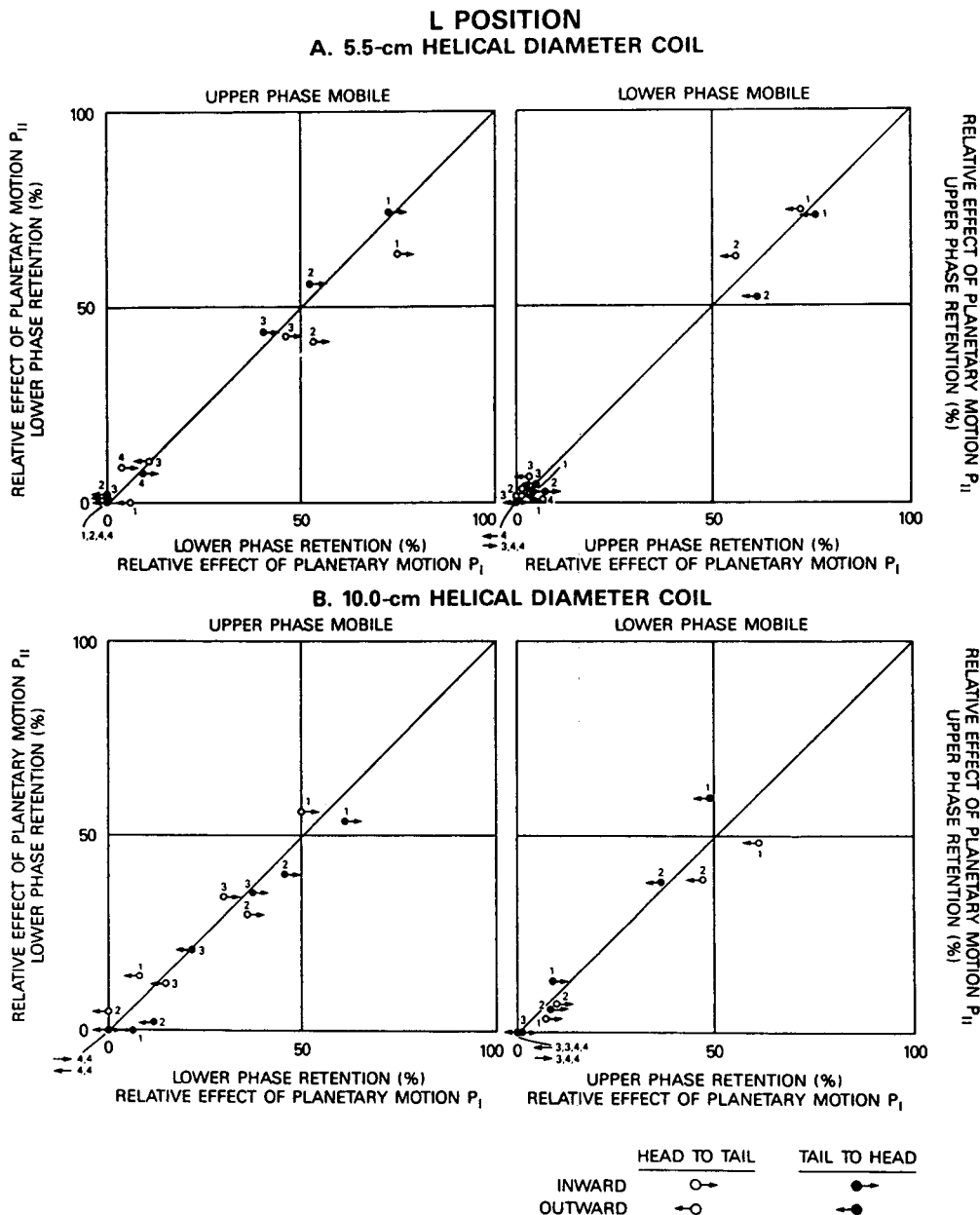


Fig. 3. *L* position: effects of the head–tail elution mode on the retention of the stationary phase. (A) 5.5-cm helical diameter coil; (B) 10.0-cm helical diameter; left: upper phase mobile; right: lower phase mobile.

strongest among those studied and it is correlated only with the choice of mobile phase to enhance the retention of stationary phase. For both diameters, *i.e.*, 5.5 cm and 10.0 cm, and for both positions, *i.e.*, *L* and $X - 1.5L$, the highest levels of retention of stationary phase are obtained with an upper mobile phase pumped in

the inward direction or a lower mobile phase pumped in the outward direction.

The diameter of the coil is also an important factor since the retention is increased by use of the 5.5 cm coil whatever the values of the other parameters. The head–tail elution modes and the direction of planetary motions P_I and P_{II}

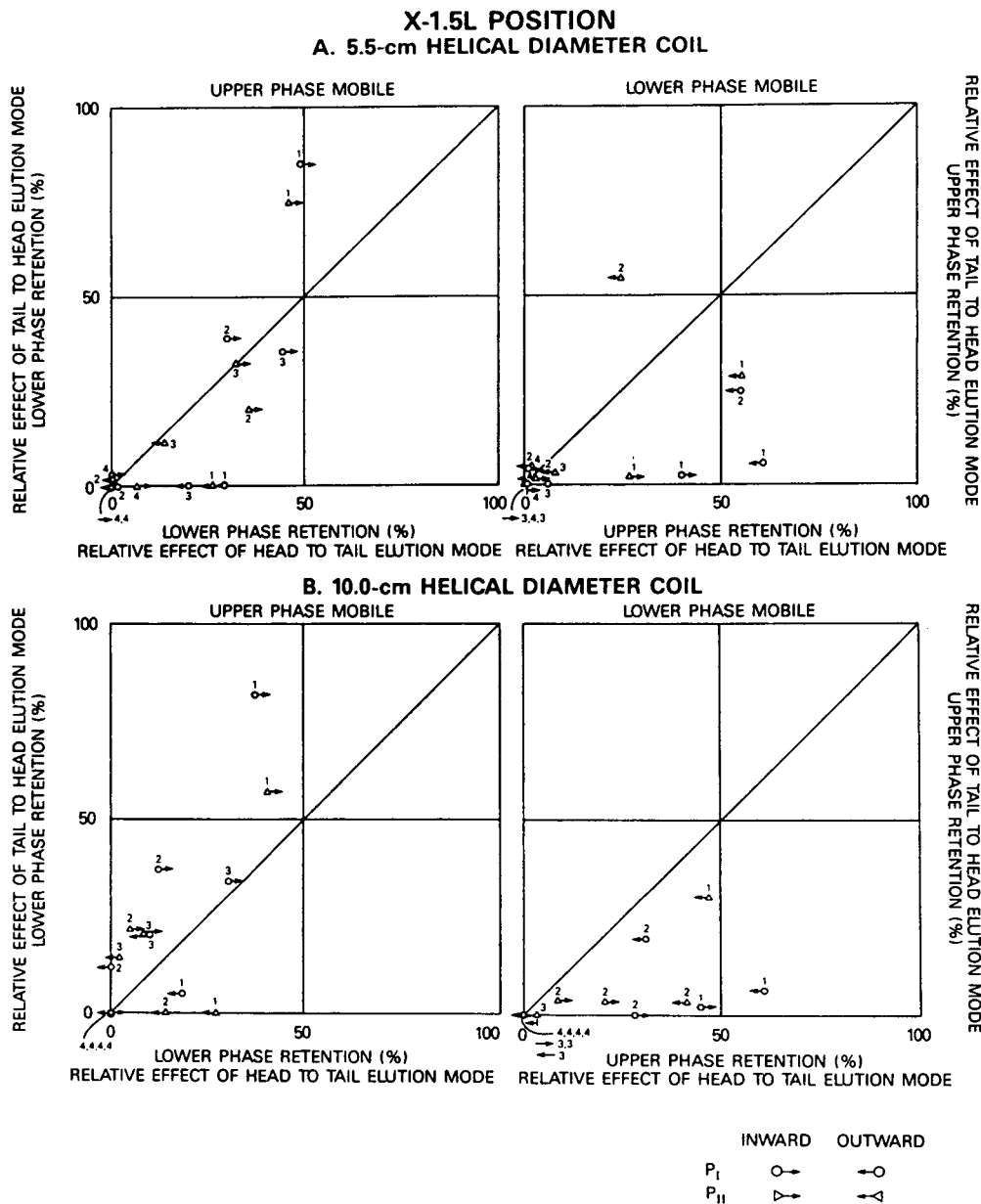


Fig. 4. $X-1.5L$ position: effects of the head–tail elution mode on the retention of the stationary phase. (A) 5.5-cm helical diameter coil; (B) 10.0-cm helical diameter; left: upper phase mobile; right: lower phase mobile.

have no effects with the L position. The head–tail factor has an effect only with the 10.0 cm coil in the $X-1.5L$ position: the best combinations are the mobile upper phase pumped in the tail-to-head mode or the mobile lower phase in the head-to-tail mode. The direction of planetary motion has an even more restricted effect as it

applies only to the 1-butanol–0.13 M $NaCl_{aq}$ (+HPC) system with the $X-1.5L$ position of the coil. When the upper phase is mobile, the P_I -T for 5.5 cm diameter and the P_I -T and P_{II} -H for 10.0 cm lead to the best retention of stationary phase. For the lower phase mobile, the P_{II} -T for 5.5 cm diameter and P_{II} -T and P_I -H for 10.0

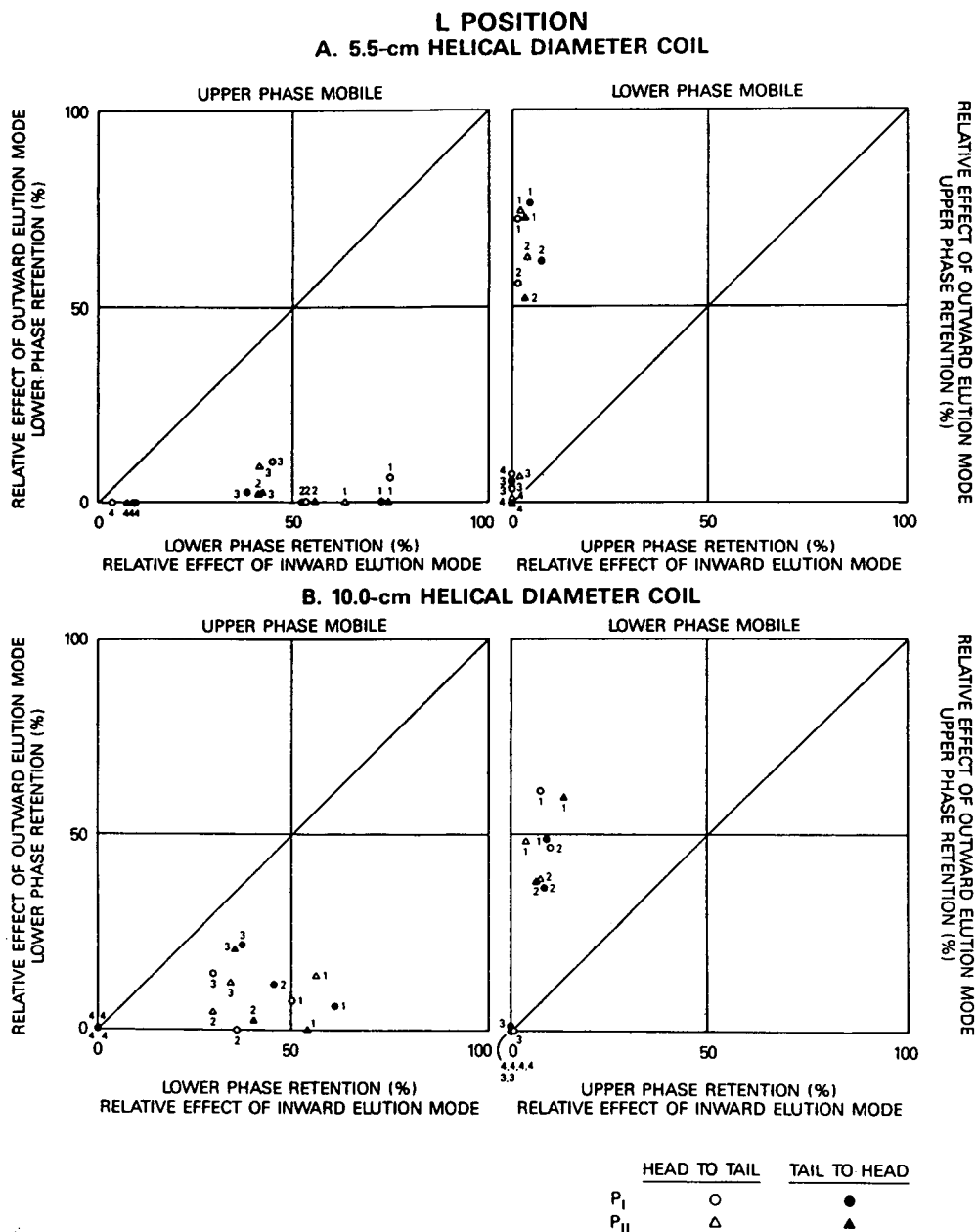
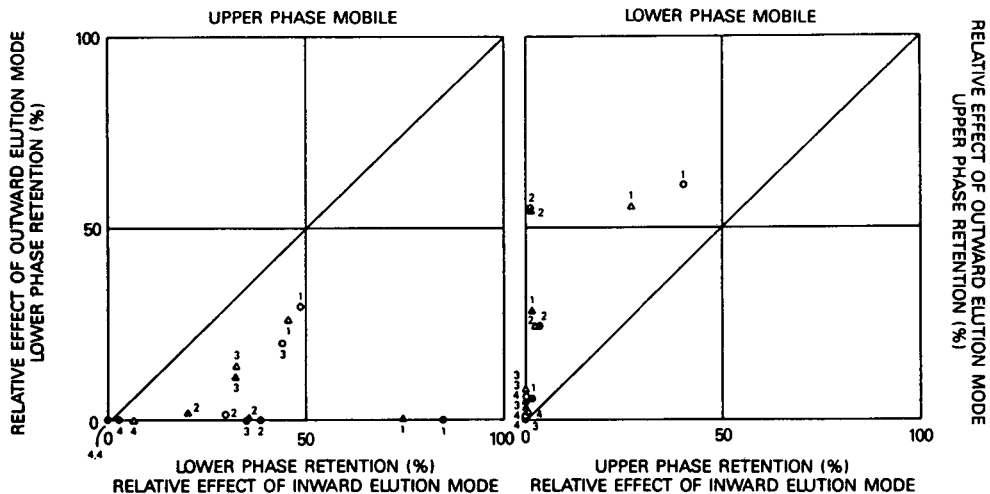


Fig. 5. *L* position: effects of the inward–outward elution mode on the retention of the stationary phase. (A) 5.5-cm helical diameter coil; (B) 10.0-cm helical diameter; left: upper phase mobile; right: lower phase mobile.

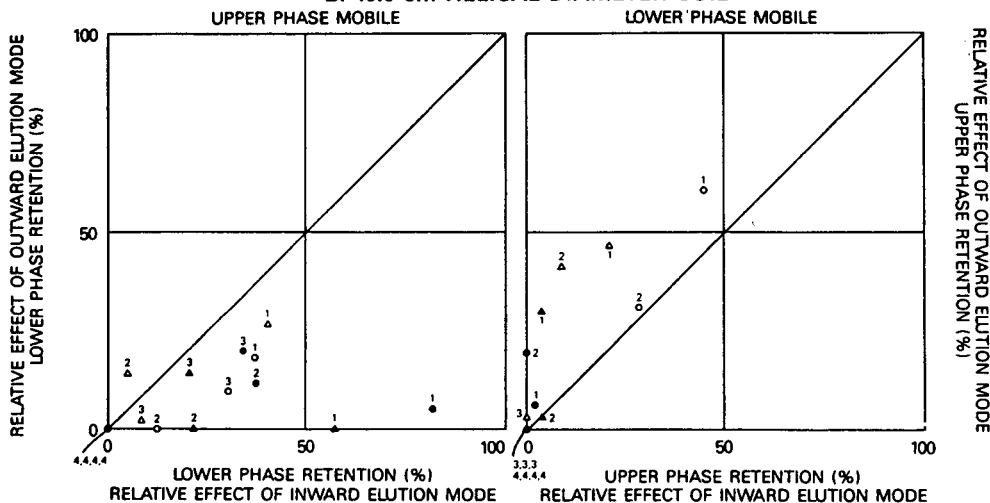
cm enhance the retention. The effect of the coil position was not studied but the overall retention measurements suggest that its influence is very small with the 5.5 cm diameter while the *L* position enhances retention for the 10.0 cm diameter.

Consequently, to achieve the highest retention of stationary phase, the three aqueous–aqueous two-phase polymer systems (numbered 2, 3 and 4) require the 5.5-cm coil with the mobile upper phase pumped inward or the mobile lower phase

X-1.5L POSITION
A. 5.5-cm HELICAL DIAMETER COIL



B. 10.0-cm HELICAL DIAMETER COIL



	<u>HEAD TO TAIL</u>	<u>TAIL TO HEAD</u>
P _I	○	●
P _{II}	△	▲

Fig. 6. X-1.5L position: effects of the inward-outward elution mode on the retention of the stationary phase. (A) 5.5-cm helical diameter coil; (B) 10.0-cm helical diameter; left: upper phase mobile; right: lower phase mobile.

pumped outward with either the *L* or *X-1.5L* coil positions. For the first solvent system, made of an organic solvent mixed with an aqueous phase, the *L* position requires the same combinations as with the other solvent systems. However, the *X-1.5L* position requires

more precise combinations: P_I-T-I for the upper phase as mobile and P_{II}-T-O for the lower phase as mobile with a 5.5-cm diameter coil.

These results are correlated with those previously obtained with a type X-LL cross-axis CPC

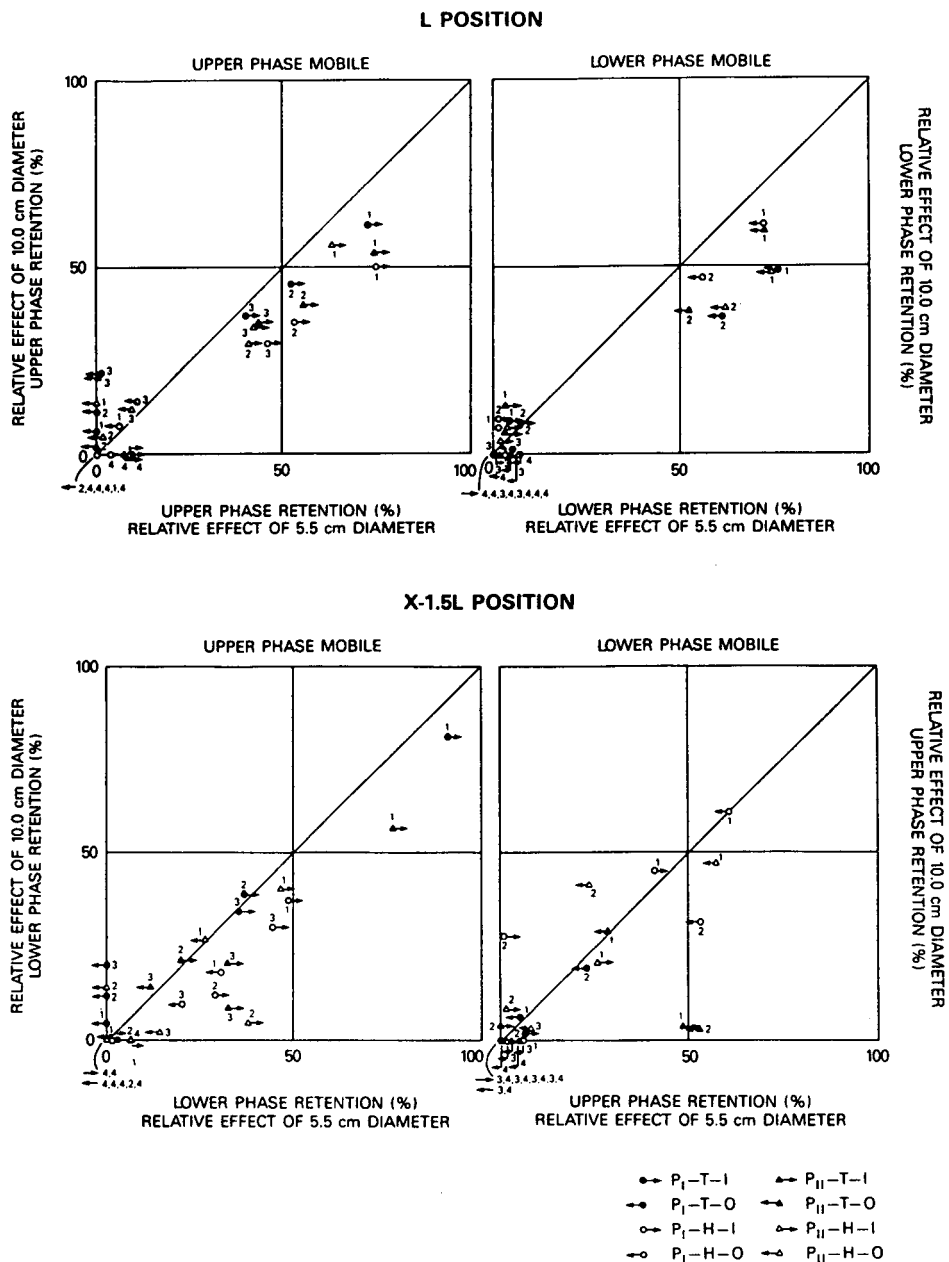


Fig. 7. Effects of the helical coil diameters with L and $X-1.5L$ positions on the retention of the stationary phase; left: upper phase mobile; right: lower phase mobile.

[4,5]. There it was concluded that the highest retention of stationary phase is obtained with the upper phase as mobile and the P_I -T-I and P_{II} -H-I combination or with the lower phase as mobile and the P_{II} -T-O and P_I -H-O combination. These results are similar to the requirements obtained

with the 1-butanol-0.13 M NaCl_{aq} (+HPC) system with the $X-1.5L$ position, except they allow the choice of two combinations instead of one when the mobile phase is chosen. For the aqueous-aqueous polymer systems (not studied on the previous X-LL prototype), the require-

ments are shared with these for organic/aqueous systems between the two cross-axis prototypes but are less precise. Consequently, the head–tail elution mode and the direction of planetary motion show no effect with aqueous–aqueous polymer two-phase systems while they have an influence on organic–aqueous two-phase systems.

SPECULATION ON THE HYDRODYNAMIC MECHANISM

Fig. 8 is intended to explain the strong correlation between the inward–outward elution mode and the choice of the mobile phase. When the lighter phase is mobile, the best retention of stationary phase is achieved with the inward elution mode, *i.e.*, from the outside end to the inside end of the column. Such a behavior is explained in Fig. 8. The descriptive model is highly simplified: it assumes the two phases are completely separated along the column, the heavier one accumulating toward the outside end of the column, pushing the lighter phase toward

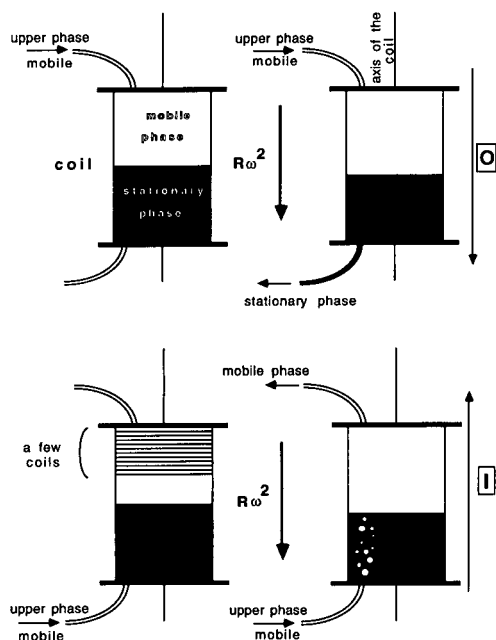


Fig. 8. Influence of the inward–outward elution mode on the retention of the heavier stationary phase inside a coil.

the inside end of the column. This model should be close to actual behavior inside columns in the L position since the head–tail elution mode has no effect. It could also be applied to the $X-1.5L$ position as far as aqueous–aqueous polymer two-phase solvent systems are considered, where no head–tail effect is involved. In the first case, the mobile phase is pumped in the outward mode. The small volumes of lighter phase continuously brought inside the column can not go through the heavier phase because they would migrate against centrifugal forces exerted in the heavier phase. Consequently, small amounts of the heavier phase are expelled from the column. In the other case, the lighter phase is introduced at the outside end of the column. The small volume of this phase continuously introduced in the column goes through the heavier phase due to a motion induced by the centrifugal forces inside the latter. As a result, the inward elution mode for the lighter mobile phase leads to better retention of the heavier stationary phase as observed in all of the experiments. However, the outward elution mode for the lighter mobile phase is able to provide a good retention of the stationary phase for some cases [*e.g.*, 1-butanol–0.13 M NaCl_{aq} (+HPC) system in the 5.5-cm coil in the $X-1.5L$ position and the P_1 -T-O mode, leading to 30% of retention]. At least two explanations are available. One is that the column is made of many coils slowing the leakage of heavier phase in the first case and possibly allowing the lighter phase to go through the heavier one. The second possibility is that the model may not apply as well to the coil in the $X-1.5L$ position: the head–tail elution mode intervenes for the 1-butanol–0.13 M NaCl_{aq} (+HPC) system. Consequently, the Archimedes' screw force may interact with the centrifugal force in the model, leading to lack of separation of the phases along the column. Such a simplified model also applies to a mobile heavier phase and a stationary lighter one. When the Archimedes' screw force appears to be small, as for coils in the L position, the model is more applicable and indeed, no reliable exceptions are shown in Tables I and II.

An analysis of the paths and the accelerations induced by cross-axis CPCs was performed in

Part II [2]. All of the parametric equations were used to plot the paths and forces induced by a column in the L and $X - 1.5L$ positions. The results showed that the paths are very similar for both coil positions: they appear as a circular path with a small deformation out of the rotation plane. The induced forces were separated into two perpendicular components relative to the tube of the coil, one in the plane of the coil, the other perpendicular to that plane and in one tangential component, in the plane of the coil. The relative importance of the tangential force over the two combined perpendicular forces was then studied for the cross-axis prototype with the L and $X - 1.5L$ coil positions. Using the column in the L position, the tangential force inside the column compared to the added perpendicular forces represents up to 16.5% with the 10.0-cm diameter and up to 9% with the 5.5-cm diameter. For the column in the $X - 1.5L$ position, this tangential force represents up to 90% with the small diameter and up to 125% with the large diameter of the combined perpendicular force. Such values explain the influence of the coil diameter. According to Fig. 7, the 5.5-cm coil diameter enhances retention of the stationary phase for both L and $X - 1.5L$ positions. This can be correlated with the relative influence of the lateral force for each position; when the diameter is increased from 5.5 cm to 10.0 cm, the lateral force is increased in value compared to the perpendicular forces. Consequently, the role of the latter is lowered; as they take part to the retention of the phases inside the column,

the retention of the stationary phase decreases. However, this explanation cannot be applied between two coil positions as they induce different force field geometries. For instance, the first solvent system can be retained up to 76% in a 5.5 cm diameter coil in the L position and up to 85% with the same coil in the $X - 1.5L$ position while the relative influence of the tangential force are 9% and 90%, respectively. One reason for this effect could be the greater role of the unilateral distribution tendency [6,7] involved with the $X - 1.5L$ position as shown by the influence of the head-to-tail or tail-to-head elution mode.

However as this tendency is not understood, a precise explanation on the effects of all the studied factors may be available only after a thorough mathematical analysis of the results [8]. Other experiments must be studied with the same solvent systems previously used on the X-LL cross-axis prototype [4].

REFERENCES

- 1 K. Shinomiya, J.-M. Menet, H.M. Fales and Y. Ito, *J. Chromatogr.*, 644 (1993) 215.
- 2 J.-M. Menet and Y. Ito, *J. Chromatogr.*, 644 (1993) 231.
- 3 G.E. Box, W.G. Hunter and J.S. Hunter, *Statistics for Experimenters*, Wiley, New York, 1978.
- 4 Y. Ito, *J. Chromatogr.*, 538 (1991) 67.
- 5 Y. Ito, E. Kitazume, M. Bhatnagar and F. Trimble, *J. Chromatogr.*, 538 (1991) 59.
- 6 Y. Ito, *J. Chromatogr.*, 207 (1981) 161.
- 7 Y. Ito, *J. Liq. Chromatogr.*, 11 (1988) 1.
- 8 J.-M. Menet, J. Goupy, K. Shinomiya and Y. Ito, in preparation.

Rapid group-type analysis of crude oils using high-performance liquid chromatography and gas chromatography

Mohammed Shahid Akhlaq

Institut für Erdölforschung, Walther-Nernst-Strasse 7, W-38678 Clausthal-Zellerfeld (Germany)

(First received October 13th, 1992; revised manuscript received February 11th, 1993)

ABSTRACT

A simple, effective and rapid high-performance liquid chromatographic (HPLC) method was developed for the separation of crude oils into different group types. The method can be used to separate crude oils, kerosenes, gasolines, middle distillates, fuel oils, etc., into various classes of aliphatics (such as straight-chain, branched and cyclic), one-, two- and three-ring aromatics, polar compounds, resins and asphaltenes. A discussion of the experimental details and data from several samples is presented.

INTRODUCTION

Group-type analysis of a given mixture is useful, because often the separation of all the compounds is not necessary and may be impracticable [1–3]. For the mineral oil industry and for research purposes it is very important to know the different group types in a given crude oil, which will contain different amounts of aliphatics, naphthenes, aromatics, naphthenoaromatics, heteroaromatics, polar compounds and colloids [4]. Efforts are made to determine all of these groups quantitatively. Doing this has following advantages: (1) with the crude oil characterization one can determine its quality and can adjust the process conditions; (2) with the knowledge of the starting material, the yield, structure and quality of the final products can be established; and (3) separation into group types can be used as pre-separation for further investigations to determine structures using HPLC, GC and mass and nuclear magnetic resonance spectrometry.

For this reason it is important to establish economical methods to characterize crude oils

more rapidly. Several HPLC methods [5–9] have been reported. The aliphatics are separated by HPLC and the remaining fractions are isolated as aromatics and polar compounds with back-flushing [6,10]. It takes about 200 min to separate a crude oil into five fractions [11]. Quantitative analyses of these fractions are carried out gravimetrically, which is very time consuming.

EXPERIMENTAL

Solvents and chemicals

The solvents used were distilled *n*-hexane and chloroform (Riedel-de Haën). Standard model compounds were purchased from Aldrich and were used as received. The crude oils used were Suria, Shingli, Matrum, Jakarta Arco and Scheerhorn oil.

Instrumentation

The HPLC system consisted of two pumps (Model 510), a UV detector (Model 484) and an RI detector (Model 410) (all from Millipore, Waters Chromatographie). Maxima 820 chromatography workstation software (Millipore, Wa-

ters Chromatographie) controlled the total HPLC instrument. A high-pressure gradient system and an electronic backflush valve were used. The gradient system is shown in Table I. The three columns used were μ Bondapak-NH₂ (Millipore, Waters Chromatographie) (300 mm \times 3.9 mm I.D.) with a particle size of 10 μ m, connected in series.

The gas chromatograph system was a Hewlett-Packard Model 5980 Series II, with flame ionization (FID) and thermal conductivity detection (TCD). A fused-silica (DB-5) capillary GC column (30 m \times 0.25 mm I.D., 0.25 μ m film thickness) was obtained from J&W Scientific. The GC oven was held 35°C for 5 min and then programmed at 5°C/min to a final temperature of 310°C, which was maintained for 10 min. A split-splitless injector was used in the split mode with a splitting ratio of 50 for all fractions.

Quantification

The relative percentages derived for each fraction required quantification by both HPLC and GC. We used an RI detector for HPLC

TABLE I

HPLC GRADIENT SYSTEM (LINEAR) FOR CRUDE OIL SEPARATION

Columns, 3 \times amino phase (300 mm \times 3.9 mm I.D.) connected in series. Mobile phase A = *n*-hexane; mobile phase B = chloroform.

Time (min)	Mobile phase		Flow-rate (ml/min)
	A (%)	B (%)	
Start	100	0	1.4
10	100	0	1.4
12	100	0	4.0
20	100	0	4.0
	Backflush		
24	90	10	4.0
32	90	10	4.0
35	50	50	2.0
60	50	50	2.0
	Re-equilibration		
75	100	0	3.0
85	100	0	3.0
90	100	0	1.4
100	100	0	1.4

because it responds to both aliphatic and aromatic compounds, whereas a UV detector will not respond to non-aromatics without an active chromophore. For the quantification of aliphatics, GC was used because it gives more reproducible results. For the GC calibration, all of the compounds in Table III were used. The response factor of the branched and cyclic aliphatics was assumed to be the same as for the corresponding normal aliphatics. To calibrate the HPLC one-ring aromatic fraction a mixture of ethylbenzene, *p*-isopropyltoluene and 1,3,5-trimethylbenzene (1:1:1, w/w/w) was used. The two-ring aromatic fraction was calibrated with naphthalene and 2-methylnaphthalene (1:1, w/w), the three-ring fraction with anthracene and phenanthrene (1:1, w/w) and the four-ring fraction with pyrene. Standard compounds for the polar and colloid fractions were not available, so these fractions were collected and the amounts of the substances present were determined gravimetrically after drying. With these amounts, the response factors were determined and accuracy was checked (Error <3%) with five different crude oils.

The HPLC or GC area counts for each fraction were multiplied by the average response factors obtained to give the relative amount of each fraction present.

RESULTS

The major problem in the analysis of crude oil is the complexity of this natural mixture, containing hundreds of different aliphatic and aromatic components [12,13]. The aliphatics consist of linear *n*-alkanes, branched-chain alkanes and cycloalkanes, while the major aromatic components are one-, two-, three- and four-ring alkylated derivatives [13]. In addition, crude oil also contains polar compounds, resins and asphaltene [11]. Most often it is useful to separate this mixture in group types. Because crude oil contains compounds from those with very low polarity such as aliphatics and naphthenes to very polar compounds such as acids and colloids, they cannot be separated and identified on one column. We used a backflush technique and

achieved the separation of crude oil into seven different fractions within 60 min.

Because in each fraction compounds with different chain lengths and substitution are present, we first investigated the chromatographic behaviour of some standard compounds. It has often been reported that the long-chain alkyl-substituted aromatics behave in chromatography like alkanes and no longer like aromatics [11]. Table II shows clearly that with the use of above method the separations of differently substituted benzene compounds occur in a very close elution range, but the pure alkane compounds separate earlier (Table III).

A standard mixture of 60 different compounds containing aliphatics (*n*-alkanes, isoalkanes and cycloalkanes), monoaromatics, diaromatics and poly- and heterocyclic compounds were selected to optimize the separation procedure. The components and their concentrations in the standard mixture were selected so as to simulate the complex chemical composition of crude oil. The separation tests carried out helped to develop and improve the analytical method.

First we investigated the 24 straight-chain compounds from C₇ to C₃₄, three branched and

TABLE II
HPLC RETENTION TIMES OF MONOAROMATIC MODEL COMPOUNDS

Substance	No. of substituents	No. of carbon atoms	Retention time (min)
Benzene	0	6	8.57
Toluene	1	7	8.67
Ethylbenzene	1	8	8.67
Hexylbenzene	1	12	8.42
Dodecylbenzene	1	18	8.23
Octadecylbenzene	1	24	8.10
<i>o</i> -Xylene	2	8	8.93
<i>m</i> -Xylene	2	8	8.93
<i>p</i> -Xylene	2	8	8.91
<i>p</i> -Ethyltoluene	2	9	8.87
<i>p</i> -Isopropyltoluene	2	10	8.86
1,3,5-Trimethylbenzene	3	9	8.96
Tetralin	–	10	9.03

TABLE III
HPLC RETENTION TIMES OF STRAIGHT-CHAIN, BRANCHED-CHAIN AND CYCLIC ALIPHATIC MODEL COMPOUNDS

Substance	No. of carbon atoms	Retention time (min)
Cyclohexane	6	7.03
<i>n</i> -Heptane	7	7.04
Cycloheptane	7	7.03
<i>n</i> -Octane	8	7.05
Isooctane	8	7.02
Cyclooctane	8	7.04
<i>n</i> -Nonane	9	7.06
<i>n</i> -Decane	10	7.06
<i>n</i> -Undecane	11	7.07
<i>n</i> -Dodecane	12	7.07
<i>n</i> -Tridecane	13	7.08
<i>n</i> -Tetradecane	14	7.09
<i>n</i> -Pentadecane	15	7.09
<i>n</i> -Hexadecane	16	7.11
<i>n</i> -Heptadecane	17	7.12
<i>n</i> -Octadecane	18	7.12
<i>n</i> -Nonadecane	19	7.13
Pristane	19	7.12
<i>n</i> -Eicosane	20	7.14
Phytane	20	7.12
<i>n</i> -Heneicosane	21	7.15
<i>n</i> -Docosane	22	7.16
<i>n</i> -Tricosane	23	7.18
<i>n</i> -Tetracosane	24	7.19
<i>n</i> -Pentacosane	25	7.21
<i>n</i> -Hexacosane	26	7.22
<i>n</i> -Octacosane	28	7.23
<i>n</i> -Triacontane	30	7.25
<i>n</i> -Dotriacontane	32	7.26
<i>n</i> -Tetracontane	34	7.28

three cyclic alkanes. Table III shows the retention times of all these compounds, which are very close ($\Delta t = 0.3$ min). As expected, the long straight-chain aliphatics elute slightly later than the short-chain aliphatics. Further, the branched-chain aliphatics separate slightly earlier than the corresponding straight-chain compounds (see octane, nonadecane and eicosane in Table III). Nevertheless, all these compounds elute very close to each other.

Better resolution of the aliphatic fraction can be achieved by GC [14–16]. A gas chromatogram of the aliphatic fraction is shown in Fig. 1.

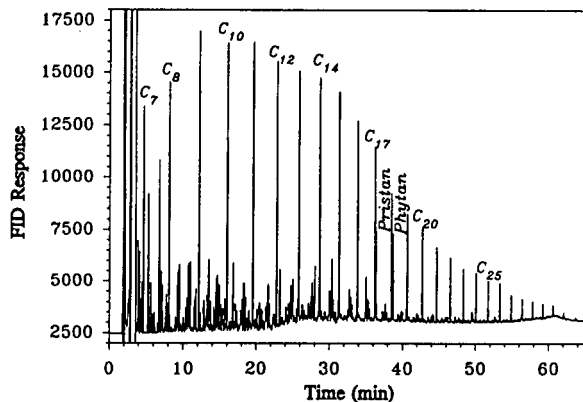


Fig. 1. Capillary gas chromatogram of the aliphatic fraction of a crude oil. Solvent, dichloromethane. A 1- μ l volume of the solution was injected in the split mode. GC conditions are given in the text.

The straight-chain compounds are separated very well, along with the branched and cyclic compounds.

Crude oils contain many different substituted benzenes. For this reason we investigated thirteen different one-ring aromatics individually. The HPLC results are given in Table II. There is a noticeable substituent dependence of the retention time. Up to a propyl substituent single and multiple substitution causes longer retention times whereas longer chains [8], such as hexyl, give short retention times.

The two-, three- and four-ring aromatic compounds are listed together with their retention times in Table IV. The compound classes are very well separated. It is noticeable that the condensed compounds need more time to elute from the column (see naphthalene and biphenyl and also anthracene and triphenylmethane). The aromatic sulphur and oxygen heterocyclic compounds are eluted as expected with the corresponding aromatic fraction. Quantification of the heterocyclic compounds is not possible because they are not well separated from the corresponding aromatic fraction. They are treated as aromatics.

We did not make any attempt to separate aromatics with more than four-ring systems, because these compounds are not expected to be present in high concentrations in crude oils (<1%). These components are eluted together

TABLE IV

HPLC RETENTION TIME OF TWO-, THREE- AND FOUR-RING AROMATIC MODEL COMPOUNDS

Substance	No. of aromatic rings	No. of carbon atoms	Retention time (min)
Naphthalene	2	10	11.82
2-Methylnaphthalene	2	11	11.95
3-Methylnaphthalene	2	11	12.03
Biphenyl	2	12	11.78
Bibenzyl	2	14	12.31
Xanthene	2	13	13.25
Dibenzothiophene	2	12	14.09
Anthracene	3	14	16.06
Phenanthrene	3	14	15.39
Triphenylmethane	3	19	15.28
Pyrene	4	16	19.67

with polar compounds in the backflush fraction. NH-, SH- and OH-substituted compounds are very polar and for this reason they eluted after the backflushing of the column. Resins and asphaltens are also eluted in the backflush fraction, but with a mobile phase containing 50% chloroform.

This method was used to separate and characterize different crude oils. Fig. 2 shows a reproducibility test with different amounts of crude oil injected. The peaks were characterized quantita-

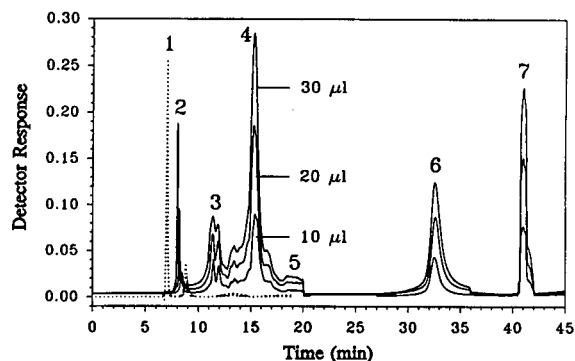


Fig. 2. HPLC of a crude oil dissolved in chloroform and filtered with a 0.25- μ m filter. Volumes of 10, 20 and 30 μ l of the crude oil solution were injected. Peaks: 1 = alkanes; 2 = one-ring aromatics; 3 = two-ring aromatics; 4 = three-ring aromatics; 5 = four-ring aromatics; 6 = polar compounds (NH-, SH-, OH-substituted compounds); 7 = colloids (asphaltens and resins). HPLC conditions are given in the text. Solid lines, UV detection (254 nm); dotted line, RI detection.

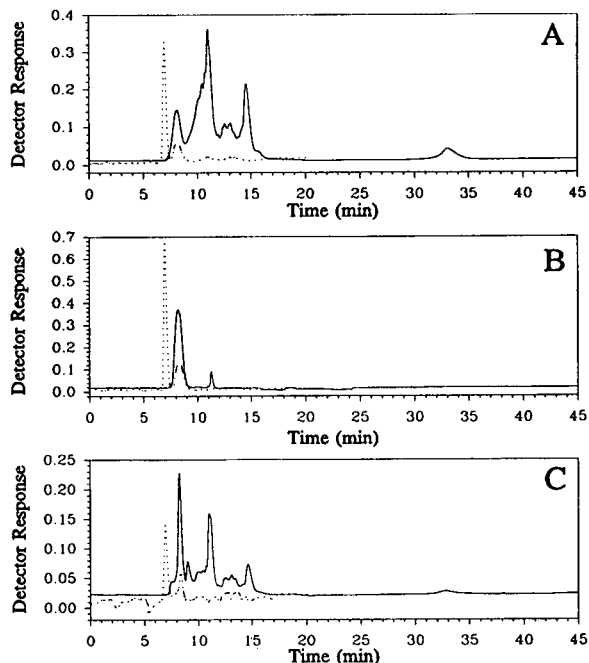


Fig. 3. HPLC of (A) diesel fuel, (B) petroleum fraction with b.p. <190°C and (C) middle distillate. A 1- μ l volume of the undiluted fuel was injected. HPLC conditions are given in the text. Solid lines, UV detection (254 nm); dotted lines, RI detection.

tively with integration and the use of response factors. Fig. 3 shows chromatograms of (A) diesel fuel, (B) a petroleum fraction with b.p.

<190°C and (C) a middle distillate. All these chromatograms show the same group-type separation as in Fig. 2 for crude oil except for the colloid-fraction. Colloids are not present in gasolines, kerosenes, middle distillates and fuel oils.

All the crude oil fractions from Fig. 2 were quantified and their relative percentages are given in Table V. We compared the results with those obtained using other methods, such as chemical separation with solvents [17] (ethyl acetate, pentane and toluene) and with column chromatography [18–20]. The results agreed very well with the classical methods, to within 10%.

CONCLUSIONS

The method described allows the separation of crude oil, fuel oil and middle distillate in their group types within 60 min. With this method one can characterize the samples quickly and without great expenditure. It is also possible to collect each fraction and effect a separation by HPLC or GC [21] (see Fig. 1), and to characterize them by infrared or NMR spectrometry or GC-MS.

Quantification of the fractions is done by integration of the corresponding peaks and using the response factors. This method is much more convenient and accurate than gravimetric meth-

TABLE V

RELATIVE QUANTITATIVE COMPOSITION (%) OF A CRUDE OIL DETERMINED USING THE HPLC METHOD AND DATA OBTAINED FROM CHEMICAL SEPARATION WITH SOLVENTS (ETHYL ACETATE, PENTANE AND TOLUENE) AND BY COLUMN CHROMATOGRAPHY (SEE TEXT)

Crude oil fraction	HPLC/GC	Chemical separation	Column chromatography
Low-boiling fraction	–	6.8	6.8
Naphthenic and paraffinic fraction	16.9	–	15.3
One-ring aromatics	54.4	–	–
Two-ring aromatics	2.2	–	44.7
Three-ring aromatics	0.4	–	–
Four-ring aromatics	0.4	–	–
Polar compounds	3.0	–	3.2
Disperse medium	–	66.3	–
Colloids (asphaltenes and resins)	24.1	27.4	25.6
Insoluble residue	2.3	–	1.9
Total %	103.7	100.5	97.5

ods, because with the latter one has to eliminate the eluent first. Quantitative elimination of the eluent is difficult and it is possible to lose some of the compounds from the one- and two-ring aromatic fractions in the drying process. .

REFERENCES

- 1 N.G. Johannsen, L.S. Ettre and R.L. Miller, *J. Chromatogr.*, 256 (1983) 393.
- 2 R.L. Miller, L.S. Ettre and N.G. Johannsen, *J. Chromatogr.*, 264 (1983) 19.
- 3 H. Engelhardt, *Erdöl Kohle Erdgas Petrochem.*, 30 (1977) 405–411.
- 4 M.S. Akhlaq, in *11. Königsteiner Chromatographietage*, GIT Verlag, Darmstadt, 1991, pp. 392–397.
- 5 S.C. Lamey, P.A. Hesbach and K.D. White, *Energy Fuels*, 5 (1991) 222–226.
- 6 J.C. Suatoni, H.R. Garber and B.E. Davis, *J. Chromatogr. Sci.*, 13 (1975) 367–371.
- 7 J.C. Suatoni and H.R. Garber, *J. Chromatogr. Sci.*, 14 (1976) 546–548.
- 8 P.L. Grizzle and J.S. Thomson, *Anal. Chem.*, 54 (1982) 1071–1078.
- 9 N.J. Tate, in G.B. Crump (Editor), *Petroanalysis '81*, Wiley, Chichester, 1982, pp. 268–284.
- 10 C.E. Östman and A.L. Colmsjö, *Fuel*, 68 (1989) 1248–1250.
- 11 A. Hollerbach, V. Meyn, G. Pusch, C. Kayser, D. Kessel, R. Meyn and I. Swaid, *DGMK-Ber.*, 202–4/2 (1989) 29–32.
- 12 I.L. Davies, K.D. Bartle, P.T. Williams and G.E. Andrews, *Anal. Chem.*, 60 (1988) 204–209.
- 13 J. Bundt, W. Herbel, H. Steinhart, S. Franke and W. Francke, *J. High Resolut. Chromatogr.*, 14 (1991) 91–97.
- 14 J.A. Appfel and H. McNair, *J. Chromatogr.*, 279 (1983) 139–144.
- 15 I.L. Davies, K.D. Bartle, G.A. Andrews and P.T. Williams, *J. Chromatogr. Sci.*, 26 (1988) 125–130.
- 16 F. Munari, A. Trisciani, G. Mapelli, S. Trestianu, K. Grob, Jr., and J.M. Colin, *J. High Resolut. Chromatogr. Chromatogr. Commun.*, 8 (1985) 601–606.
- 17 J. Wilkens and H.J. Neumann, *Bitumen Teere Asphalte Peche*, 25 (1974) 246–247.
- 18 H.H. Oelert and H.J. Neumann, *Erdöl Kohle Erdgas Petrochem.*, 29 (1976) 309.
- 19 H.H. Oelert and H.J. Neumann, *DGMK-Ber.*, 4508 (1974) 1–50.
- 20 F.P. Burke, R.A. Winschel and D.L. Wooton, *Fuel*, 58 (1979) 539–541.
- 21 M.S. Akhlaq, *J. Chromatogr.*, in preparation.

Reversed-phase high-performance liquid chromatography and chemometrics, a combined investigation tool for complex phytochemical problems

C. Baiocchi*, E. Marengo, G. Saini, M.A. Roggero and D. Giacosa

Dipartimento di Chimica Analitica, Università di Torino, Via P. Giuria 5, 10125 Turin (Italy)

(First received January 6th, 1993; revised manuscript received April 13th, 1993)

ABSTRACT

The phenolic content in the bark of poplar trees was analysed by RP-HPLC with the aim of finding some evidence of a relationship between the presence of phenols (either the total amount or the amount of an individual specific compound) and the differential resistance to the fungus *Dothichiza populea* that is found in different clones of these trees. Direct comparison of chromatographic results did not allow any useful information to be gleaned on this subject. On the other hand, the application of principal component analysis and linear discriminant analysis methods to the quantitative chromatographic data gave very promising results, allowing discrimination between resistant and susceptible poplars and the identification of phenolic compounds that are important for such discrimination.

INTRODUCTION

A connection between the resistance of poplar trees to infection by the fungus *Dothichiza populea* and the presence in their bark of some phenolic compounds providing a fungistatic activity has already been found [1–3].

The aim of this study was to determine the possibility of classifying genetically controlled hybrids of poplar trees as resistant or susceptible to the fungal infection on the basis of the phenol content of their bark.

To this end, phenolic compounds present in poplar bark were extracted, separated by reversed-phase HPLC and identified by comparing their retention times with those of suitable standards. The chromatograms provided qualitative and quantitative information that was not easily exploitable to produce a definite classification

criterion, thus it became necessary to resort to multivariate chemometric treatments, even though the original sampling programme was not formulated with a subsequent statistical treatment in mind.

For the characterization of aromatic natural products, gas chromatographic techniques coupled with such treatments have already proved to be effective in studies on olive oil [4], wine [5,6], coffee [7], tea [8] and honey bees [9]. No report of statistical treatments concerning classification of resistant and susceptible hybrids of poplar trees towards *Dothichiza* infection is currently available. In this paper principal component analysis (PCA) [10,11] and linear discriminant analysis (LDA) [12–14] methods were applied to the chromatographic data concerning poplar hybrids sampled in two different places and at regular intervals between December 1989 and June 1990. Our objective was to discover the most suitable chemical variables to perform an effective classification of poplar trees of different

* Corresponding author.

infection resistance and to evaluate the influence of seasonal and geographic factors on such a classification.

EXPERIMENTAL

Instrumentation

The HPLC equipment consisted of a Varian 5560 liquid chromatograph equipped with a UV 200 spectrophotometric detector and a 4290 integrator. The detector was operated at 270 nm.

The column was a LiChrospher RP-18 (250 × 4.6 mm I.D.), 5 μm particle size (Merck, Darmstadt, Germany). The injection was 10 μl, and the flow-rate 1.0 ml/min.

Reagents

HPLC-grade methanol and acetonitrile and a 0.57% solution of acetic acid in Millipore Milli-Q water were used as mobile phase constituents.

Chromatographic conditions

A gradient programme based on a ternary mobile phase gave the best results: acetonitrile (A), acetic acid (0.57%) water solution (B) and methanol (C). The starting conditions were 6% A, 88% B, 6% C. At 40 min the eluent composition was 6% A, 48% B and 46% C.

Sampling

The bark of three clones known to differ in resistance to *Dothichiza populea*—(a) *S. MARTINO* (S.M., resistant), (b) *LUISA AVANZO* (L.A., susceptible) and (c) I-214 (intermediate)—were sampled, in duplicate, in two different places in Italy (Casale Monferrato and Scottine). The sampling programme started in December 1989 and continued monthly until June 1990. The total number of samples collected was 96: two samples of each clone from each geographic site for eight different sampling periods.

Sample preparation

The release of phenolic compounds from poplar bark and the preparation of solutions for analytical HPLC were accomplished by performing the following procedure. About 30 mg of previously liophilized bark were added to 2.0 ml of 1.0 M sodium hydroxide in a filter

tube. The air was removed from the tube by flushing with nitrogen and the stopper secured. The suspension was shaken at 20°C for 20 h and subsequently filtered. The residue was washed with water (total volume of filtrate ca. 2.0 ml). The filtrate was acidified to pH 2.5 with 6.0 M hydrochloric acid and diluted with water to a final volume of 5.0 ml [1].

Standards

As standard substances we used the phenolic compounds more frequently proposed in previous works [2–4] as involved in the mechanism of defence against disease in poplar trees. They were: 4-hydroxy-3-methoxybenzaldehyde, 4-hydroxy-3,5-dimethoxybenzaldehyde, 4-hydroxybenzaldehyde, 4-hydroxybenzoic acid, 4-hydroxy-3-methoxycinnamic acid, 4-hydroxycinnamic acid, benzoic acid, 2-hydroxybenzoic acid, 3,5-dimethoxy-4-hydroxybenzoic acid, catechol, pyrogallol, 3,4-dihydroxybenzoic acid, 4-hydroxy-3-methoxybenzoic acid and 4-methoxybenzoic acid (Fig. 1).

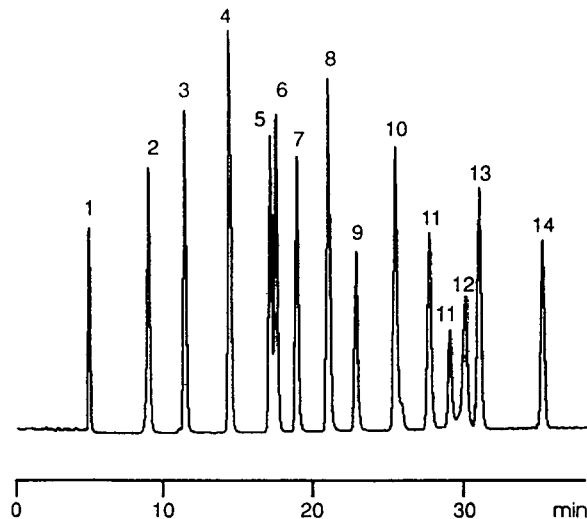


Fig. 1. Chromatographic separation of phenolic standard substances. (For elution conditions, see Experimental section.) Peaks: 1 = 4-hydroxy-3-methoxybenzaldehyde; 2 = 4-hydroxy-3,5-dimethoxybenzaldehyde; 3 = 4-hydroxybenzaldehyde; 4 = 4-hydroxybenzoic acid; 5 = 4-hydroxy-3-methoxycinnamic acid; 6 = 4-hydroxycinnamic acid; 7 = benzoic acid; 8 = salicylic acid; 9 = 4-hydroxy-3,5-dimethoxybenzoic acid; 10 = catechol; 11 = pyrogallol; 12 = 3,4-dihydroxybenzoic acid; 13 = 4-hydroxy-3-methoxybenzoic acid; 14 = 4-methoxybenzoic acid.

Chemometric methods

The data was analysed by PCA and LDA. The former is a pattern recognition method that generates new orthogonal variables, the principal components (PCs), linear combination of the original variables, so that the maximum possible amount of variance of the data is compressed in few PCs. In fact, it is theoretically possible to determine as many principal components as original variables, however they are obtained in order of decreasing contribution to the total variance, so it is usually sufficient to consider the first principal components and still retain most of the variance, that is most of information present in the original data.

PCA is a useful tool to perform variable reductions for high-dimensional complex problems. Moreover, the analysis of the new variable space (PCs space) often provides important information on the pattern of the data (*i.e.* clusters, systematic trends, etc.).

In LDA, as in the PCA technique, the aim is to reduce the number of features. However, while PCA selects a direction that retains maximal structure in a lower dimension among the data, LDA selects a direction that achieves maximum separation among the given classes. The discriminant function obtained in this way leads to a new variable which, as in principal components, is a linear combination of the original variables.

Once this direction has been found, it is possible to perform a statistical test of the significance of the separation of the groups two by two and to assign new objects to any of the two classes.

In the study we also applied a new classification algorithm that generates orthogonal discriminant directions, the orthogonal discriminant analysis (ODA) [15]. This algorithm is advantageous since it allows correct graphic visualization of the discriminant directions. This graphic visualization generally cannot be achieved with the classical LDA algorithm, whose discriminant directions are not required to be orthogonal one to each other.

The data were autoscaled before any PCA treatment in order to attribute the same *a priori* importance to the variables.

RESULTS AND DISCUSSION

Fig. 1 shows the separation of fourteen standard phenolic compounds, whereas Fig. 2 reports typical chromatographic runs regarding the analyses of the bark extracts of the resistant (a and c) and susceptible (b and d) clones. They refer to the first and the last sampling periods December and June, respectively. By comparing the chromatographic profiles obtained from the winter samples (Fig. 2a and b), definite quantitative differences between the clones can be seen. The differences are apparently remarkably reduced in the late spring samples (Fig. 2c and d). Chromatographic runs of the clone of the intermediate resistance (I-214) are not reported because they were not significantly different from those of the susceptible one (L.A.). Ten peaks identified by comparison with the retention times of the pure standards indicated in the chromatograms were used in the chemometric study. They correspond to compounds 2–11 of Fig. 1. A small number of other peaks remain unknown.

By examining the area variations of the identified peaks among the three different clones, no definite trends in the result could be found by visual inspection. So, in order to set up a useful correlation between phenolic contents and infection resistance of the poplar hybrids considered, a chemometric study was performed, though the sampling design was not programmed with a subsequent statistical treatment in mind. The chromatographic peak areas are not reported here because their number is very high.

Since there was a large sampling variation, in the total amount of phenolic compounds, owing to the various combinations of clone, geographic origin and date, but with an apparent conservation of the proportion between the areas, the calculations were performed using the percentage areas. The starting data set contained 96 samples described by ten variables each (the phenolic compounds identified and listed in Fig. 1 from 2 to 11).

The starting analysis was conducted on the whole data set containing samples of different origin, sampling period and genetic origin which, in principle, could significantly affect the phenol

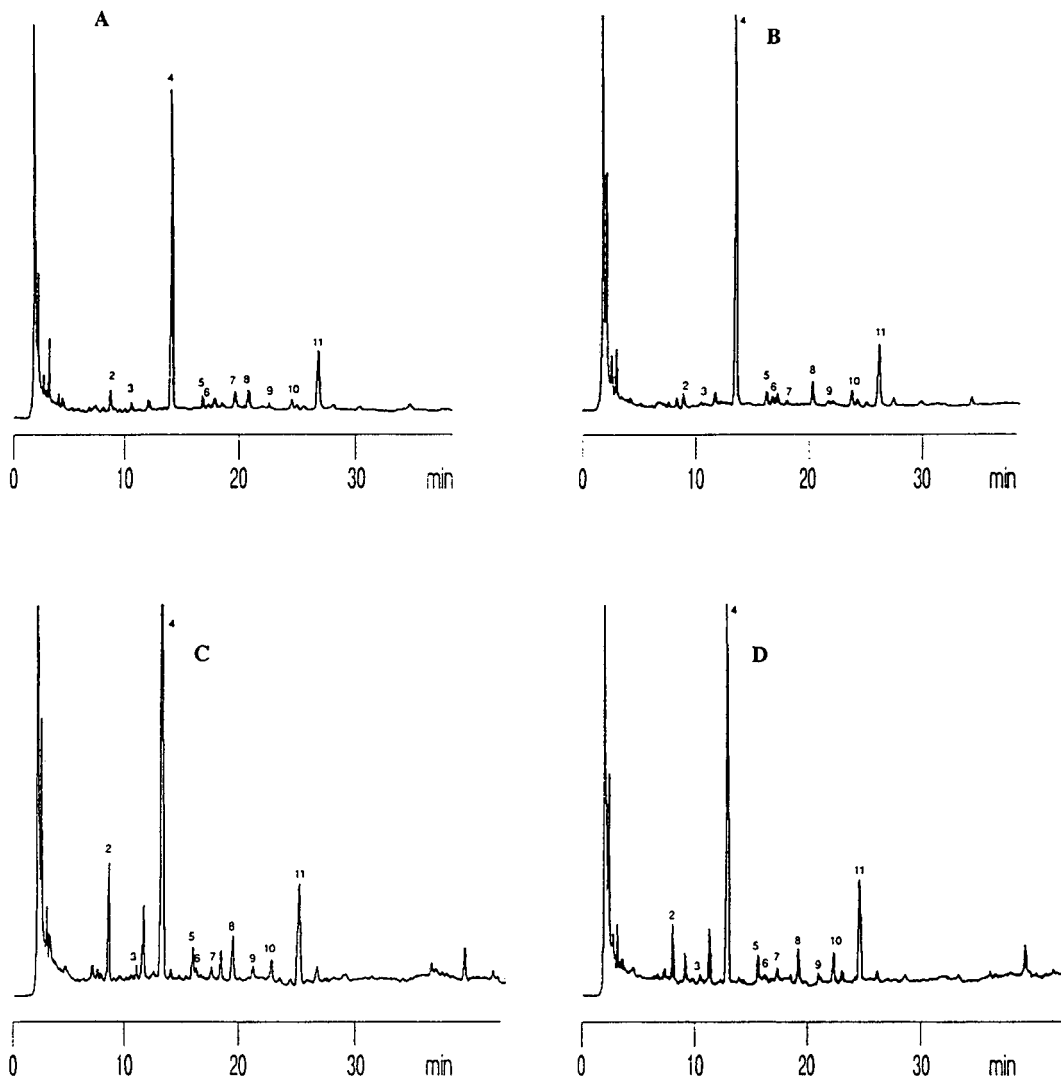


Fig. 2. Chromatographic separations of real samples (resistant and susceptible clones) at the start and the end of the sampling period. (For elution conditions, see Experimental section.) (A) Luisa Avanzo (Dec. 1989), 0.0312 AUFS; (B) S. Martino (Dec. 1989), 0.0312 AUFS; (c) Luisa Avanzo (June 1990), 0.0156 AUFS; (D) S. Martino (June 1990), 0.0156 AUFS. Peak numbers as in Fig. 1.

composition of the poplar bark extracts. After autoscaling, the complete set of the original data was subjected to PCA. The plot of the scores of the first PCs allowed the detection of two outliers (*i.e.* two anomalous samples far from any other sample), which were eliminated from the successive analysis. The new data set containing 94 samples was again autoscaled and submitted to PCA. The variance explained by the first four PCs (eigenvalue greater or around 1.0) is listed in Table I, while Table II reports the loadings of

TABLE I
VARIANCE EXPLAINED BY THE FIRST FOUR PCs
(CLONES 1, 2 AND 3)

PC	Variance (%)	Total variance (%)
1	40.2	40.2
2	14.9	55.1
3	10.7	65.8
4	9.7	75.5

TABLE II
LOADINGS OF THE FIRST FOUR PCs (CLONES 1, 2 AND 3)

Compounds	PC ₁	PC ₂	PC ₃	PC ₄
4-Hydroxy-3,5-dimethoxybenzaldehyde	0.35	-0.02	-0.21	-0.46
4-Hydroxybenzaldehyde	0.28	-0.39	-0.26	-0.12
4-Hydroxybenzoic acid	-0.47	-0.22	0.11	0.01
4-Hydroxy-3-methoxycinnamic acid	0.38	-0.21	-0.07	-0.12
4-Hydroxycinnamic acid	0.30	-0.23	0.38	0.13
Benzoic acid	0.07	-0.27	-0.42	0.78
Salicylic acid	0.33	0.13	0.50	0.30
4-Hydroxy-3,5-dimethoxybenzoic acid	0.26	-0.43	0.24	-0.04
Cathecol	0.26	0.33	-0.47	0.04
Pyrogallol	0.30	0.55	0.12	0.17

the same PCs, *i.e.* the contribution of every original variable to the definition of the PCs. The scatter plots of the samples projected on these PCs show that the PCs containing information about the difference between the clones are the second and the fourth ones. A plot of PC₂ and PC₄ presents two clusters of objects corresponding to the two clones, S.M. and L.A., slightly overlapping in the middle, and a third cluster (clone I-214) largely overlapping with the other two (Fig. 3). Since the main interest lies in the separation of resistant and susceptible clones, PCA was performed on a reduced data set containing only the hybrids S.M. and L.A. (classes 1 and 3).

The variance explained by the first four PCs

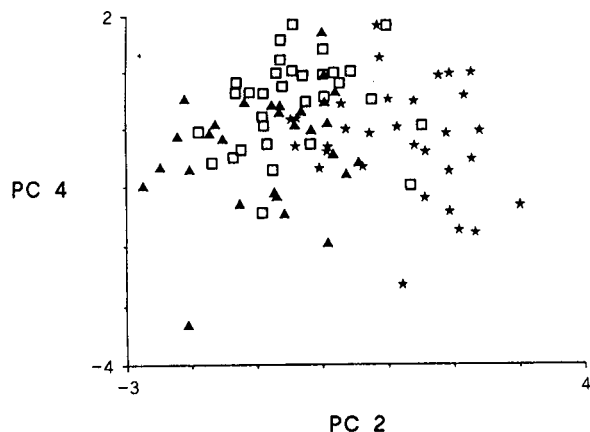


Fig. 3. Scatter plot of the scores of the objects (three types of clones) on the PCs. ★ = S. Martino; ▲ = 214; □ = Avanzo.

(eigenvalue greater or around 1.0) is given in Table III and the corresponding loadings in Table IV. The scatter plot of the scores of PC₂ and PC₄ is shown in Fig. 4. The situation is clearer and there is an improvement in the separation between the two classes, because of the elimination of the data from the samples of the intermediate resistance clone.

In order to better isolate the information traceable back to a seasonal factor, we broke down the previous general plot into a sequence of eight distinct plots in order of sampling time (Fig. 5A and B). Every plot is updated with respect to the preceding one according to the sequence of sampling period, *i.e.* it shows the preceding samples (open markers) plus the samples of the updated period (black markers). The sample origin was not considered in this step since it was found to be irrelevant in PC₂ and PC₄. As can be seen from Fig. 5, the separation of the two clones remains satisfactory for almost all sampling times. Only the data of the late

TABLE III
VARIANCE EXPLAINED BY THE FIRST FOUR PCs (CLONES 1 AND 3)

PC	Variance (%)	Total variance (%)
1	37.41004	37.41004
2	18.27317	55.68321
3	10.54750	66.23071
4	8.550346	74.78105

TABLE IV
LOADINGS OF THE FIRST FOUR PCs (CLONES 1 AND 3)

Compounds	PC ₁	PC ₂	PC ₃	PC ₄
4-Hydroxy-3,5-dimethoxybenzaldehyde	0.20	-0.59	-0.25	0.01
4-Hydroxybenzaldehyde	0.22	-0.17	0.72	0.00
4-Hydroxybenzoic acid	0.09	0.60	0.11	-0.32
4-Hydroxy-3-methoxycinnamic acid	0.39	-0.15	0.10	-0.06
4-Hydroxycinnamic acid	0.34	0.24	0.19	-0.06
Benzoic acid	0.26	0.09	0.14	0.83
Salicylic acid	0.46	-0.02	-0.24	-0.05
4-Hydroxy-3,5-dimethoxybenzoic acid	0.23	-0.27	0.30	-0.42
Cathecol	0.37	0.29	-0.11	0.08
Pyrogallol	0.41	0.05	-0.43	-0.13

spring tend to mix together, as expected. It is worth noticing that, within each sampling time, the discrimination between the two clones is very good.

However, as sampling time proceeds there is a progressive shift in the relative and absolute positions of the objects along the axes of the diagrams. Such a shift should be caused by changes in the extract composition as the season advances. In fact, the change is not random and can be explained by considering the composition of the two PCs considered. In particular, by taking into account the relative movements of the two clones, it can be observed that there are shifts along the axes attributable to changes,

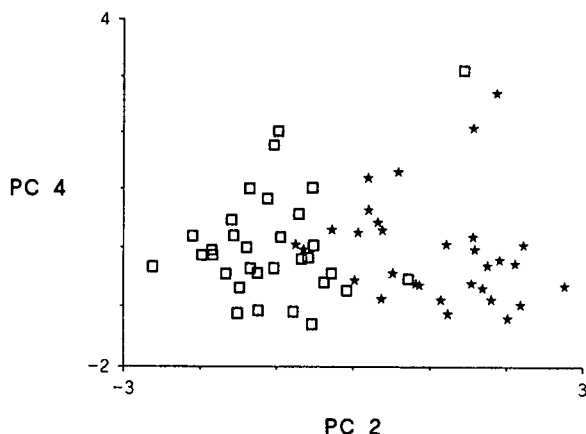


Fig. 4. Scatter plot of the scores of the reduced space of the objects (only resistant and susceptible clones) on the PCs. ★ = S. Martino; □ = Avanzo.

equal for both clones, in the percentage of the chemical components that mainly define the two PCs. At the same time there are rotations of the relative positions, which may be interpreted as different behaviours of the same chemical compounds in the two clones.

The most discriminant principal component is PC₂, which is mainly constituted by the variables corresponding to 4-hydroxy-3,5-dimethoxybenzaldehyde and 4-hydroxybenzoic acid, while PC₄ is mainly constituted by benzoic acid and 4-hydroxy-3,5-dimethoxybenzoic acid.

Very little information is available to achieve a geographic discrimination. It is apparent that the geographic variable poorly affects the characterization of the clones, the main difference being the genetic diversity and secondly the sampling period effect.

After the PCA treatment, which provides information on the pattern of the data and on the seasonal changes in the composition of the samples, we applied LDA to find the best directions for classifying the samples.

LDA was applied in turn to separate each of the clones from the others. This provided three discriminant directions. Table V reports the statistical features of the three separations and the normalized composition of the discriminant directions. The angle between the discriminating directions, easily determined from the scalar product of the vectors along the directions, is 66.6° between $R_{1,2}$ and $R_{1,3}$, 132.6° between $R_{1,2}$ and $R_{2,3}$ and 76.7° between $R_{1,3}$ and $R_{2,3}$. These

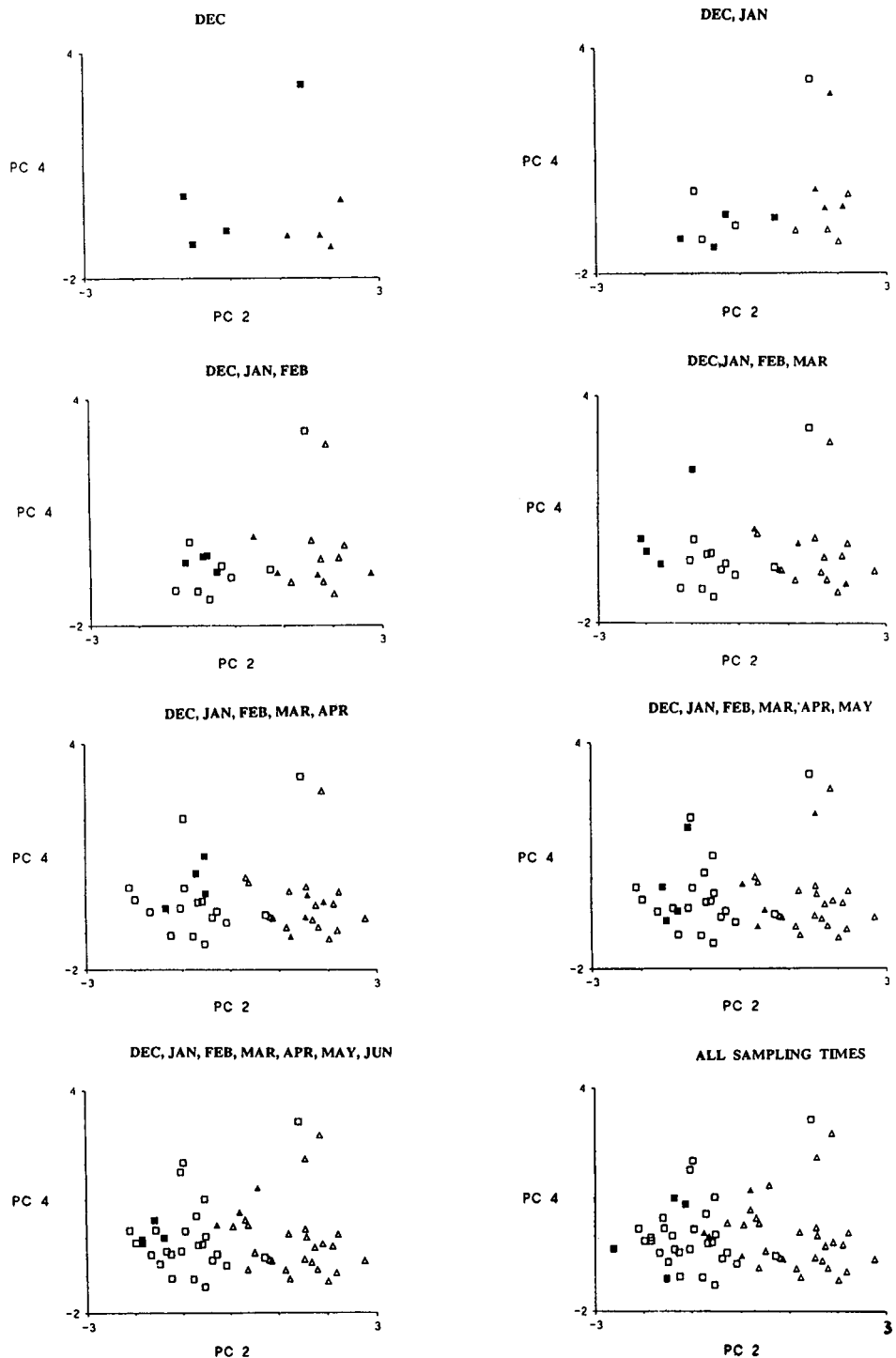


Fig. 5. Scatter plots of the reduced set of the objects of the various sampling periods in PCs. Δ = S. Martino; \square = Avanzo.

TABLE V

STATISTICAL FEATURES OF LDA SEPARATIONS AND NORMALIZED COMPOSITION OF DISCRIMINATING DIRECTIONS

Discrimination between classes 1 and 2: Mahalanobis distance: 16.20, $F_{10,49} = 20.51$

Discrimination between classes 2 and 3: Mahalanobis distance: 10.60, $F_{10,50} = 13.67$

Discrimination between classes 1 and 3: Mahalanobis distance: 20.60, $F_{10,52} = 20.60$

Compounds	Autoscaled director cosines:	Autoscaled director cosines:	Autoscaled director cosines:
4-Hydroxy-3,5-dimethoxybenzaldehyde	-0.60	0.16	-0.89
4-Hydroxybenzaldehyde	-0.02	0.12	0.06
4-Hydroxybenzoic acid	0.06	0.27	0.23
4-Hydroxy-3-methoxycinnamic acid	-0.34	-0.03	-0.09
4-Hydroxycinnamic acid	0.15	0.02	0.01
Benzoic acid	0.02	0.10	0.05
Salicylic acid	0.59	-0.58	-0.13
4-Hydroxy-3,5-dimethoxybenzoic acid	0.12	-0.11	0.13
Cathecol	-0.37	0.71	0.32
Pyrogallol	-0.06	-0.13	-0.03

directions are shown independently in Fig. 6, from which it can be seen that all classifications are satisfactory. The least separated classes are 2 and 3, for which the F -test provides a value of 13.67, which is still highly significant ($F_{50,10} = 4.2$ at the 99% confidence level); this confirms the results of the PCA step.

LDA was also applied to the separation of the samples of different geographic origin, but a very poor classification was obtained.

The application of a different LDA algorithm, namely the ODA algorithm, which provides orthogonal discriminant directions, led to the results shown in Fig. 7. It is clear that all three clones can be effectively separated on the basis of the chemical composition of the extracts.

Summing up, it was impossible to discriminate between the different clones by a direct visual inspection of the raw data alone, these being too complex. The discriminant features obtained by the chemometric treatments are not single original variables but linear combinations of variables. It is evident that the use of some multivariate statistical tools greatly improved the possibility of analysing the data structure and performing an effective classification of the clones with different resistance to fungal infection.

In conclusion, it is worth noting that such

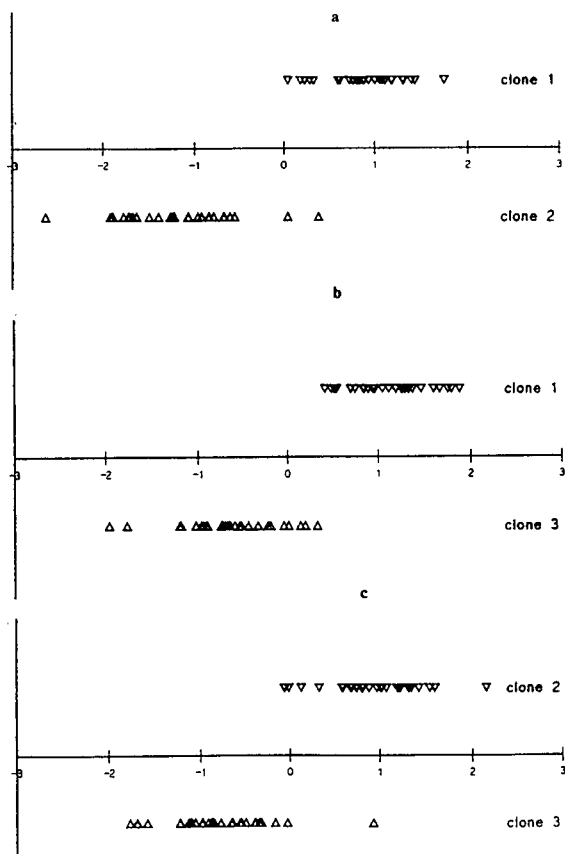


Fig. 6. Classification ability of the three clones by the discriminant directions determined by the LDA procedure. (a) Direction $R_{1,2}$; (b) direction $R_{1,3}$; (c) direction $R_{2,3}$.

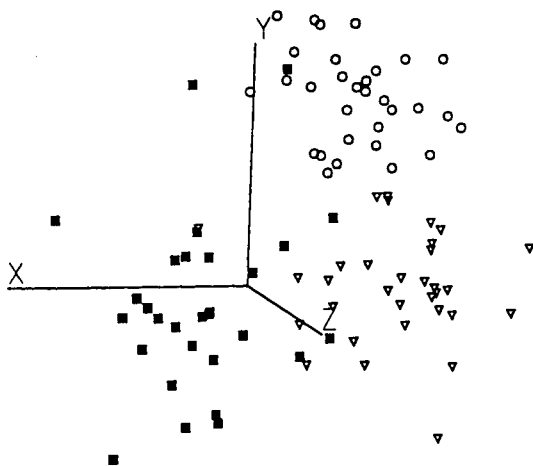


Fig. 7. Plot of the objects in the space of the three discriminant directions obtained by a different LDA algorithm.

information was obtained from data not particularly suitable for treatment with the method adopted. A new sampling plan much more tailored on the statistical requirements is almost accomplished and a further chromatographic and chemometric study is in progress in our laboratory.

REFERENCES

- 1 S. Pukacka, *Arbor. Korn.*, 20 (1975) 227.
- 2 S. Pukacka, *Arbor. Korn.*, 25 (1980) 257.

- 3 Y. Chuanhe, Y. Wang and Z. Zhongming, presented at *International Poplar Commission, XVIIIth Session, Beijing, September 5–8, 1988*.
- 4 M. Forina and E. Tiscornia, *Ann. Chim. (Rome)*, 72 (1982) 143.
- 5 I.E. Frank, B.R. Kowalski, *Anal. Chim. Acta*, 162 (1984) 241.
- 6 W.E. Kwan and B.R. Kowalski, *J. Food Sci.*, 43 (1978) 1320.
- 7 K. Wada, S. Oghama, H. Sasaki and M. Shimoda, *Agr. Biol. Chem.*, 51 (1987) 1745.
- 8 L. Xiande, P. Van Espen and F. Adams, *Anal. Chim. Acta*, 200 (1987) 421.
- 9 R. Valcarce and G.G. Smith, *Chemom. Intell. Lab. Syst.*, 6 (1989) 157.
- 10 J.C. Davis, *Statistics and Data Analysis in Geology*, Wiley, New York, 2nd ed., 1986, p. 524.
- 11 S. Wold, *Technometrics*, 20 (1978), 397.
- 12 D.L. Massart, B.G.M. Vandeginste, S.N. Deming, Y. Michotte and L. Kaufman, *Chemometrics: a Textbook*, Elsevier, Amsterdam, 1988, p. 330.
- 13 K.V. Mardia, J.T. Kent and J.M. Bibby, *Multivariate Analysis*, Academic Press, London, 1979.
- 14 M. James, *Classification Algorithms*, Collins, London, 1985.
- 15 E. Marengo and R. Todeschini, presented at *X congresso Nazionale della Divisione di Chimica Analitica della Società Chimica Italiana, Turin, Sept. 16–19, 1991*.

Retention behaviour of aromatic sulphonic acids in reversed-phase ion-pair liquid chromatography with methanol and acetonitrile as organic modifiers

Hanfa Zou*, Yukui Zhang, Mingfang Hong and Peichang Lu

National Chromatographic R & A Centre, Dalian Institute of Chemical Physics, Academia Sinica, Dalian 116011 (China)

(First received March 9th, 1993; revised manuscript received April 8th, 1993)

ABSTRACT

The capacity factors of phenylamine- and naphthylaminesulphonic acids in reversed-phase ion-pair liquid chromatography were measured. The equations $\log k' = \log k_w - S\varphi$ and $\log k' = \log k_w + A\varphi^2 - S\varphi$ to describe the effects of methanol and acetonitrile concentration were compared. It has been observed that the effect of organic modifier concentration up to $\varphi = 0$ on retention follows the empirical equation $\log k' = \log k_w - S\varphi$. It was found that the effect of acetonitrile on retention is stronger than that of methanol, which is the same as the order of their elution strengths observed in RP-HPLC.

INTRODUCTION

Reversed-phase ion-pair liquid chromatography (RP-IPC) is widely used in separations of organic and inorganic ions. Retention can be regulated by the properties and concentrations of the organic modifier and counter ion and by using a competing ion with the same charge as the analyte. Many models of RP-IPC have been published [1–7] and excellent reviews have appeared [1,8]. In recent years, the electrostatic model with the use of the Gouy–Chapman theory has been applied to IPC [9–14]. The effects of chromatographic variables such as organic modifier concentration [13], ion-pair reagent [15], inorganic salt concentration [16], column temperature [17] and solute properties such as hydrophobicity and charge [18,19] on retention have been investigated. It has been observed that both hydrophobicity and solute charge play a very important role in retention in RP-IPC and in most instances the retention

order in RP-IPC for organic ions with the same charge is the same as in RP-HPLC [20]. In this work, the retention behaviour of sulphonic acids in RP-IPC with tetrabutylammonium iodide as ion-pair reagent and methanol and acetonitrile as organic modifiers was studied.

EXPERIMENTAL

Materials

The phenylamine- and naphthylaminesulphonic acids (Table I) were obtained from the Dyestuff Laboratory, Chemical Engineering Department, Dalian University of Sciences and Technology. Standard solutions were prepared in water. Doubly distilled water was used throughout. Methanol, tetrabutylammonium iodide (TBAI), NaH_2PO_4 , NaOH, KCl and HCl were of analytical-reagent grade.

Apparatus

RP-IPC experiments were carried out on a stainless-steel column (150×4.6 mm I.D.) packed with Spherisorb- C_{18} (10 μm) (Phase

* Corresponding author.

Separations, Deeside, UK) at room temperature (26°C). The column was packed at the National Chromatographic R & A Centre, Dalian, China. The mobile phases contained methanol, acetonitrile and water in different proportions with constant concentrations of TBAI ion-pair reagent (4 mmol/l), NaH₂PO₄ (10 mmol/l) and KCl (10 mmol/l) and with a pH of 7.00. Mobile phase was delivered with a Waters (Milford, MA, USA) Model 510 pump. Eluates were detected at 254 nm. Samples were loaded with a U6K syringe-loading sample injector. The pH value of the organic modifier solution was measured with an SA-720 pH meter (Orion Research, Chicago, IL, USA). As discussed by Karger *et al.* [21], with up to 25% of organic modifier in the aqueous eluent, the systematic error in pH measured pH in a mixed solvent and standardizing with aqueous buffer is much less than 0.1 pH unit. The flow-rate was 1.0 ml/min. All experimental data was processed using a personal computer.

RESULTS AND DISCUSSION

Relationship between retention and organic modifier concentration

The retention times of each sulphonic acid were measured twice with different methanol

and acetonitrile concentrations from 0.22 to 0 volume fraction and the difference between the two retention times in each instance was less than 3%. Pre-equilibration of the column for 30 min was applied when changing the mobile phase composition. The capacity factors of test solutes calculated from retention times are given in Tables I and II. In reversed-phase high-performance liquid chromatography (RP-HPLC), according to the solubility parameter concept [22], the relationship between solute retention and organic modifier concentration can be described by

$$\log k' = \log k_w + A\varphi^2 - S\varphi \quad (1)$$

where $\log k_w$ is the capacity factor obtained by extrapolation of retention data from binary eluents to 100% water, A and S are constants for a given solute–eluent combination and φ is the volume fraction of the organic modifier in the aqueous eluent. Snyder *et al.* [23] showed that over a volume fraction range of at most 0.1–0.9, eqn. 1 can be simplified as a good approximation to

$$\log k' = \log k_w - S\varphi \quad (2)$$

In RP-IPC, a retention equation identical with eqn. 2 was used to describe the effect of organic modifier concentration on retention. The results

TABLE I

CAPACITY FACTORS OF PHENYLAMINE- AND NAPHTHYLAMINESULPHONIC ACIDS AT DIFFERENT METHANOL CONCENTRATIONS

Solute	Volume fraction of methanol, φ (v/v)				
	0.22	0.15	0.08	0.04	0
1,3-Diaminobenzene-4-sulphonic acid	0.130	0.420	0.712	0.987	1.52
1-Aminobenzene-4-sulphonic acid	0.146	0.419	0.699	0.936	1.56
1-Aminobenzene-3-sulphonic acid	0.394	0.885	1.81	2.80	4.31
1,3-Diaminobenzene-4,6-disulphonic acid	0.441	1.02	2.70	4.00	6.91
1-Amino-4-methylbenzene-2-sulphonic acid	0.842	1.97	4.19	6.74	10.21
1-Aminonaphthalene-5-sulphonic acid	1.26	3.02	8.10	13.08	23.07
2-Aminonaphthalene-4,7-disulphonic acid	1.72	4.81	17.72	35.17	68.95
2-Aminonaphthalene-4,8-disulphonic acid	1.64	5.37	18.26	36.48	74.11
2-Aminonaphthalene-5-sulphonic acid	3.57	9.45	29.33	50.56	90.52
2-Aminonaphthalene-3,6-disulphonic acid	2.24	8.08	31.08	87.33	133.9
2-Aminonaphthalene-4,6,8-trisulphonic acid	2.95	10.02	45.19	95.57	191.3
2-Aminonaphthalene-3,6,8-trisulphonic acid	3.70	10.25	49.15	102.0	201.6

TABLE II

CAPACITY FACTORS OF PHENYLAMINE- AND NAPHTHYLAMINESULPHONIC ACIDS AT DIFFERENT ACETONITRILE CONCENTRATIONS

Solute	Volume fraction of acetonitrile, $\varphi(v/v)$				
	0.22	0.15	0.08	0.04	0
1,3-Diaminobenzene-4-sulphonic acid	0.090	0.224	0.539	0.769	1.52
1-Aminobenzene-4-sulphonic acid	0.077	0.256	0.571	0.833	1.56
1-Aminobenzene-3-sulphonic acid	0.122	0.474	1.20	1.98	4.31
1,3-Diaminobenzene-4,6-disulphonic acid	0.135	0.635	1.80	3.09	6.91
1-Amino-4-methylbenzene-2-sulphonic acid	0.224	0.737	2.40	4.39	10.21
1-Aminonaphthalene-5-sulphonic acid	0.410	1.36	4.52	9.39	23.07
2-Aminonaphthalene-4,7-disulphonic acid	0.378	1.98	8.06	18.75	68.95
2-Aminonaphthalene-4,8-disulphonic acid	0.330	1.66	7.84	19.65	74.11
2-Aminonaphthalene-5-sulphonic acid	0.660	2.76	13.19	33.33	90.52
2-Aminonaphthalene-3,6-disulphonic acid	0.474	2.43	12.98	34.36	133.9
2-Aminonaphthalene-4,6,8-trisulphonic acid	0.680	4.24	24.04	53.41	191.3
2-Aminonaphthalene-3,6,8-trisulphonic acid	0.756	4.40	25.49	60.12	201.6

TABLE III

LOG k_w , S AND A IN EQN. 1 OBTAINED BY REGRESSION ANALYSIS OF THE EXPERIMENTAL DATA IN TABLES I AND II

Solute	Methanol–water				Acetonitrile–water			
	Log k_w	S	A	r	Log k_w	S	A	r
1,3-Diaminobenzene-4-sulphonic acid	0.148	2.496	-9.528	0.9936	0.157	5.593	0.730	0.9980
1-Aminobenzene-4-sulphonic acid	0.155	3.066	-6.030	0.9924	0.160	4.467	-5.621	0.9970
1-Aminobenzene-3-sulphonic acid	0.631	4.490	-0.902	0.9994	0.596	5.962	-3.639	0.9971
1,3-Diaminobenzene-4,6-disulphonic acid	0.836	5.365	-0.320	0.9993	0.800	6.070	-6.430	0.9974
1-Amino-4-methylbenzene-2-sulphonic acid	1.009	4.590	-1.482	0.9999	0.991	7.923	2.263	0.9994
1-Aminonaphthalene-5-sulphonic acid	1.362	5.939	0.865	0.9998	1.348	9.034	5.374	0.9997
2-Aminonaphthalene-4,7-disulphonic acid	1.851	8.027	2.883	0.9995	1.790	11.38	6.572	0.9979
2-Aminonaphthalene-4,8-disulphonic acid	1.870	7.708	0.828	1.0000	1.833	12.39	8.848	0.9989
2-Aminonaphthalene-5-sulphonic acid	1.962	6.437	-0.004	0.9996	1.946	10.93	5.782	0.9999
2-Aminonaphthalene-3,6-disulphonic acid	2.172	7.983	-1.662	0.9971	2.096	13.10	9.857	0.9993
2-Aminonaphthalene-4,6,8-trisulphonic acid	2.299	8.403	0.093	0.9993	2.243	11.11	0.987	0.9987
2-Aminonaphthalene-3,6,8-trisulphonic acid	2.333	8.878	3.391	0.9979	2.279	11.29	1.893	0.9995

of regression analysis of the experimental data shown in Tables I and II according to eqn. 1 are given in Table III. The plots of $\log k'$ vs. φ according to eqn. 2 for the data in Tables I and II are given in Figs. 1 and 2; Tables IV and V give the values of $\log k_w$ and S in eqn. 2 obtained by taking or not taking into account, respectively, the k' values at $\varphi = 0$.

It can be seen that the regression coefficients with eqns. 1 and 2 are higher than 0.99 for all solutes, except for 1-aminobenzene-4-sulphonic acid and 1,3-diaminobenzene-4-sulphonic acid in Table IV, the reason for which is probably the low numerical value of k' , giving a high uncertainty. The values of $\log k_w$ and S obtained with eqn. 1 are close to those given by eqn. 2 with methanol as the organic modifier; their relative difference is less than 10% for ten of the twelve solutes. However, the relative difference between the values of S obtained with eqns. 1 and

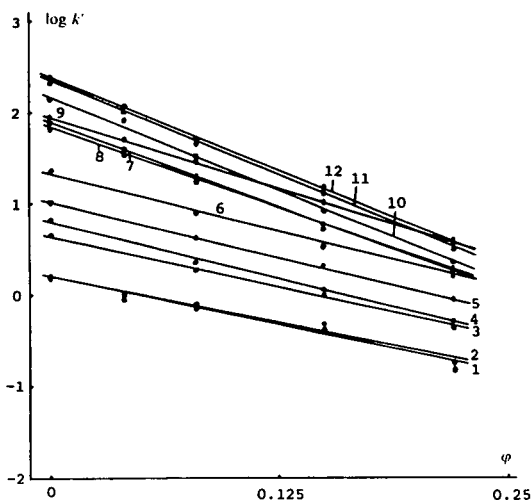


Fig. 1. Plots of $\log k'$ vs. φ according to eqn. 2 with methanol as organic modifier. 1 = 1,3-Diaminobenzene-4-sulphonic acid; 2 = 1-aminobenzene-4-sulphonic acid; 3 = 1-aminobenzene-3-sulphonic acid; 4 = 1,3-diaminobenzene-4,6-disulphonic acid; 5 = 1-amino-4-methylbenzene-2-sulphonic acid; 6 = 1-aminonaphthalene-5-sulphonic acid; 7 = 2-aminonaphthalene-4,7-disulphonic acid; 8 = 2-aminonaphthalene-4,8-disulphonic acid; 9 = 2-aminonaphthalene-5-sulphonic acid; 10 = 2-aminonaphthalene-3,6-disulphonic acid; 11 = 2-aminonaphthalene-4,6,8-trisulphonic acid; 12 = 2-aminonaphthalene-3,6,8-trisulphonic acid.

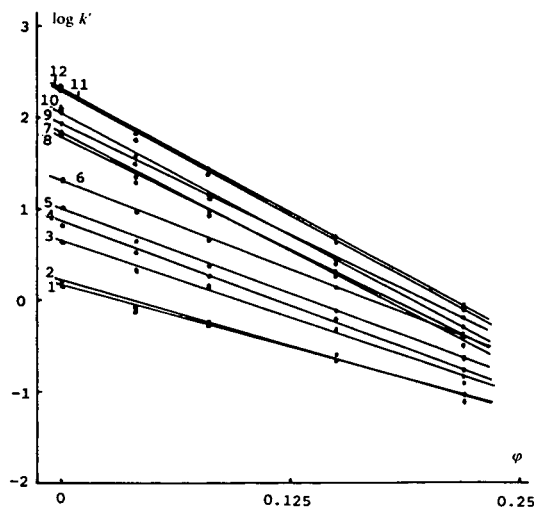


Fig. 2. Plots of $\log k'$ vs. φ according to eqn. 2 with acetonitrile as organic modifier. Compound numbers as in Fig. 1.

2 is larger than 10% for eight of the twelve solutes with acetonitrile as the organic modifier. The regression coefficients with eqn. 1 are only slightly higher than those with eqn. (2), which means that both eqns. 1 and 2 describe well the effect of organic modifier concentration on retention in our experimental system. The value of A in eqn. 1 varies from 3.391 to -9.528 with methanol and from -6.430 to 9.857 with acetonitrile as the organic modifier. The reason is probably the minor statistical weight in regression analysis giving high uncertainty to the A values. The φ^2 term in eqn. 1 makes a much smaller contribution to the retention than the φ term does. In general, the effect of the φ^2 term on retention with acetonitrile as an organic modifier is stronger than that with methanol as an organic modifier. The regression coefficients with eqn. 1 considering or not considering the data at $\varphi = 0$ are fairly close and the relative differences in the parameters $\log k_w$ and S between two instances are less than 5% in most cases. The above results mean that eqn. 2 can accurately describe the effect of organic modifier concentration on retention up to $\varphi = 0$ in our experimental system, but eqn. 2 is a better approximation for methanol than for acetonitrile, which is usually observed in RP-HPLC.

TABLE IV

LOG k_w AND S IN EQN. 2 OBTAINED BY LINEAR REGRESSION ANALYSIS OF THE EXPERIMENTAL DATA IN TABLE I

Solute	Not taking into account data at $\varphi = 0$			Taking into account data at $\varphi = 0$		
	Log k_w	S	r	Log k_w	S	r
1,3-Diaminobenzene-4-sulphonic acid	0.230	4.768	0.9793	0.205	4.614	0.9855
1-Aminobenzene-4-sulphonic acid	0.188	4.390	0.9817	0.191	4.403	0.9888
1-Aminobenzene-3-sulphonic acid	0.638	4.699	0.9997	0.636	4.691	0.9998
1,3-Diaminobenzene-4,6-disulphonic acid	0.836	5.426	0.9988	0.838	5.436	0.9993
1-Amino-4-methylbenzene-2-sulphonic acid	1.027	4.980	0.9997	1.018	4.921	0.9997
1-Aminonaphthalene-5-sulphonic acid	1.350	5.707	0.9996	1.357	5.747	0.9997
2-Aminonaphthalene-4,7-disulphonic acid	1.829	7.357	0.9987	1.834	7.386	0.9992
2-Aminonaphthalene-4,8-disulphonic acid	1.860	7.493	1.0000	1.865	7.524	1.0000
2-Aminonaphthalene-5-sulphonic acid	1.968	6.474	0.9995	1.962	6.438	0.9996
2-Aminonaphthalene-3,6-disulphonic acid	2.240	8.712	0.9978	2.182	8.352	0.9971
2-Aminonaphthalene-4,6,8-trisulphonic acid	2.317	8.496	0.9991	2.299	8.382	0.9993
2-Aminonaphthalene-3,6,8-trisulphonic acid	2.321	8.179	0.9961	2.313	8.124	0.9975

Relationship of retention values in different mobile phases

Cross-comparison of the log k' values at the same volume fraction of methanol and acetonitrile and the ion-pair reagent concentration in the eluents revealed two effects: first, the retention order of sulphonic acids was not different between the two organic modifiers, and second, sulphonic acids were retained in the column much longer by methanol–water than by acetonitrile–water mixtures. For instance, 2-aminonaphthalene-4,6,8-trisulphonic acid eluted at 45 min with methanol–water (0.08:0.92). The same compound eluted only at 24 min with acetonitrile–water (0.08:0.92). The parameter S in eqn. 2 with acetonitrile–water as the eluent is much larger than that with methanol–water, which means that there is a much stronger effect of

acetonitrile on the retention of sulphonic acids than that of methanol in RP-IPC, which agrees with the results observed by Bartha *et al.* [14] that the effect of acetonitrile on the adsorbed amount of ion-pair reagent is stronger than that of methanol, and also agrees with the order of elution strength as an organic modifier in RP-HPLC. It is clear that the hydrophobic interaction plays an important role in the adsorption of ion-pair reagents on the stationary surface and the retention of ionic solutes in RP-IPC.

The results of linear regression of the log k' values, log k_w and S between the two organic modifiers are given in Figs. 3, 4 and 5, respectively. The regression coefficients for the correlation of log $k'_{(\text{ACN})}$ vs. log $k'_{(\text{MeOH})}$ and log $k_{w(\text{ACN})}$ vs. log $k_{w(\text{MeOH})}$ are higher than 0.99, but that of $S_{(\text{ACN})}$ vs. $S_{(\text{MeOH})}$ is only 0.957. The lower

TABLE V

LOG k_w AND S IN EQN. 2 OBTAINED BY LINEAR REGRESSION ANALYSIS OF THE EXPERIMENTAL DATA IN TABLE II

Solute	Not taking into account data at $\varphi = 0$			Taking into account data at $\varphi = 0$		
	Log k_w	S	r	Log k_w	S	r
1,3-Diaminobenzene-4-sulphonic acid	0.123	5.245	0.9981	0.153	5.430	0.9980
1-Aminobenzene-4-sulphonic acid	0.194	5.718	0.9920	0.193	5.717	0.9951
1-Aminobenzene-3-sulphonic acid	0.601	6.667	0.9944	0.618	6.773	0.9965
1,3-Diaminobenzene-4,6-disulphonic acid	0.838	7.495	0.9935	0.839	7.501	0.9960
1-Amino-4-methylbenzene-2-sulphonic acid	0.943	7.209	0.9998	0.977	7.418	0.9993
1-Aminonaphthalene-5-sulphonic acid	1.266	7.531	0.9999	1.315	7.836	0.9988
2-Aminonaphthalene-4,7-disulphonic acid	1.659	9.353	0.9993	1.750	9.917	0.9971
2-Aminonaphthalene-4,8-disulphonic acid	1.686	9.831	1.0000	1.780	10.41	0.9975
2-Aminonaphthalene-5-sulphonic acid	1.864	9.349	0.9998	1.914	9.659	0.9991
2-Aminonaphthalene-3,6-disulphonic acid	1.943	10.33	1.0000	2.031	10.91	0.9977
2-Aminonaphthalene-4,6,8-trisulphonic acid	2.192	10.61	0.9990	2.237	10.89	0.9989
2-Aminonaphthalene-3,6,8-trisulphonic acid	2.229	10.63	0.9996	2.267	10.87	0.9994

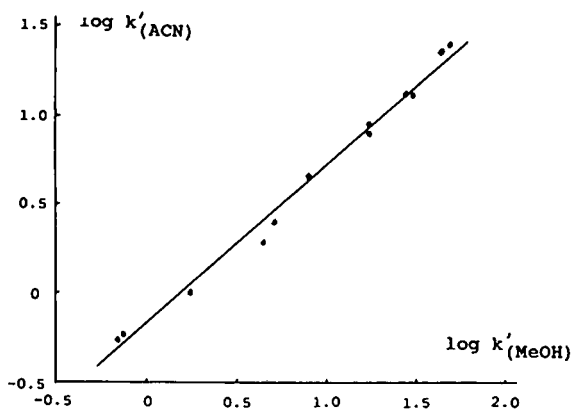


Fig. 3. Results of linear regression analysis of $\log k'$ values between the two organic modifiers with volume fraction 0.08. For experimental conditions, see text. Regression equation: $\text{Log } k'_{(\text{ACN})} = -0.141 + 0.873 \log k'_{(\text{MeOH})}$, $r = 0.9972$, $n = 12$.

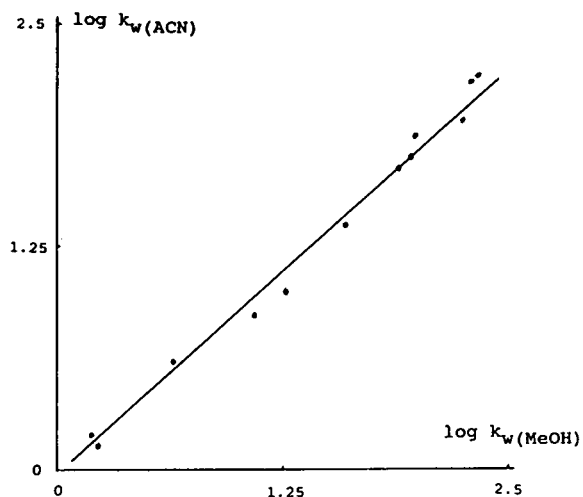


Fig. 4. Result of linear regression analysis of the $\log k_w$ values between the two organic modifiers. For experimental conditions, see text. Regression equation: $\text{Log } k_w(\text{ACN}) = -0.004 + 0.935 \log k_w(\text{MeOH})$, $r = 0.9964$, $n = 12$.

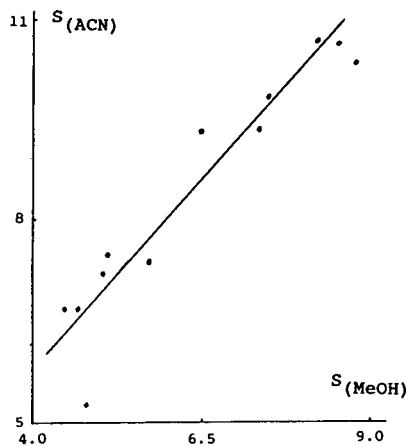


Fig. 5. Result of linear regression analysis of the S values between the two organic modifiers. For experimental conditions, see text. Regression equation: $S_{(\text{ACN})} = 0.987 + 1.149 S_{(\text{MeOH})}$, $r = 0.9568$, $n = 12$.

regression coefficient for $S_{(\text{ACN})}$ vs. $S_{(\text{MeOH})}$ may be caused from the facts that there is some difference in selectivity between methanol and acetonitrile mixtures and the low numerical value for some solutes such as 1,3-diaminobenzene-4-sulphonic acid resulted in an uncertainty of the S value. For example, the regression coefficient is 0.973 for the eleven solutes excluding 1,3-diaminobenzene-4-sulphonic acid.

ACKNOWLEDGEMENT

Financial support from the Natural Science Foundation of China is gratefully acknowledged.

REFERENCES

- 1 B.A. Bidlingmeyer, *J. Chromatogr. Sci.*, 18 (1980) 525.
- 2 A. Tilly-Melin, Y-Askemark, K.G. Wahlund and G. Schill, *Anal. Chem.*, 51 (1979) 976.

- 3 B.A. Bidlingmeyer, S.N. Deming, W.P. Price, Jr., B. Sachok and M. Petrusek, *J. Chromatogr.*, 186 (1979) 419.
- 4 C.T. Huang and R.B. Taylor, *J. Chromatogr.*, 202 (1980) 333.
- 5 P.T. Kinnsinger, *Anal. Chem.*, 49 (1977) 883.
- 6 J.H. Knox and R.A. Hartwick, *J. Chromatogr.*, 204 (1981) 3.
- 7 S. Afrashtehfer and F.F. Cantwell, *Anal. Chem.*, 54 (1982) 2422.
- 8 Cs. Horvath and W.R. Melander, in M.T.W. Hearn (Editor), *Ion-Pair Chromatography—Theory and Biological and Pharmaceutical Application*, Marcel Dekker, New York, 1985, p. 27.
- 9 J. Stahlberg, *J. Chromatogr.*, 356 (1986) 231.
- 10 A. Bartha and J. Stahlberg, *J. Chromatogr.*, 535 (1990) 181.
- 11 H. Liu and F.F. Cantwell, *Anal. Chem.*, 63 (1990) 2032.
- 12 P.-C. Lu, H.-F. Zou and Y.-K. Zhang, *Mikrochim. Acta*, III (1990) 35.
- 13 H.-F. Zou, Y.-K. Zhang and P.-C. Lu, *J. Chromatogr.*, 545 (1990) 59.
- 14 A. Bartha, Gy. Vigh and J. Stahlberg, *J. Chromatogr.*, 506 (1990) 85.
- 15 M.-F. Hong, H.-F. Zou, Y.-K. Zhang and P.-C. Lu, *Acta Chim. Sin.*, 51 (1993) 178.
- 16 Y.-K. Zhang, H.-F. Zou, M.-F. Hong and P.-C. Lu, *Chromatographia*, 32 (1991) 538.
- 17 H.-F. Zou, Y.-K. Zhang, M.-F. Hong and P.-C. Lu, *Chromatographia*, 35 (1993) 390.
- 18 H.-F. Zou, Y.-K. Zhang, M.-F. Hong and P.-C. Lu, *Chromatographia*, 32 (1991) 329.
- 19 H.-F. Zou, Y.-K. Zhang, M.-F. Hong and P.-C. Lu, *J. Chromatogr.*, 625 (1992) 169.
- 20 H.-F. Zou, Y.-K. Zhang, X.-B. Wen and P.-C. Lu, *J. Chromatogr.*, 523 (1990) 247.
- 21 B.L. Karger, J.N. Lepage and N. Tanaka, in Cs. Horvath (Editor), *High Performance Liquid Chromatography—Advances and Perspectives*, Vol. 1, Academic Press, New York, 1980, p. 130.
- 22 P.J. Schoenmakers, H.A.H. Billiet, R. Tijssen and L. de Galan, *J. Chromatogr.*, 149 (1978) 519.
- 23 L.R. Snyder, J.W. Dolan and J.R. Gant, *J. Chromatogr.*, 165 (1979) 3.

High-performance liquid chromatographic separation of enantiomeric amino acids on bis[carbamoyl(alkyl)methylamino]-6-chloro-*s*-triazine-derived chiral stationary phases

Jer-Yann Lin^{*} and Mei-Hui Yang^{*}

Department of Chemistry, National Taiwan University, Taipei 10764 (Taiwan)

(First received February 8th, 1993; revised manuscript received April 15th, 1993)

ABSTRACT

The synthesis and chiral recognition ability of a series of four chiral stationary phases (CSPs) containing 2,4-bis[carbamoyl(alkyl)methylamino]-6-chloro-*s*-triazine (designated phase A) are described. The synthesis of these CSPs is achieved through amide formation by bonding 2,4-bis[carboxy(alkyl)methylamino]-6-chloro-*s*-triazine onto 3-aminopropyl silica gel. Such phases are quite effective for high-performance liquid chromatographic separation of a racemic mixture of five typical amino acids. The chromatographic behaviour of these CSPs was studied. Comparison of these CSPs with the *s*-triazine-derived CSP (designated phase B), which bears a tripeptide chiral moiety, is also discussed. The present study clearly indicates that an *s*-triazine-terminated CSP derived from certain L-amino acids (phase A), instead of tripeptide, is effective enough for the separation of enantiomeric amino acids.

INTRODUCTION

In our previous report [1], a highly selective *s*-triazine-modified C₁₈ column for HPLC was prepared. The chromatographic efficiency and selectivity of the bonded phase were evaluated from the separability of a mixture of twelve aromatic hydrocarbons. Better performance was achieved on the prepared column than on some commercially available C₁₈ columns. Also, the bonded phase so prepared showed better chemical stability. We therefore considered that the presence of an *s*-triazine ring in the bonded phase system not only led to a convenient reproducible synthetic way of introducing a hy-

drocarbon moiety to the silica surface but also played an important role, possibly due to a $\pi-\pi$ interaction with aromatic analytes, in the separation of aromatic hydrocarbons.

In a study of chiral stationary phases (CSPs) for HPLC, Oi *et al.* [2] reported that the *s*-triazine derivative of tripeptide ester bonded to silica gel (Fig. 1, phase B), when used as a CSP in HPLC, gave good enantioselectivity for di-nitrobenzoyl (DNB)-derivatized enantiomers of amino acids. It is possible that, by alternative bonding with the *s*-triazine terminus, an L-amino acid derivative instead of a tripeptide ester derivative (Fig. 1, phase A) may be effective enough in the chiral recognition process owing to the increasing rigidity of this terminal moiety. Furthermore, from the viewpoint of the synthetic advantage, as we described previously [3,4], an amide linkage could be formed effectively

* Corresponding author.

* Present address: Department of Mathematics and Science Education, National Teachers College, Tainan, Taiwan.

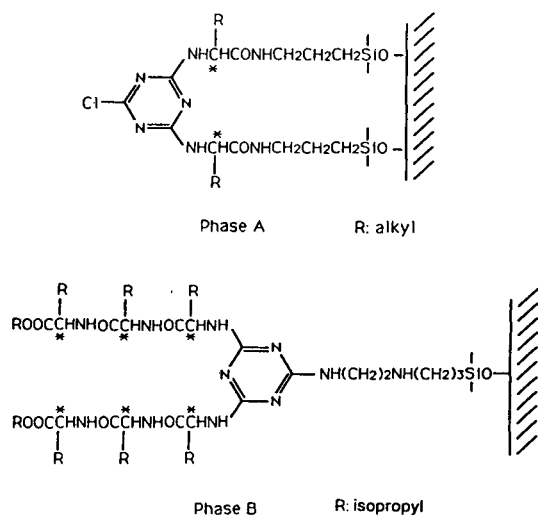


Fig. 1. The structures of chiral stationary phases.

through an active ester transformation. Thus, an amide formation would be more favourable than a nucleophilic substitution for introducing the chiral moiety of the *s*-triazine derivative to aminopropylsilanized silica.

The aim of this work was to evaluate the performance of *s*-triazine linking to different positions of silanized silica in the separation of enantiomeric amino acids by HPLC. Thus, bis(*L*-amino acid)-substituted *s*-triazine-derived CSPs were prepared and the chiral recognition ability of these sorbents was investigated. It was found that not only is the preparation of the *s*-triazine-terminal CSPs favourable, but these phases also exhibit excellent recognition ability for DNB-derivatized racemic amino acids in reversed-phase chromatography.

EXPERIMENTAL

Chemicals

The silica gel used was Nucleosil (pore size 100 Å; particle size 10 μm; surface area 350 m²/g), obtained from Macherey–Nagel.

All reagents used to prepare the bonded CSPs were reagent grade: cyanuric chloride (Fluka), 3-aminopropyltriethoxysilane (APS, Chisso), dicyclohexylcarbodiimide (DCC, Merck), *L*-amino acids (Sigma) and *N*-hydroxysuccinimide (Aldrich). The solvents used for HPLC were

LC-grade methanol and reversed-osmosis deionized water.

Preparation of *s*-triazine derivatives of *L*-amino acids

Three derivatives of *s*-triazine prepared in this study were 2,4-bis(*L*-alanyl)-6-chloro-*s*-triazine (I), 2,4-bis(*L*-valyl)-6-chloro-*s*-triazine (II) and 2,4-bis(*L*-leucyl)-6-chloro-*s*-triazine (III). These compounds were synthesized by a general procedure as follows. Anhydrous sodium carbonate (0.042 mol) and the *L*-amino acid (0.02 mol) were dissolved in 50 ml of water, then a solution of cyanuric chloride (0.02 mol) in acetone (10 ml) was added with stirring. The mixture was heated at 45–50°C for 30 min. The product was precipitated by acidifying with dilute hydrochloric acid, filtered, and washed with pure water until no more chloride ion could be detected in filtrate by silver nitrate solution, and dried under vacuum in the presence of P₂O₅ to give the expected product quantitatively. The melting points of compounds I, II and III were determined to be 170–172, 166–168, and 70–72°C, respectively. The characteristic IR data (potassium bromide, cm⁻¹) for compounds I–III are summarized: ν(O–H) 2600–3600, ν(C–H) 2970, ν(N–H) 3300, ν(C=O) 1710, ν(*s*-triazine ring) 1500–1600. ¹H-NMR(C²H₃O²H) showed peaks at δ1.2(d, 6H) and δ4.4(q, 2H) for compound I; δ0.79(d, 12H), δ2.2(m, 2H) and δ4.4(d, 2H) for compound II; δ0.98(d, 12H), δ1.65(m, 6H) and δ4.6(t, 2H) for compound III. Elemental analysis showed: C:H:N = 3.67:4.21:2.40 (calculated, C:H:N = 3.72:4.15:2.46) for compound I; C:H:N = 45.20:5.81:20.33 (calculated, C:H:N = 45.15:5.79:20.26) for compound II; C:H:N = 48.09:6.33:18.89 (calculated, 48.19:6.43:18.74) for compound III.

Preparation of APS-modified silica gel

Silica gel (3 g) dried at 180°C for 10 h was suspended in dry toluene (100 ml). After APS (3 ml) had been added, the reaction mixture was refluxed under nitrogen for 10 h with stirring. After cooling, the APS-modified silica was collected by filtration and washed exhaustively with toluene, chloroform, methanol and diethyl ether, and then dried under vacuum in the presence of

TABLE I
CHARACTERISTICS OF APS-SILICA AND THE CSPs

	APS-silica	CSP-I	CSP-IIa	CSP-IIb	CSP-III
Elemental analysis					
C (%)	5.69	9.29	9.26	10.96	8.97
N (%)	1.65	2.60	2.87	2.85	2.69
Surface coverage ^a					
(mmol/g)	1.17	0.17	0.17	0.17	0.15
(μ mol/m ²)	3.34	0.49	0.49	0.49	0.43
End-capped ^b	-	+	-	+	+

^a The number of moles of *s*-triazine derivative of L-amino acids grafted per gram or unit surface area of APS-silica (based on N%).

^b + = End-capped by trimethylchlorosilane; - = not end-capped.

P₂O₅. The result of elemental analysis is given in Table I.

Preparation of CSPs

CSP-I, CSP-IIa, CSP-IIb and CSP-III were prepared by the following general procedure. The *s*-triazine derivative (5 mmol) and N-hydroxysuccinimide (0.01 mol) were dissolved in dimethylformamide (100 ml) and then DCC (0.01 mol) was added. The mixture was stirred first at 0°C for 1 h and thereafter at room temperature for 24 h. After removal of the suspended solid dicyclohexylurea, 3 g of APS-silica gel were added and the mixture stirred gently at 0°C for 1 h and then at room temperature for 48 h. The prepared CSP was collected and washed thoroughly with dimethylformamide, methanol, pure water, methanol and ether, and dried under vacuum in the presence of P₂O₅ to give the uncapped CSP.

The uncapped CSP (3 g) was suspended in toluene (100 ml), and trimethylchlorosilane (3 ml) was added at 0°C and stirred for 1 h, then at 40°C for 4 h under nitrogen. The reaction mixture was filtered and washed with toluene, methanol and ether, and dried under vacuum to give the capped CSP. The results of elemental analyses of all the prepared CSPs are given in Table I.

Chromatographic studies

Stainless-steel columns (250 mm × 4 mm I.D.) were packed by the balanced-density slurry tech-

nique with methanol as mobile phase under a head pressure of 720 kg/cm². The chromatographic experiments were carried on Waters HPLC system equipped with a Model 6000A pump, a U6K injector and a Model 440 UV ($\lambda = 254$ nm) detector. The analytes were derivatized with 3,5-dinitrobenzoyl chloride by a routine method before injection.

RESULTS

The CSPs were prepared conveniently by a three-step reaction, as shown in Fig. 2. In the first step, acetone-water binary solvents were chosen as reaction solvents and the proper ratio by volume was 1:5. Using this proper ratio of acetone-water binary solvents, L-amino acids without any derivatization were able to react with cyanuric chloride to give the expected disubstituted products in one step with high yield and high purity (supported by elemental analysis and m.p. results). It is noteworthy that the *s*-triazine derivatives must be transferred to an active ester before being bonded to APS-silica gel in the second synthetic procedure. Without active ester formation, the dicyclohexylurea, which was the by-product of amide formation, could not be completely removed from the reaction product and would exist in the prepared silica gel. When this unpurified bonded silica gel was used for column packing, unusually high column pressure and poor chromatographic resolution were obtained.

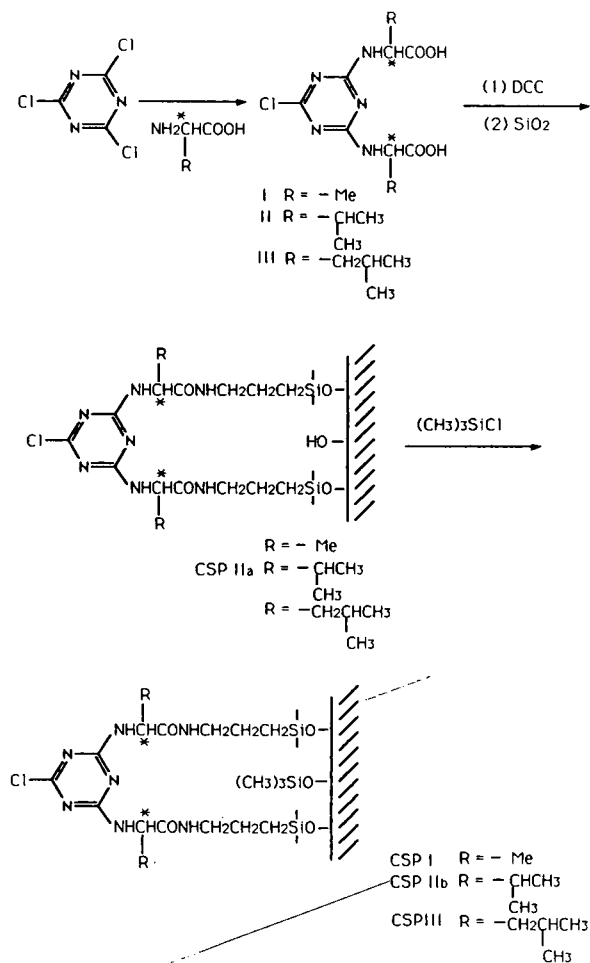


Fig. 2. The preparation procedure of chiral stationary phases.

The presence of the *s*-triazine derived chiral ligands on the silica surface of the prepared CSPs was characterized by elemental analysis (Table I). The surface coverage of the *s*-triazine chiral moiety on the silica gel was found to range from 0.15 to 0.17 mmol/g (0.43–0.49 $\mu\text{mol}/\text{m}^2$) based on nitrogen percentage. Further surface characterization was done by using the method of trifluoroacetic acid hydrolysis and HPLC identification [5]. The bonded-phase silica gel was hydrolysed in hot trifluoroacetic acid aqueous solution to cleave the amide linkage of the bonded-phases and followed by an HPLC identification of the components of these hydrolysed mixtures with the corresponding authentic samples (I–III).

The chromatographic results for the separation of five racemic amino acids on the prepared CSPs are summarized in Table II. It shows that there is little difference in α values of four CSPs. For convenience, CSP-II was chosen as the representative CSP to be further investigated and the typical chromatograms are shown in Figs. 3 and 4. The enantiomers of five racemic amino acids chosen in this study can be all resolved in these prepared CSPs. The racemic amino acids were reacted with dinitrobenzoyl chloride before being injected into the HPLC system and the chromatographic peaks were identified with the corresponding optically pure L-amino acids.

As shown in Table II, the capacity factor of a

TABLE II

HPLC SEPARATION OF DNB-DERIVATIZED RACEMIC AMINO ACIDS ON CSPs

The separation factor of the enantiomers, α , is the ratio of their capacity factors, and k'_1 is the capacity factor for the first-eluted enantiomer (D-form). The analytes were reacted with dinitrobenzoyl chloride before injection.

Analyte	CSP-I ^a		CSP-IIa ^b		CSP-IIb ^b		CSP-III ^b	
	k'_1	α	k'_1	α	k'_1	α	k'_1	α
Alanine	1.53	1.19	5.36	1.15	3.53	1.15	1.29	1.19
Valine	1.69	1.08	8.50	1.08	3.29	1.13	1.76	1.10
Leucine	2.34	1.21	8.86	1.15	4.88	1.15	2.82	1.19
Methionine	2.26	1.18	7.79	1.15	5.00	1.18	2.65	1.18
Phenylalanine	3.84	1.11	9.50	1.10	7.58	1.11	4.76	1.15

^a Mobile phase: 20% aqueous methanol–0.05 M ammonium hydroxide pH 6.8.

^b Mobile phase: 20% aqueous methanol–0.01 M ammonium hydroxide pH 7.0.

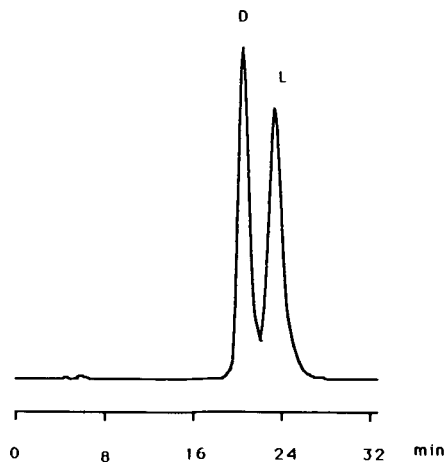


Fig. 3. The chromatogram for the resolution of dinitrobenzoyl-D,L-leucine on CSP-IIb. Mobile phase: methanol-water (20:80), 0.01 M ammonium acetate, pH 7.0, flow-rate: 1.5 ml/min.

given analyte on CSP-IIa is larger than that on CSP-IIb under the same chromatographic conditions. Because the structure and the surface coverage of the chiral moiety of CSP-IIa are the same as that of CSP-IIb, the only difference is whether or not the unreacted surface silanol was end-capped by trimethylchlorosilane (Fig. 2).

The capacity factors of a given analyte on the CSP-IIb were decreased when the pH values of

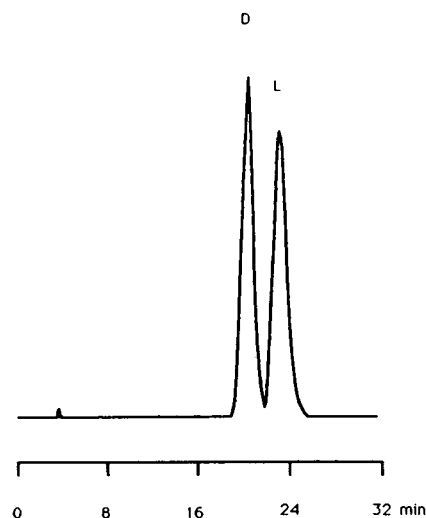


Fig. 4. The chromatogram for the resolution of dinitrobenzoyl-D,L-methionine on CSP-IIb. Mobile phase: methanol-water (20:80), 0.01 M ammonium acetate, pH 7.0, flow-rate: 1.3 ml/min.

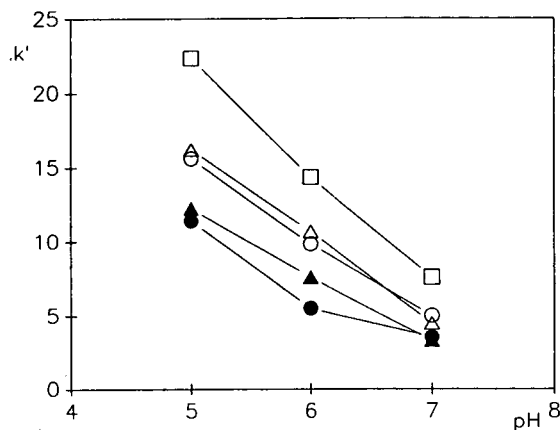


Fig. 5. The effect of the pH of mobile phase on the k_1' of analytes for chromatographic resolution of racemic amino acids on CSP-IIb. Mobile phase: methanol-water (20:80), ammonium acetate 0.01 M. Amino acids analytes were reacted with dinitrobenzoyl chloride before injection to HPLC. k_1' is the first-eluted enantiomer of the amino acid (D-form). ○ = Methionine; ● = alanine; △ = leucine; ▲ = valine; □ = phenylalanine.

mobile phases were increased from pH 5.0 to 7.0. Fig. 5 shows the effect of the pH value of the mobile phase on the capacity factor, k_1' , of the analytes on CSP-IIb. Five amino acids, after reaction with dinitrobenzoyl chloride, were chosen as analytes. Chromatographic results

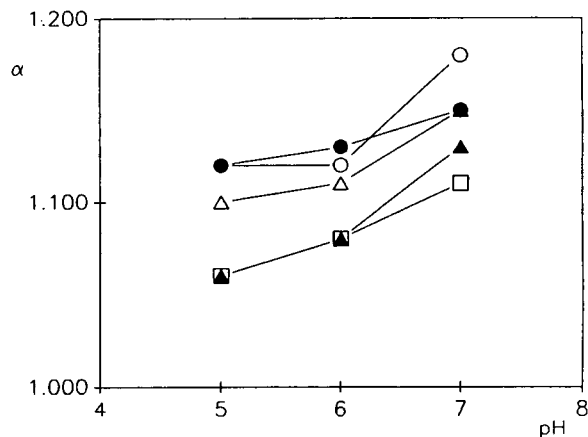


Fig. 6. The effect of the pH of mobile phase on the α -values of analytes for the resolution of enantiomers on CSP-IIb. Mobile phase: methanol-water (20:80), 0.01 M ammonium acetate. Amino acids analytes were reacted with dinitrobenzoyl chloride before injection into the HPLC system. Symbols as in Fig. 5.

indicated that the k' of D-valine, for example, was 12.5 when the pH of mobile phase was 5.0, but was only 3.3 when the pH of the mobile phase was 7.0.

However, the separation factor of a given racemic amino acid on the CSP-IIb is slightly increased when the pH of the mobile phase is increased from 5.0 to 7.0. Fig. 6 shows the effect of the pH value of the mobile phase on the separation factors, α , of enantiomers of analytes on CSP-IIb. Chromatographic results indicated that the α -value of the racemic DNB-methionine, for example, was 1.13 when the pH of the mobile phase was 5.0 but increased to 1.18 when the pH of the mobile phase was 7.0.

DISCUSSION

Preparation and characterization of CSPs

In general, non-esterified amino acids are poorly soluble in the organic solvents, while cyanuric chloride is little soluble in water but is soluble in organic solvent. In this study, it was found that using the proper ratio of the acetone–water solvent (1:5), a complete disubstituted reaction of L-amino acid with cyanuric chloride would occur at 40–50°C. In the preparation of CSPs, the presence of N-hydroxysuccinimide not only favours amide formation, but also leads to easy exclusion of dicyclohexylurea, a by-product precipitated from amide formation, before the subsequent addition of APS-modified silica. As a result, it prevents the extreme increase in column pressure caused by the fine particles of the by-product.

The double-bonded *s*-triazine structure on the CSP (Fig. 2) was assumed as a result of the synthetic procedure. But it was also supported indirectly by the chromatographic peak shape in the separation of DNB-derivatized amino acids in the reversed phase. The fact that no peak tailing occurred suggested the absence of carboxylic groups, which would be the other end-moiety of a single-bonded *s*-triazine derivative, on the surface of CSP.

Chromatographic properties of CSPs

The hydrophobic character of the prepared CSPs is illustrated by their chromatographic

behaviours. As shown in Table II, the capacity factors of analytes increase with an increase in the carbon number of the analytes. Moreover, the relationship between the capacity factors of analytes and the pH of the mobile phase, as shown in Fig. 5, also indicates that longer retention is obtained for the relatively hydrophobic carboxylic acids in their acid form rather than in carboxylate form of a given analyte on CSP-IIb.

The chromatographic results suggested that the uncapped silanol groups on the silica surface of CSP do not contribute to the discrimination of the enantiomers of analytes chosen in this study. As shown in Table II, the capacity factors on the CSP-IIa, in which silanol groups were not capped, are larger than those on the end-capped CSP-IIb, but the separation factors are almost unchanged on both CSPs. To this is attributed the fact that the free silanol sites on the CSP-IIa contributed to longer retention for the analytes but not to the chiral recognition.

In Fig. 6, the phenomenon of larger α -values of the DNB-amino acids on CSP-IIb in a higher pH mobile phase can be explained by the fact that there is an effective stereoselective interaction between the analyte, in carboxylate form in a high-pH solution, and CSP. Thus, the carboxylate form, which provides a stronger basic site, might form hydrogen bonds with the acidic site (N–H) of the amide linkage in CSP.

Table II shows that the prepared *s*-triazine-terminal CSPs afford effective enantioselectivity for DNB-derivatized racemic amino acids and that the D-enantiomer always elutes first in reversed-phase conditions. Obviously, a π – π interaction between the analyte (DNB derivative) and the *s*-triazine moiety of the CSP contributes to the chiral recognition.

Comparison of phase A and phase B

Although both of the CSPs (Fig. 1) contain an *s*-triazine moiety, phase A is derived from L-amino acids and phase B is derived from a tripeptide. Moreover, the bonding model of chiral moiety to the silica surface is also different. Phase B contains six chiral centres and four amide functional groups with the *s*-triazine ring on the inner part of the connection arm, while phase A contains only two chiral centres and two

amide groups with the *s*-triazine ring on the terminal of the brush of CSP. It is suggested that the terminal bis(L-amino acid)-substituted *s*-triazine moiety on the CSP seems to be conformationally “stiffer”, and therefore more favourable for chiral recognition.

CONCLUSIONS

The present results clearly indicate that the CSP with an *s*-triazine ring on the terminal of the brush (phase A), derived from L-amino acids instead of tripeptide, is effective enough to resolve the enantiomers of amino acids. The preparation of the CSPs is convenient by bonding 2,4-bis[carboxy(alkyl)methylamino]-6-chloro-*s*-triazine onto APS–silica gel through amide formation. The chromatographic results reveal that the CSPs show hydrophobic character

and can recognize DNB-derivatized racemic amino acids in reversed-phase HPLC.

ACKNOWLEDGEMENT

The authors thank the National Science Council, Taiwan, for financial support.

REFERENCES

- 1 M.H. Yang, C.E. Lin and J.K. Fan, *Silicon Material Research Program (Monograph Series, No. 1)*, National Science Council, Taiwan, 1986, p. 75.
- 2 N. Oi, M. Nagase and Y. Sawada, *J. Chromatogr.*, 292 (1984) 427.
- 3 J.Y. Lin and M.H. Yang, *J. Chin. Chem. Soc.*, 38 (1991) 543.
- 4 M.H. Yang and J.Y. Lin, *J. Chromatogr.*, 631 (1993) 165.
- 5 B. Feibush, M.J. Cohen and B.L. Karger, *J. Chromatogr.*, 282 (1983) 3.

Observation of a conformational effect in peptide molecule by reversed-phase high-performance liquid chromatography

Michal Lebl

Selectide Corporation, 1580 E. Hanley Boulevard, Tucson, AZ 85737 (USA)

(Received February 23rd, 1993)

ABSTRACT

RP-HPLC of analogues of oxytocin containing a reduced peptide bond was studied using various columns and buffers. Anomalous behavior of one analogue served as a basis for the discussion of possible conformational consequences of this substitution.

INTRODUCTION

Reversed-phase liquid chromatography has been used for conformational studies in peptide chemistry by several workers [1–7], because the interaction of a peptide with the rigid hydrophobic surface may provide information about the flexibility of the peptide chain or about the accessibility of various hydrophobic residues in the chain, depending on its conformation. Extensive studies in this field have been performed by Hodges' and Houghten's groups [1–6], who synthesized several model peptides containing the same amino acid residues and showed that their retention depends on their most probable conformation. Another paper [7] speculated about the similar conformation of a number of oxytocin analogues based on the fact that their retentions followed the same dependence as those of similarly modified benzene derivatives.

Recently we have synthesized a range of oxytocin analogues with one peptide bond at a time replaced with a CH_2NH bond [8]. We found that in almost all instances the biological activity of these analogues was substantially decreased if not completely eliminated. The two exceptions

were the analogues with CH_2NH replacement between Cys and Tyr in positions 1 and 2 and between Pro and Leu in positions 7 and 8. In the former instance the analogue was a fairly potent inhibitor and in the latter it was an active agonist. We were interested in establishing whether this activity change is reflected by a change in retention on a reversed-phase material.

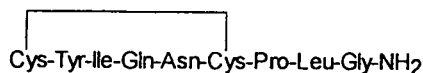
EXPERIMENTAL

The analogues used in this study were the same as those synthesized earlier [8]. Isocratic high-performance liquid chromatography (HPLC) was carried out on an SP-8800 instrument equipped with an SP-8450 detector and SP-4290 integrator (all from Spectra Physics, Santa Clara, CA, USA). We used columns of Vydac C_{18} (250×4 mm I.D., $5 \mu\text{m}$) (Separations Group, Hesperia, CA, USA) and Separon SI C_{18} (250×4 mm I.D., $5 \mu\text{m}$) (Tessek, Prague, Czech Republic). The mobile phases used were mixtures of methanol with either 0.05% trifluoroacetic acid in water or 0.1 M ammonium acetate (pH 7.5). Chromatography was per-

formed at room temperature with a flow-rate of 1 ml/min.

RESULTS AND DISCUSSION

The retention times of the oxytocin analogues containing the reduced peptide bond (**II-IX**) were compared with those of oxytocin (**I**) using two different columns with reversed phases and buffers of acidic and neutral pH. As can be seen from Table I, reduction of peptide bond resulted in the expected decrease in the retention times with an acidic mobile phase, and therefore in increased hydrophilicity, in all but one instance. The most pronounced decrease was observed for **IV** and **VIII**, where the reduced bond is situated between Ile and Asn or at the carboxyterminus of the molecule. This behavior can be explained by the relatively high exposure of these bonds to the exterior of the molecule (thus increasing its



Oxytocin

hydrophilicity), as they are claimed to connect (in the native molecule) the corner residues of putative β -turns. A relatively small decrease in retention time was observed for **IX**, with the reduced bond between Leu and C-terminal Gly. However, **II** showed an increased retention in the comparison with the parent molecule oxytocin.

The overall hydrophobicities calculated from the partial hydrophobicities of all the structural elements in the molecules of **II-IX** are apparently identical (the secondary amino group is completely ionized) and therefore the higher retention of **II** in an acidic mobile phase can be explained only by the better interaction of this compound with the stationary phase. Inaccessibility of the generated amino group might explain the smaller than expected decrease in retention time, but it cannot explain its increase.

Retention times in a neutral mobile phase may not reflect precisely the hydrophobicity of the analogues, as under these conditions amino groups might be ionized to different extents, depending on the character of the amino acid residue. Therefore, we did not attempt to draw any conclusions from the behavior of the analogues in a neutral mobile phase. The com-

TABLE I
RETENTION CHARACTERISTICS OF OXYTOCIN ANALOGUES

No.	Analogue	k'			
		Vydac C ₁₈		Separon SI C ₁₈	
		pH 2 ^a	pH 7.5 ^b	pH 2 ^c	pH 7.5 ^d
I	Oxytocin (OXT)	9.00	6.74	7.56	5.77
II	[¹ Ψ ² -CH ₂ NH]OXT	13.25	7.89	10.62	6.13
III	[² Ψ ³ -CH ₂ NH]OXT	2.37	11.86	2.46	9.93
IV	[³ Ψ ⁴ -CH ₂ NH]OXT	1.94	6.67	2.05	5.91
V	[⁴ Ψ ⁵ -CH ₂ NH]OXT	4.50	6.54	4.15	5.69
VI	[⁵ Ψ ⁶ -CH ₂ NH]OXT	3.87	6.40	4.07	5.32
VII	[⁶ Ψ ⁷ -CH ₂ N]OXT	2.37	4.86	2.53	5.12
VIII	[⁷ Ψ ⁸ -CH ₂ NH]OXT	2.06	9.03	2.36	7.08
IX	[⁸ Ψ ⁹ -CH ₂ NH]OXT	6.75	8.96	5.24	6.86

^a 27.5% MeOH.

^b 38% MeOH.

^c 45% MeOH.

^d 57% MeOH.

parison of two mobile phases might be further complicated by their different ionic strengths and the use of different counter ions [3].

A peptide bond imposes certain restrictions on the conformation of the peptide chain, which is released when it is replaced with the CH₂NH group. We have shown recently [9] that the steric fixation of the aromatic side-chain in position 2 in oxytocin had a dramatic effect on its biological activity. It is well known (for a review, see, e.g., ref. 10) that the hydrophobicity of the amino-terminal position of the oxytocin molecule is responsible for the interaction with its uterotonic receptor. A change in configuration of the aromatic amino acid in position 2 led to the design of potent uterotonic inhibitors. Elimination of steric restrictions by peptide group replacement led to a similar result to a change in configuration in this position. Also, in both instances the retention on a reversed phase was substantially increased. (For the behavior of analogues containing D-amino acids in position 2, see refs. 11–13.)

We can speculate that the increased retention of II in an acidic mobile phase on a reversed phase reflects a conformational relaxation in the amino-terminal part of the oxytocin molecule, which correlates well with the properties of a uterotonic inhibitor that were observed for this analogue.

ACKNOWLEDGEMENT

This work was supported in part by the Czechoslovak Academy of Sciences, Grant No. 45531.

REFERENCES

- 1 N.E. Zhou, P.D. Semchuk, C.M. Kay and R.S. Hodges, in R.S. Hodges and C.T. Mant (Editors), *HPLC of Peptides and Proteins: Separation, Analysis and Conformation*, CRC Press, Boca Raton, FL, 1991, p. 643.
- 2 J.M.R. Parker, D. Guo and R.S. Hodges, *Biochemistry*, 25 (1986) 5425.
- 3 D. Guo, C.T. Mant and R.S. Hodges, *J. Chromatogr.*, 386 (1987) 205.
- 4 S.E. Blondelle and R.A. Houghten, *Pept. Res.*, 4 (1991) 12.
- 5 J.M. Ostresh, K. Buttner and R.A. Houghten, in R.S. Hodges and C.T. Mant (Editors), *HPLC of Peptides and Proteins: Separation, Analysis and Conformation*, CRC Press, Boca Raton, FL, 1991, p. 633.
- 6 S.E. Blondelle and R.A. Houghten, *Biochemistry*, 31 (1992) 12688.
- 7 M. Lebl, *J. Chromatogr.*, 242 (1982) 342.
- 8 M. Lebl, M. Souček, J. Trojnar, R. Kasprzykovska and J. Slaninová, *Int. J. Pept. Protein Res.*, submitted for publication.
- 9 M. Lebl, P. Hill, W. Kazmierski, L. Karászová, J. Slaninová, I. Frič and V.J. Hruby, *Int. J. Pept. Protein Res.*, 36 (1990) 321.
- 10 K. Jošt, M. Lebl and F. Brtník (Editors), *CRC Handbook of Neurohypophyseal Hormone Analogs*, CRC Press, Boca Raton, FL, 1987.
- 11 B. Larsen, B.L. Fox, M.F. Burke and V.J. Hruby, *Int. J. Pept. Protein Res.*, 13 (1979) 12.
- 12 M. Lebl, *J. Chromatogr.*, 264 (1983) 459.
- 13 M. Lebl, T. Barth, L. Servitová, J. Slaninová and K. Jošt, *Collect. Czech. Chem. Commun.*, 50 (1985) 132.

Interaction of catechol-2,3-dioxygenase of *Pseudomonas putida* with immobilized histidine and histamine

Karsten Haupt and M.A. Vijayalakshmi*

Laboratoire de Technologie des Séparations, Université de Technologie de Compiègne, B.P. 649, 60206 Compiègne Cedex (France)

(First received June 16th, 1992; revised manuscript received March 26th, 1993)

ABSTRACT

Catechol-2,3-dioxygenase (EC 1.13.11.2) from *Pseudomonas putida* as a model enzyme was purified from a bacterial crude extract in one step using affinity chromatography on immobilized histamine. In order to understand better the nature of the interaction, the adsorption of the enzyme on different gels having histidine and histamine coupled to Sepharose 4B was studied. The dissociation constants determined in the temperature range 4–37°C by an equilibrium binding analysis are between $0.95 \cdot 10^{-7}$ and $2.8 \cdot 10^{-7}$ M and between $2.6 \cdot 10^{-7}$ and $4.0 \cdot 10^{-7}$ M for histamine-carboxyhexyl Sepharose and histidyl-carboxyhexyl Sepharose, respectively. The standard enthalpy and entropy changes are different for these two gels, reflecting the different natures of the forces involved in the interaction.

INTRODUCTION

Amino acids have been used as pseudo-bio-specific ligands in affinity chromatography for several years [1]. For example, arginine, tryptophan and lysine have been coupled to Sepharose for the purification of fibronectin, cellulase and plasminogen [2–4]. Histidine has also been used as a ligand to adsorb proteins [1,5–7]. Owing to its numerous properties such as weak hydrophobicity and charge-transfer ability and a wide range of pK_a values [8,9], which make it unique among the amino acids, it can be used as a general ligand in pseudo-biospecific chromatography [5]. Several workers have observed that the fixation of the ligand to the matrix via a spacer arm can greatly improve the binding properties of the gel towards the molecule to be separated. Thus El-Kak and Vijayalakshmi [7] increased the binding capacity, yield and purification factor during the purification of mouse

IgG on immobilized histidine by using amino-hexyl as a spacer arm. These parameters were also improved by using histamine instead of histidine. However, there is not much information about the adsorption mechanism and the nature of the interaction forces on which the histidine-ligand affinity chromatography is based.

In this work, the interaction of catechol-2,3-dioxygenase (C-2,3-D) (EC 1.13.11.2) from *Pseudomonas putida* BL 3 as a model enzyme with different supports with immobilized histidine and histamine was studied. This enzyme is an extradiol-type dioxygenase and catalyses the conversion of catechol to 2-hydroxy-muconic 6-semialdehyde with the insertion of two atoms of molecular oxygen [10]. The enzyme consists of four identical subunits with a molecular mass of 35 155 [11,12] and contains 4 g-atom of iron(II) per mole of enzyme [11,13]. It is unstable in air owing to the oxidation of iron(II) to iron(III) [14]. The enzyme, which has already been purified by other methods [13], showed a high affinity for histamine-carboxyhexyl Sepharose (hista-CH Sepharose) and histidyl-carboxyhexyl

* Corresponding author.

Sepharose (his-CH Sepharose) gels. This paper describes the purification of the enzyme with these gels and the determination of the thermodynamic constants of the protein–ligand interaction by a non-chromatographic method using equilibrium binding analysis in order to understand better the nature of the interaction.

EXPERIMENTAL

Materials

Sepharose 4B and carboxyhexyl- and aminohexyl-Sepharose 4B were obtained from Pharmacia (Uppsala, Sweden). 1-Ethyl-3-(3-dimethylaminopropyl)carbodiimide, L-histidine and histamine were obtained from Sigma (St. Louis, MO, USA). All other reagents were of analytical-reagent grade.

The *Pseudomonas putida* BL3 biomass was supplied by Dr. Schöpp (Department of Biochemistry, University of Leipzig, Leipzig, Germany). This strain, which is a derivative of the strains BL1 and ATCC 33015 [15], obtained after plasmid transfer by Ackermann [16], was fermented on benzyl alcohol as carbon source.

Preparation of the gels coupling histidine and histamine

His-CH Sepharose and histidyl-aminohexyl Sepharose were prepared by coupling histidine to carboxyhexyl Sepharose 4B and aminohexyl Sepharose 4B, respectively, by carbodiimide at pH 4.5–6 with constant stirring for 16 h at room temperature as described by the manufacturer. Hista-CH Sepharose was prepared in the same manner by coupling histamine to carboxyhexyl Sepharose 4B. Histidine Sepharose was prepared as described previously [3] by coupling histidine to Sepharose 4B activated with epichlorohydrin. The proposed structures of the gels are shown in Fig. 1.

Preparation of the enzyme crude extract

After suspension of the bacterial cells in 25 mM Tris–HCl buffer (pH 7.5) to an absorbance of $A_1^{600} = 12$, the cells were disrupted in an Aminco French pressure cell at 5000 p.s.i. (1 p.s.i. = 6894.76 Pa). The resulting suspension was centrifuged for 2 h at 10 000 g and the

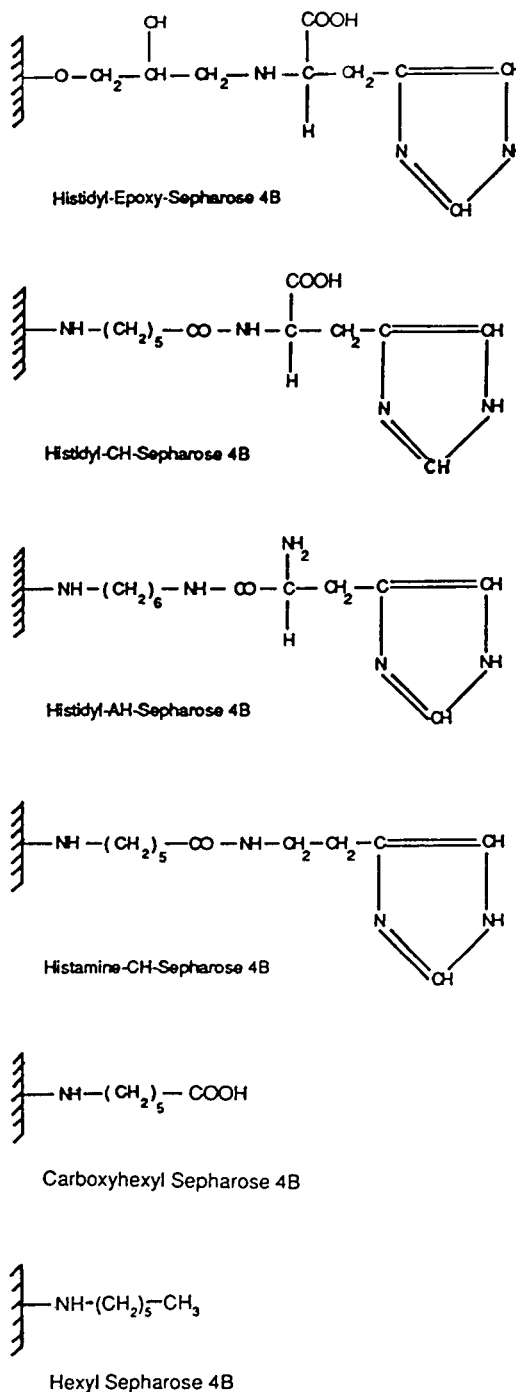


Fig. 1. Proposed structures of the various gels.

supernatant (crude extract), which had a protein concentration of about 4 mg/ml, was directly applied for chromatography.

Chromatographic procedures

Purification was performed at 20°C using a jacketed column (4 cm × 1.2 cm I.D.) containing hista-CH Sepharose which was thermostated using a water-bath connected to a refrigeration unit (Bioblock). The column was connected to an automated Econo liquid chromatographic system (Bio-Rad Labs.). Chromatography was carried out at a flow-rate of 35 ml/h. A 3–10-ml volume of the crude extract was injected into the column after equilibration with 25 mM Tris-HCl buffer (pH 7.5). Elution was performed at the same flow-rate with 25 mM Tris-HCl buffer (pH 7.5) containing increasing amounts of sodium chloride (0.1–1 M). The absorbance of the eluate was measured at 280 nm; fractions of 2 ml were collected. After each experiment, the column was washed with three column volumes of a 0.05 M sodium hydroxide solution followed by water and finally by the equilibration buffer.

Enzyme assay

The activity of catechol-2,3-dioxygenase was assayed spectrophotometrically by measuring the increase in absorbance at 375 nm as described by Nozaki [14]. One unit of enzyme activity is defined as the amount that catalyses the formation of 1 μmol of the product per minute at 20°C.

Protein determination

The protein concentration was determined by the method of Bradford [17]. Crystalline bovine serum albumin was used as a reference protein. In the crude extract, protein was determined according to Kalb and Bernlohr [18]. This method uses the absorbances at 230 and 260 nm and eliminates the interference of nucleic acids.

Native polyacrylamide gel electrophoresis

The purity of the separated enzyme was analysed by native polyacrylamide gel electrophoresis as described by Davis [19] using a 7.5% (w/v) gel. The gel was stained with Coomassie Brilliant Blue. The method described by Müller *et al.* [20] was used to stain for enzyme activity. The gel was incubated for 10 min in a 1 mM solution of ammonium iron(II) sulphate in 25 mM Tris-HCl

buffer (pH 7.5), followed by a 1 mM solution of catechol in the same buffer. A yellow band appeared after a few minutes.

Equilibrium binding analysis

The equilibrium binding experiments were carried out according to the method described by Hutchens *et al.* [21]. The gel was equilibrated with 25 mM 3-(N-morpholino)propane sulphonic acid (MOPS) buffer (pH 7.5) (hista-CH Sepharose) or 25 mM 2-(N-morpholino)ethane sulphonic acid (MES) buffer (pH 6) (his-CH Sepharose) and then allowed to settle. A homogeneous suspension was then prepared with an equal volume of the equilibration buffer, 40-μl aliquots of which were added to a series of Eppendorf incubation tubes (1.5 ml) in duplicate containing 100 μl of the protein solution at various concentrations in the equilibration buffer (between 80 and 1000 μg/ml). For the equilibrium binding experiments, a twice rechromatographed and additionally gel filtration-purified preparation of C-2,3-D was used (during preparation, buffer solutions containing 15% of ethanol were used to prevent oxidative inactivation of the enzyme). The tubes were incubated for 30 min in a thermostated water-bath with intermittent gentle rotation to give adequate mixing. The period of 30 min was chosen from preliminary incubation of a series of control tubes at different temperatures, which did not show any change in the supernatant protein concentration after 20 min. The suspensions were then centrifuged at 180 g for 30 s using a thermostated centrifuge and 100 μl of the clear supernatant were taken from each tube to determine the concentration of the unbound protein.

The data were analysed according to Hutchens *et al.* [21] using linear Scatchard plots obtained from the equation $[PL]/[P] = -1/K_D \cdot [PL] + L_t/K_D$, which was obtained from the Langmuir adsorption isotherm after derivation and linearization. The slope gives the dissociation constant K_D of the protein–ligand complex and the intercept gives the maximum binding capacity L_t ; $[P]$ is the concentration of unbound protein and $[PL]$ the concentration of the protein–ligand complex at equilibrium. $[PL]$ can be calculated from

$[PL] = [P_0] - [P]$, where $[P_0]$ is the total protein concentration applied to the gel.

The thermodynamic parameters for the adsorption can be obtained by determining K_D at different temperatures. From the Van't Hoff reaction isotherm $\Delta G = \Delta G^0 - RT \ln K_D$, at equilibrium when $\Delta G = 0$, the equation $\Delta G^0 = RT \ln K_D$ is obtained. ΔG^0 can be calculated at a given temperature from the dissociation constant. The temperature dependence of K_D is given by the Van't Hoff reaction isobar. In its integrated form, $\ln K_D = \Delta H^0/RT + l$ (l is an integration constant), when plotting $\ln K_D$ versus $1/T$, ΔH^0 is given by the slope if a straight line is obtained (in this case, ΔH^0 does not depend on temperature [22]). From the Gibbs–Helmholtz relationship, $\Delta G^0 = \Delta H^0 - T \Delta S^0$, the standard entropy change ΔS^0 can be obtained.

RESULTS

The adsorption of catechol-2,3-dioxygenase on a series of Sepharose gels was studied. The best results concerning the adsorption and elution conditions and the recovery of enzyme activity were obtained with his-CH Sepharose at pH 6 and with hista-CH Sepharose at pH 6–8 (Table I). On histidyl Sepharose and histidyl-amino-hexyl Sepharose the adsorption was very low. Carboxyhexyl Sepharose as a reference gel did

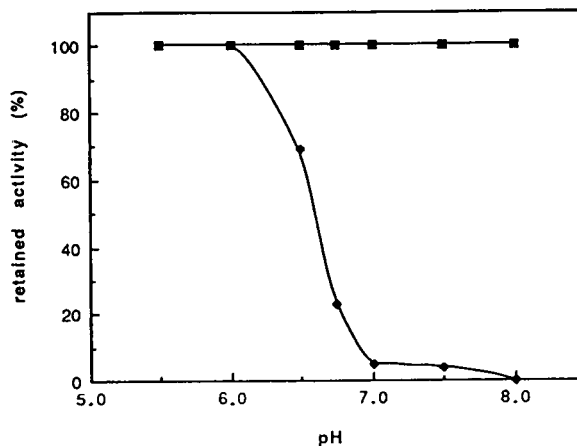


Fig. 2. pH dependence of the adsorption of catechol-2,3-dioxygenase on (◆) his-CH Sepharose and (■) hista-CH Sepharose.

not adsorb the enzyme, whereas on hexyl Sepharose no elution could be achieved under mild conditions using 1 M NaCl in the elution buffer.

The effect of the pH of the adsorption buffer on the retention of catechol-2,3-dioxygenase on hista-CH Sepharose and his-CH Sepharose was investigated. The first gel showed an adsorption of 100% of the enzyme which did not depend on the pH, whereas for his-CH Sepharose the retention was nearly 100% up to pH 6 but decreased to 5% at pH 7 (Fig. 2).

TABLE I

RETENTION OF CATECHOL-2,3-DIOXYGENASE ON DIFFERENT SUPPORTS DEPENDING ON THE pH OF ADSORPTION

RA is retained activity and ECA is eluted cumulating activity at 0.2–1 M NaCl in the elution buffer

Support	pH 6		pH 7		pH 8	
	RA (%)	ECA (%)	RA (%)	ECA (%)	RA (%)	ECA (%)
Histidyl Sepharose	20	12	0	0	0	0
Histidyl-AH Sepharose	23	10	0	0	0	0
His-CH Sepharose	100	70	5	5	0	0
Hista-CH Sepharose	100	65	100	100	100	100
Carboxyhexyl Sepharose	0	0	0	0	0	0
Hexyl Sepharose	100	0	100	0	100	0

Chromatography on hista-CH Sepharose

Chromatography was carried out at pH 7.5 on hista-CH Sepharose because the enzyme is unstable at pH values lower than 6.5.

The result of the chromatography on hista-CH Sepharose is shown in Fig. 3. The first large peak contains the unbound protein. Peak 2 contains the protein eluted with 0.1 M NaCl in the buffer. In these peaks no C-2,3-D activity could be detected. The enzyme was eluted with 0.15 M NaCl (peak 3), whereas peak 4 (0.3 M NaCl) and peak 5 (1 M NaCl) did not contain any enzyme activity. The specific activity of C-2,3-D increased from 4.9 U/mg in the crude extract to 53 U/mg (purification factor 11); the affinity yield was 42%.

In a native polyacrylamide gel electrophoresis, peak 3 showed an intense protein band with only traces of contaminating proteins (Fig. 4, lane 2). Staining for enzyme activity proved that the main band corresponded to C-2,3-D.

Equilibrium binding experiments

The equilibrium binding experiments were carried out at different temperatures (see Table II). In the Scatchard plots, straight lines were obtained (Fig. 5). The K_D and L_t values calculated from the Scatchard plots are given in Table II. The dissociation constant of the protein–ligand complex decreases with increasing temperature, ranging from $2.8 \cdot 10^{-7}$ to $9.5 \cdot 10^{-8}$ M for hista-CH Sepharose, and increases with in-

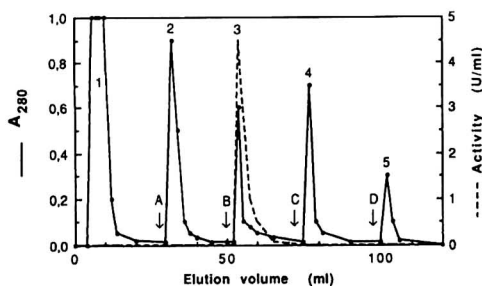


Fig. 3. Elution pattern of the crude extract on hista-CH Sepharose at 20°C. Elution with (A) 0.1 M NaCl, (B) 0.15 M NaCl, (C) 0.3 M NaCl and (D) 1.0 M NaCl in Tris-HCl buffer (pH 7.5). The numbers 1–5 indicate the protein peaks obtained.

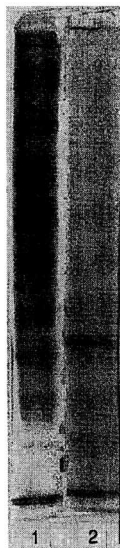


Fig. 4. Native polyacrylamide gel electrophoresis of the active fractions of the chromatography on hista-CH Sepharose. 1 = Crude extract; 2 = peak 3.

creasing temperature from $2.6 \cdot 10^{-7}$ to $4.0 \cdot 10^{-7}$ M for his-CH Sepharose. The apparent maximum binding capacity was found to be between 4 and 6 mg protein/ml gel and between 1.8 and 2.2 mg/ml gel, respectively. In the plot of $\ln K_D$ versus $1/T$, straight lines were obtained (Fig. 6). The ΔH^0 values calculated from this plot were 5.6 kcal/mol for hista-CH Sepharose and -2.2 kcal/mol for his-CH Sepharose (Table II). The ΔG^0 values calculated for the different temperatures ranged from -8.3 kcal/mol at 4°C to -9.9 kcal/mol at 37°C and from -8.3 kcal/mol at 4°C to -9.1 kcal/mol at 37°C, respectively (Table II). The ΔS^0 values are 49.8 cal/mol·K for hista-CH Sepharose and 22.2 cal/mol·K for his-CH Sepharose (Table II).

The K_D values of the protein–ligand complex with hista-CH Sepharose were also determined in the presence of different concentrations of NaCl as neutral salt (relative to solvent structuring ability [23]) and a cosmotropic salt $[(NH_4)_2SO_4]$. The results are shown in Fig. 7. K_D increases with increasing NaCl concentration up to 0.2 M and then remains approximately

TABLE II

DISSOCIATION CONSTANTS (K_D) AND MAXIMUM BINDING CAPACITIES (L_i) DETERMINED AT DIFFERENT TEMPERATURES FOR HISTA-CH SEPHAROSE AND HIS-CH SEPHAROSE

r is the correlation coefficient in the linear regression, ΔH^0 is the standard enthalpy change, ΔS^0 the standard entropy change and ΔG^0 the standard free energy change calculated from the dissociation constants.

Parameter	Hista-CH Sepharose				His-CH Sepharose		
	4°C	15°C	26°C	37°C	4°C	20°C	37°C
K_D ($10^{-7} M$)	2.8	2.3	1.6	0.95	2.6	3.2	4.0
L_i (mg/ml)	4.5	4.3	6.0	5.6	1.9	2.0	2.2
r	0.98	0.98	0.98	0.98	0.99	0.99	0.99
ΔH^0 (kcal/mol) ^a		5.6				-2.2	
ΔS^0 (cal/mol · K) ^a		49.8				22.2	
ΔG^0 (kcal/mol) ^a	-8.2	-8.7	-9.3	-9.8	-8.3	-8.7	-9.2

^a 1 cal = 4.184 J.

constant up to a concentration of 2 *M*. In presence of $(NH_4)_2SO_4$, K_D reaches a maximum at a concentration of 0.3 *M* whereas at higher concentrations better adsorption is obtained. In $(NH_4)_2SO_4$ at a concentration of more than 1.3 *M* the enzyme protein is not fully soluble.

DISCUSSION

The difference in retention of the enzyme on the different gels shows that adsorption depends on several factors such as hydrophobic and electrostatic interactions and hydrogen bonding, which can change with the surrounding pH depending on the *pK* values of the different chemical groups involved; interactions are thus modified, as can be seen for his-CH Sepharose (Fig. 2). The increase in adsorption of the enzyme on his-CH Sepharose as compared with histidyl Sepharose might be due to the added carboxyhexyl arm, as histidine is probably not accessible by large molecules such as C-2,3-D. Comparing the adsorption of the enzyme to his-CH Sepharose and to carboxyhexyl Sepharose as reference gel, we can conclude that the imidazole ring is necessary for adsorption. The poor retention on histidyl-aminohexyl Sepharose might be due to an electrostatic repulsion by the positively charged amino group. Apparently, coupling of a hexyl arm alone to Sepharose

renders the gel very hydrophobic and elution cannot be achieved under mild conditions.

Chromatography on hista-CH Sepharose shows that this gel has a good specificity for C-2,3-D, which is expressed by the high affinity ($K_D = 0.23 \mu M$ at 15°C; see Table II), and good resolution. Starting from a bacterial crude extract containing a large number of proteins (Fig. 4, lane 1), we observed in the purest fractions eluted with 0.15 *M* NaCl in native polyacrylamide gel electrophoresis an intense protein band (Fig. 4, lane 2) which corresponds to C-2,3-D, as revealed by an active coloration according to ref. 20. In addition, elution was achieved under very mild conditions. The specific activity for the purified enzyme of 53 U/mg is less than indicated in ref. 13, which is probably due to the oxidative inactivation of the C-2,3-D during the chromatographic procedures. This effect can be overcome by the addition of 15% of ethanol to all the eluting buffers, which also increased the yield from 42% to about 80%. In this instance, the elution pattern was not changed except that the elution volumes decreased (data not shown).

We chose to work with hista-CH Sepharose for the purification of the enzyme owing to the good capacity and resolution of the gel and the possibility of working at pH values above 7 where the enzyme is more stable. Chromatographic results on his-CH Sepharose at pH 6 showed that

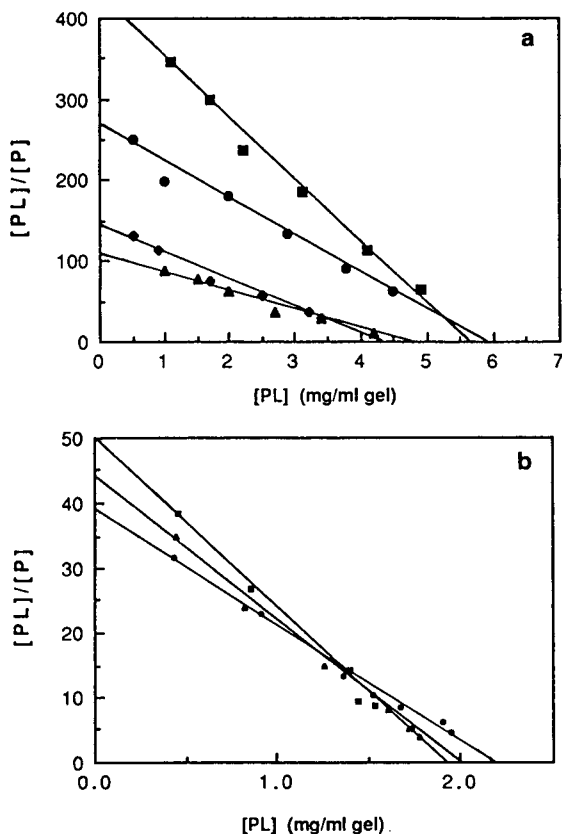


Fig. 5. (a) Scatchard plots of the equilibrium binding analysis of the adsorption of catechol-2,3-dioxygenase on his-CH Sepharose at different temperatures: \blacksquare = 37; \bullet = 26; \blacklozenge = 15; \blacktriangle = 4°C. (b) Scatchard plots of the equilibrium binding analysis of the adsorption of catechol-2,3-dioxygenase on his-CH Sepharose at different temperatures: \bullet = 37; \blacktriangle = 20; \blacksquare = 4°C.

the activity yield is low but the resolution is equal to that obtained with his-CH Sepharose.

The interaction of C-2,3-D with his-CH Sepharose and his-CH Sepharose was studied more thoroughly by using an equilibrium binding analysis. This method was put forward by Hutchens and co-workers [21,24], who studied the interactions of model proteins with immobilized transition metals. With a Scatchard plot, the dissociation constant of the protein–ligand complex and the maximum binding capacity can be determined. The latter may be higher when determined in a dynamic mode owing to the formation of a Nernst layer on the surface of the gel beads. As shown by Hutchens *et al.* [21], this method gives the same results as those obtained

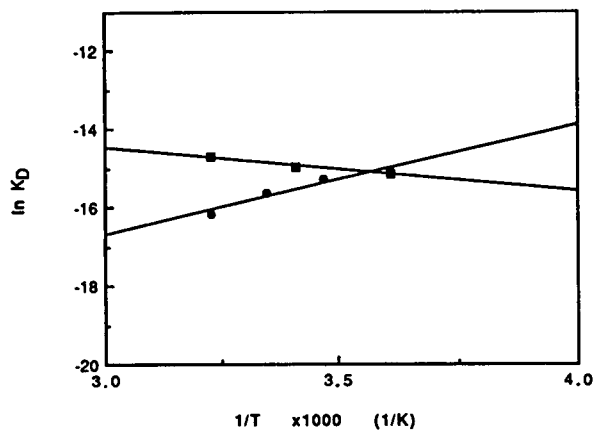


Fig. 6. Dependence of the dissociation constant of the enzyme-immobilized ligand complex on temperature. \blacksquare = His-CH Sepharose; \bullet = his-CH Sepharose.

by chromatographic methods (frontal analysis, zonal elution). In addition, the requirement in protein is low and the time of manipulation is short.

We determined the dissociation constants for the adsorption of C-2,3-D on the immobilized ligand at different temperatures (Table II). The increase in adsorption with temperature (K_D decreases) as determined for his-CH Sepharose (Table II) implies that hydrophobic forces are important for the interaction. Similar results were reported by Cacace and Sada [25] for hydrophobic adsorptions. With his-CH Sepha-

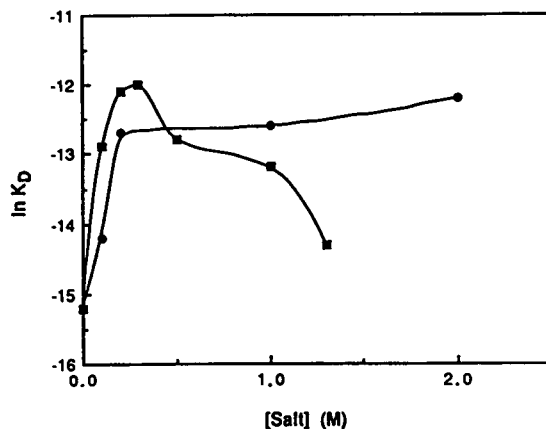


Fig. 7. Dissociation constant K_D of the catechol-2,3-dioxygenase-his-CH Sepharose complex at different concentrations of (●) NaCl and (■) $(NH_4)_2SO_4$.

rose the adsorption decreased with increasing temperature, which is probably due to the supplementary interaction possibility given by the charged carboxyl group. For this gel, electrostatic forces and hydrogen bonding play a more important role in the adsorption process than with hist-CH Sepharose. As is already well known, hydrophobic interactions are the only ones of the interactions discussed above that increase with temperature [26]. This is probably due to a conformational change of the protein molecule when adsorbed on a hydrophobic matrix [27], which is facilitated at higher temperatures. For hist-CH Sepharose, the temperature dependence of the dissociation constants is smaller than for hist-CH Sepharose, indicating that the contribution of hydrophobic forces and the others discussed above to the interaction is well balanced.

The standard free energy value calculated from the dissociation constants is not different for the two gels, but the additional carboxyl group causes a change in the standard enthalpy which is positive for hist-CH Sepharose and negative for hist-CH Sepharose, and the positive standard entropy also decreases. This is not surprising because hydrophobic interactions cause a net disordering of the system and the entropy increases. These results indicate that the adsorption might be entropy driven with hist-CH Sepharose and more enthalpy driven for hist-CH Sepharose. In the presence of an increasing concentration of ammonium sulphate as cosmotropic salt, hydrophobic interactions are favoured, which is shown by the decrease in K_D values for hist-CH Sepharose when using salt concentrations higher than 0.5 M. In the presence of a neutral salt (NaCl) this effect was not observed (Fig. 7).

In conclusion, we can say that histidine and histamine can be successfully used as ligands in affinity chromatography and proteins can be specifically purified even from a mixture of a large number of proteins such as a bacterial crude extract. The contribution of the different molecular forces to the adsorption process depends thereby on different factors such as the coupling mode of the ligand to the polymer support, the presence or not of a spacer arm, the

structure of the adsorption site of the molecule to be purified and the adsorption conditions. It seems also that not histidine or histamine alone but the ensemble of amino acid, spacer arm and polymer support is the real ligand.

ACKNOWLEDGEMENT

We gratefully thank Dr. Schöpp of the Department of Biochemistry, University of Leipzig, for carrying out the fermentational work and supplying the biomass.

REFERENCES

- 1 M.A. Vijayalakshmi, *Trends Biotechnol.*, 7 (1989) 71.
- 2 M. Vuento and A. Vaheri, *Biochem. J.*, 183 (1979) 331.
- 3 M.A. Vijayalakshmi and J. Porath, *J. Chromatogr.*, 177 (1979) 201.
- 4 L. Suamri, F. Spitz and L. Arzadon, *J. Biol. Chem.*, 251 (1976) 3693.
- 5 S. Kanoun, L. Amourache, S. Krishnan and M.A. Vijayalakshmi, *J. Chromatogr.*, 376 (1986) 259.
- 6 A. Akoum, M.A. Vijayalakshmi, P. Cardon, B. Fournet, M. Sigot and J.F. Guespin-Michel, *Enzyme Microb. Technol.*, 9 (1987) 426.
- 7 A. El-Kak and M.A. Vijayalakshmi, *J. Chromatogr.*, 570 (1991) 29.
- 8 G.M. Blackburn, H.L.H. Dodds and D.J. Shire, in R.M.S. Semellie (Editor), *Chemical Reactivity and Biological Role of Functional Groups in Enzymes (Biochemical Society Symposia, Vol. 31)*, Academic Press, London, 1970, p. 81.
- 9 W.P. Jenks, in R.M.S. Semellie (Editor), *Chemical Reactivity and Biological Role of Functional Groups in Enzymes (Biochemical Society Symposia, Vol. 31)*, Academic Press, London, 1970, p. 259.
- 10 O. Hayaishi, M. Nozaki and M.T. Abbott, in D. Boyer (Editor) *The Enzymes, Part B, Vol. XII*, Academic Press, London, 3d ed., 1975, p. 140.
- 11 M. Nozaki, *Top. Curr. Chem.*, 78 (1979) 145.
- 12 C. Nakai, H. Kagamiyama, M. Nozaki, T. Nakazawa, S. Inouye, Y. Ebina and A. Nakazawa, *J. Biol. Chem.*, 258 (1983) 2923.
- 13 C. Nakai, K. Hori, H. Kagamiyama, T. Nakazawa and M. Nozaki, *J. Biol. Chem.*, 248 (1983) 2916.
- 14 M. Nozaki, *Methods Enzymol.*, 17A (1970) 522.
- 15 W. Schöpp, C. Toasperm and H. Tauchert, *J. Basic Microbiol.*, 25 (1985) 187.
- 16 J.U. Ackermann, *Dissertation zur Promotion A*, University of Leipzig, Leipzig, 1984.
- 17 M.M. Bradford, *Anal. Biochem.*, 72 (1976) 248.
- 18 V.F. Kalb, Jr., and R.W. Bernlohr, *Anal. Biochem.*, 82 (1977) 362.
- 19 B.J. Davis, *Ann. N.Y. Acad. Sci.*, 121 (1964) 404.

- 20 R. Müller, S. Haug, J. Eberspächer and F. Lingens, *Hoppe-Seyler's Z. Physiol. Chem.*, 358 (1977) 797.
- 21 T.W. Hutchens, T.-T. Yip and J. Porath, *Anal. Biochem.*, 170 (1988) 168.
- 22 G. Fischer in A. Schellenberger (Editor), *Enzymkatalyse*, Gustav Fischer, Jena, 1990, p. 25.
- 23 K.D. Collins and M.M. Washabaugh, *Q. Rev. Biophys.*, 18 (1985) 323.
- 24 T.W. Hutchens and T.-T. Yip, *Anal. Biochem.*, 191 (1990) 160.
- 25 M.G. Cacace and A. Sada, *J. Chromatogr.*, 376 (1986) 103.
- 26 V.V. Mozhaev and K. Martinek, *Enzyme Microb. Technol.*, 6 (1984) 50.
- 27 S. Lin, P. Oroszlan and B.L. Karger, *J. Chromatogr.*, 536 (1991) 17.

Efficient separation of natural ribonucleotides by low-pressure anion-exchange chromatography

Tomáš Cihlář* and Ivan Rosenberg

Institute of Organic Chemistry and Biochemistry, Czech Academy of Sciences, Flemingovo nám 2, 166 10 Prague 6 (Czech Republic)

(First received October 15th, 1992; revised manuscript received January 18th, 1993)

ABSTRACT

Chromatographic conditions for the separation of twelve purine and pyrimidine ribonucleotides (mono-, di- and triphosphates) by ion-exchange chromatography were investigated. Two types of anion exchangers with tertiary or quaternary ammonium functionalities (DEAE and QAE types) were compared. Parameters examined included pH of the mobile phase, elution buffer composition and flow-rate. Excellent resolution of all compounds in 50 min was achieved with a strongly basic anion exchanger in the formate form using a linear gradient of ammonium formate with constant formic acid concentration in the mobile phase. The proposed method utilizes (1) a strongly basic anion exchanger based on a macroporous hydrophilic organic polymer, (2) a volatile elution buffer system which permits one-run purification of nucleotides (no further column operation is required, *e.g.*, desalting) and (3) low-pressure liquid chromatographic equipment with simple column preparation. The method was applied to the purification of [U-¹⁴C]adenosine-5'-diphosphate and other radiolabelled nucleotides and their analogues in order to obtain highly radiochemically pure compounds.

INTRODUCTION

Forty years ago, a strong anion exchanger (based on styrene-divinylbenzene copolymer, Dowex type) was applied for the first time for the separation of nucleotides [1], and subsequently the same material has frequently been utilized for this purpose [2–4]. DEAE-Sephadex [5], PEI-cellulose [6], acriflavine gel [7] and, in particular cases, cation exchangers [8,9] were also applied for separations of nucleotide mixtures.

The introduction of microparticulate materials as efficient packing sorbents [10–12] allowed the development of high-performance liquid chromatography (HPLC). Several workers have reviewed methods of nucleotide analysis using HPLC [13–15]. This area includes two method-

ologies: anion-exchange chromatography [16–21] and reversed-phase chromatography on octadecyl-bonded silica gel [22–24]. The latter is often used in a mode of ion-pair chromatography employing tetra-*n*-butylammonium [25–27], trimethyl- or triethylammonium [28] and *n*-heptyltriethylammonium [29] cations as counter ions. Modern high-performance anion-exchange chromatography mostly utilizes quaternary ammonium functionalities and phosphate- or chloride-based buffers. To increase the column efficiency and/or selectivity of separation, water-miscible organic modifiers [17,30–32] have been introduced.

Our previous experience with nucleoside and nucleotide separations using a strongly basic anion exchanger of the benzyltrimethylammonium type [33] based on a rigid macroporous hydrophilic copolymer of 2-hydroxyethyl methacrylate and ethylene glycol dimethacrylate [34–36] (Separon HEMA series) prompted us to use

* Corresponding author.

in further studies medium-basic (diethylaminoethyl type) and strongly basic (triethylammoniummethyl type) exchangers derived from the same matrix. These commercially available exchangers exhibit very good mechanical properties, excellent chemical resistance at extreme pH values and negligible volume changes caused by variations in ionic strength and pH of the mobile phase.

In this work, we studied the chromatographic behaviour of twelve ribonucleotides with respect to the pH and composition of the mobile phase, flow-rate and type of anion exchanger used. The influence of these parameters on the elution order of the compounds is discussed. We found conditions for the baseline separation of all twelve components using a strongly basic anion exchanger (QAE type) in the formate form. We applied this chromatographic system to the purification of some ^3H - and ^{14}C -labelled nucleotides and their analogues intended for metabolic studies. In all instances we achieved highly efficient separations and obtained compounds with radiochemical purities of more than 98%.

Although this chromatographic work is directed towards the area of the micropreparation of nucleotides from mixtures after chemical or enzymatic synthesis at micromolar levels, the method can also be used for the analytical separation of nucleotides in biological materials. Further studies concerning especially the influence of temperature on the nucleotide separation and optimization of the anion-exchange packing procedure are in progress.

EXPERIMENTAL

Separon HEMA-1000 Q (QAE type, particle size $10\ \mu\text{m}$, $0.60\ \text{mequiv./g}$) and Separon HEMA-1000 DEAE (DEAE type, particle size $15\ \mu\text{m}$, $1.22\ \text{mequiv./g}$) (the molecular mass exclusion limit of the basic matrix is 10^6 , determined for dextrans), were obtained from Laboratorní přístroje (Prague, Czech Republic). 5'-Monophosphates of adenosine (AMP), cytidine (CMP), guanosine (GMP), uridine (UMP) and cytidine 5'-triphosphate (CTP) were purchased from Sigma (St. Louis, MO, USA).

5'-Diphosphates of adenosine (ADP), cytidine (CDP), guanosine (GDP) and uridine (UDP) and 5'-triphosphates of adenosine (ATP), guanosine (GTP) and uridine (UTP) were obtained from Boehringer (Mannheim, Germany).

The liquid chromatograph consisted of an LCP 3001 high-pressure, pulse-free pump with a GP 3 gradient programmer (low-pressure side gradient formation), a UV detector operating at 254 nm, a TZ 4620 line recorder and a CI 100 computing integrator (all from Laboratorní přístroje). A sample loop injector was purchased from Knauer (Bad Homburg, Germany). A glass column ($150\ \text{mm} \times 8\ \text{mm}$ I.D.) including adjustable end-pieces was made in the Institute mechanical workshop.

Preparation of the anion-exchanger column

Ion exchangers were converted into the chloride form by gradual rinsing with sodium hydroxide ($1\ \text{mol/l}$; $50\ \text{ml}$ per gram of the resin), water, dilute hydrochloric acid ($1\ \text{mol/l}$; $100\ \text{ml}$ per gram of the resin) and again with water to neutral pH of the filtrate. Further decantation of the resin in acetone ($100\ \text{ml/g}$; three times) provided dust-free material which was dried *in vacuo* at room temperature for 15 h. A slurry of the exchanger in water (20%, w/v) was transferred into the glass column at a flow-rate of $3\ \text{ml/min}$. After bed settling (bed height *ca.* $130\ \text{mm}$) the column was closed with an adjustable end-piece and the bed was then compressed by hand to the final height of $120\ \text{mm}$. The column was washed either with potassium chloride solution ($1\ \text{mol/l}$, $50\ \text{ml}$) or with ammonium formate solution ($2\ \text{mol/l}$, $100\ \text{ml}$) at a flow-rate of $3\ \text{ml/min}$ and finally equilibrated with the appropriate starting buffer.

Chromatography

Chromatography was usually performed for 60 min at a flow-rate of $1\ \text{ml/min}$. The pressure never exceeded 10 bar. Elution of nucleotides from the resin in the chloride form was achieved using a linear gradient of potassium chloride from 0.05 to $0.35\ \text{mol/l}$ at various pH values of the leading buffer (potassium phosphate, $0.05\ \text{mol/l}$). The appropriate pH was adjusted by

addition of dilute phosphoric acid or potassium hydroxide solution.

In separations using a strong anion exchanger in the formate form, a linear gradient of ammonium formate from 0 to 0.6 mol/l at various formic acid concentrations (ranging from 0 to 0.15 mol/l) was used.

A representative mixture of nucleotides was injected into the column in microgram amounts (10 μ g of each per 100 μ l of the sample).

Determination of radiochemical purity

The samples (2 kBq) were analysed by ion-pair HPLC using a 250 \times 4.6 mm I.D. Separon RPS SGX (7 μ m) column (Tessek, Prague, Czech Republic). Elution buffer A contained 0.05 mol/l $(\text{NH}_4)_2\text{HPO}_4$ and 0.003 mol/l tetrabutylammonium hydrogensulphate (pH 6.8); buffer B had the same composition but contained 20% (v/v) acetonitrile. The separation was carried out for 30 min with a linear gradient

from A–B (95:5) to A–B (40:60) and with a flow-rate of 1 ml/min. The radioactivity of 0.5-ml fractions was measured using a Beckman LS-6000A scintillation counter following the addition of 5 ml of Aquasafe 300 scintillation cocktail (Zinsser Analytic, UK).

RESULTS AND DISCUSSION

Effect of pH and buffer composition

The pH of the mobile phase is one of the most important factors for the resolution of species by ion-exchange chromatography. In this work, the effect of pH in the range 3–9 on the retention time (expressed as the capacity factor, k') was studied. Generally, both exchangers showed the expected separation patterns (Fig. 1a and b).

At low pH, the retention was decreased owing to the mutual weaker ionic interactions between nucleotides and the exchanger. This is caused both by suppression of phosphate group dissocia-

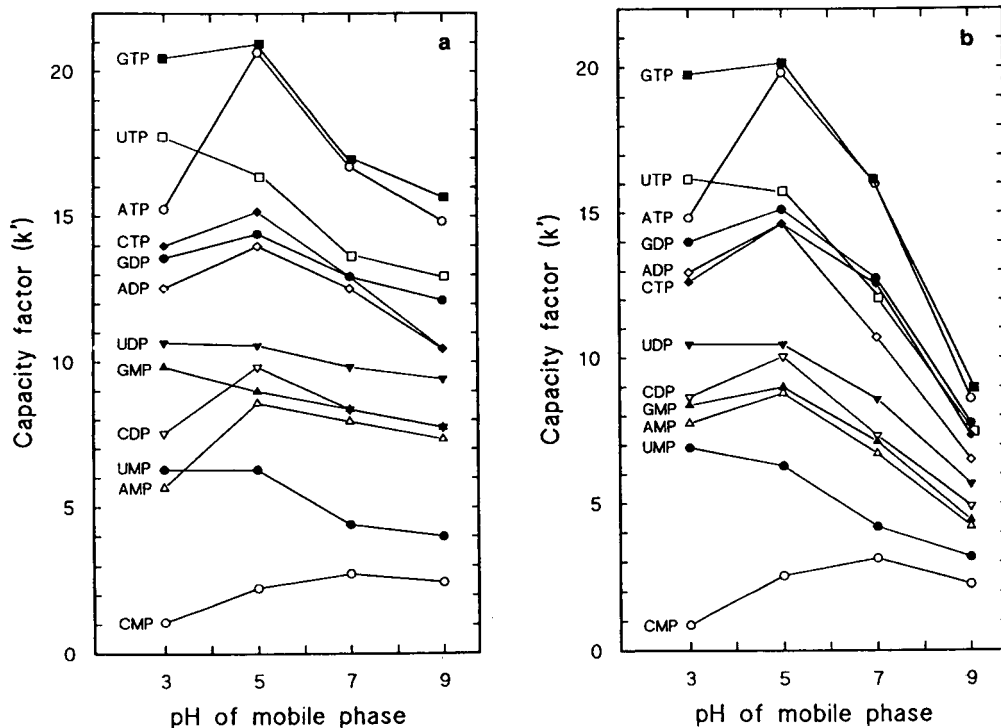


Fig. 1. Dependence of the capacity factor (k') of particular ribonucleotides on the pH of the mobile phase. Separations were performed on (a) Separon HEMA-1000 Q and (b) Separon HEMA-1000 DEAE with a 60-min linear gradient of KCl from 0.05 to 0.35 mol/l at a flow-rate 1 ml/min. The mobile phase contained 0.05 mol/l potassium phosphate adjusted to a given pH.

tion and by protonation of the amino groups of cytosine, adenine and guanine. In our experiments, adenine nucleotides showed the largest and uracil nucleotides the smallest shortening of retention. Although the retention maximum of most of the compounds started around pH 5, such conditions interfere with the desired separation, especially of purine nucleotides, using either exchanger.

As the pH increases to the basic region, the retention of nucleotides decreases and different behaviours of the two exchangers are observed. The shortening of retention is greater for the medium-basic anion exchanger because partially deprotonated diethylaminoethyl groups of the resin do not permit such strong interactions with phosphate groups of the nucleotides.

The desired separation of nucleotides using the QAE-type exchanger in the chloride form was achieved at pH 3, where only the CTP–GDP pair was not separated (Fig. 2).

In subsequent studies the QAE type of exchanger in the formate form was chosen. It was observed that not only the ionic strength but also the concentration of formic acid in the mobile phase substantially affect the quality of separation. We kept the gradient slope and concentration range of ammonium formate constant

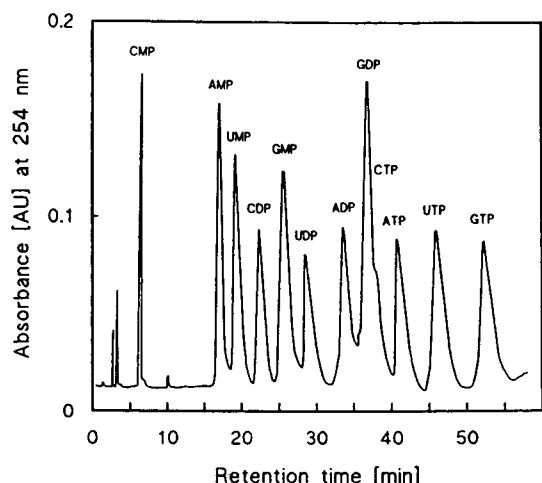


Fig. 2. Chromatography of a mixture of twelve ribonucleotides on Separon HEMA-1000 Q under the conditions described in Fig. 1. The pH of the mobile phase was adjusted to 3.0.

and in each run only the molarity of formic acid was changed. It was found that formic acid at concentrations up to 0.09 mol/l significantly affected capacity factors of the nucleotides (Fig. 3). Above this concentration (up to 0.15 mol/l), the capacity factors were found to be independent of formic acid concentration (data not shown). The best resolution of all twelve ribonucleotides was achieved at 0.06 mol/l formic acid. We also studied this separation system using a basic pH of the mobile phase. In this instance formic acid was replaced with ammonia solution. However, the quality of the separation decreased very significantly under these conditions.

An attempt to increase the efficiency of nucleotide separation using organic modifiers in the mobile phase [methanol and acetonitrile up to 50% (v/v) were used] failed completely. Contrary to expectation, we observed a significant

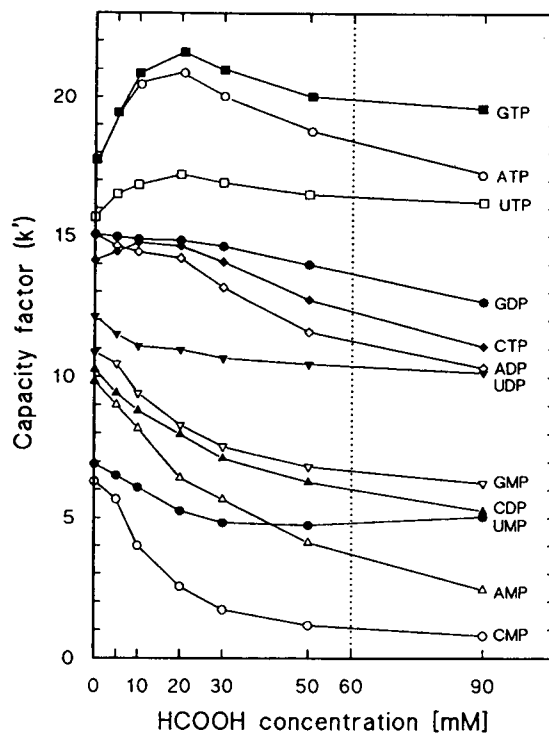


Fig. 3. Dependence of the capacity factor (k') of individual nucleotides on the concentration of formic acid in the mobile phase. Separations were performed on Separon HEMA-1000 Q with a 60-min linear gradient of ammonium formate from 0 to 0.60 mol/l at a flow-rate 1 ml/min. The mobile phase contained an appropriate concentration of formic acid.

decrease in the efficiency of separation (data not shown).

Effect of flow-rate

Under the most favourable chromatographic conditions using the exchanger in the formate form, we studied the influence of flow-rate on the quality of resolution (expressed as the resolution factor R_s) in the range 0.5–1.5 ml/min. The separation of four pairs of nucleotides was substantially affected by this parameter (Fig. 4). We found the usual dependence for the well separated pairs CDP–GMP, UDP–ADP and CTP–GDP up to 1.2 ml/min. Higher flow-rates decreased only the resolution of CDP–GMP.

A completely different behaviour was found for the ADP–CTP pair. We did not observe any significant resolution at flow-rates up to 1.0 ml/min, but a dramatic change occurred at 1.2 ml/min, where a baseline separation was obtained.

The optimum resolution of all twelve nucleotides was achieved at a flow-rate of 1.2 ml/min (linear speed 2.4 cm/min). Fig. 5 shows the chromatogram for this run and Table I gives the retention times (t_R), capacity factors (k'), res-

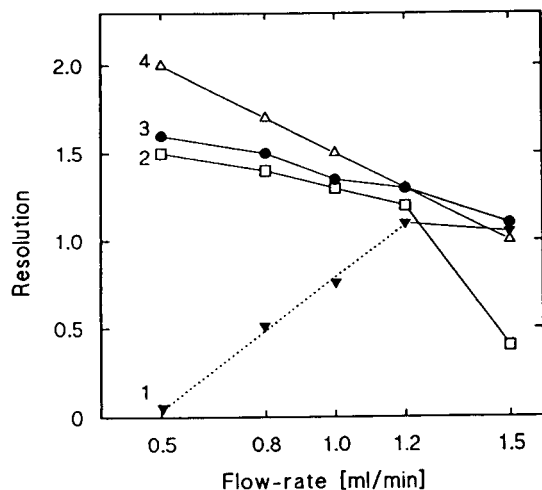


Fig. 4. Dependence of the resolution factor (R_s) of four neighbouring pairs of nucleotides on the flow-rate of the mobile phase. The separations were performed on Separon HEMA-1000 Q using a 60-min linear gradient of ammonium formate from 0 to 0.60 mol/l. The mobile phase contained 0.06 mol/l formic acid. Pairs of nucleotides: 1 = ADP–CTP; 2 = CDP–GMP; 3 = CTP–GDP; 4 = UDP–ADP.

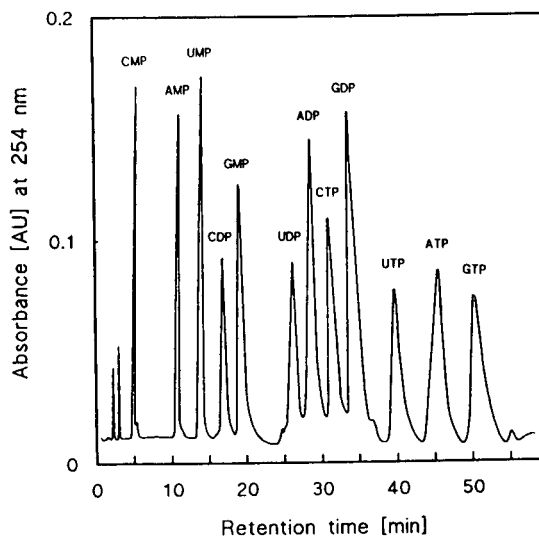


Fig. 5. Chromatography of a mixture of twelve ribonucleotides on Separon HEMA-1000 Q under the conditions given in Fig. 4. The flow-rate of the mobile phase was 1.2 ml/min.

olution factors (R_s), number of theoretical plates (N), heights equivalent to a theoretical plate (HETP) and asymmetry factors (A_s).

Use of the system for purification of radiolabelled nucleotides

Chromatography on the strongly basic anion exchanger was used to purify several radiolabelled nucleotides and nucleotide analogues that we needed with very high radiochemical purity for metabolic studies.

[U- 14 C]ADP can be mentioned as an example of such a purification procedure. Storage at -20°C for several years resulted in partial decomposition of this labelled compound and it was necessary to remove the impurities before it could be used. The one-step purification procedure was performed as follows: 7.4 MBq of the sample (specific activity 13 GBq/mmol) were applied to a column of Separon HEMA-1000 Q in the formate form and purified using a 30-min linear gradient of ammonium formate from 0 to 0.3 mol/l with 0.06 mol/l formic acid. A 3-ml fraction corresponding to the elution of [U- 14 C]ADP was collected, evaporated and co-dis-

TABLE I

CHROMATOGRAPHIC RESULTS FOR RIBONUCLEOTIDE SEPARATION USING THE STRONGLY BASIC ANION EXCHANGER SEPARON HEMA-1000 Q

Linear gradient of ammonium formate from 0 to 0.6 mol/l for 60 min. The mobile phase contained 0.06 mol/l formic acid. Flow-rate, 1.2 ml/min.

Ribonucleotide	t_R (min)	k'	N	HETP (μm)	R_s	A_s
CMP	4.9	1.0	3330	37		1.0
AMP	11.8	3.9	3090	39	9.8	1.1
UMP	13.7	4.7	2460	49	1.7	1.1
CDP	17.0	6.1	2510	48	2.3	1.3
GMP	18.8	6.8	1960	61	1.2	2.3
UDP	27.5	10.5	3140	38	4.0	1.6
ADP	29.7	11.4	3690	32	1.3	2.2
CTP	32.2	12.4	3990	30	1.1	2.1
GDP	35.0	13.6	3720	32	1.3	2.4
UTP	41.5	16.3	4240	28	2.3	2.3
ATP	46.0	18.2	4056	30	1.4	1.9
GTP	50.6	20.1	3530	34	1.3	3.0

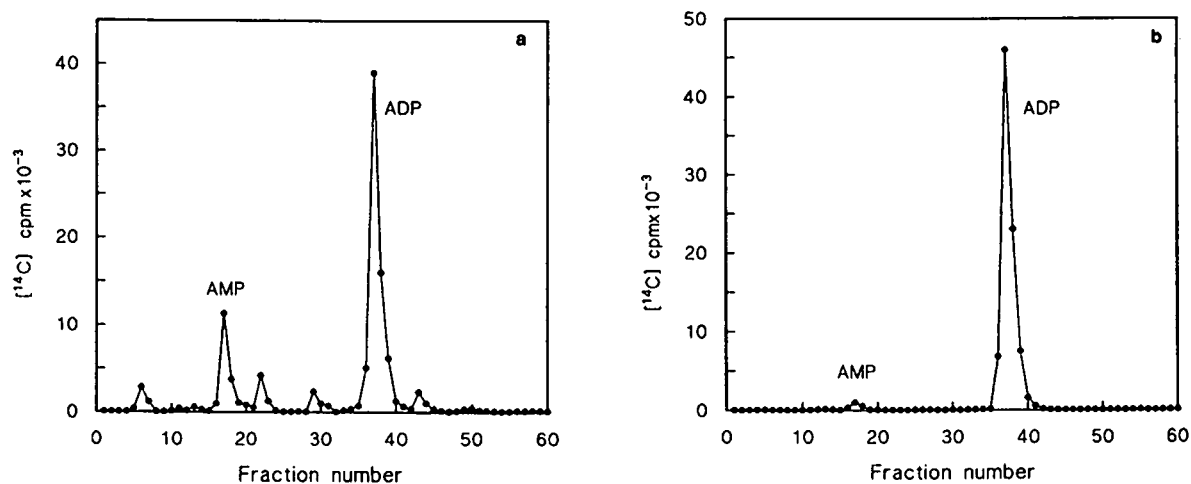


Fig. 6. Radiochemical purity of $[U-^{14}\text{C}]$ ADP (a) before and (b) after purification on Separon HEMA-1000 Q. Analysis was carried out using ion-pair HPLC under the conditions described in Experimental.

tilled several times with water on a Speedvac to remove traces of the elution buffer components. The radiochemical purity of the sample was found to be higher than 98% using ion-pair HPLC. Fig. 6 shows the purity of [U-¹⁴C]ADP before and after purification. Similar results were achieved in the purification of [U-¹⁴C]AMP, [U-¹⁴C]GMP and several ³H- and ¹⁴C-labelled nucleotide analogues.

Use of the volatile elution buffer system enables the purification to be carried out rapidly and simply and therefore this procedure is suitable especially for the purification of higher phosphates of nucleotides because of their lower stability.

ACKNOWLEDGEMENT

This work was supported by Grant No. 45508 of the Grant Agency of the Czech Academy of Sciences.

REFERENCES

- W.E. Cohn, *J. Am. Chem. Soc.*, 71 (1949) 2275.
- N.G. Anderson, J.G. Green and M.L. Barber, *Biochemistry*, 6 (1963) 153.
- H.W. Heldt and M. Klingenberg, *Methods Enzymol.*, 10 (1967) 482.
- M. Hori, *Methods Enzymol.*, Vol. 10 (1967) 381.
- I.A. Caldwell, *J. Chromatogr.*, 44 (1969) 331.
- K.H. Pflueger, *Anal. Biochem.*, 81 (1977) 136.
- J.M. Egly, *J. Chromatogr.*, 215 (1981) 243.
- F.R. Blattner and M.P. Erickson, *Anal. Chem.*, 18 (1967) 220.
- F. Murakami, S. Rokushita and H. Hatano, *J. Chromatogr.*, 53 (1970) 584.
- C.B. Horváth, B. Preiss and S.R. Lipsky, *Anal. Chem.*, 39 (1967) 1422.
- C.B. Horváth and S.R. Lipsky, *Anal. Chem.*, 41 (1969) 1227.
- J.J. Kirkland, *J. Chromatogr. Sci.*, 8 (1969) 72.
- P.R. Brown, *High Pressure Liquid Chromatography*, Academic Press, New York, 1973.
- C. Horváth, *Methods Biochem. Anal.*, 21 (1973) 79.
- J.X. Khym, *Analytical Ion-exchange Procedures in Chemistry and Biology*, Prentice-Hall, Englewood Cliffs, NJ, 1974, pp. 168–182.
- A. Floridi, C.A. Palmerini and C. Fini, *J. Chromatogr.*, 138 (1977) 203.
- H.E. Edelson and J.G. Lawless, C.T. Wehr and S.R. Abbott, *J. Chromatogr.*, 174 (1979) 409.
- E. Freese, Z. Olempska-Beer and M. Eisenberg, *J. Chromatogr.*, 284 (1984) 125.
- E. Nissinen, *Anal. Biochem.*, 106 (1980) 497.
- R.A. De Abreu, J.M. Van Baal, J.A.J.M. Bakkeren, C.H.M.M. De Bruyn and E.D.A.M. Schretlen, *J. Chromatogr.*, 227 (1982) 45.
- R.P. Singhal, *Eur. J. Biochem.*, 43 (1974) 245.
- M.W. Taylor, H.V. Hershey, R.A. Levine, K. Coy and S. Olivelle, *J. Chromatogr.*, 219 (1981) 133.
- H. Martinez-Valdez, R.M. Kothari, H.V. Hershey and M.W. Taylor, *J. Chromatogr.*, 247 (1982) 307.
- A. Wakizaka, K. Kurosaka and E. Okuhara, *J. Chromatogr.*, 162 (1979) 319.
- N.E. Hoffman and J.C. Liao, *Anal. Chem.*, 49 (1977) 2231.
- J. Harmenberg, A.H.J. Karlsson and G. Gilljam, *Anal. Biochem.*, 161 (1987) 26.
- R.T. Toguzov, Y.V. Tikhonov, A.M. Pimenov, V.Y. Prokudin, W. Dubiel, M. Ziegler and G. Gerber, *J. Chromatogr.*, 434 (1988) 447.
- Ch.Y. Ip, D. Ha, P.W. Morris, M.L. Puttemans and D.L. Venton, *Anal. Biochem.*, 147 (1985) 180.
- R.A.V. Hodge and R.M. Perkins, *Antimicrob. Agents Chemother.*, 33 (1989) 223.
- R.P. Singhal and W.E. Cohn, *Biochemistry*, 12 (1973) 1532.
- R.P. Singhal and W.E. Cohn, *Anal. Biochem.*, 45 (1972) 585.
- R.P. Singhal, *Arch. Biochem. Biophys.*, 152 (1972) 800.
- I. Rosenberg and A. Holý, *Czech. Pat.*, AO 209268 (1983).
- J. Čoupek, M. Křiváková and S. Pokorný, *J. Polymer. Sci., Poly. Symp.*, 42 (1973) 18.
- J. Volková, M. Křiváková, M. Patzelová and J. Čoupek, *J. Chromatogr.*, 76 (1973) 159.
- J. Hradil, M. Křiváková, P. Starý and J. Čoupek, *J. Chromatogr.*, 79 (1973) 99.

CHROMSYMP. 2855

Coupled-column reversed-phase liquid chromatography–UV analyser for the determination of polar pesticides in water

E.A. Hogendoorn

Laboratory of Organic Analytical Chemistry, National Institute of Public Health and Environmental Protection (RIVM), P.O. Box 1, 3720 BA Bilthoven (Netherlands)

U.A.Th. Brinkman

Department of Analytical Chemistry, Free University, De Boelelaan 1083, 1081 HV Amsterdam (Netherlands)

P. van Zoonen*

Laboratory of Organic Analytical Chemistry, National Institute of Public Health and Environmental Protection (RIVM), P.O. Box 1, 3720 BA Bilthoven (Netherlands)

(First received October 9th, 1992; revised manuscript received April 8th, 1993)

ABSTRACT

Coupled-column RPLC with UV detection using direct large volume injections of up to 4 ml can be used for the rapid and sensitive determination of single polar pesticides in environmental water samples. The limits of determination for pesticides such as bentazone and isoproturon are 0.1 $\mu\text{g/l}$ in real-life samples and the sample throughput is 5–7/h. Linearity is observed over at least three decades and the repeatability is satisfactory (relative standard deviations 3–7% at spiking levels of 0.1–0.5 $\mu\text{g/l}$). The set-up is fully automated and shows good robustness. The coupled-column RPLC–UV analyser has successfully been used in several monitoring programmes.

INTRODUCTION

Today there is a growing concern over the contamination of drinking-water sources by pesticides. The European Community (EC) Directive on the Quality of Water Intended for Human Consumption states (in paragraph OJL 229 30.80) that the concentration of pesticides and related products should not exceed the level of 0.1 $\mu\text{g/l}$ for individual compounds and 0.5 $\mu\text{g/l}$ for total pesticides. Consequently, there is a

need for fast, sensitive and reliable techniques for the determination of pesticides in aqueous environmental samples. Ideally, it should be possible to meet the above requirements by injecting an aqueous sample of interest into an analyser without any sample pretreatment.

In many laboratories reversed-phase column liquid chromatography (RPLC) is routinely used to determine polar pesticides in environmental water samples. In almost all instances, however, time consuming sample pretreatment is required and the total analytical procedure cannot be carried out on-line. Still, in recent years an important step forward has been made by the

* Corresponding author.

further development of so-called coupled-column or column-switching procedures which involve prepreparation of a sample on the first —often low-efficiency— column, heart-cutting of the analyte-containing fraction to the second column and final analysis of this fraction on the latter —invariably high-efficiency— column. If such procedures are based on RPLC-type separations and are used for the analysis of aqueous samples, it is an additional advantage that relatively large volumes can be injected without causing extensive band broadening. In other words, a certain degree of on-line trace enrichment can be effected. Such approaches are well documented [1–8] and do not require further discussion. However, problems are encountered when highly polar analytes have to be determined. Retention now is low even on highly hydrophobic C₁₈-bonded-silica phases and, consequently, trace enrichment becomes difficult because the analyte starts to elute during injection. Moreover, clean-up becomes less efficient, because the possibility of separating the analytes of interest from the invariably present early-eluting interferences will be rather limited.

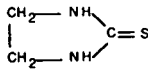
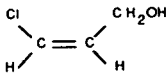
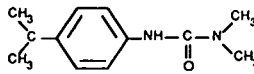
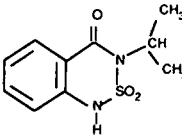
In recent papers, we have used the above

approach for the trace-level determination of three very polar analytes, viz. chloroallyl alcohol (CAAL) [9], ethylenethiourea (ETU) [10] and methylisothiocyanate (MITC) [11]. When two LC columns of essentially the same high efficiency were used in a coupled-column LC–UV set-up, the solutes of interest could be determined in water samples down to a level of 1 µg/l by means of direct large-volume (200–800 µl) injections. The total time of analysis was a mere 5–7 min. Unfortunately, however, each of the quoted analytes displayed one distinctly unfavourable characteristic, viz. very low retention on C₁₈-bonded silica (ETU), an extremely non-selective detection wavelength (CAAL), or a small molecular extinction coefficient (MITC) (see Table I). This prevented a further improvement of the on-line system performance to meet the EC requirement of a 0.1 µg/l detection limit. (To achieve that, RPLC–UV had to be preceded by off-line liquid–liquid extraction.)

Still, the simplicity of coupled-column LC and its high sample throughput of 7–10 h make it rather attractive for screening purposes if (single) analytes that are somewhat less polar than ETU, CAAL and MITC, and have similar or slightly

TABLE I

DETAILS OF POLAR COMPOUNDS ANALYSED BY MEANS OF LARGE-VOLUME-INJECTION COLUMN-SWITCHING RPLC WITH UV DETECTION

Parameter	Ethylenethiourea (ETU)	Chloroallyl alcohol (CAAL)	Methylisothiocyanate (MITC)	Isoproturon	Bentazone
Formula			$H_3C-N=C=S$		
Water sol. (g/l)	20	Infinite	8	0.07	0.5
k' ^a	1.6	7.0	20	>100	>100
λ (nm)	233	205	237	244	220
ϵ (l/mol cm)	18 000	10 000	3000	17 000	25 000
Sample vol. (ml)	0.20	0.20	0.77	4.00	2.00
LOD (µg/l) ^b	1	1	1	0.1	0.1
Time of analysis (min)	5	7	7	10	10

^a On 5-µm Hypersil ODS; mobile phase, pure water for ETU/CAAL/MITC/isoproturon and aqueous 0.1% phosphoric acid for bentazone.

^b Detection limit (signal-to-noise ratio = 3) of analyte in ground, surface and rain water.

better UV detection characteristics, have to be determined. In other words, coupled-column RPLC-UV using direct large-volume injections may well prove to be an elegant monitoring method for a large majority of the many medium-polarity pesticides in use today. In the present paper this is demonstrated using isoproturon and bentazone, two typical representatives of this class of compounds, as test solutes (Table I).

EXPERIMENTAL

Materials

Isoproturon and bentazone (content > 99.5%) were obtained from Dr. S. Ehrenstorfer (Promochem, Wesel, Germany). Acetonitrile (HPLC-grade S), methanol (HPLC grade) and phosphoric acid (analytical-reagent grade, 89% pure) were from Rathburn (Walkburn, UK), Promochem and Merck (Darmstadt, Germany), respectively. HPLC-grade water was obtained by purifying demineralized water in a Milli-Q system (Millipore, Bedford, MA, USA). A 1000 µg/ml stock solution of each pesticide was prepared in acetonitrile. For LC analysis the stock solution of isoproturon was diluted in HPLC-grade water and the stock solution of bentazone in a 0.02 M phosphate buffer, pH 2.3. The diluted solutions were kept in a refrigerator at 4°C.

RPLC analyser

The schematic of the coupled-column RPLC analyser is shown in Fig. 1. The system consists of two isocratic Model 305 LC pumps (P-1 and P-2) from Gilson (Villiers-le-Bel, France), a Model 232 autosampler (AS) from Gilson equipped with a Type 7010 high-pressure column-switching valve (HP) from Rheodyne (Berkeley, CA, USA), a Model 116 variable-wavelength UV-Vis detector (D) from Gilson and two analytical separation columns, both packed with 3-µm C₁₈ Microspher from Chrompack (Bergen op Zoom, Netherlands) with dimensions of 50 × 4.6 mm I.D. (C-1) and 100 × 4.6 mm I.D. (C-2), respectively.

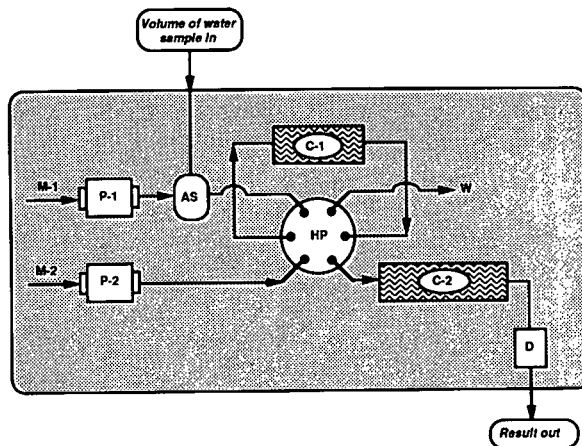


Fig. 1. Schematic of the coupled-column RPLC analyser. M-1, M-2 = first and second mobile phases; C-1, C-2 = first and second C₁₈ separation columns; P-1, P-2 = LC pumps; AS = autosampler; HV = high-pressure switching valve; D = UV detector; W = waste.

Procedures

Isoproturon. Approximately 20 ml of sample were passed through a 0.45-µm Millex filter (Millipore) and collected in an autosampler vial of 20 ml. A volume of 4.00 ml was taken from this vial and injected onto C-1. After injection, column-switching RPLC was carried out using a clean-up volume of 5.85 ml (injection volume included) of M-1 [acetonitrile–water (47.5:52.5, v/v) at 1 ml/min], and, after switching C-1 on-line with C-2, a transfer volume of 0.40 ml of M-1 (duration, 24 s). In this instance, separation on C-2 was performed with a mobile phase, M-2, having the same composition and flow-rate as M-1. UV detection was at 244 nm.

Bentazone. A 20 ml water sample was acidified by adding 20 µl of phosphoric acid, passed through a 0.45-µm filter and collected in an autosampler vial. A volume of 2.00 ml was taken from this vial and injected onto C-1. After injection, a clean-up volume of 4.65 ml (injection volume included) of M-1 [methanol–0.02 M phosphate buffer, pH 2.3 (50:50, v/v)] at 1 ml/min was used. Analyte transfer was carried out for 27 s (0.45 ml of M-1) after switching C-1 on-line with C-2. Separation on C-2 was carried out with methanol–0.02 M phosphate buffer, pH 2.7 (50:50, v/v), at 1 ml/min as mobile phase M-2; UV detection was at 220 nm.

Both of the above procedures were fully automated. Quantification was done by peak height comparison after RPLC–UV of equal volumes of aqueous standard and sample solutions.

RESULTS AND DISCUSSION

In several earlier studies, the main parameters governing analyte detectability and sensitivity in coupled-column RPLC have been discussed, and a general scheme for method development has been represented [11]. Briefly, there are two basic requirements. Firstly, one needs sufficient pre-separation between the analyte and UV-absorbing ionic species, such as anions and humic acids, in order to enhance the selectivity of the chromatographic process. Secondly, relatively large sample volumes have to be introduced into the RPLC system without undue band broadening in order to obtain the desired low limits of detection. Table I shows the relevant properties of the five compounds discussed in this paper. As outlined in the Introduction, when only one out of the three key characteristics (k' , λ_{\max} , ϵ_{\max}) is unfavourable, direct 200–800 μl sample analysis still yields limits of detection of 1 $\mu\text{g/l}$.

Obviously, sample analysis using the coupled-column RPLC analyser of Fig. 1 will permit one to reach the EC drinking-water limit of detection of 0.1 $\mu\text{g/l}$ for all analytes having marginally better characteristics than the three compounds referred to above, *i.e.* for essentially all (polar) pesticides and many related individual compounds of current interest. In order to verify this assumption, isoproturon and bentazone—which can be considered to possess typically “average” characteristics within the quoted class of compounds—were selected as test solutes. As can be calculated from their molecular extinction coefficients included in Table I, injection volumes of about 4.00 ml (isoproturon) or 2.00 ml (bentazone) should be sufficient to reach a 0.1 $\mu\text{g/l}$ detection limit. Because of the high k' values in purely aqueous solutions, such volumes can be injected without causing serious additional band broadening. However, one should bear in mind that the total volume of mobile phase used in this type of analysis typically is less than 10 ml.

In other words, a sample injection of more than 1 ml represents a significant part of the total chromatographic process, *i.e.* the most polar interferences will start to elute during injection. To put it differently, in the proposed procedures sample injection is the first step of a (multi)step-gradient elution with the sample as the first mobile phase. In practice, no additional band broadening was observed by us for the present large-volume injections of isoproturon and bentazone. That is, the requirement concerning analyte detectability can obviously be met.

As regards selectivity, it lies at hand to use an earlier simulation programme for the development of methods using step-gradient elution [12]. Unfortunately, this approach cannot easily be used for the determination of polar compounds in aqueous samples, because the interfering peak(s) originating from the matrix cannot be defined properly by plots of $\ln k'$ vs. mobile phase composition, as it required for this simulation programme. Especially in the case of acidic compounds such as bentazone, interferences show up as a broad (tailing) hump, eluting in the same region as the analytes [13]. Trial and error seems to be the only way to obtain an acceptable solution. Still, on the basis of earlier experiences, we can define two major boundary conditions, *viz.* (i) the clean-up volume, which is the volume of mobile phase M-1 used on column C-1, should at least be twice the dead volume of that column, and (ii) the capacity factor of the analyte in the mobile phases M-1 and M-2 should be between 2 and 5, in order to achieve short times of analysis and good sensitivity. On the basis of the above considerations, coupled-column RPLC–UV procedures were elaborated for isoproturon and bentazone. Since, in such procedures, the somewhat contradictory demands of large-volume injections and high sensitivity/selectivity have to be met, large-diameter (4.6 mm I.D.) analytical columns packed with high-efficiency material (3- μm Microspher C₁₈) were invariably used.

Determination of isoproturon

Initial experiments showed acetonitrile to be preferable to methanol because of slightly better peak shapes and a lower operational pressure.

Acetonitrile–water (50:50, v/v) —which gave $k' = 3$ for isoproturon— was the first choice as mobile phase M-1. Under these conditions sample volumes of up to at least 4.00 ml could be injected without any noticeable band broadening compared with 100- μ l injections. Using the same mobile phase compositions for M-1 and M-2, and a suitably adjusted small transfer volume, isoproturon could now be determined down to a level of 0.1 μ g/l in aqueous standard solutions. However, for spiked surface water samples the separation between analyte and matrix interferences in the first part of the chromatogram was not sufficient. Improved results were obtained by lowering the eluotropic strength of both M-1 and M-2 (47.5% instead of 50% of acetonitrile). The application of gradient elution, *i.e.* the use of different percentages of acetonitrile in M-1 and M-2, did not improve selectivity and/or sensitivity substantially. Using a clean-up volume of 5.75 ml on column C-1—that is 4.00 ml of injected water sample plus 1.75 ml of M-1 (!)— and a transfer volume of 0.40 ml of M-1, isoproturon could be determined in surface water samples

down to a level of 0.1 μ g/l. A typical example of a real-life analysis is shown in Fig. 2.

The repeatability of the procedure was tested with surface water. Samples spiked with 0.2–0.5 μ g/l isoproturon showed a mean recovery of 98% and a relative standard deviation (R.S.D.) of 2.8% ($n = 8$). Calibration curves were linear ($r = 0.9998$) over the range 0.1–200 μ g/l (Five data points in duplicate.)

Determination of bentazone

When analysing water samples for an acidic compound such as bentazone, two additional boundary conditions are important during method development. The pH of mobile phase M-1 should be as low as possible for the processing of large sample volumes, pH 2.3 being about the best one can achieve when working with alkyl-modified silicas. In addition, modifier-based gradients should be avoided in order to prevent interferences due to the continuous release of humic and/or fulvic acids from the column during such a gradient.

The analytical columns, C-1 and C-2, were the same as in the previous example. In this instance, however, mobile phases based on methanol–phosphate buffer were preferred (cf. Ref. 14). With pH 2.3–2.7, the capacity factor of bentazone was about 3 when using methanol–phosphate buffer (50:50, v/v) as mobile phase. Under these conditions, a sample of up to at least 2.00 ml could be injected on C-1 without additional band broadening of the bentazone peak.

Fig. 3 gives a nice impression of the problems encountered in the development of the coupled-column procedure for bentazone. As can be seen, small changes in the mobile phase composition have a dramatic impact on the final result. As in earlier studies, a conventional step gradient was used. Fig. 3A shows the chromatogram obtained with a step gradient from 50 to 60% methanol, which, apparently, releases quite a lot of interferences. However, omitting the step gradient does not provide enough selectivity, as is demonstrated in Fig. 3B. Fig. 3C shows that the combined use of a modifier and a pH gradient has a distinctly beneficial influence, but quantification of bentazone will still be rather

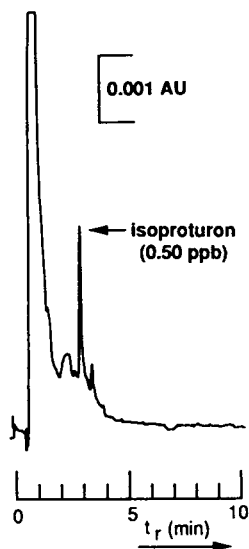


Fig. 2. Column-switching RPLC–UV (244 nm) using direct 4.0-ml sample injection of (A) a surface water sample spiked with 0.5 μ g/l (ppb) isoproturon and (B) a blank surface water. Displayed chromatograms start after clean-up on C-1. For LC conditions, see Experimental section.

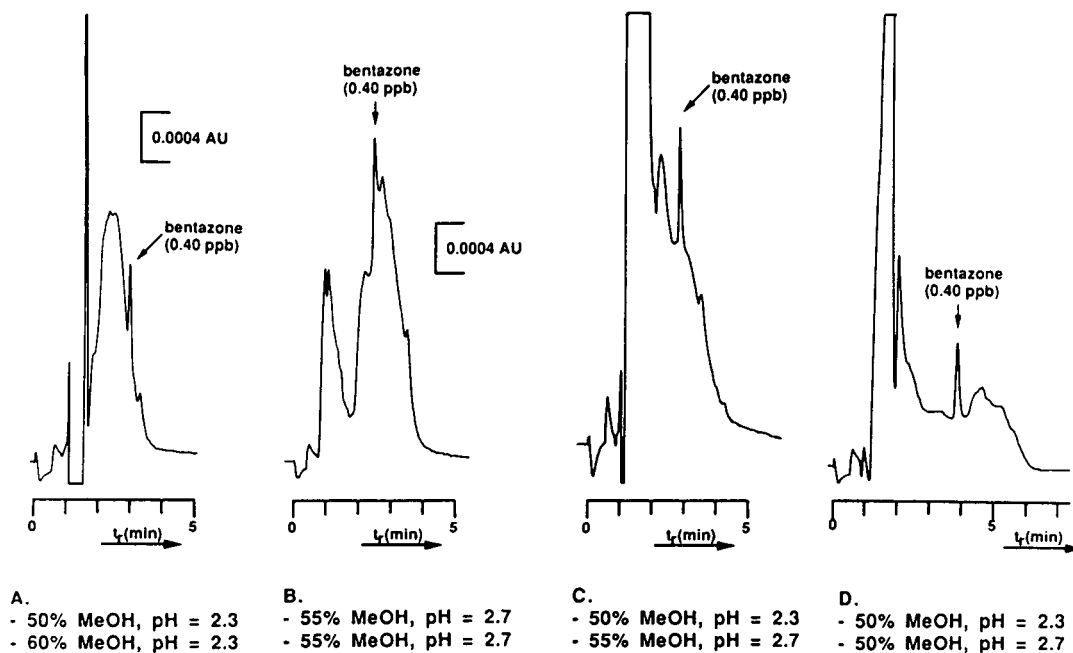


Fig. 3. Selectivity effected with the different step gradients given above using coupled-column RPLC of a surface water containing $0.40 \mu\text{g/l}$ bentazone, using direct sample injection (2.00 ml). Clean-up volumes: A, C and D, 4.65 ml of M-1 and B, 3.75 ml of M-1; transfer volumes: A, C and D, 0.50 ml of M-1 and B, 0.40 ml of M-1; MeOH = methanol. For LC conditions, see text. Displayed chromatograms start after clean-up on C-1.

difficult. In the end, restricting ourselves to a pH step gradient only gave the best approach, as can be seen from Fig. 3D. This figure also shows that the final goal of a coupled-column procedure enabling detection at the $0.1 \mu\text{g/l}$ level has been reached. As an illustration of the potential of the procedure, the results of RPLC–UV analyses of a drinking and a surface water sample spiked with bentazone at the $0.1 \mu\text{g/l}$ level are shown in Fig. 4. Compared with our earlier procedure, which involved a manual liquid–liquid extraction [14], the gain in sample throughput is considerable (total time of analysis, 8–10 min; seven samples per hour).

It is an interesting feature of the present heart-cutting procedures that only a small fraction of the interfering material reaches the second column, C-2, and subsequently, of course, the detector. This is nicely illustrated in Fig. 5 for a surface water sample; in this instance, the clean-up time, t_c , is included in the RPLC–UV traces shown. When processing a series of samples, the next analysis can be started shortly (*ca.* 0.5 min)

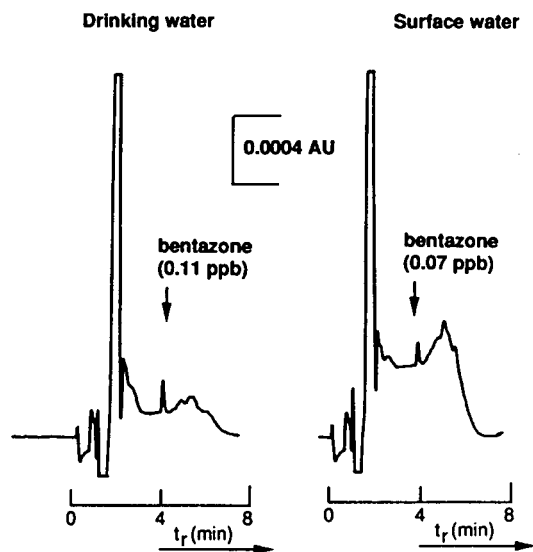


Fig. 4. Column-switching RPLC–UV (220 nm) with direct sample injection (2.00 ml) of a drinking water and a surface water sample spiked with *ca.* $0.1 \mu\text{g/l}$. For LC conditions, see Experimental section. Displayed chromatograms start after clean-up on C-1.

TABLE II

DETERMINATION OF BENTAZONE IN SURFACE WATER BY RPLC-UV USING LIQUID-LIQUID EXTRACTION (LLE) OR DIRECT LARGE-VOLUME INJECTION

Sample No.	Bentazone content ($\mu\text{g/l}$) found using	
	LLE	Direct sampling
1	0.06	0.08
2	0.37	0.40
3	<0.02	<0.05
4	0.66	0.71
5	0.35	0.33

after analyte transfer to column C-2. The real time of analysis therefore is only about 8 min.

Calibration curves were linear ($r = 0.9999$) over the range $0.11\text{--}110 \mu\text{g/l}$ (five data points in duplicate). The recovery of bentazone from drinking water spiked at the 1.1 and $0.11 \mu\text{g/l}$ level was 98% (R.S.D., 0.5% ; $n = 5$) and 86% (R.S.D., 5.7% ; $n = 6$), respectively. Similar results were obtained for rain water. Two real-life surface water samples containing bentazone were analysed on five consecutive days. The reproducibilities were 6.0% and 6.5% at the $0.40 \mu\text{g/l}$ and $0.08 \mu\text{g/l}$ level, respectively. Five surface water samples were analysed both by the

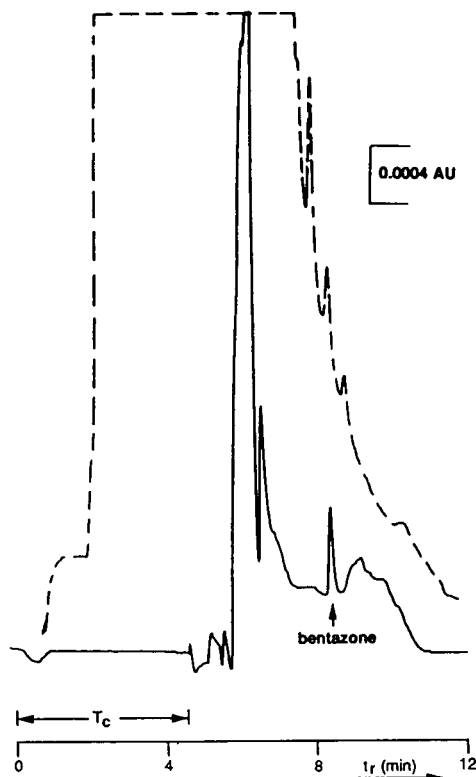


Fig. 5. RPLC-UV (220 nm) of a surface water sample containing $0.40 \mu\text{g/l}$ bentazone; injection volume, 2.00 ml . Solid line, chromatogram obtained with the coupled-column procedure (see Experimental section); dashed line, chromatogram obtained with the same two columns coupled on-line without column switching using a mobile phase of methanol- 0.02 M phosphate buffer, pH 2.7 (50:50, v/v) at 1 ml/min ; t_c , clean-up time on C-1 with coupled-column procedure.

TABLE III

TYPICAL RESULTS OF REAL-LIFE WATER SAMPLE ANALYSES USING THE COUPLED-COLUMN RPLC-UV ANALYSER

Date	Pesticide	Type of sample	No. of samples investigated	No. of positive samples	Pesticide content ($\mu\text{g/l}$)
11/10/91	Bentazone	Surface water	5	5	0.1-0.7
07/09/92	Bentazone	Ground water	8	3	0.3-0.5
07/09/92	Isoproturon	Surface water	5	0	<0.1
10/09/92	Methabenzthiazuron	Surface water	7	0	<0.1
19/10/92	Linuron	Surface water	12	12	2-8
30/01/93	Bentazone	Ground water	12	4	0.4-90
09/02/93	Bentazone	Ground water	10	8	2-10

present method and by the earlier method involving liquid–liquid extraction. As listed in Table II, the agreement between the two sets of results was fully satisfactory.

CONCLUSIONS

Coupled-column RPLC with UV detection using direct large-volume injections is a highly useful technique for the rapid trace analysis of single polar pesticides in aqueous environmental samples such as drinking, ground and surface water. For compounds with LC retention and UV detectability characteristics typical for this class of compounds, detection limits are of the order of 0.1 $\mu\text{g/l}$. The results presented in this paper demonstrate the viability of this approach, which features a throughput of 5–7 samples per hour. The coupled-column RPLC–UV analyser used in our studies is fully automated and has shown good robustness over a period of more than 16 months. Typical results of monitoring programmes carried out during this period of time for bentazone and isoproturon as well as two other pesticides, metribuzine and linuron, are summarized in Table III. The development of the various dedicated procedures was relatively rapid in all instances.

REFERENCES

- 1 M.W.F. Nielen, A.J. Valk, R.W. Frei, U.A.Th. Brinkman, Ph. Mussche, R. de Nijs, B. Ooms and W. Slink, *J. Chromatogr.*, 393 (1987) 69.
- 2 C.H. Marvin, I.D. Brindle, C.D. Hall and M. Chiba, *J. Chromatogr.*, 503 (1990) 167.
- 3 M.-C. Hennion, P. Subra, V. Coquart and R. Rosset, *Fresenius' J. Anal. Chem.*, 339 (1991) 488.
- 4 V. Coquart and M.-C. Hennion, *J. Chromatogr.*, 585 (1991) 67.
- 5 R.B. Geerdink, C.A.A. van Balkom and H.J. Brouwer, *J. Chromatogr.*, 481 (1989) 275.
- 6 E.R. Brouwer, I. Liska, R.B. Geerdink, P.C.M. Fintrop, W.H. Mulder, H. Lingeman and U.A.Th. Brinkman, *Chromatographia*, 32 (1991) 445.
- 7 R. Reupert, I. Zube and E. Plöger, *LC·GC Int.*, 5 (1992) 43.
- 8 J. Slobodnik, E.R. Brouwer, R.B. Geerdink, W.H. Mulder, H. Lingeman and U.A.Th. Brinkman, *Anal. Chim. Acta*, 268 (1992) 55.
- 9 E.A. Hogendoorn, A.P.J.M. de Jong, P. van Zoonen and U.A.Th. Brinkman, *J. Chromatogr.*, 511 (1990) 243.
- 10 E.A. Hogendoorn, P. van Zoonen and U.A.Th. Brinkman, *Chromatographia*, 31 (1991) 285–292.
- 11 E.A. Hogendoorn, C. Verschraagen, U.A.Th. Brinkman and P. van Zoonen, *Anal. Chim. Acta*, 268 (1992) 205.
- 12 E.A. Hogendoorn, R. Hoogerbrugge, C.E. Goewie, P. van Zoonen and P.J. Schoenmakers, *J. Chromatogr.*, 522 (1991) 113.
- 13 J.V. Sancho-Llopis, F. Hernández-Hernández, E.A. Hogendoorn and P. van Zoonen, *Anal. Chim. Acta*, 283 (1993) in press.
- 14 E.A. Hogendoorn and C.E. Goewie, *J. Chromatogr.*, 475 (1989) 432.

Direct column liquid chromatographic enantiomer separation of the coumarin anticoagulants phenprocoumon, warfarin, acenocoumarol and metabolites on an α_1 -acid glycoprotein chiral stationary phase

Jan Xaver de Vries* and Eva Schmitz-Kummer

Abteilung Klinische Pharmakologie, Medizinische Klinik der Universität, Bergheimerstrasse 58, W-6900 Heidelberg (Germany)

(First received January 15th, 1993; revised manuscript received April 15th, 1993)

ABSTRACT

The enantiomers of the racemic coumarin anticoagulants phenprocoumon (PH) and metabolites (4'-, 6-, 7- and 8-hydroxy-PH), warfarin (WA) and metabolites (6-, 7-hydroxy-WA and the two diastereomeric WA alcohols) and acenocoumarol were resolved by column liquid chromatography using an immobilized α_1 -acid glycoprotein stationary phase; elution was performed using a phosphate buffer and isopropanol gradient with and without dimethyloctylamine as modifier, and detection by ultraviolet or fluorescence. The advantages of this method are: the procedure is simple and fast and does not require pre-column derivatization; the configuration of the enantiomers can be assigned by comparison with a reference sample with already known absolute configuration; the optical purities of these compounds can be analysed with high sensitivity; the method can be applied to the determination of the enantiomers in biological samples.

INTRODUCTION

Column liquid chromatographic (HPLC) separation of enantiomers on chiral stationary phases has been extensively investigated during recent years since many bioactive substances are chiral and enantiomers may show different biological activities [1-4].

The 4-hydroxycoumarin oral anticoagulants phenprocoumon (PH) (**1**), warfarin (WA) (**7**) and acenocoumarol (AC) (**13**) (Fig. 1) are used in human therapy for the treatment and preven-

tion of thromboembolic disorders [5,6]. These drugs are chiral but are available and administered as racemates [7].

Pharmacokinetic studies concerning the enantioselective elimination of coumarin anticoagulants after racemic drug administration require assays with resolution of enantiomers [7-10]. WA and PH have been previously resolved by HPLC using chiral phases [11-13]; however, only the metabolites from WA have been resolved, using a lengthy procedure with pre-column derivatization, separation by normal-phase HPLC and detection by fluorescence after post-column aminolysis [14].

α_1 -Acid glycoprotein chiral stationary phases

* Corresponding author.

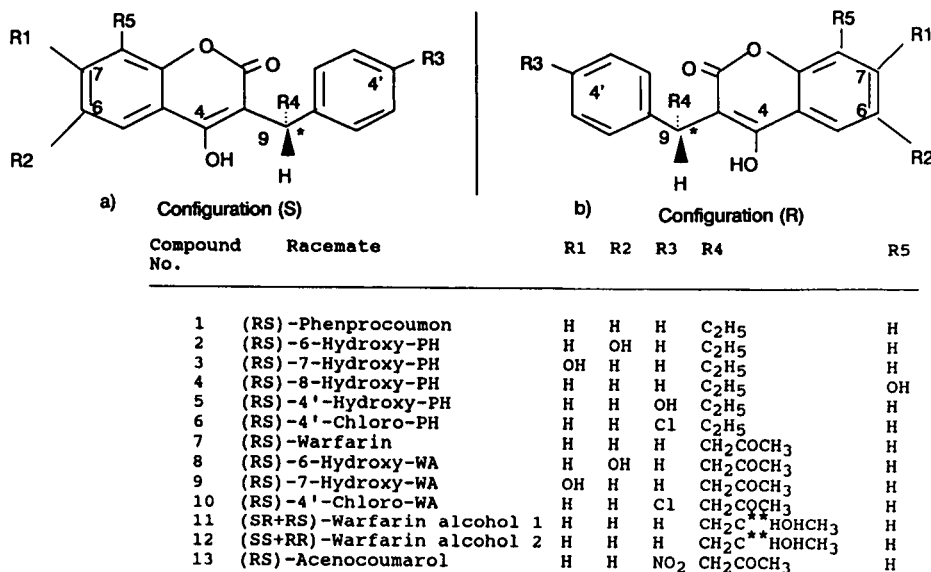


Fig. 1. Structures and configurations of oral anticoagulants and their metabolites [\star and $\star\star$ are chiral centres at C-9 and C-11, respectively; compound numbers followed by a or b correspond to a configuration at C-9 of (S) or (R), respectively].

have been used for the separation of enantiomers and stereoisomers of a large number of compounds [15–18]; in the present study we report on the use of this phase for the direct HPLC separation of the enantiomers of PH, WA, their metabolites and AC.

EXPERIMENTAL

Chemicals

Racemic warfarin (7) and 4'-chlorowarfarin (10) were commercially available (Sigma Chemie, Deisenhofen, Germany); (RS)-phenprocoumon (1), (S)-(-)-phenprocoumon (1a), (R)-(+)-phenprocoumon (1b) and (RS)-4'-chloro-phenprocoumon (6) were gifts from Hoffman-La Roche (Basle, Switzerland); (S)-(-)-acenocoumarol (13a) and (S)-(-)-warfarin (7a) were gifts from Dr. H.H.W. Thijssen, (Department of Pharmacology, University of Limburg, Netherlands); racemic acenocoumarol (13) was obtained from Ciba-Geigy (Wehr, Germany). Racemic hydroxy-phenprocoumon metabolites (6-OH-PH, 7-OH-PH, 8-OH-PH and 4'-OH-PH) (2–5), racemic warfarin metabolites (6-OH-WA, 7-OH-WA) (8, 9) and the racemic diastereomeric warfarin alcohols 1 and 2 (11, 12)

were obtained in our laboratories by chemical synthesis [19–21].

WA alcohols 1 and 2 (11, 12) were obtained by reduction of racemic WA (7) with sodium borohydride, separation by silica gel column chromatography and recrystallization [21]; alcohol 1 (11) (isolated from fractions 11–24) showed m.p. 169–173°C (Lit. [21], 173–175°C), R_F 0.49 (Lit. [21], 0.46), $^1\text{H NMR}$ (in C^2HCl_3), δ (ppm) (No. of protons)(multiplicity)(assignment): 7.0–7.8 (9H) (m) (aromatic), 4.60 (1H) (d,d) (C9-H), 3.8 (1H) (m) (C11-H), 2.1–2.5 (2H) (m) (C10-HH), 1.30 (3H) (d) (C12C-H3); alcohol 2 (12) (isolated from fractions 32–56) showed m.p. 159–165°C (Lit [21], 162–168°C), R_F 0.39 (TLC, Lit. [21], 0.21), $^1\text{H NMR}$ (in C^2HCl_3): 7.2–7.8 (9H) (m) (aromatic), 4.70 (1H) (tr) (C9-H), 4.0 (1H) (m) (C11-H), 2.1–2.6 (2H) (m) (C10-HH), 1.35 (3H) (d) (C12C-H3); UV spectra of 11 and 12 were identical to those reported in the literature [22]. Warfarin alcohols 1a (SR) (11a) and 2a (SS) (12a) were obtained similarly by reduction of optically pure (S)-(-)-WA (7a) and were a gift from Dr. H.H.W. Thijssen.

N,N-Dimethyloctylamine (DMOA) (99%) was obtained from Fluka Feinchemikalien (Neu-Ulm, Germany); reagents and solvents for chro-

matography were analytical grade. Solvents for HPLC were filtered and degassed with helium before chromatography.

Equipment and chromatographic conditions

HPLC analysis was performed with a Model 1090 M liquid chromatograph with ternary solvent delivery system, autosampler, UV-visible photodiode-array detector, fluorescence detector M1046 and a Model 79994A computer workstation for system control and data handling (Hewlett Packard, Waldbronn, Germany). The photodiode-array detection (DAD) wavelengths were set at 276 and 312 nm and on-line spectra were recorded in the range 210–400 nm; fluorescence excitation and emission wavelengths were set at 292 and 380 nm, respectively; the enantiomers were separated with a Chiral-AGP column (100 × 4 mm I.D., spherical 5- μ m particles; ChromTech, Norsborg, Sweden) and a guard column (10 × 3 mm) filled with the same material.

The following elution systems were used. Elution system 1: solvent A, 0.01 M aqueous phosphate buffer pH 7.0; solvent B, 2-propanol. Elution system 2: solvent A, 0.1 M aqueous phosphate buffer pH 7.0; solvent B, 2-propanol. Elution system 3: solvent A, 0.01 M aqueous phosphate buffer pH 7.0 modified with 0.001 M dimethyloctylamine; solvent B, 2-propanol modified with 0.001 M dimethyloctylamine. For all elution systems the same linear gradient parameters were used: solvent B 0–20% in 10 min, 15 min with 20% B and 10 min equilibration with 100% solvent A before the next injection. The solvent flow-rate was 0.9 ml/min and the operating pressure and temperature were 10–12 MPa and 20–25°C, respectively. After an analysis series the column was washed with an aqueous 10% 2-propanol solution for 15 min. Aliquots of 1–2 μ l of methanolic solutions were injected; larger volumes were injected in phosphate buffer solutions.

Thin-layer chromatography was run on silica gel plates with the solvent toluol–ethyl formate–formic acid (10:5:1; v/v/v) [22] and the spots were visualized under an ultraviolet lamp.

¹H NMR spectroscopy was performed on a Bruker Model FT AM-360 instrument at 360

MHz; substances were dissolved in deuterated chloroform or dimethylsulphoxide and tetramethylsilane was used as reference; spectra were obtained by Dr. C. Deus and Professor Dr. H. Friebolin (Institute of Organic Chemistry, University of Heidelberg, Germany); UV spectra (in methanol acidified with 1% 0.1 M hydrochloric acid) were run on a Kontron Model Uvikon 910 spectrophotometer.

RESULTS AND DISCUSSION

Enantiomeric separation

The structures of the oral anticoagulants and metabolites are given in Fig. 1. HPLC separation of the enantiomers of the racemic parent drugs PH (1), WA (7) and AC (13) are shown in Fig. 2A–C; Fig. 3 shows the liquid chromatographic separation of some metabolite racemates; Fig. 3A is from 4'-OH-PH (5), Fig. 3B from 6-OH-PH (8) and Fig. 3C from WA alcohol 2 (12). Several solvent combinations and elution systems were evaluated by varying the pH, ionic strength and modifier; elution system 3 showed the best enantiomeric separations of the individual racemates, with the exception of 6-OH-WA (8) and 7-OH-WA (9), which could, however, be separated with systems 1 and 2, respectively. 4'-Chloro-PH (6) and 4'-chloro-WA (10) were also analysed as they are used as internal standard for total PH and WA assays; 4'-chloro-WA (10) could not be resolved. The (*S*) enantiomers of PH (1a) and WA (7a) eluted before their respective (*R*) enantiomers, but for AC (13) the elution order is reversed (Table I). Chromatographic data are shown in Table I. Only small volumes (1–2 μ l) of solutions in organic solvents can be injected due to band broadening of chromatographic peaks; aqueous solutions must be used when injecting larger volumes. Retention times are reproducible within $\pm 2\%$. The limit of detection of PH, WA and their metabolites using fluorescence detection, and of AC with UV detection, was 10–20 ng; the reported main metabolites from AC, 6-hydroxy-AC and 7-hydroxy-AC, were not available. No racemization was detectable during the solution or chromatographic procedures of pure enantiomers. The standard chromatographic systems and pa-

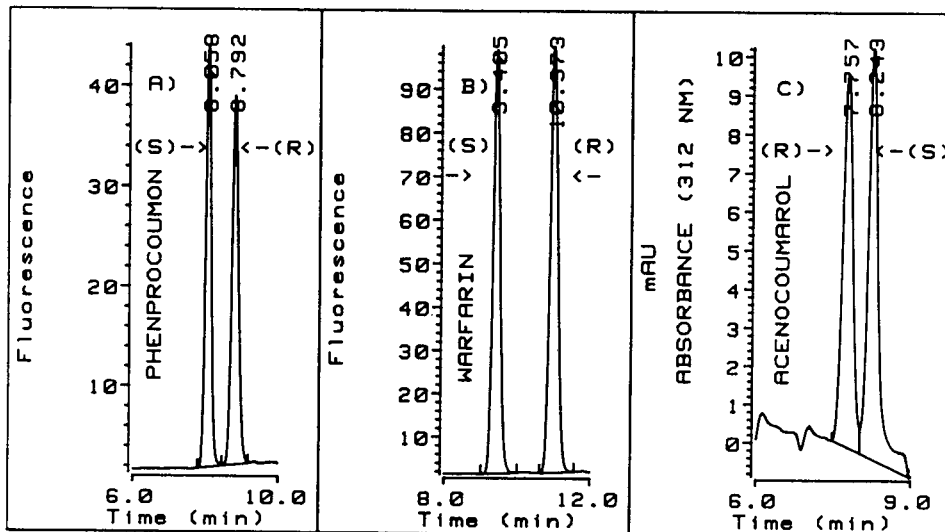


Fig. 2. HPLC separation of the enantiomers of racemic coumarin anticoagulants (elution system 3). (A) Phenprocoumon (1); (B) warfarin (7); (C) acenocoumarol (13). Configuration assignments are indicated in the chromatograms.

rameters mentioned in the Experimental section can, however, be further modified and optimized for a specific separation. Although limitations and drawbacks of protein-derived chiral stationary phases have been reported [2,3], the present

chromatographic conditions showed higher selectivity for the direct separation of coumarin anticoagulants and metabolites than the previously used chiral phase of the donor-acceptor type [13]; stationary phase stability is satisfactory

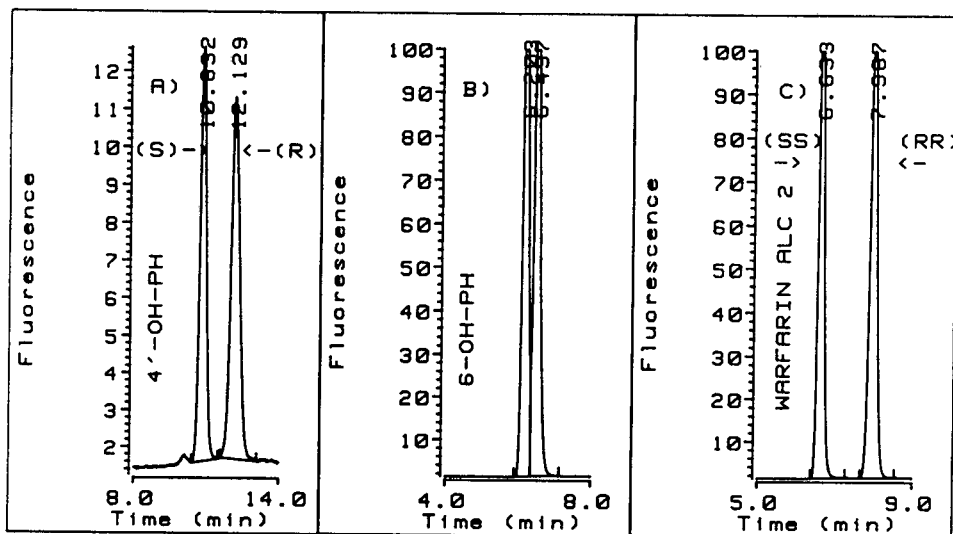


Fig. 3. HPLC separation of the enantiomers of some racemic coumarin anticoagulant metabolites (elution system 3). (A) 4'-Hydroxyphenprocoumon (5); (B) 6-hydroxyphenprocoumon (2); (C) warfarin alcohol 2 (12).

TABLE I

COLUMN CAPACITY FACTORS (k') AND SELECTIVITIES (α) FOR THE ENANTIOMERIC SEPARATION OF COUMARIN ANTICOAGULANTS AND THEIR METABOLITES

N.S. = No separation; (R) and (S) C-9 configuration assignments.

Compound No.	Elution system 1			Elution system 2			Elution system 3		
	k'_1	k'_2	α	k'_1	k'_2	α	k'_1	k'_2	α
1	8.02 (S)	9.23 (R)	1.15	9.13 (S)	10.70 (R)	1.17	7.15 (S)	8.51 (R)	1.18
2	6.80 (N.S.)			5.65 (N.S.)			4.36	4.63	1.06
3	4.03	4.20	1.04	5.13 (N.S.)			2.82	2.92	1.03
4	4.78	5.09	1.06	5.90	6.03	1.02	4.69	5.08	1.08
5	9.24	10.77	1.16	10.51	13.02	1.23	8.36	9.48	1.13
6	12.7 (N.S.)			10.97 (N.S.)			8.94	9.15	1.02
7	6.92 (S)	7.57 (R)	1.09	7.67 (S)	8.44 (R)	1.10	6.04 (S)	6.67 (R)	1.10
8	3.44	3.70	1.07	3.98 (N.S.)			2.82	2.92	1.03
9	2.94	3.14	1.06	3.33	3.59	1.07	2.49 (N.S.)		
10	11.10 (N.S.)			8.92 (N.S.)			7.35 (N.S.)		
11	6.50 (SR)	7.07 (RS)	1.08	6.78 (SR)	7.60 (RS)	1.12	5.42 (SR)	6.00 (RS)	1.10
12	5.83 (SS)	7.07 (RR)	1.21	6.15 (SS)	7.47 (RR)	1.21	4.74 (SS)	5.91 (RR)	1.24
13	6.67 (R)	8.14 (S)	1.21	7.77 (R)	8.17 (S)	1.05	5.72 (R)	6.14 (S)	1.07

as more than 800 analyses were performed before loss of column efficiency.

Configuration assignment

The absolute configuration of the enantiomers of PH, WA and AC (**1**, **7**, **13**) was determined previously by chemical and chiroptical methods [23–26]. The configurations of the parent drugs were assigned in the present work by injecting the pure enantiomers (**1a**, **1b**, **7a**, **11a**, **12a**, **13a**) in the HPLC system and comparing their retention times and UV on-line spectra; the present HPLC method allows the determination of the configuration of the anticoagulant drugs with small samples.

However, the absolute configuration of the enantiomers of the phenolic metabolites from PH (**2–5**) and WA (**8,9**) has not been assigned yet and pure metabolite enantiomers were not available. The racemic diastereomeric warfarin alcohols **1** (**11**) (9R, 11S + 9S, 11R) and **2** (**12**) (9R, 11R + 9S, 11S) were obtained by chemical reduction of racemic warfarin and column chromatography according to Chan *et al.* [21]; the chromatographic behaviour and the spectral and

physical properties of our synthetic compounds corresponded to that of the literature [21,22]; the denominations warfarin alcohols **1** and **2** were based on migration rates on silica and have been retained. The optically pure diastereomeric warfarin alcohols **1a** (**11a**) (9S, 11R) and **2a** (**12a**) (9S, 11S) were obtained by chemical reduction of the (S) (–) WA enantiomer.

Optical purity

The optical purities of the compounds can be evaluated quantitatively; a 1% impurity of one of the enantiomers can be detected in the presence of the antipode with less material and higher sensitivity than in polarimetry.

Analysis of biological samples

The HPLC enantiomer separation of the coumarin anticoagulants and their metabolites is fast and simple, and presents advantages over those that require derivatization [10].

GC–MS analysis of methylated WA and PH and their metabolites has been reported but this requires the synthesis and administration of

specific ^{13}C -labelled enantiomer mixtures (pseudoracemates) of the parent drugs [27,28]; however, these assays are not applicable to studies with patients on long-term therapy with racemic anticoagulant administration [7].

The described HPLC method can be applied to biological samples; although enantiomer pairs are well resolved, different metabolites may overlap during chromatography (see Table I).

CONCLUSIONS

Several advantages of the above-described method for the direct liquid chromatographic separation of the coumarin anticoagulant enantiomers of phenprocoumon, warfarin, acenocoumarol and metabolites on α_1 -acid glycoprotein chiral stationary phase are reported: it is a simple and fast procedure not requiring precolumn derivatization; the absolute configuration of the parent drugs can be assigned using small amounts of material; the optical purities of these compounds can be determined with high sensitivity; it can be applied to the determination of enantiomers in biological samples.

ACKNOWLEDGEMENTS

We thank Dr. H.H.W. Thijssen (Department of Pharmacology, University of Limburg, Netherlands), Hoffman-La Roche (Basle, Switzerland) and Ciba-Geigy (Wehr, Germany) for samples, Dr. C. Deus and Professor Dr. H. Friebolin (Institute of Organic Chemistry, University of Heidelberg, Germany) for the ^1H NMR spectra.

REFERENCES

- 1 A.M. Krustulovic, *J. Pharm. Biomed. Anal.*, 6 (1988) 641.
- 2 W.H. Pirkle and T.C. Pochapsky, *Adv. Chromatogr.*, 27 (1987) 73.
- 3 W.H. Pirkle and T.C. Pochapsky, *Chem. Rev.*, 89 (1989) 347.
- 4 D.W. Armstrong and S.M. Han, *Crit. Rev. Anal. Chem.*, 19 (1988) 175.
- 5 P.W. Majerus, G.J. Broze, J.P. Miletich and D.M. Tollefsen, *Goodman and Gilman's The Pharmacological Basis of Therapeutics*, Pergamon Press, New York, 8th ed., 1991, p. 1311.
- 6 E. Zimmermann and H. Mörl, in G. Schettler and E. Weber (Editors), *Internistische Therapie in Klinik und Praxis*, G. Thieme, Stuttgart, 1985, p. 466.
- 7 J.X. De Vries, U. Völker and E. Weber, *Hämostaseologie*, 11 (1991) 60.
- 8 N.H.G. Holford, *Clin. Pharmacokin.*, 11 (1986) 483.
- 9 K. Williams and E. Lee, *Drugs*, 30 (1985) 333.
- 10 S. Toon, K.J. Hopkins, F.M. Garstang, B. Diquet, T.S. Gill and M. Rowland, *Br. J. Clin. Pharmacol.*, 21 (1986) 187.
- 11 I.W. Wainer and Y.Q. Chu, *J. Chromatogr.*, 455 (1988) 316.
- 12 Y.Q. Chu and I.W. Wainer, *Pharm. Res.*, 5 (1988) 680.
- 13 J.X. De Vries and U. Völker, *J. Chromatogr.*, 493 (1989) 149.
- 14 C. Banfield and M. Rowland, *J. Pharm. Sci.*, 73 (1984) 1392.
- 15 J. Hermansson, *J. Chromatogr.*, 269 (1983) 71.
- 16 J. Hermansson and M. Enquist, *J. Liq. Chromatogr.*, 9 (1986) 621.
- 17 M. Enquist and J. Hermansson, *J. Chromatogr.*, 519 (1990) 285.
- 18 I. Fitos, J. Visy, M. Simonyi and J. Hermansson, *J. Chromatogr.*, 609 (1992) 163.
- 19 L.D. Heimark, S. Toon, L.W. Low, D.C. Swinney and W.F. Trager, *J. Labell. Comp. Radiopharmac.*, 23 (1985) 137.
- 20 E. Bush and W.F. Trager, *J. Pharm. Sci.*, 72 (1983) 830.
- 21 K.K. Chan, R.J. Lewis and W.F. Trager, *J. Med. Chem.*, 15 (1972) 1265.
- 22 R.J. Lewis and W.F. Trager, *J. Clin. Invest.*, 49 (1970) 907.
- 23 B.D. West, S. Preis, C.H. Schroeder and K.P. Link, *J. Am. Chem. Soc.*, 83 (1961) 2676.
- 24 B.D. West and K.P. Link, *J. Heterocycl. Chem.*, 2 (1965) 93.
- 25 C.R. Wheeler and W.F. Trager, *J. Med. Chem.*, 22 (1979) 1122.
- 26 E.J. Valente, W.R. Porter and W.F. Trager, *J. Med. Chem.*, 21 (1978) 231.
- 27 E.D. Bush, I.K. Low and W.F. Trager, *Biomed. Mass Spectrom.*, 10 (1983) 395.
- 28 L.D. Heimark and W.F. Trager, *Biomed. Mass Spectrom.*, 12 (1985) 67.

Analysis of paralytic shellfish poisoning toxins by automated pre-column oxidation and microcolumn liquid chromatography with fluorescence detection[☆]

Mojmir Janeček^{☆☆} and Michael A. Quilliam^{*}

Institute for Marine Biosciences, National Research Council of Canada, 1411 Oxford Street, Halifax, Nova Scotia B3H 3Z1 (Canada)

James F. Lawrence

Health Protection Branch, Food Research Division, Bureau of Chemical Safety, Food Directorate, Ottawa, Ontario, K1A 0L2 (Canada)

(Received April 19th, 1993)

ABSTRACT

Periodate oxidation of the toxins responsible for paralytic shellfish poisoning (PSP) yields fluorescent purines suitable for trace analysis by reversed-phase LC. Mobile phases containing perfluorinated acids, such as heptafluorobutyric acid, as ion-pair agents were found to provide high capacity factors for the oxidized products. Gradient elution on a microbore column with large volume injections and fluorescence detection permitted the detection of femtomole quantities of PSP toxins. A fully automated pre-column oxidation procedure was developed for an LC autosampler system in order to improve precision and allow unattended analyses. The complete method was applied successfully to various samples, including shellfish and toxic phytoplankton.

INTRODUCTION

Paralytic shellfish poisoning (PSP) is a world-wide problem caused by consumption of shellfish that have accumulated potent neurotoxins produced by toxigenic dinoflagellates, such as those belonging to the genus *Alexandrium* [1]. The PSP toxins include saxitoxin (STX) and several of its derivatives formed by addition of sulfo, hydroxysulfate and N-1-hydroxyl groups (Fig. 1).

The AOAC mouse bioassay is used routinely

by regulatory laboratories for the determination of PSP toxins [2]. Although this method has the advantage of being non-selective and therefore well suited for protection of the public, it is recognized that bioassay suffers from considerable variability [3] and gives little information on toxin composition. In addition, there is pressure from animal rights groups to discontinue such tests; some European countries have banned them already.

The most commonly used chemical method for the analysis of PSP toxins is the combination of liquid chromatography (LC) with on-line post-column oxidation and fluorescence detection [4,5]. This approach evolved from earlier work by Bates and Rapoport [6] which showed that STX could be oxidized to a fluorescent purine by

* Corresponding author.

☆ NRCC No. 34869.

☆☆ On leave from Institute of Analytical Chemistry, Czech Academy of Sciences, Brno, Czech Republic.

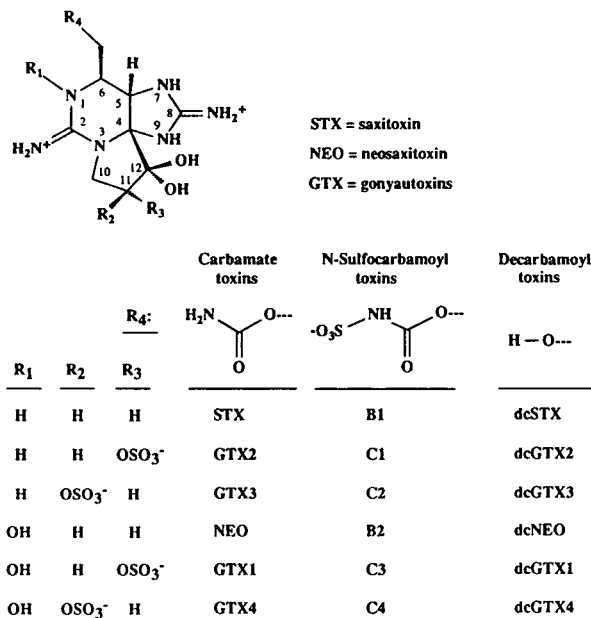


Fig. 1. Structures of the principal toxins responsible for paralytic shellfish poisoning (PSP).

hydrogen peroxide under alkaline conditions. Since this original procedure proved unsuitable for the N-1-hydroxylated PSP toxins, better oxidizing agents such as *tert.*-butyl hydroperoxide [4] or periodate [5] are used in post-column oxidation systems in order to detect all PSP toxins. Unfortunately, the set up and operation of such equipment is quite complex and requires considerable daily maintenance.

Recently, an alternative LC technique was reported [7,8]. The method involves a pre-column oxidation of the toxins followed by reversed-phase gradient elution and fluorescence detection of the oxidized products. Since the products are more amenable to reversed-phase LC than the precursor toxins, an octadecylsilica (C₁₈) column may be used to obtain better separation efficiencies than those possible using the PRP-1 column recommended in the most commonly used post-column method [5]. A mobile phase containing aqueous ammonium formate was found to provide good peak shape and reproducibility. In addition, the composition of the reaction mixture for pre-column periodate oxidation was optimized to improve fluorescent

product yield and a solid-phase extraction cleanup was established to reduce interference from co-extractives and to perform group separations of the toxins [8].

The objectives of the work described here were as follows: (a) to investigate additional mobile phases for the reversed-phase chromatography of oxidized PSP toxins; (b) to improve the sensitivity and reproducibility of the analysis by using a microbore column, large volume injection, and fully automated pre-column oxidation reaction; and (c) to apply the method to shellfish and phytoplankton samples.

EXPERIMENTAL

Chemicals

Trifluoroacetic acid and acetonitrile were purchased from BDH (Poole, UK), heptafluorobutyric acid (HFBA) and periodic acid from Sigma (St. Louis, MO, USA), and tridecafluoroheptanoic acid from Aldrich (Milwaukee, WI, USA). Distilled water was further purified by passage through a Milli-Q (Millipore, Bedford, MA, USA) water purification system equipped with ion-exchange and carbon filters. All other reagents were of analytical-reagent grade. Purified standards of PSP toxins were kindly provided by Dr. M.V. Laycock (Institute for Marine Biosciences, Halifax, Canada).

Equipment

Chromatography was performed using an HP1090M liquid chromatograph (Hewlett-Packard, Palo Alto, CA, USA) equipped with a ternary DR5 solvent delivery system, variable volume injector/autosampler, and automated pre-column sample preparation system. The system was controlled by an HP7994A Pascal ChemStation, which enables the user to customize and automate various sample manipulations including pre-column derivatizations at ambient and elevated temperatures. The LC effluent was monitored with an HP1046A dual monochromator fluorescence detector fitted with the standard 4.5- μ l flow cell. Stainless steel capillaries with internal diameter of 0.12 mm served as connection tubing.

A digital PMH63 pH meter (Radiometer, Copenhagen, Denmark) was used for the measurement of pH of mobile phases and oxidation mixtures. A Model 5415 microcentrifuge (Brinkmann, Westbury, NY, USA) was used for sample preparation. A vacuum manifold system was used for solid-phase extraction clean-up (Supelco, Bellefonte, PA, USA).

LC columns

Stainless-steel columns (25 cm × 1.0 mm I.D. and 10 cm × 2.1 mm I.D.) were packed by the slurry technique using an ethanol–glycerol (50:50, v/v) suspension under a pressure of 50 MPa. LiChrospher-100 RP-18 (Merck, Darmstadt, Germany) with particle diameter of 5 μm was used as a sorbent. Packing solvent (ethanol) was delivered by a single piston air-driven pump (Shandon, Cheshire, UK). Packed columns were tested on an apparatus consisting of an MPLC Micropump (Applied Biosystems, Santa Clara, CA, USA), a manual injector fitted with 0.5-μl loop (Valco, Houston, TX, USA) and a μLC-10 UV spectrophotometer with 0.5-μl flow cell (ISCO, Lincoln, NB). Anthracene was used for measurement of column efficiency, with a mobile phase of aqueous 80% acetonitrile at a flow-rate of 50 or 200 μl/min (for 1.0 or 2.1 mm I.D. columns, respectively) and detection at 260 nm.

Sample extraction

Shellfish tissue samples were extracted in 0.1 M HCl according to the AOAC mouse bioassay procedure [2]. Extracts were cleaned using a LC-18 octadecylsilica solid phase extraction cartridge (Supelco) [7] or by ultracentrifugation through a 10 000 NMWL filter (Millipore, Bedford, MA, USA) at 10 000 g for 20 min. Toxic phytoplankton extracts were kindly provided by Dr. A.D. Cembella (Institute for Marine Biosciences, Halifax, Canada). Cells of the marine dinoflagellate *Alexandrium* in unialgal culture (isolate Gt429, CCMP Collection, Bigelow Labs., Boothbay Harbour, ME, USA) and in natural mixed phytoplankton assemblages (from Gaspé, Québec, Canada) were sonicated in 0.03 M acetic acid followed by centrifugation (10 000

g, 10 min) and filtration (0.22-μm Millex filter, Millipore).

Pre-column oxidation and LC analysis

Sample derivatization was based on a periodate oxidation which converts all PSP toxins to fluorescent derivatives. The composition of the oxidation mixture and procedures for manual reaction were the same as described earlier [8]. The oxidation mixture was prepared daily. Automated reactions and analyses were carried out with reagents and samples placed in individual crimp-top plastic vials in the HP1090 auto-sampler. The latter were controlled through the "Injector Program" which is part of the standard HP7994A ChemStation software. The details of

TABLE I

INJECTOR PROGRAM USED FOR AUTOMATED PRE-COLUMN OXIDATION REACTION AND INJECTION

LC conditions: 25 cm × 1.0 mm I.D. column packed with 5 μm LiChrospher-100 RP18 (*N* = 11 000); mobile phase: A = 10 mmol/l HFBA in water adjusted to pH 4.2 with NH₄OH, B = acetonitrile, gradient from 0 to 20% B over 20 min; 100 μl/min flow-rate; fluorescence detection (335 nm excitation, 400 nm emission). A 12-min column equilibration time was used between analyses. Vial 0 = Periodate oxidation reagent (1:1:1 mixture of 0.03 M periodic acid, 0.3 M Na₂HPO₄ and 0.3 M ammonium formate adjusted to pH 9.0 with 1 M NaOH; prepared daily); vial 1 = water for needle rinse; vial 2 = acetic acid (1:1 mixture of water and glacial acetic acid).

Line	Function		
1	Draw: 7.0 μl	from:	Vial: 0
2	Draw: 0.0 μl	from:	Vial: 1
3	Draw: 4.0 μl	from:	Sample
4	Draw: 0.0 μl	from:	Vial: 1
5	Draw: 7.0 μl	from:	Vial: 0
6	Mix: 7.0 μl	cycles:	3
7	Wait: 1.7 min		
8	Draw: 0.0 μl	from:	Vial: 1
9	Draw: 2.0 μl	from:	Vial: 2
10	Mix: 5.0 μl	cycles:	2
11	Inject		
Total injection volume: 20.0 μl			

the entire method, including reagent compositions and LC conditions, are given in Table I.

RESULTS AND DISCUSSION

LC conditions

The previously published pre-column oxidation method [8] used a mobile phase of aqueous ammonium formate (100 mmol/l, pH 6) with a gradient from 0% to 5% acetonitrile and a reversed-phase Supelcosil LC-18 column. Although this system provided excellent performance for the oxidized PSP toxins, alternative mobile and stationary phases have been investigated in this work in an attempt to increase the retention of the analytes. This was desirable in order to facilitate high sensitivity analyses through the use of large injection volumes (see below).

In our past experience, we have found that 0.1% (v/v) (9 mmol/l) trifluoroacetic acid (TFA) in aqueous acetonitrile is an excellent mobile phase for the analysis of basic compounds [9]. The acidic conditions (pH 2.1) suppress interactions of the analytes with active silanol sites in the column resulting in symmetrical peak shapes, while the TFA anion acts as an effective ion-pair agent resulting in increased retention. Preliminary experiments, carried out on short, narrow bore (10 cm × 2.1 mm I.D.) columns, showed that most of the PSP oxidation products behaved well with such a mobile phase in combination with several different stationary phases (Zorbax Rx-C18, Vydac 201TP, LiChrospher RP-18, etc.). LiChrospher RP-18 (5 μm particle size) was selected as the sorbent for the remainder of the project because it is commercially available in bulk and proved most suitable in our hands for the preparation of high efficiency microbore columns (see below). Under isocratic conditions, with 10% acetonitrile in the mobile phase, it was observed that the retention times of the analytes increased with increasing concentration of TFA (up to 9 mmol/l). Since pH varies with the concentration of TFA, experiments were conducted to study the effect of pH, independent of TFA concentration. The mobile phase pH was controlled by the addition of NH₄OH. With a constant TFA concentration of 10 mmol/l and the pH adjusted over the range 2

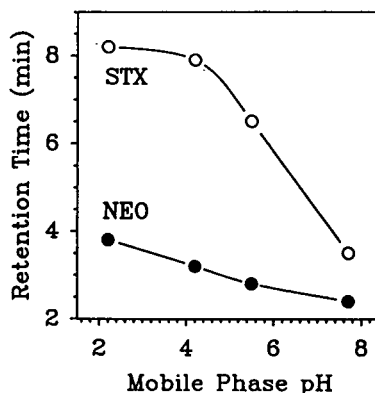


Fig. 2. Effect of mobile phase pH on the retention of the oxidized PSP toxins, saxitoxin (STX) and neosaxitoxin (NEO), in isocratic reversed-phase LC. The mobile phase contained 10 mmol/l trifluoroacetic acid (TFA) adjusted to the specified pH with NH₄OH. Other conditions as in Table II.

to 8, the greatest retention was achieved at low pH. Fig. 2 shows the effect of pH on the retention times of oxidized NEO and STX.

These results can be attributed to the formation of strong hydrophobic ion pairs between the oxidized toxins and the TFA. The toxins lose their positive charge as the solution pH approaches their dissociation constants (for unoxidized STX, $pK_a = 8.1$), and consequently ion pairs would not be created effectively at high pH. Peak shape and separation selectivity appeared

TABLE II

EFFECT OF ADDITION OF VARIOUS ACIDS TO THE MOBILE PHASE ON THE RETENTION OF OXIDIZED NEOSAXITOXIN (NEO) AND SAXITOXIN (STX)

Column: LiChrospher-100 RP-18 (10 cm × 2.1 mm I.D.) at ambient temperature; mobile phase: isocratic 10% acetonitrile, 10 mmol/l acid, adjusted to pH 4.2 with 1 M NH₄OH; flow-rate: 200 μl/min.

Ion-pair agent (at 10 mmol/l)	Retention time (min)	
	NEO	STX
Formic acid [HCOOH]	2.5	4.4
Acetic acid [CH ₃ COOH]	2.6	4.5
TFA [CF ₃ COOH]	3.6	7.9
HFBA [C ₃ F ₇ COOH]	13.1	23.6
TDFHA [C ₆ F ₁₃ COOH]	41.5	72.3

best at pH 4.2, so this was used for all subsequent experiments.

In an attempt to further increase retention and to test the ion-pair hypothesis, other acid modifiers were investigated. As shown in Table II, formic acid and acetic acid gave similar low retention times for oxidized NEO and STX at pH 4.2, but retention times were increased dramatically with longer chain perfluorinated acids. Retention with HFBA was approximately triple that of TFA, and tridecafluoroheptanoic acid (TDFHA) tripled that of HFBA. The longer-chain perfluorinated acids presumably form ion pairs with greater hydrophobicity, resulting in a stronger retention of analyte on the octadecylsilica stationary phase. This means that a higher percentage of acetonitrile can be used with HFBA or TDFHA to give similar retention values to those with TFA. It also means that a larger volume of aqueous sample may be injected in a gradient elution experiment starting from an initial 0% organic. As discussed below, this feature was used to improve sensitivity and to facilitate a fully automatic system. Since TDFHA (a solid at room temperature) proved difficult to dissolve, caused considerable foaming of the mobile phase due to its surfactant nature and is also quite expensive, HFBA was selected as the ion-pair agent for subsequent work.

Initial gradient elution experiments were conducted on the 2.1 mm I.D. LiChrospher RP-18 column. Using aqueous HFBA (adjusted to pH 4.2 with NH_4OH) as solvent A and acetonitrile as solvent B, the mobile phase was programmed from 0 to 20% B over 10 min. This resulted in a slight change in buffer concentration through the run but this did not seem to cause any problems. Fig. 3 presents some representative chromatograms for six individual toxin standards that were available in high purity. The chromatogram for GTX1 + 4 (data not shown) was very similar to that of GTX2 + 3. C3 + 4 was not available to us as a standard but a chromatogram for a mixture of C1 to C4 indicated that the products of C3 + 4 are the same as those for C1 + 2. Recently, we have reported the use of combined liquid chromatography–mass spectrometry (LC–MS) to characterize the oxidation products of the PSP toxins [10]. Fig. 4 presents the proposed structures of the major products. As can be seen in

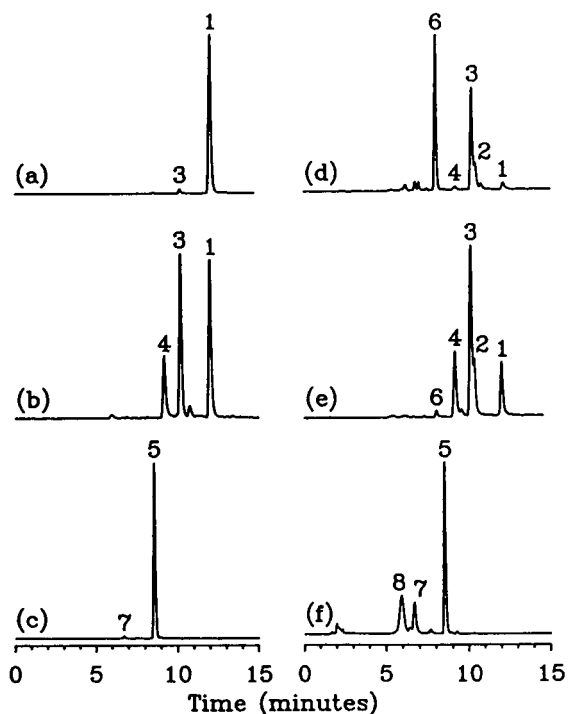
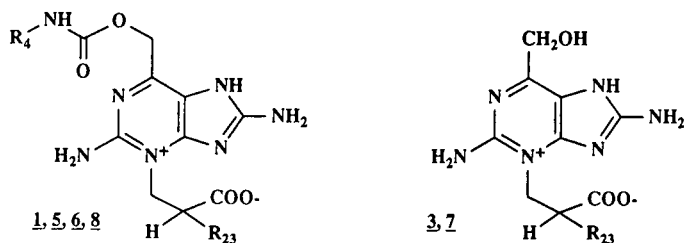


Fig. 3. Gradient elution LC analysis of oxidized toxin standards: (a) STX; (b) NEO; (c) GTX2 + 3; (d) B1; (e) B2; (f) C1 + 2. GTX2 + 3 and C1 + 2 are equilibrium mixtures of the epimeric toxins GTX2 and GTX3 and C1 and C2, respectively. GTX1 + 4 gives a similar result to that of GTX2 + 3, with a slightly larger peak 7. Oxidation reactions were performed manually; toxin concentrations before the oxidation reaction were approximately 100 $\mu\text{g}/\text{ml}$. LC conditions: gradient from 0 to 20% (over 10 min) acetonitrile in aqueous 10 mmol/l HFBA (adjusted to pH 4.2 with NH_4OH); 10 cm \times 2.1 mm LiChrospher RP-18 column; 200 $\mu\text{l}/\text{min}$ flow-rate; 1 μl injection volume; fluorescence detector gain set at 2^9 . For peak Nos., see Fig. 4.

Figs. 3 and 4, STX and the GTX and C toxins yielded primarily single products (1 and 5, respectively) while NEO and the B toxins yielded several products (1, 2, 3, 4 and 6) under the oxidation conditions employed. Excellent peak shapes were observed for all toxins and this encouraged us to proceed with development of a microcolumn (1 mm I.D.) LC method.

Microcolumn LC

One of the advantages of gradient elution is the possibility of improving concentration detection limits through the on-column trace enrichment effect [11]. This effect allows the use of large injection volumes, provided that the sam-



Prod. No. ^a	R ₄	R ₂₃ ^b	Precursors	Prod. No. ^a	R ₂₃	Precursors
<u>1</u>	H	H	STX, NEO, (B1), (B2)	<u>3</u>	H	dSTX, NEO, B1, B2, (STX)
<u>5</u>	H	OSO ₃ H	GTX1-4, C1-4	<u>7</u>	OSO ₃ H	(C1-4), (GTX1-4)
<u>6</u>	SO ₃ H	H	B1, B2	<u>2, 4</u>	unknowns	(dSTX), (NEO), (B1), (B2)
<u>8</u>	SO ₃ H	OSO ₃ H	(C1-4)			

^a Oxidation product number (peak no. in Figures).

^b R₂₃ = either R₂ or R₃ (see Figure 1).

() = minor product from these toxins.

Fig. 4. Proposed structures for the oxidation products of the PSP toxins. These were based on fluorescence and mass spectra, as well as relative retention times [10]. Table III presents the relative yields and retention times of the products from the different toxins.

ple is dissolved in a solvent with a low eluotropic strength and that analytes have high retention factors. From preliminary experiments, it was found that up to 90 μ l of oxidized reaction mixture could be injected on the 2.1 mm I.D. column using the HFBA mobile phase and gradient elution described above, without substantial band-broadening. On a 4.6 mm I.D. column, this translates to a 420- μ l injection volume. Although our LC autoinjection system could have been reconfigured to allow such large volumes, it was more convenient to keep the system in the standard configuration (25 μ l maximum) required for other routine analyses. Therefore, to fully utilize the trace enrichment effect, we continued our work on 1.0 mm I.D. microbore columns. Although such an approach is more difficult to implement on conventional LC systems, it has the advantage that less sample is consumed to achieve the same concentration detection limit (*i.e.*, a lower mass detection limit). As indicated later, this is very useful for certain applications such as the analysis of plankton samples.

LiChrospher RP-18 microcolumns (25 cm \times

1.0 mm I.D.), prepared in our laboratory using the slurry packing technique, gave moderately high efficiencies ($N = 11\,000$, measured using a micro-LC-UV detector equipped with a 0.5- μ l flow cell). When the columns were used on the HP1090 LC system, a relatively high flow-rate of 100 μ l/min was used to both decrease analysis time and ensure compatibility with the pumping system and the size of the flow cell (4.5 μ l) in the fluorescence detector. The large size of the flow cell concerned us a great deal before starting the experiment, since a 0.5–1- μ l flow cell size is normally used for microbore work. However, we were surprised to find that column efficiency was deteriorated by only 20% over that measured on the micro-LC system. This was deemed quite acceptable, since the detection sensitivity associated with a large flow cell compensated for the extra band broadening. Our observations are supported by a recent report [12] which showed that it is the design of the flow cell and connecting tubing rather than the absolute flow cell volume that is of primary importance, and that it is possible to use certain commercially available LC detectors fitted with

conventionally sized flow cells in microbore column work. The HP1046A fluorescence detector used in our study seems to have a design suitable for microbore work.

Using gradient elution with the HFBA–aqueous acetonitrile mobile phase, it was possible to inject 20 μ l of oxidation reaction solution without significant band broadening. This represents a 20-fold increase over the normal 1- μ l injection volume for a 1.0 mm I.D. column. Fig. 5 demonstrates clearly the high-efficiency separations that are possible with such a system. Fig. 5a shows the chromatogram from a 20- μ l injection of a mixture of GTX2 + 3 and NEO, oxidized by a manual reaction according to the earlier method [8]. Similarly, Fig. 5c shows the chromatogram resulting from a mixture of STX and B2. In

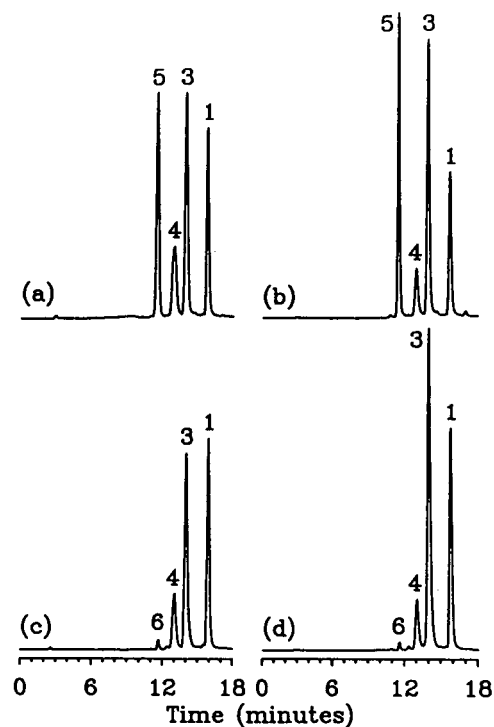


Fig. 5. Analyses of 2 standard PSP toxin mixtures by LC using manual (a, c) and automated (b, d) pre-column oxidation. Mixture 1 (a, b) contained GTX2 + 3 and NEO at 1.2 and 4.4 μ g/ml, respectively. Mixture 2 (c, d) contained B2 and STX at 3.3 and 5.0 μ g/ml, respectively. Peak 1 in (c, d) is due to STX mainly, but there is a small contribution from B2, especially in the manual reaction. LC conditions: see Table I; 20 μ l injection volume for both manual and automated reactions; fluorescence detector gain set at 2^{11} .

general, with this system, we have obtained better separation efficiency, peak shape and baseline stability than with the previous ammonium formate mobile phase [8]. Some changes in the order of elution of analytes were observed, however. Table III provides a listing of the retention times of the oxidized PSP toxins on the microcolumn system.

Automated reaction system

Most pre-column derivatization methods suffer from the disadvantage of being labor-intensive and relatively imprecise due to potentially poor volumetric and reaction time control. The latter is quite important for the pre-column oxidation procedure since both reaction time and the time between completion of the reaction and LC analysis can affect relative proportions and overall yields of oxidation products. A fully automated reaction could improve precision and allow unattended analyses.

Several commercially-available LC auto-sampler systems permit automated derivatizations to be performed prior to LC analysis. The HP1090 LC system used in this study can perform such reactions through the HP Chem-Station's "Injector Program". User-defined volumes of reagents and sample may be drawn into a reaction capillary where they are mixed, allowed to react, and then injected on the column. An injector program that allows the current pre-column oxidation procedure is listed in Table I. It uses a 4.0- μ l aliquot of sample mixed first with 14 μ l of oxidation reagent and then with 2.0 μ l of concentrated acetic acid. The entire injection sequence including the 1.7-min reaction time takes 3 min. It is important to note that the oxidation reaction is pH-dependent. It was reported previously [8] that the optimum pH for the oxidation reagent was 8 for the manual reaction, and that samples should be adjusted to pH 8 before reaction to avoid buffer effects from the sample matrix. For the automated reaction it was observed that the fluorescence response for STX and GTX2 + 3 reached a maximum at pH 9; the response for NEO decreased gradually with increased pH over the range of 8 to 10.5. An oxidation reagent pH of 9 was selected as a

TABLE III

RETENTION TIMES AND RELATIVE YIELDS OF OXIDATION PRODUCTS FOR VARIOUS PSP TOXINS USING THE FULLY AUTOMATED OXIDATION PROCEDURE

Product code ^a	Retention time (min) ^b	Relative yield (%) ^c							
		STX	dcSTX	NEO	B1	B2	GTX2 + 3	GTX1 + 4	C1 + 2 ^e
1	15.9	99		30	2	3			
2	14.3		25	1	1	1			
3	14.0	1	75	60	30	80			
4	13.0 ^d			10	2	12			
5	11.2						99	96	75
6	11.2				65	2			
7	4.8						1	4	10
8	3.8 ^d								15

^a Oxidation product code numbers refer to structures in Fig. 4 and are used to identify peaks in chromatograms.

^b Conditions: as in Table I.

^c Approximate relative yield of products from each toxin estimated from relative peak heights; insufficient standards to give relative sensitivities between toxins.

^d Broad peak.

^e Expected products for C3 + 4 also, but no individual standards were available.

compromise. A pH meter was used to adjust pH to ensure the best reproducibility.

Fig. 5b and d shows the chromatograms resulting from the automated pre-column oxidation of the same standard solutions analyzed after manual reaction in Fig. 5a and c, respectively. While there is no deterioration in the separations due to the automated reaction, there are some slight changes in relative responses for the toxins. For the automated reaction of NEO, there is an increase of product 3 relative to products 1 and 4 (Fig. 5b vs. 5a). The same observations are true for B2 (Fig. 5d vs. 5c), which is converted to essentially the same array of products as NEO in addition to compound 6. In comparing Fig. 5c and d, it is important to keep in mind that B2 and STX contribute to peak 1, with B2 contributing somewhat less in Fig. 5d due to its increased conversion to 3. The reasons for the different profiles with the automated system are not completely understood at this time; the profiles are highly reproducible, however.

Table III presents the retention times and relative proportions of the oxidation products observed for the automated analyses of all the toxins that were available to us. Because toxin

standards with accurate concentrations were not available, the relative sensitivities for each toxin can not be presented at this time. Accurate calibration will be very important for the future implementation of this method, as the relative molar response factors of the different toxins appear to vary considerably. Of course, this has also been a major problem with the post-column oxidation LC method [4,5]. Since completion of this project, accurate calibration solutions for STX, NEO and GTX2 + 3 have become publicly available from the NRC Marine Analytical Chemistry Standards Program.

The reproducibilities of both the automated and manual methods were compared by performing replicate analyses. The results indicated that the automated method is much more reproducible than the manual method. The relative standard deviations (R.S.D., $n = 6$) for peak areas of STX, NEO and GTX2 + 3 standards were as follows: (a) 11, 18 and 18%, respectively, for manual reaction; (b) 3.5, 3.4 and 2.2%, respectively, for automated reaction. Retention times for the gradient elution procedure were also found to be very reproducible (0.1 to 0.2% R.S.D.). It should be mentioned, however, that

since the column was left at ambient temperature in our experiments, there were some variations from day to day when the room temperature changed. It is recommended that the column temperature be thermostatically controlled for the best long-term retention time reproducibility. Good linearity of response and zero intercepts were observed for calibration curves generated by the automated analysis of serially diluted solutions of STX, NEO and GTX2 + 3.

The combination of the large volume injection with microbore LC makes this one of the most sensitive methods for the measurement of PSP toxins. An example of the trace analysis of a diluted toxin standard mixture is shown in Fig. 6, along with that of a blank reaction. Estimated values for the detection limits of STX, NEO and GTX2 + 3, listed in Table IV, are in the low femtomole range. These are about 80 times more sensitive than the Sullivan and Wekell post-column oxidation method [5] based on mass detection limits. Concentration detection limits are as low as 0.35 pmol/l for GTX2 + 3 and 1 pmol/l for STX. Accurate estimates for the detection limits of other toxins can not be provided until reliable standards are available,

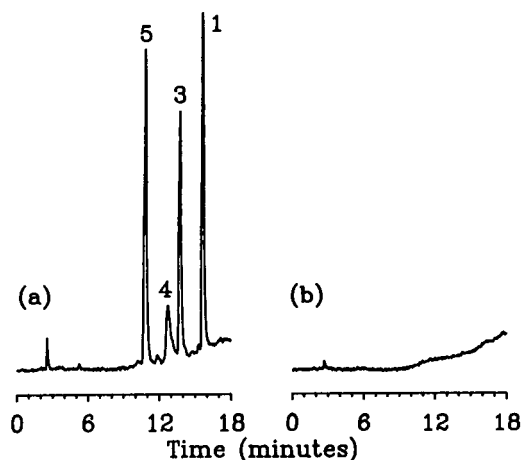


Fig. 6. Automated pre-column oxidation LC analyses of: (a) a low-level PSP toxin standard mixture, containing GTX2 + 3, NEO and STX at 16, 50 and 33 ng/ml, respectively; and (b) a blank reaction. LC conditions: see Table I; fluorescence detector gain set at 2^{18} .

TABLE IV

ESTIMATED DETECTION LIMITS ACHIEVED IN THE FULLY AUTOMATED ANALYSIS PROCEDURE

LC conditions as in Fig. 5 and Table I, detector gain = 2^{18} , 4 μ l sample reacted (20 μ l reaction mixture injected). MDQ = Minimum detectable quantity injected on-column (estimate for $S/N = 3$); MDC = minimum detectable concentration in the sample extract (estimate for $S/N = 3$).

Analyte	MDQ		MDC	
	pg	fmol	ng/ml	pmol/l
STX	1.2	4.0	0.30	1.0
NEO ^a	2.2	7.0	0.56	1.8
GTX2 + 3	0.6	1.5	0.14	0.35

^a Based on the principal product (3) for NEO.

although from the present work they all appear to be of the same order of magnitude.

Application to samples

Some practical applications of the automated pre-column oxidation/microcolumn method are illustrated in Figs. 7 and 8. An extract of a contaminated scallop liver currently being examined as a candidate reference material for PSP toxins gave the chromatogram in Fig. 7a, after a simple cleanup through a C_{18} solid-phase extraction cartridge [8]. Two outstanding peaks were observed corresponding to products from GTX2 + 3 and STX; one very weak peak was observed corresponding to the product from NEO. Concentrations were estimated to be 23, 3.6 and 19 μ g/g in the original tissue for GTX2 + 3, NEO and STX, respectively; these results are in good agreement with those from analyses using the post-column oxidation system [5]. A similar chromatogram was acquired from raw scallop liver extract after centrifugation through a molecular mass 10 000 filter. The chromatogram from an extract of mussel tissue contaminated at 1 μ g/g total toxin (as determined by mouse bioassay) is given in Fig. 7b. The presence of C's, GTX's, NEO and STX is indicated. This was confirmed using the post-column oxidation system.

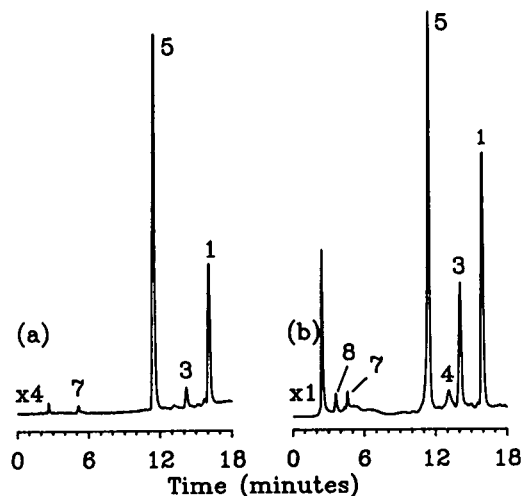


Fig. 7. Analyses of extracts of shellfish contaminated with PSP toxins using the automated pre-column oxidation procedure: (a) scallop liver (candidate reference material); (b) mussel tissue with 1 $\mu\text{g/g}$ STX equivalent by mouse bioassay. LC conditions: see Table I; fluorescence detector gain set at 2^{14} for (a) and 2^{17} for (b); 250 μg tissue equivalent injected for each.

The monitoring of phytoplankton is an important activity that can allow warnings to be issued to aquaculturists when plankton blooms

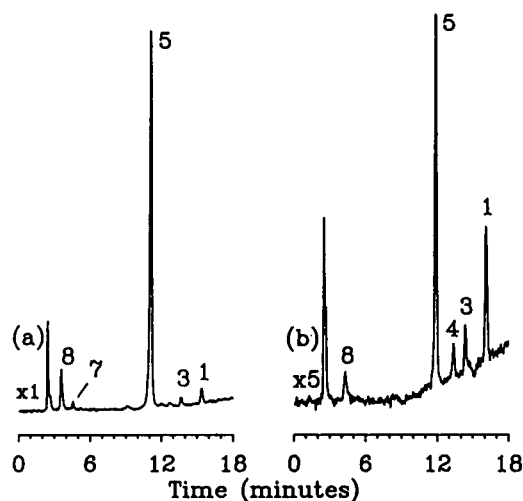


Fig. 8. Analyses of phytoplankton samples containing endogenous levels of PSP toxins using the automated pre-column oxidation procedure: (a) *Alexandrium tamarense* (Gt429), equivalent of 60 cells injected; (b) *Alexandrium excavatum* in a mixed phytoplankton sample, equivalent of 20 cells of *Alexandrium* injected. LC conditions: see Table I; fluorescence detector gain set at 2^{18} .

are starting or have occurred. A simple, rapid and sensitive assay for PSP toxins would be a useful tool for such monitoring programs to determine if a bloom is in fact toxic. We have tested a number of plankton samples and found that the present automated pre-column oxidation method should be very useful for screening plankton samples. Fig. 8a shows the results obtained for an extract of cultured *A. tamarense* (Gt429). The analysis was performed on the equivalent of only 60 cells. Similarly, an extract of *Alexandrium excavatum* cells in a natural phytoplankton assemblage (Gaspé) gave the chromatogram in Fig. 8b. This represents the analysis of the equivalent of only 20 *Alexandrium* cells. The main toxins observed in this sample were the GTX's, but small amounts of C's, NEO and STX were also present. Non-toxic plankton samples gave no significant peaks upon analysis.

CONCLUSIONS

Automated pre-column oxidation coupled with LC and fluorescence detection is a very sensitive and reproducible method for the routine screening analysis of PSP toxins. The method is more sensitive and far easier to perform on a routine basis than is the post-column oxidation method. However, due to the formation of identical oxidation products from some toxins and multiple products from others, the method is less useful than the post-column oxidation for research work directed at understanding the distribution of toxin structures.

The very high mass sensitivity provided by the microcolumn-based technique makes it very useful for the screening of phytoplankton samples for PSP toxins. Since an analysis may be achieved with fewer than 100 cells, it should be relatively easy to perform "cell-picking" experiments from mixed phytoplankton populations.

Although the microcolumns provide the highest mass sensitivity, it is important to keep in mind that an automated pre-column oxidation reaction is also applicable to conventional chromatographic systems. Indeed, we have had good success with both 2.1 and 4.6 mm I.D. columns

and we have been able to implement the method on other manufacturers' autosampler systems.

ACKNOWLEDGEMENTS

The authors are grateful to Dr. M.V. Laycock for PSP toxin standards, Dr. A.D. Cembella for the plankton extracts, Dr. P.G. Sim for the scallop tissue extract and Mr. W.R. Hardstaff and Mr. R. Richards for technical assistance. Funding for this project was provided in part by Health and Welfare Canada.

REFERENCES

- 1 Y. Shimizu, in A.T. Tu (Editor), *Handbook of Natural Toxins: Marine Toxins and Venoms*, Marcel Dekker, New York, 1988, p. 63.
- 2 *Official Methods of Analysis*, Associations of Official Analytical Chemists, Arlington, VA, 14th ed., 1984, sections 18.086–18.092; 15th ed., 1990, section 959.08G.
- 3 D.L. Park, W.N. Adams, S.L. Graham and R.C. Jackson, *J. Assoc. Off. Anal. Chem.*, 69 (1986) 547.
- 4 Y. Oshima, M. Machida, K. Sasaki, Y. Tamaoki and T. Yasumoto, *Agric. Biol. Chem.*, 48 (1984) 1707.
- 5 J.J. Sullivan and M.M. Wekell, in D.E. Kramer and J. Liston (Editors), *Seafood Quality Determination*, Elsevier/North-Holland, New York, 1987, p. 357.
- 6 H.A. Bates and H. Rapoport, *J. Agric. Food Chem.*, 23 (1975) 237.
- 7 J.F. Lawrence, C. Menard, C.F. Charbonneau and S. Hall, *J. Assoc. Off. Anal. Chem.*, 74 (1991) 404.
- 8 J.F. Lawrence and C. Menard, *J. Assoc. Off. Anal. Chem.*, 74 (1991) 1006.
- 9 S. Pleasance, P. Blay and M.A. Quilliam, *J. Chromatogr.*, 558 (1991) 155.
- 10 M.A. Quilliam, M. Janecek and J.F. Lawrence, *Rapid Comm. Mass Spec.*, in press.
- 11 K. Slais, D. Kourilova and M. Krejci, *J. Chromatogr.*, 282 (1983) 363.
- 12 D.N. Mallett and B. Law, *J. Pharm. Biomed. Anal.*, 9 (1991) 53.

Ultratrace anion analysis of high-purity water

A column comparison

Michael W. Martin* and Russel A. Giacomini

Analytical Technology Division, Eastman Kodak Company, 66 Eastman Avenue, Rochester, NY 14650-2140 (USA)

(Received April 5th, 1993)

ABSTRACT

Several vendor columns were employed in a comparison of columns aimed at optimized separation and quantitation of ultratrace (*i.e.*, high pg/ml to low ng/ml) levels of anions in high-purity water. The anionic profile of feed water will vary depending on the source; however, anions of most interest in high-purity water applications were chromatographed. The anions tested included fluoride, acetate, formate, chloride, nitrite, bromide, nitrate, phosphate, sulfate, and oxalate. Isocratic methods were used without exception and all separations were made under chemically suppressed conditions employing a Dionex AMMS-1 suppressor with 12.5 mM sulfuric acid as regenerant. All eluents were prepared from either sodium carbonate–sodium hydrogencarbonate or 50% (w/w) sodium hydroxide solution. Columns evaluated in this study included Dionex AS4A, AS9, and AS10, Sarasep AN1 and AN2, and Waters IC-PAK Anion HR. Comparisons were made on the basis of chloride retention, resolution of fluoride and acetate, column efficiency on nitrite and sulfate peaks, capacity, and run time. Column durability was not thought to be an issue because of the nature of the samples. Dionex AS10, Sarasep AN2 and Waters IC-Pak Anion HR columns were deemed acceptable though no single column met every requirement.

INTRODUCTION

Over the years, two methods have emerged as on-line means of ultratrace analysis by ion chromatography. The first is merely a large volume injection technique [1,2]. In this case, between 0.5 and 2.0 ml have been successfully injected onto an ion chromatography column. The major drawback to this technique is the huge ensuing water dip that masks weakly retained species such as fluoride, acetate, and formate. The second and more popular method uses one or two switching valves and a concentrator column which is loaded off-line from the analytical column but switched in-line prior to elution of the solutes [3–5]. Large sample volumes, up to 100 ml, can be handled by this scheme as the concentrator column interstitial volume is of the

order of 0.4 ml. Concentrator column procedures are not as straightforward as they might appear. Jackson and Haddad [6] have elegantly described the complexities of this strategy.

Haddad and Heckenberg [7,8] have extensively studied factors that make up a precise and quantitative preconcentration for single-column ion chromatography (SCIC) and recommended a single pump with two high pressure switching valves. Jackson and Haddad [9] found the use of a monovalent aromatic acid at pH < 6 avoided interference by bicarbonate and provided good loading, washing, and backflushing characteristics from the concentrator column. In addition, they studied the effects of sample loading parameters [10] and ion-exchange capacity of the concentrator column [11] on achieving optimal preconcentration. Their aim was to achieve a precise and quantitative loading of the components in the sample such that these components

* Corresponding author.

would be quantitatively transferred onto the analytical column in a tight band with retention characteristics: $4 < k' < 30$ in an eluent compatible with the requirements of SCIC.

Harvey [12] evaluated several Dionex columns for a one-step gradient procedure separating eleven anions of interest in nuclear power industry applications. In particular, he cited the need to separate fluoride, acetate, formate, and chloride. Because of elution problems with hydrogencarbonate/carbonate eluents, he found the Omni-Pac PAX 100 column with a hydroxide step gradient and chemical suppression provided the needed resolution and run time for this application.

We have found the preparation of hydroxide eluents for gradient use to be somewhat tedious necessitating trap columns while maintaining a CO₂ free headspace over the eluent [13]. In addition, we have seen retention time shifts, especially for weakly retained anions, from eluent to eluent and baselines upon which it is difficult for data systems to perform integration without recalculation by the user. Also, gradients necessitate a post run equilibration period that usually requires about 10 column volumes of eluent. For these reasons, we prefer an isocratic separation with a stable and robust eluent such as hydrogencarbonate–carbonate.

Aside from the work of Harvey [12], little has been done to specify requirements for ultratrace anion applications. Our application requires the elution and separation of weakly retained anions such as fluoride and acetate as well as strongly retained anions such as sulfate in a suppression mode. The recent introduction of new IC columns of higher capacity, notably the Dionex AS10 and Sarasep AN2, may offer an advantage towards this end. In our work, the separation of fluoride, acetate, and chloride is essential. Thus, we have evaluated several low-capacity IC columns (Dionex AS4A and AS9, Sarasep AN1 and Waters IC-Pac Anion HR) along with two columns of somewhat higher capacity (Sarasep AN2 and Dionex AS10). The comparison is based on resolution of fluoride and acetate, chloride retention, total run time, and column efficiency. In addition, we desire baseline resolution of fluoride, acetate, chloride, nitrite,

bromide, nitrate, phosphate, and sulfate in twenty minutes. Of less importance in our application is the selectivity of these columns towards formate and oxalate as these anions have been observed in the work of others [12].

EXPERIMENTAL

Reagents

Reagent-grade water from a Milli-Q system (Millipore, Bedford, MA, USA) was used throughout this work. Sodium carbonate and sodium hydrogencarbonate were standard reference materials obtained from NIST (National Institute of Standards and Technology, Gaithersburg, MD, USA). Sodium hydroxide, 50% (w/w), was Fisher certified reagent (Fisher Scientific, Fair Lawn, NJ, USA). Sulfuric acid used to prepare regenerant was ULTREX Ultrapure reagent (J.T. Baker, Phillipsburg, NJ, USA). Sodium nitrate used to measure column capacities was reagent-grade material (EM Industries, Cherry Hill, NJ, USA). Anion standards for fluoride, chloride, nitrite, bromide, nitrate, and sulfate were prepared from certified 1000 µg/ml stock solutions (Alltech, Deerfield, IL, USA). The oxalate standard was prepared from J.T. Baker primary standard oxalic acid, formate from reagent grade sodium formate (Aldrich, Milwaukee, WI, USA), and acetate from suprapure sodium acetate (Alfa/Johnson Matthey, Ward Hill, MA, USA).

Instrumentation

All column test chromatograms were performed on a Dionex 4500i, polyether ether ketone (PEEK) version (Dionex, Sunnyvale, CA, USA) with a Spectra-Physics 8875 autosampler (Spectra-Physics, Fremont, CA, USA) and 20-µl loop. Sulfuric acid regenerant at 12.5 mM concentration was delivered with a Dionex AutoRegen module. The Dionex system was controlled and data acquired with a Dionex AutoIon 450. The columns and corresponding eluents used in this study are found in Table I. Flow-rates used with all columns was 1.0 ml/min. A Waters 600E pump (Millipore, Milford, MA, USA) equipped with a Rheodyne 9125 metal-free injector valve (Rheodyne, Cotati,

TABLE I
ANION-EXCHANGE COLUMN SPECIFICATIONS

Columns	Manufacturer	Dimensions (mm)	Particle size (μm)	Eluent
IonPac AS4A	Dionex	250 × 4	15	1.4 mM Carbonate, 1.3 mM hydrogencarbonate
IonPac AS9	Dionex	250 × 4	15	1.5 mM Carbonate, 0.56 mM hydrogencarbonate
IonPac AS10	Dionex	250 × 4	8.5	90 mM Hydroxide
AN1	Sarasep	250 × 4.6	8	1.4 mM Carbonate, 1.3 mM hydrogencarbonate
AN2	Sarasep	250 × 4.6	8	1.6 mM Carbonate, 2.1 mM hydrogencarbonate
IC-Pak Anion HR	Waters	75 × 4.6	6	1.2 mM Carbonate, 1.1 mM hydrogencarbonate

CA, USA) was used with a Kratos 783 variable-wavelength UV detector (Applied Biosystems, Ramsey, NJ, USA) at 245 nm (this wavelength was chosen to provide a 0.7 AU response with 10 mM nitrite) to measure column capacities. A Waters 590 pump and events unit controlled a Waters solvent switching valve and an Eldex Model E series B sample pump in the trace enrichment studies. Data acquisition for the Waters systems was made with a Nelson 2600 through series 760 interfaces.

Column capacity studies

Columns were converted to the hydroxide form by pumping with 1 M sodium hydroxide for 1 h. The excess base was pumped out with water until the conductivity dropped to 1 μS . The column was connected directly between the 9125 valve and the UV detector with a minimum of 0.010 inch I.D. PEEK tubing. While pumping water at 1.0 ml/min, the data system was started simultaneously with a switch from water to 10 mM sodium nitrite. An S-shaped curve was obtained and the time required to achieve 90% of the absorbance in the upper plateau region was determined for t (i.e., the nitrate breakthrough time) in the equations below. The choice of 90% absorbance was somewhat arbitrary but reflected the fact that some of the curves were not symmetrical in shape. The delay volume due to the column alone, V_M , was obtained by measuring the time required for an injected

water dip to elute from the column after conversion of the resin to the nitrite form. The system delay volume $(V_D)_{\text{TOT}}$ could be measured by removing the column, replacing with a zero-dead volume fitting, and repeating the eluent switching experiment. After returning to water, the delay volume between the injector and detector, $(V_D)_{\text{INJ}}$, was obtained by injecting 25 μl of nitrite into water and measuring the time to the beginning of the nitrite response. Pump flow rates were verified gravimetrically with each measurement. The column capacity could then be calculated from the following relationship.

$$Ft = (V_D)_{\text{TOT}} + V_M - (V_D)_{\text{INJ}} + C/E$$

Solving the above equation for C , the capacity, one obtains

$$C = [Ft - (V_D)_{\text{TOT}} - V_M + (V_D)_{\text{INJ}}]E$$

In the above equations C is the column capacity in $\mu\text{equiv.}$, E is the eluent concentration in mM, F is the flow-rate in ml/min, t is the time to achieve 90% maximum absorbance in min, and the volume quantities are defined in the text above and are in ml.

Trace enrichment studies

The Eldex pump had a bubble trap placed on the inlet tubing just prior to the pump head. This pump was operated at a flow-rate of 1.50 ml/min. A single switching valve design [3,4], where the solutes are backflushed from the concen-

TABLE II
TRACE ENRICHMENT PROGRAM

Time (min)	Event or action
0.0	Flush lines to injector valve with the sample (analytical column off-line)
5.0	Load sample on the concentrator column (analytical column off-line)
8.0	Backflush the solutes onto the analytical column and data acquisition
10.0	Rotate valve back to load
33.0	End run and data acquisition

trator column, was employed and controlled by the events unit of the Waters 590 pump. A Dionex AS9 was used as the concentrator column and loaded with water sample for 3.0 min. Most applications typically preconcentrate 10 to 30 ml of sample; however, we prefer smaller volumes, of the order of 5 ml, to help minimize spreading of weakly retained anions along the concentrator column [5,10]. Between samples, the inlet line to the Eldex pump was purged with the next sample by opening the bubble trap and allowing several milliliters to run to waste as the solvent inlet line provides the greatest dead volume between samples. The anions were eluted by backflushing the concentrator column for 2.0 min onto the analytical column. The program sequence may be found in Table II. The analytical column was either a Dionex AS9 or a Sarasep AN2 (Sarasep, Santa Clara, CA, USA). A Dionex AMMS-1 suppressor was used with 12.5 mM sulfuric acid delivered at 2 ml/min pneumatically with helium. A Dionex CDM-2 was employed as detector. Samples were collected in polypropylene bottles that had been presoaked in high-purity water overnight [4].

RESULTS AND DISCUSSION

There are several desirable features for a routine analytical method for the determination of trace anions in water. These applications require pg/ml to low ng/ml level detection limits for anions. Preferably, the method will be isocratic. This eliminates the need for column re-

equilibration associated with running gradients, thus increasing sample throughput. A run time of less than 20 min is desirable. A robust method, in particular, a stable easily maintained eluent, is also needed.

There are ten anions that are commonly measured in high-purity water applications: fluoride, acetate, formate, chloride, nitrite, bromide, nitrate, phosphate, sulfate and oxalate. In our experience, we have observed all of these with the exception of formate and oxalate. Chloride is always seen at some level. This may be a combination of sampling and the ubiquitous nature of chloride. Because of this, k' for chloride of at least 1.0 for adequate retention is essential.

Acetate is frequently observed in our applications and at exceptionally high levels (hundreds of ng/ml). Because of its weak retention, separation from fluoride is important. Thus, a column that gives resolution between fluoride and acetate of at least 1.0 is desirable.

In addition to the above criteria, there are other features that are important although not specific requirements for this method; *viz.*, columns providing good efficiency (*i.e.*, >15 000 plates/m) and good peak shapes. Also, if possible in this hypothetical isocratic run, baseline resolution of all ten components would be an ideal feature.

Table III gives a compilation of the columns with emphasis on retention of fluoride, chloride, and the last eluting anion. Figs. 1-6 are chromatograms of the ten anions on each column. Only three columns meet the criteria of $k' \geq 1.0$ for chloride (Dionex AS10, Sarasep AN2 and Waters Anion Pak HR). In fact, the Waters

TABLE III
RETENTION OF SELECTED ANIONS

Columns	V_0	$k'(F)$	$k'(Cl)$	k' (last)
Dionex AS4A	1.6	0.20	0.70	8.62
Dionex AS9	1.4	0.17	0.74	11.2
Dionex AS10	2.4	0.30	2.28	10.2
Sarasep AN1	2.9	0.46	0.83	4.82
Sarasep AN2	3.0	0.52	1.02	6.17
Waters HR	1.3	1.00	2.40	13.3

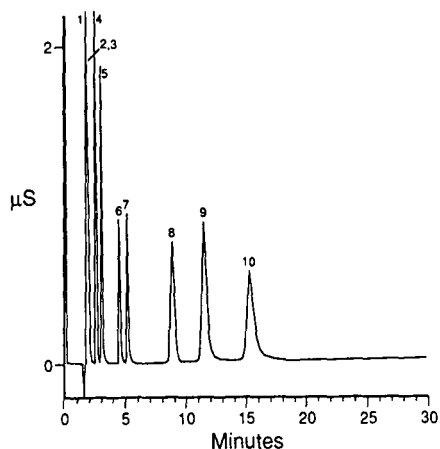


Fig. 1. Ten anions separated on a Dionex AS4A column. Conditions can be found in Table I. The flow-rate is 1.0 ml/min. Peaks: 1 = fluoride; 2 = acetate; 3 = formate; 4 = chloride; 5 = nitrite; 6 = bromide; 7 = nitrate; 8 = phosphate; 9 = sulfate; 10 = oxalate.

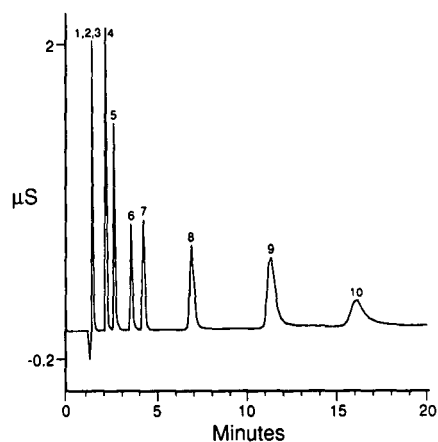


Fig. 2. Ten anions separated on a Dionex AS9 column. Conditions can be found in Table I. The flow-rate is 1.0 ml/min. Peaks as in Fig. 1.

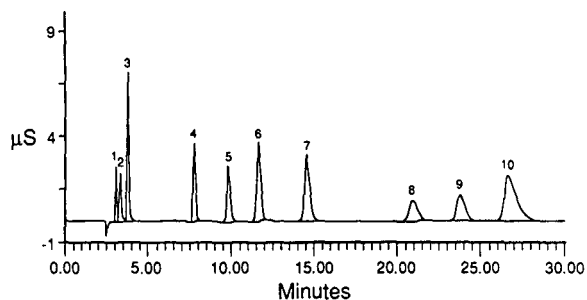


Fig. 3. Ten anions separated on a Dionex AS10 column. Conditions can be found in Table I. The flow-rate is 1.0 ml/min. Peaks: 1 = fluoride; 2 = acetate; 3 = formate; 4 = chloride; 5 = nitrite; 6 = sulfate; 7 = oxalate; 8 = phosphate; 9 = bromide; 10 = nitrate.

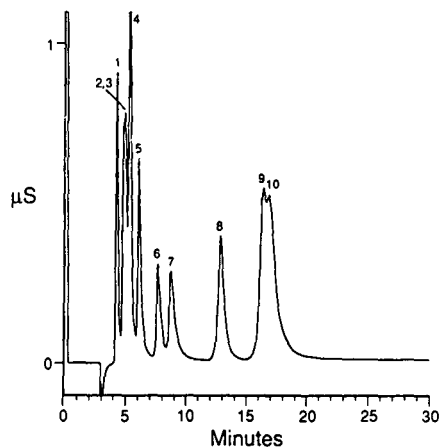


Fig. 4. Ten anions separated on a Sarasep AN1 column. Conditions can be found in Table I. The flow-rate is 1.0 ml/min. Peaks as in Fig. 1.

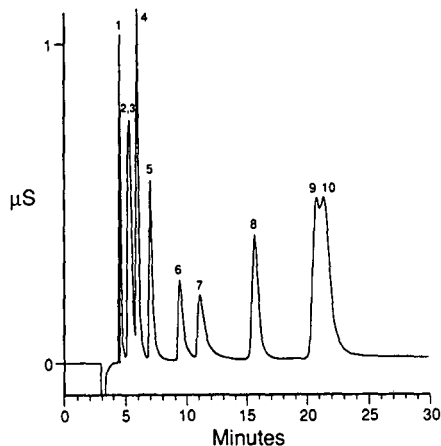


Fig. 5. Ten anions separated on a Sarasep AN2 column. Conditions can be found in Table I. The flow-rate is 1.0 ml/min. Peaks as in Fig. 1.

column shows appreciable retention of fluoride ($k' = 1.0$). The criteria for a run time < 20 min is met or nearly met by all the columns studied under the conditions of Table I.

Resolution of four pairs of closely eluting anions is given in Table IV. The pair of primary interest (fluoride and acetate) are well resolved on the Dionex AS10, Sarasep AN2 and Waters columns. The latter two actually meet the criteria of resolution of 1.0 or greater. Resolutions of formate/acetate and sulfate/oxalate are poor on the Sarasep AN2 column but of far less importance because of the absence of for-

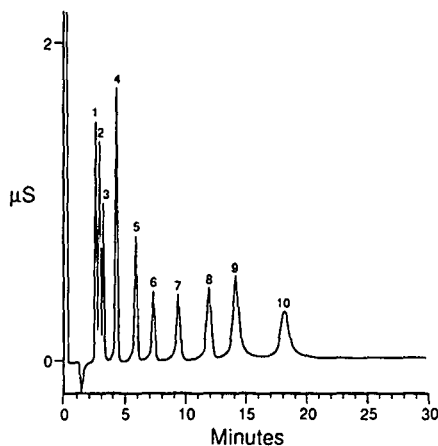


Fig. 6. Ten anions separated on a Waters IC-Pak Anion HR column. Conditions can be found in Table I. The flow-rate is 1.0 ml/min. Peaks as in Fig. 1.

mate and oxalate in these samples. Other applications may require separation of the latter two anions from acetate and sulfate, respectively. Viewing the chromatograms obtained on each

column, only the Dionex AS10 and Waters Anion Pak HR column are capable of resolution of all ten anions. Haddad *et al.* [14] found the Waters column to be superior to others used in SCIC based on a number of criteria.

Table V compares efficiencies of the columns as calculated from the width at half-height. For the most part, all columns meet the somewhat arbitrary conditions of 15 000 plates/m. The Dionex AS10 column has an exceptionally high efficiency. This may be due to the design of this pellicular/macroporous packing [15]. The peak shapes exhibited on all columns are excellent except for the Waters column where the peaks are exceedingly asymmetrical with uncharacteristic shoulders on the front and back of each peak. This column is not normally used with carbonate-type eluents and because of its methacrylate structure may be subject to some hydrolysis at high pH, although this was not confirmed in this study.

A recent example from our laboratory will

TABLE IV
RESOLUTION OF SELECTED PAIRS OF ANIONS

Column	$R_s(\text{OAc}/\text{F})$	$R_s(\text{OAc}/\text{COO})$	$R_s(\text{NO}_3/\text{Br})$	$R_s(\text{SO}_4/\text{oxalate})$
Dionex AS4A	0.39	0.58	2.50	4.45
Dionex AS9	0.00	0.00	2.98	4.42
Dionex AS10	0.88	1.88	2.37	4.79
Sarasep AN1	2.87	0.10	1.58	0.35
Sarasep AN2	2.17	0.26	1.89	0.61
Waters HR	1.39	1.54	4.04	3.66

TABLE V
COLUMN EFFICIENCIES AND CAPACITIES

Column	N (nitrite) ^a	N (sulfate) ^a	Capacity
Dionex AS4A	22 000	16 000	40
Dionex AS9	14 000	14 000	38
Dionex AS10	44 000	36 000	140
Sarasep AN1	16 000	25 000	39
Sarasep AN2	15 000	21 000	61
Waters Anion HR	18 000	18 000	41

^a All units are plates/m. Calculation based on the following equation: $N = 5.54 (t_R/w_h)^2$, where w_h is the peak width at half-height.

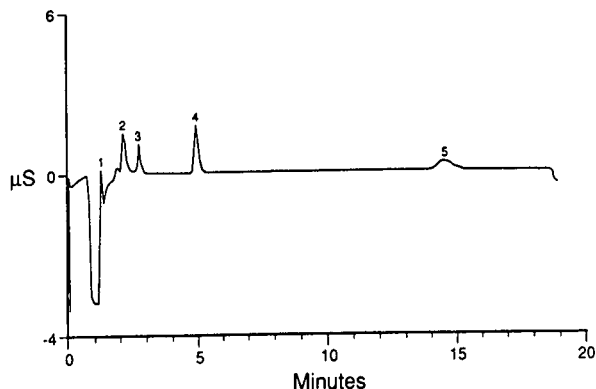


Fig. 7. Trace enrichment of standard on Dionex AS9. Conditions can be found in Table I. The flow-rate is 1.0 ml/min. Peaks: 1 = fluoride; 2 = chloride; 3 = nitrite; 4 = nitrate; 5 = sulfate.

serve to illustrate the importance of acetate and fluoride resolution. A chromatogram of a five-anion standard (fluoride, chloride, nitrite, nitrate and sulfate) on a Dionex AS9 column is shown in Fig. 7. Note the fluoride peak eluting from the inverted tail of the water dip. A sample run at that time showed a large peak at the retention time of fluoride; see Fig. 8. This peak was initially reported as fluoride to the customer. On further discussion with the customer, the possibility of so large a fluoride contaminant in the water purification system seemed remote. Running an acetate standard, an identical retention time with fluoride was confirmed.

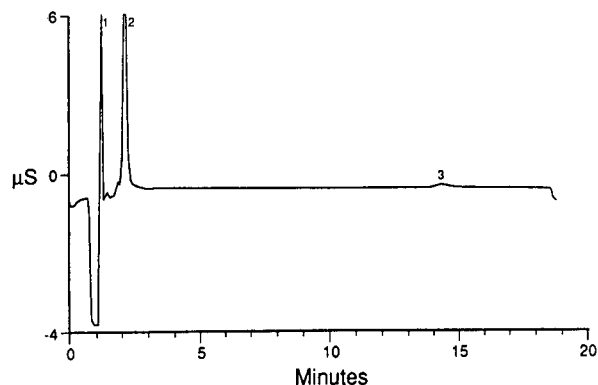


Fig. 8. Trace enrichment of ultrapure water on a Dionex AS9. Conditions can be found in Table I. The flow-rate is 1.0 ml/min. Peaks: 1 = unknown; 2 = chloride; 3 = sulfate.

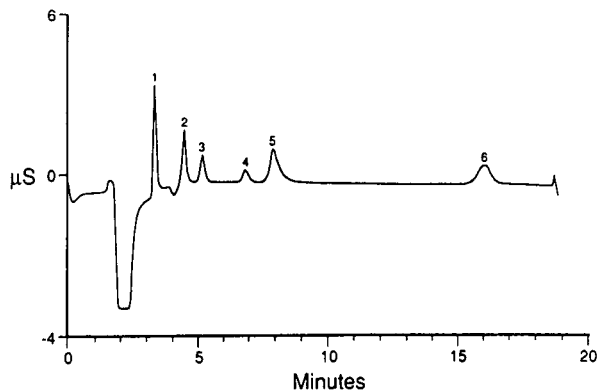


Fig. 9. Trace enrichment of standard on a Sarasep AN2. Eluent is 2.0 mM sodium carbonate and 2.5 mM sodium hydrogencarbonate at 1.0 ml/min. Peaks: 1 = fluoride; 2 = chloride; 3 = nitrite, 4 = bromide; 5 = nitrate; 6 = sulfate.

The Sarasep AN2 column was designed with this high-purity water application in mind. In Fig. 9, six anions (fluoride, chloride, nitrite, bromide, nitrate and sulfate) are separated on the Sarasep AN2 column. Note the fluoride is well out of the water dip. On the date this standard was run, another sample containing the unknown peak that eluted at the retention time of fluoride on the Dionex AS9 column was received. Fig. 10 shows this chromatogram and clearly the large anion in the sample is not fluoride. An acetate standard showed a good retention time and peak shape match with this unknown peak.

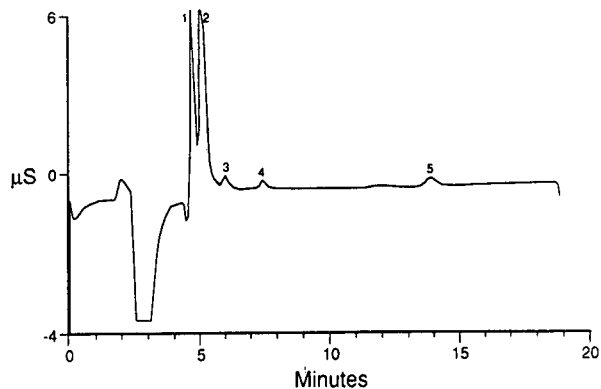


Fig. 10. Trace enrichment of ultrapure water on a Sarasep AN2. Conditions as in Fig. 9. Peaks: 1 = unknown; 2 = chloride; 3 = bromide; 4 = nitrate; 5 = sulfate.

CONCLUSIONS

Six commercially available columns were studied to determine suitability for a high-purity water analysis. Traditional IC columns that are used to separate the seven anions of primary interest in general IC applications (fluoride, chloride, nitrite, bromide, nitrate and sulfate) were not suitable in an isocratic mode for this high-purity water application. New columns that combine excellent fluoride retention with reasonable elution of the last peak are far superior in this regard. An additional criterion of importance is resolution of weak organic acids such as acetate from fluoride. Three vendor columns were found to be suitable for most criteria, although no column fulfilled all. Sodium hydrogencarbonate and sodium carbonate eluents are preferred in suppressed IC because they are easily prepared and stable. The salts are available from NIST providing a traceable source. It must be stressed that each application will have its own requirements. For example, if oxalate and formate are impurities of interest, the Sarasep AN2 column will not adequately resolve these from sulfate and acetate, respectively.

REFERENCES

1 A.L. Heckenberg and P.R. Haddad, *J. Chromatogr.*, 299 (1984) 301.

- 2 T. Okada and T. Kuwamoto, *J. Chromatogr.*, 350 (1985) 317.
- 3 R.A. Wetzel, C.L. Anderson, H. Schleicher and G.D. Crook, *Anal. Chem.*, 51 (1979) 1532.
- 4 M.A. Fulmer, J. Penkrot and R.J. Nadalin, in D. Mulik and E. Sawicki (Editors), *Ion Chromatographic Analysis of Environmental Pollutants*, Vol. 2, Ann Arbor Sci. Publ., Ann Arbor, MI, 1979, Ch. 32, p. 381.
- 5 K.M. Roberts, D.T. Gjerde and J.S. Fritz, *Anal. Chem.*, 53 (1981) 1691.
- 6 P.E. Jackson and P.R. Haddad, *J. Chromatogr.*, 439 (1988) 37.
- 7 P.R. Haddad and H.L. Heckenberg, *J. Chromatogr.*, 318 (1985) 279.
- 8 A.L. Heckenberg and P.R. Haddad, *J. Chromatogr.*, 330 (1985) 95.
- 9 P.E. Jackson and P.R. Haddad, *J. Chromatogr.*, 355 (1986) 87.
- 10 P.R. Haddad and P.E. Jackson, *J. Chromatogr.*, 367 (1986) 301.
- 11 P.E. Jackson and P.R. Haddad, *J. Chromatogr.*, 389 (1987) 65.
- 12 S. Harvey, *J. Chromatogr.*, 546 (1991) 125.
- 13 M.W. Martin and R.A. Giacomini, in P. Jandik and R.M. Cassidy (Editors), *Advances in Ion Chromatography*, Vol. 1, Century International, Medfield, MA, 1989, p. 119.
- 14 P.R. Haddad, P.E. Jackson and A.L. Heckenberg, *J. Chromatogr.*, 346 (1988) 139.
- 15 C.A. Pohl, presented at the *International Ion Chromatography Symposium 1990, San Diego, CA, September 30, 1990*.

CHROMSYMP. 2851

Evaluation of ion-exchange chromatography for nitrate determination in wastewaters[☆]

S. Bignami, M.L. Daví*, C. Milan, M. Moretti and F. Navarra

Settore Chimico-Ambientale, Presidio Multizonale di Prevenzione, USL 31, Corso Giovecca 169, I-44100 Ferrara (Italy)

(First received February 12th, 1993; revised manuscript received April 3rd, 1993)

ABSTRACT

Two methods of nitrate measurement have been compared: colorimetric with salicylate and conductimetric with ion-exchange chromatography. For samples with low nitrate concentrations, the salicylate method is similar to the ion chromatographic method. However, for samples with high nitrate concentrations, such as wastewaters from biological plants, ion-exchange chromatography is preferable: it is more accurate, even after dilution, and is not subject to interferences by organic or inorganic constituents.

INTRODUCTION

Nitrate is the most oxidized form of nitrogen compound produced by the biological decomposition of organic matter. It is frequently found in effluents after biological treatment. Nitrate in river water can arise from sewage effluents, drainage from agricultural land treated with artificial nitrogen fertilizers and from effluents of certain industries (*e.g.* chemicals, explosives and fertilizers) [1]. Under certain circumstances, nitrates can stimulate the growth of algae to such an extent as to cause problems for the aquatic life (eutrophication).

The Italian law relevant to wastewaters is Legge Merli No. 319/76, in which the limit for nitrate nitrogen is either 20 or 30 mg/l (N), depending on their use. More precisely, in this

law two references (Tables A and C) are fixed for wastes in surface water or in public sewers. The same law establishes the limits for chloride and sulphate anions, respectively 1000 mg/l and 1200 mg/l, in both surface water and sewers. In Italy wastewater samples frequently contain chloride concentrations near the maximum allowable limit, whereas sulphate is usually much lower than the allowable limit.

EXPERIMENTAL

Apparatus

For the salicylate method [2], a Beckman DU20 spectrophotometer was used at 420 nm, with matched silica cells of 1 cm light path. Chromatography was performed on a Dionex system 2000i/SP ion chromatograph equipped with a conductivity detector (range 30 μ S) with suppression (Model AMMS). A separator column (HPIC-AS4A) with a guard column (HPIC-AG4A) was used. The volume of the sample loop was 50 μ l. The integrator model was HP 3390A. The eluent used was 1.8 mM sodium carbonate plus 1.7 mM sodium bicarbonate at a

* Corresponding author.

[☆] Presented at the *International Ion Chromatography Symposium 1992, Linz, September 21–24, 1992*. The majority of the papers presented at this symposium were published in *J. Chromatogr.*, Vol. 640 (1993).

flow-rate of 2 ml/min. The suppressor was regenerated with 0.0125 M sulphuric acid.

Reagents

Purified water was obtained from a Milli-Q purification system (Millipore). All the solutions were prepared from analytical reagent-grade chemicals: sodium salicylate solution (0.5 g in 100 ml) and Seignette salt solution (sodium and potassium tartrate 60 g in 1 l, basified with sodium hydroxide 400 g in 1 l). The acidifying agent was concentrated sulphuric acid.

Methods

The determination of nitrate is difficult because of the relatively complex procedures required, the high probability that interfering constituents will be present and the limited concentration ranges of the various techniques. The official Italian method for nitrate in wastewater is a colorimetric analysis with sodium salicylate to form a coloured dye [3]. It allows measurement of nitrate at concentrations between 0.5 and 5.0 mg/l as nitrogen. Interlaboratory tests using this method have verified its applicability [4].

A 1-ml volume of sodium salicylate was added to 10 ml of sample in a porcelain dish and the solution evaporated in a water bath. After cooling the residue, 2 ml of concentrated sulphuric acid was added and carefully mixed to completely rinse the dish surface. After 10 min, 15 ml of deionized water and 15 ml of Seignette salt solution were added and mixed. The resultant yellow solution was analysed spectrophotometrically at 420 nm [5].

The main disadvantage of this method is the presence in most samples of interfering substances: coloured compounds, iron, nitrites and chlorides. When the chloride concentration is greater than 400 mg/l, treatment with silver sulphate is suggested to precipitate silver chloride. However, this procedure is not ideal because of the precipitate is difficult to eliminate.

Alternatively, ion-exchange chromatography (IEC) provides a single instrumental technique that may be used for rapid and sequential measurement of common anions [6]. The minimum

detectable concentration of an anion is a function of the sample size and the conductivity scale used. In this work, with a range of 30 $\mu\text{S}/\text{cm}$ and a 50- μl sample loop, the minimum detectable concentration is 0.05 mg/l as nitrogen. The main disadvantages of this method are: any substance that has a retention time coinciding with that of any anion to be determined will interfere; a high concentration of an ion also interferes with the resolution of the others [7]. Therefore, it is necessary to respect the maximum tolerable concentration of interfering anion. For example, the concentration ratios for the nitrates are [8,9]:

$$\text{NO}_3^-/\text{Cl}^- \quad 1:500 \text{ mg/l}$$

$$\text{NO}_3^-/\text{Br}^- \quad 1:100 \text{ mg/l}$$

$$\text{NO}_3^-/\text{SO}_4^{2-} \quad 1:500 \text{ mg/l}$$

RESULTS AND DISCUSSION

The accuracy of the IEC method was verified by analysing a stock standard solution of anhydrous potassium nitrate in deionized water, 2.50, 5.00 or 10.00 mg/l as nitrate. These solutions were successively diluted (1:2.5, 1:5, 1:10) to obtain the same final concentrations. The chromatography calibration was obtained using four concentration levels of nitrate. One of these was at a concentration near, but above, the minimum detectable concentration, and the other concentrations were as near as possible to the expected range of values found in real samples. The working calibration curve was verified daily by the measurement of the 5.00 mg/l nitrate calibration standard.

In Table I the average experimental concentrations for the different dilutions are reported; the relative error (RE) percentage was calculated by five repeated measurements. The results show that the same concentrations obtained by suitable dilutions give a similar relative error percentage. For wastewater and sewage samples analysed in this paper, RE was lower than 10%.

The accuracy and precision of the salicylate and IEC methods were compared. Potassium nitrate standard solutions, at different concentrations, were prepared and five determinations

TABLE I

AVERAGE EXPERIMENTAL CONCENTRATIONS AND RELATIVE ERROR PERCENTAGE FOR THE DIFFERENT DILUTIONS

Theor. conc.	2.50 mg/l		5.00 mg/l		10.00 mg/l	
Dilutions	Average expt. conc. (mg/l)	RE (%)	Average expt. conc. (mg/l)	RE (%)	Average expt. conc. (mg/l)	RE (%)
Just like	2.54	1.6	5.08	1.6	10.36	3.6
1:2.5	1.02	2.0	2.04	2.0	4.05	1.2
1:5	0.54	8.0	1.04	4.0	2.04	2.0
1:10	0.29	16.0	0.53	6.0	1.03	3.0

TABLE II

COMPARISON OF ACCURACY AND PRECISION FOR NITRATE STANDARDS

Nitrate (mg/l)	Nitrogen (mg/l)	Salicylate method mg/1N		IEC method mg/1N	
		$\bar{x} \pm S.D.$	RE (%)	$\bar{x} \pm S.D.$	RE (%)
0.20	0.05	0.09 ± 0.0034	+80	0.051 ± 0.0026	+2
1.00	0.22	0.26 ± 0.0022	+18	0.230 ± 0.0020	+5
2.00	0.45	0.51 ± 0.0046	+13	0.463 ± 0.0029	+3
2.50	0.56	0.61 ± 0.0029	+9	0.576 ± 0.0011	+3
5.00	1.13	1.22 ± 0.0050	+8	1.145 ± 0.0022	+1
8.86	2.00	2.21 ± 0.0036	+10	2.054 ± 0.0025	+3
10.00	2.26	2.46 ± 0.0015	-9	2.323 ± 0.0026	+3

for each method were made. The standard deviations of the average values and the RE values are indicated in Table II.

A comparison of the linearity range and of the minimum detectable concentration between the different methods is shown in Table III.

The effects of chloride concentration on the nitrate determination were studied because chloride is present in all real samples. The salicylate and IEC methods were compared in three different chloride concentration ranges (Fig. 1A): $Cl^- > 1000$ mg/l; $Cl^- 100$ – 1000 mg/l; $Cl^- < 100$ mg/l. It was verified that the IEC is applicable in the following conditions:

(a) $Cl^- > 1000$ mg/l, when the concentration

of nitrate is greater than 2.0 mg/l, with dilution 1:10.

(b) $Cl^- 100$ – 1000 mg/l, when nitrates are between 1.0 and 20.0 mg/l, with dilution 1:5, and

TABLE III

COMPARISON OF LINEARITY RANGE AND MINIMUM DETECTABLE CONCENTRATION

Method	Linearity range (mg/l as N)	Minimum detectable conc. (mg/l as N)
Salicylate	0.5–5.0	0.5
IEC	0.05–4.00	0.05

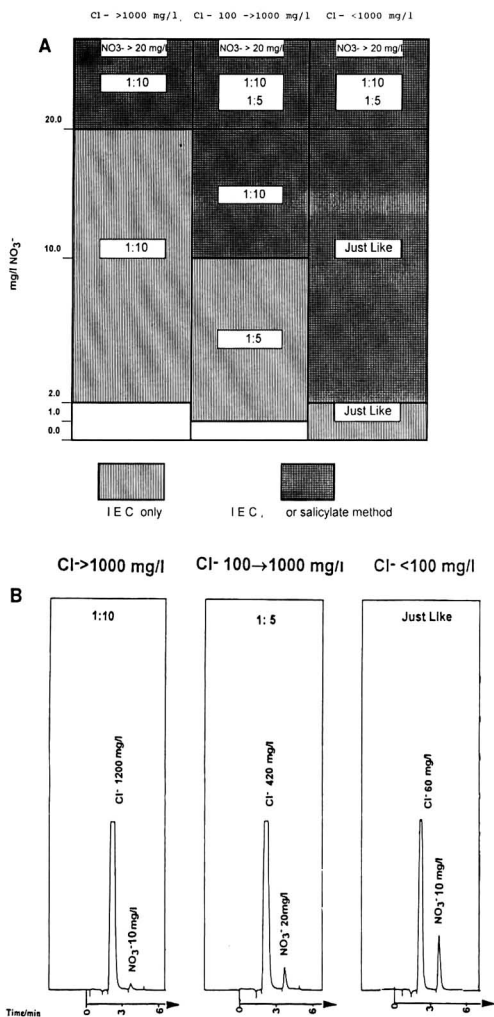


Fig. 1. (A) Chloride interferences in the nitrate determination. (B) Chromatograms of variable chloride–nitrate ratio.

when nitrates are higher than 20.0 mg/l, with dilution 1:5 or 1:10.

(c) Cl⁻ < 100 mg/l, when nitrates are higher than 0.2 mg/l, without dilution, and when nitrates are higher than 20.0 mg/l, with dilution 1:5, or 1:10.

The most suitable dilutions for the simultaneous determination of nitrate and chloride are shown in Fig. 1B.

This study also verified that, in complex matrices analysis, excellent results can be obtained by IEC. The advantages include:

(1) Simultaneous reduction in interferences, either organic or inorganic. Also, when the chemical oxygen demand (COD) value was higher than 100 mg/l as oxygen, it was possible to determine nitrates without organic anion interferences. Coloured compounds that may influence the UV or visible measurements did not cause any problems.

(2) Rapid and sequential analysis that allows different anions to be determined simultaneously.

(3) Elimination of hazardous reagent use.

(4) Small samples volumes are required.

(5) The greater sensitivity of the IEC method allows the analysis of samples with a low concentration of nitrate, but high concentration of chloride, for which the dilution is necessary.

For all these reasons, it is to be hoped that in future the ion-exchange chromatography method becomes an approved national procedure.

REFERENCES

- 1 L. Klein, *River Pollution*, Vol. II, Butterworths, London, 1962, p. 23.
- 2 J. Rodier, *L'Analyse de l'Eau*, Dunod, Paris, 7th ed., 1984, p. 200.
- 3 Istituto di Ricerca sulle Acque-Centro Nazionale Ricerche, *Azoto Nitrico, D-004*, Rome, Dec. 1987.
- 4 R. Mosello, R. Baudo, G. Tartari, M. Camusso, G. Marengo, H. Muntau, A. Barbieri and G. Righetti, *Documenta dell'Istituto Italiano di Idrobiologia*, 18, CNR, Verbania Pallanza, 1989, p. 54.
- 5 L.S. Clesceri, A.E. Greenberg and R.R. Trussell, *Standard Methods for the Examination of Water and Wastewater*, 17th ed., 1989 Section 4500-NO B, p. 4.132.
- 6 D. Jenke, *Anal. Chem.*, 53 (1981) 1356.
- 7 M.I. Bynum, *Anal. Chem.*, 53 (1981) 1936.
- 8 *Method 38405*, DIN, Germany, 1989.
- 9 *Method 876*, UNICHIM, Milan, 1990.

Determination of nitrate in surface waters by ion-exchange chromatography after oxidation of total organic nitrogen to nitrate[☆]

M.L. Daví*, S. Bignami, C. Milan, M. Liboni and M.G. Malfatto

Settore Chimico-Ambientale, Presidio Multizonale di Prevenzione, USL 31, Corso Giovecca 169, I-44100 Ferrara (Italy)

(First received February 12th, 1993; revised manuscript received April 3rd, 1993)

ABSTRACT

The official method for the determination of organic nitrogen in surface water consists of a Kjeldahl distillation to reduce nitrogen to ammonia, followed by colorimetric or volumetric determination. The purpose of this work is to determine whether the Valderrama method can be used as an alternative procedure. The Valderrama method estimates total nitrogen, either organic or inorganic, after oxidation to nitrate. The first step is an oxidative digestion in an autoclave in the presence of potassium persulphate, boric acid and sodium hydroxide. Nitrate is then determined colorimetrically, after acidification by concentrated sulphuric acid, or by ion-exchange chromatography, without acidification. This last procedure takes advantage of some important features of ion-exchange chromatography: greater sensitivity than UV methods, rapid analysis, high selectivity and, thus, low matrix interferences.

INTRODUCTION

Organic nitrogen substances in surface waters arise principally from animal and vegetable proteins and from synthetic organic compounds used in agricultural practice (for example triazine herbicides), or used as dyes in various manufactures. They find their most important application in the dyeing and printing of textiles, but are also used to some extent for dyeing paper and leather, in the preparation of certain inks and in photography. Industrial wastes containing proteins include food processing and canning wastes, gelatine manufacturing

wastes and slaughterhouse, dairy and tannery wastes [1].

Decomposition of nitrogen organic matter by either aerobic or anaerobic bacteria gives rise to ammonia. The oxidation of ammonia by aerobic bacteria (nitrification) produces first nitrites and then nitrates. An undesirable effect of nitrate in surface water destined for human consumption has been featured in the medical literature [2]. It has been shown that young infants receiving artificial feeds of milk diluted with water containing more than about 10–20 mg/l nitrogen as nitrate may develop “methaemoglobinaemia”.

EEC Directive No. 80/778, regarding the characteristics of the water for human consumption, imposes three classes of concentrations (A_1 , A_2 , A_3) for Kjeldahl nitrogen: 1, 2 and 3 mg/l as nitrogen, respectively. The analytical procedures used in this work are the Kjeldahl [3] and Valderrama methods [4].

The first method determines nitrogen in the

* Corresponding author.

[☆] Presented at the *International Ion Chromatography Symposium 1992, Linz, September 21–24, 1992*. The majority of the papers presented at this symposium were published in *J. Chromatogr.*, Vol. 640 (1993).

trinegative state. If ammonia nitrogen is not removed in the initial phase of the procedure, "organic nitrogen" can be obtained by subtracting ammonia nitrogen from Kjeldahl nitrogen. Alternatively, the Valderrama method proposes an oxidation of the nitrogen to nitrate at elevated temperature by persulphate in alkaline medium. "Organic nitrogen" can be obtained as follows: total nitrogen – (ammonia + nitrite + nitrate) nitrogen.

EXPERIMENTAL

Apparatus

For the Valderrama method, a Perkin Elmer 550S spectrophotometer was used at 220 nm, with matched silica cells of 1 cm light path. Chromatography was performed on a Dionex System 2000i/SP ion chromatograph equipped with a conductivity detector (range 30 μ S) with suppression (Model AMMS). A separator column (HPIC-AS4A) with a guard column (HPIC-AG4A) was used. The volume of the sample loop was 50 μ l. The integrator model was HP 3390A. The eluent solution (flow-rate 2.0 ml/min) consisted of 1.8 mM sodium carbonate and 1.7 mM sodium bicarbonate; the regenerant for AMMS was 0.0125 M sulphuric acid. For the Kjeldahl method, the digestion and distillation apparatus are described in ref. 5.

Reagents

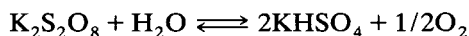
Purified water was obtained from a Milli-Q purification system (Millipore); all other reagents (sulphuric acid, sodium carbonate and bicarbonate) were of analytical reagent grade. The oxidizing solution was prepared from potassium persulphate (50 g/l), boric acid (30 g/l) and sodium hydroxide (14 g/l). The reagents used in the Kjeldahl method are listed in ref. 5.

Methods

The macro-Kjeldahl method was applied to 500 ml sample in an 800-ml Kjeldahl flask. A 50-ml aliquot of digestion reagent (sulphuric acid, potassium sulphate and mercuric sulphate catalyst) was carefully added to the distillation flask [6]. The solution was heated until the volume was reduced to about 25–50 ml, and

copious white fumes were observed. The digestion was continued for an additional 30 min, then the solution was cooled, diluted to 300 ml with water, mixed, and distilled. A distillate volume of 200 ml was collected below the surface of 50 ml of a 0.02 M sulphuric acid solution and the ammonia was determined spectrophotometrically using the phenate method [7].

In the Valderrama method the water sample (50 ml) was pipetted into a glass bottle and potassium persulphate, dissolved in sodium hydroxide solution, was added. The bottle was closed, heated in an autoclave at 120°C for 1 h, and then cooled. The oxygen available for the oxidation appears from the equation:



The heating time must be long enough to decompose the excess persulphate. This requisite excess is dependent not so much on the amount of nitrogen in the sample, but rather on the total amount of oxidizable substances, primarily organic matter. The chemical oxygen demand (COD) value of the sample should not appreciably exceed 10% of the oxygen available from the persulphate [8]. In our river samples, the COD value is 15–30 mg/l as oxygen, therefore 0.09 mmol of $\text{K}_2\text{S}_2\text{O}_8$ in 50 ml of sample were used. In this way, the presence of sulphate due to persulphate decomposition does not interfere in the determination of nitrate, because a nitrate–sulphate concentration ratio of 1:500 is maintained [9,10]. The obtained nitrates are determined by ion-exchange chromatography (IEC) or spectrophotometrically at 220 nm, after acidification by concentrated sulphuric acid.

RESULTS AND DISCUSSION

In samples from the river Po, collected at Pontelagoscuro (Ferrara), organic nitrogen was determined by using the Kjeldahl, Valderrama UV and Valderrama IEC methods. It has been shown by many authors that ammonia, EDTA, urea, carbamates, pyridine, glycine, proteins and their partial decomposition products are quantitatively oxidized to nitrate, whereas the oxidation of compounds containing nitrogen-to-nitro-

TABLE I

COMPARISON OF RECOVERY PERCENTAGE FOR AMMONIUM SULPHATE, GLYCINE AND UREA STANDARDS ADDED TO SURFACE WATER SAMPLES

Method	Recovery (%)					
	Ammonium sulphate spike		Glycine spike		Urea spike	
	0.05 mg/1 N	0.5 mg/1 N	0.05 mg/1 N	0.5 mg/1 N	0.05 mg/1 N	0.5 mg/1 N
Kjeldahl	ND	97	ND	98	ND	100
Valderrama UV	107	110	97	104	106	102
Valderrama IEC	101	100	99	106	100	99

ND = Not detected.

gen bonds seems to be incomplete [11]. In this paper experimental trials were performed to determine the recoveries by oxidation of the following nitrogen compounds: ammonium sulphate, glycine and urea added to surface water samples. For every compound tested, the fortified sample matrix technique was used. In the laboratory, a known quantity of each analyte was added to an aliquot of Po river sample. The spiked field sample matrix was analysed exactly as a field sample. In the recoveries from spiked river Po water samples, the organic nitrogen amount already present in the water sample was subtracted, after having determined it by means of the average values obtained by the IEC

Valderrama method. The obtained mean recovery percentages for two spike concentrations are reported in Table I. The comparison between the organic-free water and surface water recoveries was made to establish whether the sample matrix affected the analytical results, but no different recoveries was obtained. In Table II the relative error percentage obtained by the Valderrama UV and Valderrama IEC methods for organic-free water spiked with ammonium sulphate, glycine and urea standards at different concentrations are reported. The mean recovery percentages in Table I and the relative error percentages in Table II are the results of five replicate determinations.

TABLE II

COMPARISON BETWEEN VALDERRAMA UV AND VALDERRAMA IEC METHOD OF RELATIVE ERROR PERCENTAGE FOR AMMONIUM SULPHATE, GLYCINE AND UREA STANDARDS, ADDED TO ORGANIC-FREE WATER

Theor. conc. (mg/1 N)	RE (%)					
	Ammonium sulphate		Glycine		Urea	
	UV	IEC	UV	IEC	UV	IEC
0.50	+4	+6	+10	+3	+14	+3
1.00	+8	+5	+12	+4	+20	+3
2.00	+8	+3	+2	+4	-11	+1
3.00	-10	+4	-4	+3	-3	-2
5.00	-9	+6	-3	+2	-4	-5

TABLE III
COMPARISON OF MINIMUM DETECTABLE CONCENTRATION (MDC)

Method	MDC (mg/1N)
Kjeldahl	0.5
Valderrama UV	0.5
Valderrama IEC	0.05

A comparison of minimum detectable concentration in the three examined procedures is shown in Table III. In Fig. 1 a chromatogram of river Po water, after digestion, is shown.

The Valderrama method for "total nitrogen" determination is relatively simple and rapid and allows the estimation of low concentrations of organic nitrogen by subtracting the other nitrogen forms. It has been found experimentally that nitrate determination by IEC is more accurate than by the UV method as the relative errors (RE) in Table II show, and that the minimum detectable concentration is the lowest among the three described procedures. However, the ac-

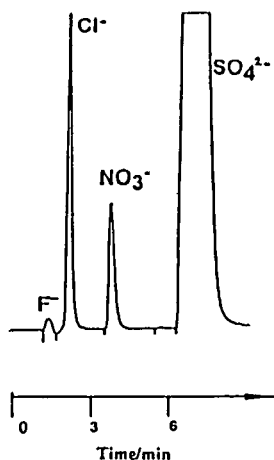


Fig. 1. Chromatogram of river Po water after digestion.

curacy of the analysis will be dependent on the nature of nitrogen compounds and on their relative concentrations. Unlike the spectrophotometric method, dissolved, coloured compounds do not interfere with the IEC determination. Recoveries of nitrogen substances added to natural water samples, obtained by Valderrama method, are very satisfactory, independent of their chemical nature (inorganic salt, amide, amino acid). For each kind of sample, it is advisable to adjust the amount of peroxy reagent, depending on the organic matter content of the sample. In this case, if it is not possible to dilute the oxidized solution, the sulphate must be eliminated before the IEC injection.

The results obtained in this paper show that the Valderrama method, modified by IEC, can be successfully used in place of the Kjeldahl method, to analyse surface water.

REFERENCES

- 1 L. Klein, *River Pollution*, Vol. II, Butterworths, London, 1962, pp. 26, 32–33, 202–203.
- 2 G. Gilli, *Igiene dell'Ambiente e del Territorio*, Edizioni Medico Scientifiche, 1989, pp. 294–296.
- 3 J. Kjeldahl, *Anal. Chem.*, 22 (1883) 366.
- 4 J.C. Valderrama, *Mar. Chem.*, 10 (1981) 109.
- 5 L.S. Clesceri, A.E. Greenberg and R.R. Trussell (Editors), *Standard Methods for the Examination of Water and Wastewater*, 17th ed., Washington, 1989, Section 4500-N org B, pp. 4.144–4.147.
- 6 G.B. Morgan, J.B. Lackey and F.W. Gilcreas, *Anal. Chem.*, 29 (1957) 833.
- 7 L.S. Clesceri, A.E. Greenberg and R.R. Trussell (Editors), *Standard Methods for the Examination of Water and Wastewater*, 17th ed., Washington, 1989, Section 4500-NH₃ D, pp. 4.120–4.121.
- 8 F. Nydahl, *Water Res.*, 12 (1978) 1123.
- 9 *Method 38405*, DIN, Germany, 1989.
- 10 *Method 876*, UNICHIM, Milan, 1990.
- 11 J. Ebina, T. Tsutsui and T. Shirai, *Water Res.*, 17 (1983) 1721.

Alkali flame ionization detector for gas chromatography using an alkali salt aerosol as the enhancement source

Eric D. Conte and Eugene F. Barry*

Department of Chemistry, University of Massachusetts Lowell, Lowell, MA 01854 (USA)

(First received January 29th, 1993; revised manuscript received April 6th, 1993)

ABSTRACT

A new design of an alkali flame ionization detector (AFID) is presented and differs from other configurations in that the enhancement source is introduced as an aerosol into a flame ionization detector (FID) rather than as a stationary solid bead positioned above a FID flame. This aerosol enters the detector as a hydrogen flame located perpendicular to the FID jet. Because the present design permits a constant and fresh supply of alkali salt to reach the detector, detector response does not fatigue over time. This AFID design also allows for operation as a FID by implementing a simple pneumatic procedure. This paper will deal with the performance and optimization of the detector in the phosphorous mode. The linear range for triethylphosphate exceeds four orders of magnitude. Selectivity ratios are in the four orders of magnitude range and detection limits for organophosphorus compounds studied ranged from 2.38 to 14.2 pg P/s.

INTRODUCTION

The earliest version of the alkali flame ionization detector (AFID) [1,2] dates back to 1964. In these initial designs an alkali salt was placed on the collector electrode and heated by a conventional flame. For phosphorus-containing compounds, the sensitivity of response increased by approximately two orders of magnitude compared to the FID, although a drawback was unreproducible response. The lifetime of the alkali source was limited by its volatilization which resulted in detector instability and gradual fatigue in response. Further improvements in detector design have been reported by Coahran and others [3–8] who positioned a compacted form of the alkali salt upon the FID jet. Unfortunately, this configuration where the alkali salt was placed in a concentric manner around the FID jet resulted in the same problems of limited lifetime and instability as the initial design.

In an alternative design, known as the flameless alkali sensitized detector (FASD), reported by Kolb and Bischoff [9], the alkali salt compacted in a more stable glass bead was ionized electrically above the FID flame. Additional designs involving electrical heating [10–14] have been reported. These designs offered improved performance in comparison with the earlier designs, but exhibited decreased sensitivity over time and necessitated frequent replacement of exhausted alkali salt sources.

The enhancement mechanism is not well understood, although mechanisms have been suggested [9,15,16] where nitrogen and phosphorus compounds are converted into free radicals during their elution into the flame. The free radicals are transformed into organic anions by the donation of electrons from alkali atoms (Li, Na, K, Rb and Cs) through either a solid- or gas-phase process. The ion current that is formed through this operation is responsible for the observed signal enhancement.

The proposed aerosol arrangement described in this paper circumvents several of these earlier

* Corresponding author.

problems including source replacement and gradually fatiguing response over time by providing a constant introduction of the alkali salt through ultrasonic generation. Previous work using a pneumatic alkali salt design on packed columns was performed in our laboratory [17]. The selectivity ratios, detection limits and optimization parameters of this detector in the phosphorus mode are discussed for organophosphorus pesticides.

EXPERIMENTAL

Materials

The pesticides used in the study include parathion (99% purity), diazinon (99%), chlorpyrifos (99.9%), malathion (98.5%) (ChemService, West Chester, PA, USA) while azinophosmethyl (99%) and methyl parathion (99.8%) were supplied by the Environmental Protection Agency, Research Triangle Park, NC, USA. Reagent-grade triethylphosphate and tributylphosphate were obtained from Eastman Kodak, Rochester, NY, USA whereas hexamethylphosphoramide, triethylphosphonoacetate, and penta-decane were acquired from Aldrich, Milwaukee, WI, USA. Organophosphorus standard solutions were prepared in reagent grade acetone at the following concentrations: phorate (4.23 $\mu\text{g}/\text{l}$), disulfoton (6.30 $\mu\text{g}/\text{l}$), tetraethylpyrophosphate (TEPP) (4.02 $\mu\text{g}/\text{l}$), parathion (6.09 $\mu\text{g}/\text{l}$), dimethoate (3.92 $\mu\text{g}/\text{l}$) and methyl parathion (7.08 $\mu\text{g}/\text{l}$). Solvents used to dissolve the phosphorus compounds were carbon tetrachloride, methylene chloride and *n*-hexane (J.T. Baker, Phillipsburg, NJ, USA), *n*-tetradecane (Aldrich) and cyclohexane (Alltech, Deerfield, IL, USA). Reagent-grade alkali salts employed for aerosol generation were potassium chloride, cesium chloride (J.T. Baker), rubidium chloride, sodium chloride (Fisher Scientific, Pittsburgh, PA, USA) and lithium chloride (Mallinckrodt, St. Louis, MO, USA).

Instrumentation

The gas chromatographic system was a Model 5890A (Hewlett-Packard, Avondale, PA, USA) equipped with a split/splitless injector. An HP-1 fused-silica capillary column, 30 m \times 0.25 mm

I.D., film thickness 0.25 μm , was utilized for all separations. The injector and detector temperatures were maintained at 220°C; helium was employed as carrier gas and operated at a linear velocity of 23 cm/s. The detector signal was filtered through a resistance-capacitance (RC) circuit having a time constant of 1.03 s and processed by an IBM-compatible computer (Model ZW-248-82; Zenith Data Systems, Benton Harbor, MI, USA) using Lab Calc software (Galactic Industries, Salem, NH, USA). All chromatograms were digitally smoothed using Savitsky-Golay five-point smoothing.

Glass-ware apparatus

The glass-ware apparatus used for aerosol generation is depicted in Fig. 1 where an inverted 250-ml erlenmeyer flask (b) was positioned to initially contain the aerosol produced from a home ultrasonic humidifier (a) (Model 691-100, Sunbeam, Hattiesburg, MS, USA). On the mouth of the flask was placed a 10 cm \times 10 cm polystyrene film (c) which was secured by silicon adhesive. Two glass tubes were

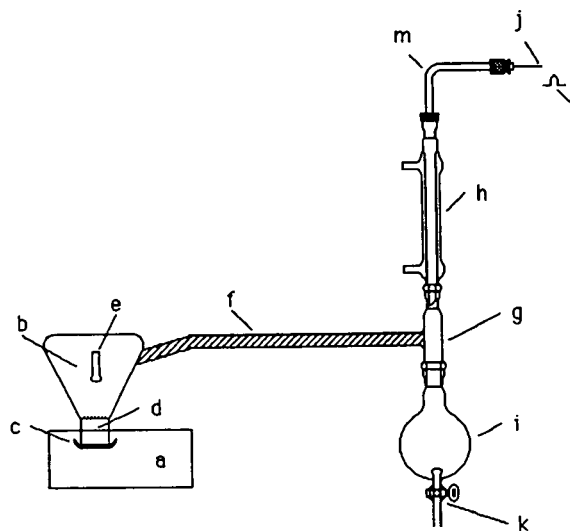


Fig. 1. AFID glass-ware apparatus. a = Ultrasonic nebulizer; b = 250-ml erlenmeyer flask; c = polystyrene film; d = alkali salt solution; e = hydrogen and nitrogen gas inlet; f = outlet tube for desolvation system wrapped in heating tape; g = T-joint adapter; h = condensation tube; i = 35-ml round-bottom flask; j = alkali flame jet; k = stopcock; l = FID jet; m = tube connecting condensation tube with alkali flame tip.

attached to the flask. The first tube (e) (50 mm \times 3 mm I.D.) to which was connected the flame-support hydrogen and nitrogen flow streams and a second tube (f) (240 mm \times 10 mm I.D.) 90° to the other tube contained the heated aerosol stream. This latter tube exiting the flask was fitted with a T adapter (g) which connected a condensation tube (h) (Wheaton, cat. No. 333970) and a 35-ml round-bottom flask (i) to collect condensate. Tube f was wrapped with heating tape to maintain the temperature at 110°C. A stopcock (k) was installed on the round bottom flask to facilitate removal of condensate. An additional tube (m) (80 mm \times 7 mm I.D.) was connected to the top of the condensation tube allowing a direct path to the detector through the use of a 1/4 in. (1 in. = 2.54 cm) plastic nut and a stainless-steel 1/4 to 1.16 in. reducing anion at the end of which was connected a stainless-steel tube (j) (30 mm \times 0.71 mm I.D.). The stainless-steel tube (j) is located perpendicular to the FID jet (l) in the detector chamber and is used as the alkali metal salt flame jet as illustrated in Fig. 2.

The original HP detector base was replaced with one fabricated from brass (n) [60 mm

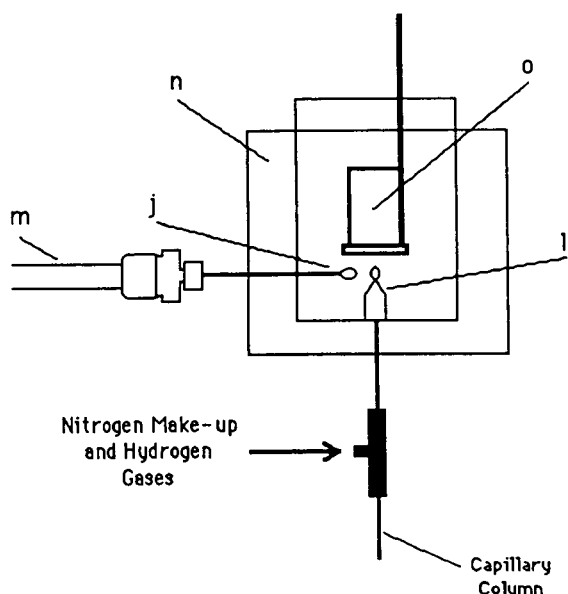


Fig. 2. Schematic diagram of the AFID. j = alkali flame jet; l = FID jet; m = tube connecting condensation tube with alkali flame tip; n = detector base; o = collector electrode.

(length) \times 40 mm (width) \times 40 mm (height)] into which holes were drilled to accommodate the alkali flame jet (10 mm \times 3 mm), (8 mm) for the FID jet, (1 mm) air, (1 mm) for the electrical ground of the FID jet, (2 mm) for the temperature thermocouple, and (10 mm) for the detector heater cartridge. The end of the capillary column was inserted at a position 1 mm below the tip of the FID jet. A stainless-steel 1/8 in. Swagelok T was used to modify existing flow channels which permitted hydrogen and nitrogen make-up gas to enter the FID jet. The collector electrode, which was composed of a 24 mm diameter aluminum disk, the heater, thermocouple, and FID jet were all connected to the existing electronic modules of the gas chromatograph.

RESULTS AND DISCUSSION

A solution containing 36.5 ng P/ μ l triethylphosphate in hexane was used for phosphorus optimization. With a 2- μ l injection and a column split ratio of 142:1 a final analyte mass of 0.51 ng P reached the TID. Optimization graphs for five detector gases are presented in Figs. 3 and 4. For the alkali aerosol flame, nitrogen and hydrogen gases were used to optimize two variables, the flame temperature and the amount of aerosol swept to the detector. These two gases were found to yield the optimal signal response at flow-rates of 90 ml/min and 47 ml/min for nitrogen and hydrogen, respectively. For the

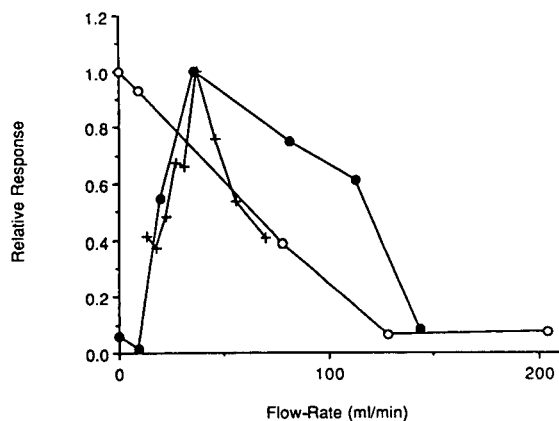


Fig. 3. FID hydrogen (+), make-up (●), and air (○) flow-rate optimizations.

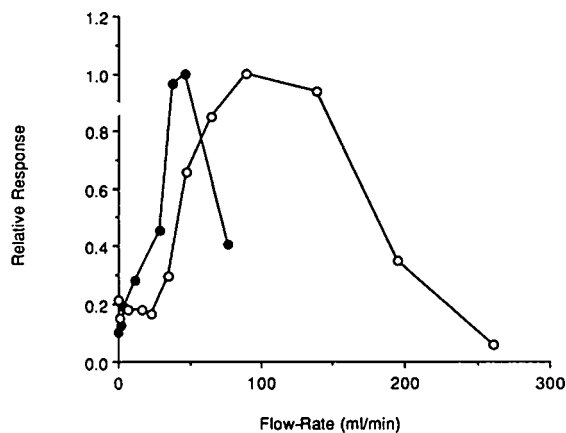


Fig. 4. Alkali nitrogen (O) and alkali hydrogen (●) flow-rate optimizations.

FID jet, the make-up flow (nitrogen) was optimized at 36 ml/min while the flow of hydrogen was optimized at 38 ml/min. Because both flames were housed in a single detector assembly, a single supply of air was used as the oxidant. A flow-rate of 0 ml/min produced the maximum peak response. This need for a rich flame is demonstrated by noting increasing response with decreasing air flow-rate. Because the detector is not a completely closed system, atmospheric oxygen is the sole contributor to flame support. The vertical gap between the flame jets and the horizontal displacement of the flame jets relative to each other were optimized at 3 mm and 5 mm, respectively, as shown in Fig. 5. Optimum response was also noted when the alkali flame jet, being electrically neutral, was positioned to be in direct contact with the collector electrode. Distinct flame formations attached to the orifice of each flame jet were observed when the collector electrode was removed.

The effect of introducing 100 $\mu\text{g/ml}$ aqueous solutions of CsCl, RbCl, KCl, LiCl, and NaCl on detector response was investigated. As displayed in Fig. 6, maximum response is associated with KCl and decreases with increasing molecular mass. The effect of varying KCl concentration from 0 to 1000 $\mu\text{g/ml}$ on selectivity was also explored and is illustrated in Fig. 7 for a separation of malathion and parathion in cyclohexane. The condensation tube maintained at 0°C elimi-

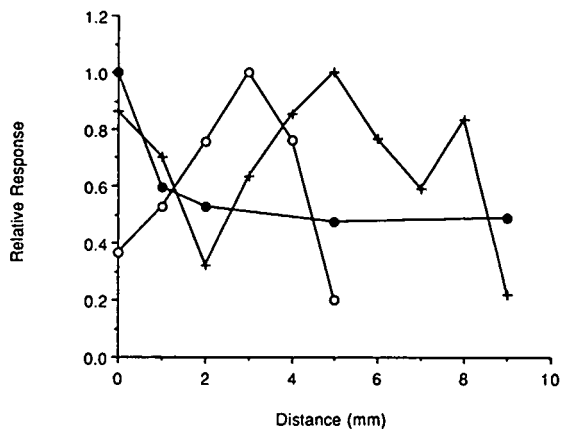


Fig. 5. Detector flame and collector distances optimization. Horizontal displacement distance of the flames (+), vertical gap distance of the flames (O) and collector distance from alkali flame jet (●).

nated the possibility of leaching and subsequent transport of alkali vapors into the alkali flame jet. Decreasing response for cyclohexane with increasing salt concentration is observed along with the high selectivity of the phosphorus-containing analytes. A concentration of 400 $\mu\text{g/ml}$ KCl created the problem of coating the collector electrode with a fine layer of salt over time and thus creating an unstable baseline. However, a concentration of 100 $\mu\text{g/ml}$ KCl completely alleviated this problem with no significant deposition of salt on the FID jet or collector electrode.

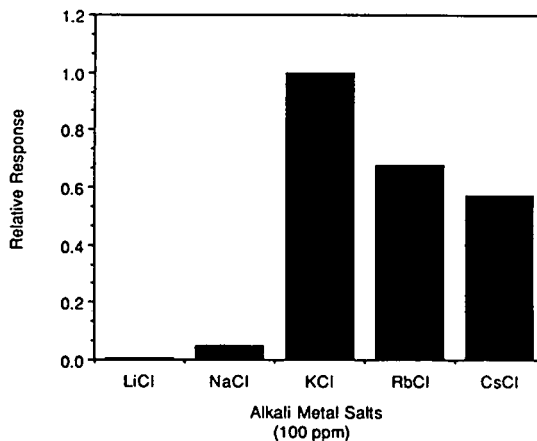


Fig. 6. Alkali salt optimization. ppm = $\mu\text{g/ml}$.

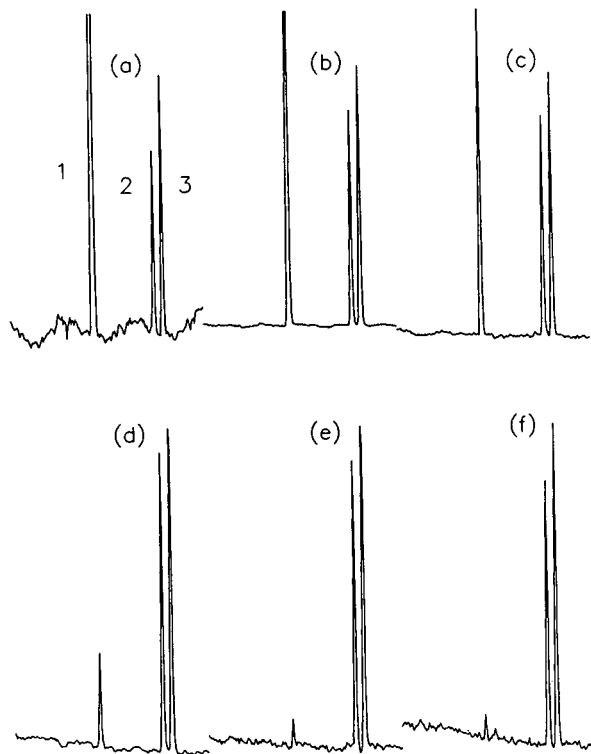


Fig. 7. Effect of KCl concentration. Peaks: 1 = cyclohexane; 2 = parathion 2.67 ng P; 3 = malathion 2.31 ng P. KCl concentrations: (a) blank, (b) 400 ng/ml, (c) 4.00 $\mu\text{g/ml}$, (d) 40.0 $\mu\text{g/ml}$, (e) 400 $\mu\text{g/ml}$, (f) 1000 $\mu\text{g/ml}$. GC conditions: column temperature, 150°C; split ratio of 150:1; 2- μl injection.

Detection limits, linearity and selectivity

Minimum detectable mass rates were determined by dividing three times the standard deviation of the baseline noise by the slope of the calibration curve and the analyte peak at half-height. The standard deviation of the noise is given by $s_B = N_{p-p}/r$, where N_{p-p} is the peak-to-peak noise and r is 5 for random Gaussian noise [18]. Minimum detectable mass rates for five organophosphorus pesticides are presented in Table I and range from 2.38 pg P/s for disulfoton to 14.2 pg P/s for dimethoate. Detector linearity was approximately 4.5 orders of magnitude determined with triethylphosphate as the solute. The separation of six organophosphorus pesticides at the low nanogram level is displayed in Fig. 8.

In Table II selectivity ratios for various or-

TABLE I

MINIMUM DETECTABLE MASS RATE (MDMR) OF SELECTED ORGANOPHOSPHORUS PESTICIDES

Compound	MDMR (pg P/s)
Disulfoton	2.38
Phorate	2.81
Parathion	5.29
Methyl parathion	11.7
Dimethoate	14.2

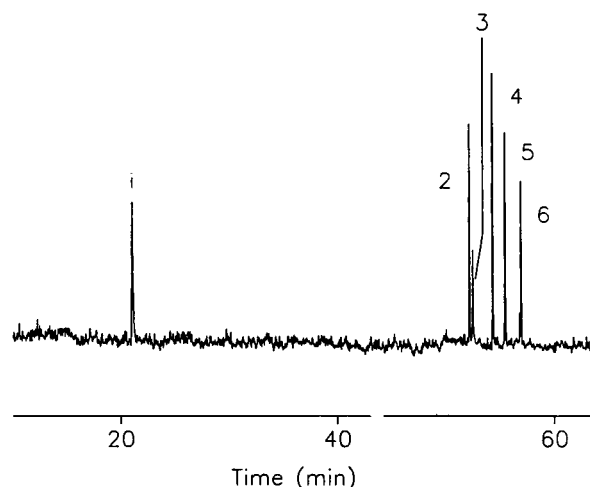


Fig. 8. Separation of an organophosphorus pesticide mixture with AFID detection. Peaks: 1 = TEPP 1.23 ng P; 2 = phorate 0.80 ng P; 3 = dimethoate 0.76 ng P; 4 = disulfoton 1.02 ng P; 5 = methyl parathion 1.29 ng P; 6 = parathion 0.92 ng P. GC conditions: column temperature: 50°C (1 min), 2°C/min to 140°C (10 min), 10°C/min to 240°C (8 min); split ratio of 3:1; 2- μl injection.

TABLE II

SELECTIVITY RATIOS OF SELECTED ORGANOPHOSPHORUS COMPOUNDS

Compound	Selectivity ratio (g P/g C)
Hexamethylphosphoamide	10 700
Malathion	20 400
Methyl parathion	25 400
Chlorpyrifos	26 800
Parathion	32 700
Tributylphosphate	35 200
Azinphosmethyl	39 000
Triethylphosphonoacetate	73 200

ganophosphorus species are presented, which all fall in the 10^4 range. The ratios were obtained by calculating the ratio of the organophosphorus compound response per mass unit of phosphorus to the ratio of tetradecane response per mass unit of carbon. The effect of chlorinated solvents on contamination of the alkali source, known to decrease the sensitivity of nitrogen–phosphorus detectors, was also explored. An alkali salt introduced in aerosol form circumvents this situation. Repetitive one microliter injections which corresponded to 16 ng of phorate and 21 ng of parathion in carbon tetrachloride were made to monitor detector stability over a 9-h period at 15-min intervals. Peak areas of phorate and parathion were compared and found to be constant and suggests no evidence of decreased sensitivity due to contamination.

Applications

This detector design also permits one to revert detector operation back to a FID by sim-

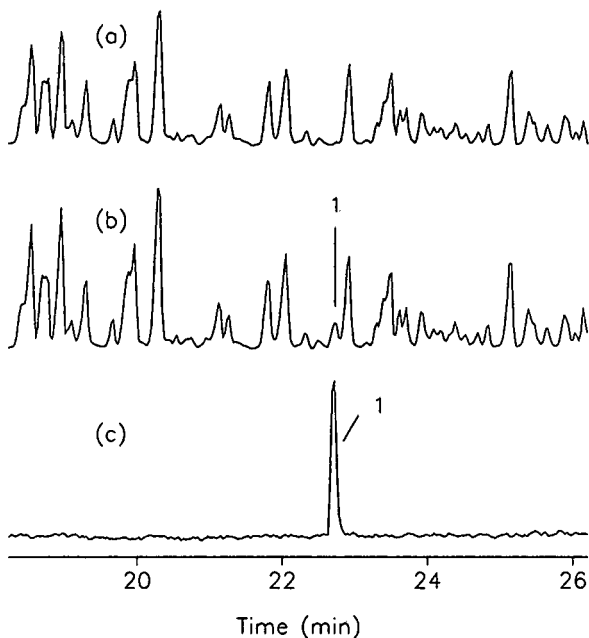


Fig. 9. Parallel FID and AFID chromatograms of gasoline. (a) FID chromatogram; (b) FID chromatogram of triethylphosphate (TEP) spiked into gasoline; peak 1 represents 5.1 ng of TEP; (c) parallel AFID chromatogram of b. GC conditions: column temperature: 30°C (1 min), 3°C/min to 185°C (5 min); split ratio of 150:1; 2- μ l injection.

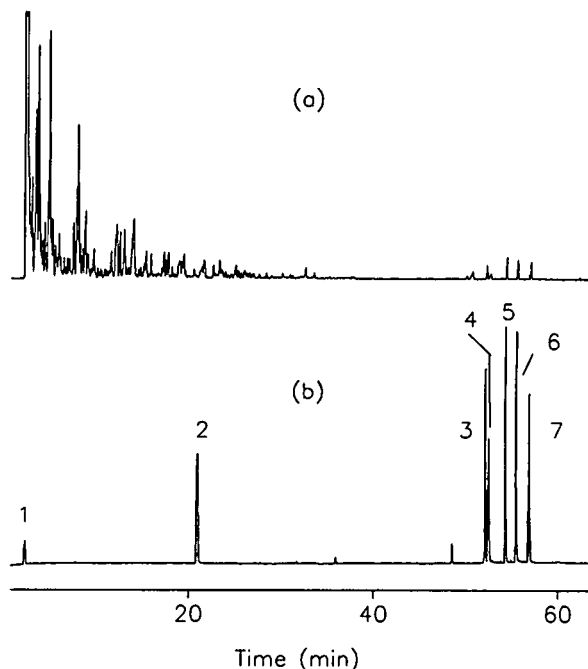


Fig. 10. Parallel chromatograms of gasoline spiked with six organophosphorus pesticides with (a) FID and (b) AFID. Peaks: 1 = acetone; 2 = TEPP 120 ng; 3 = phorate 141 ng; 4 = dimethoate 117 ng; 5 = disulfoton 118 ng; 6 = methyl parathion 210 ng; 7 = parathion 181 ng. GC conditions: column temperature: 50°C (1 min), 2°C/min to 140°C (10 min), 10°C/min to 240°C (8 min); split ratio of 50/1; 2 μ l injection volume.

ply shutting off the ultrasonic nebulizer and the nitrogen and hydrogen flows supplying the alkali salt flame. Fig. 9a is a segment of a capillary separation of a gasoline sample with FID detection, while the chromatograms in Fig. 9b and c illustrate the separation of gasoline spiked with triethylphosphate (peak 1 at 5.1 ng P). Fig. 9b is detected in the FID mode, while Fig. 9c illustrates the selectivity of the detector in the phosphorus mode. Further applications of detector selectivity are depicted in Fig. 10 of several organophosphorus pesticides spiked in gasoline and in Figs. 11 and 12 for commercial pesticide preparations in a complex matrix.

CONCLUSIONS

Although commercial FASD versions may offer improved detection limits and selectivity ratios, the linear range of this aerosol configura-

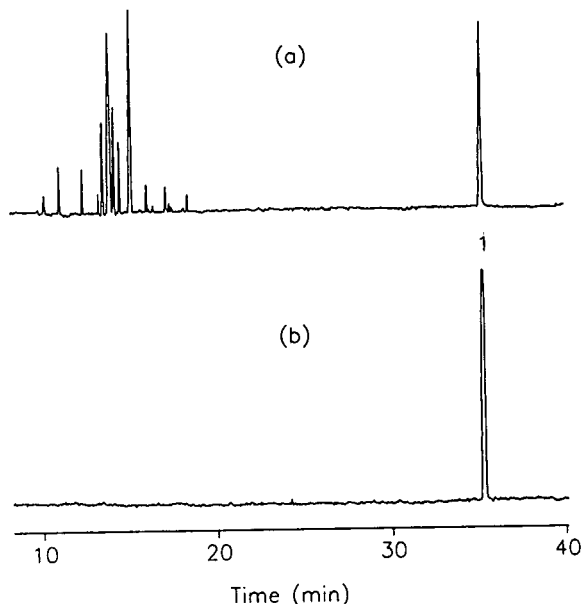


Fig. 11. Parallel chromatograms of a commercial Ortho diazinon preparation with (a) FID and (b) AFID. Peak 1 represents 36.8 ng P diazinon. GC conditions: column temperature: 40°C (5 min), 6°C/min to 250°C; split ratio of 150:1; 2- μ l injection of 1:10 dilution of preparation in acetone.

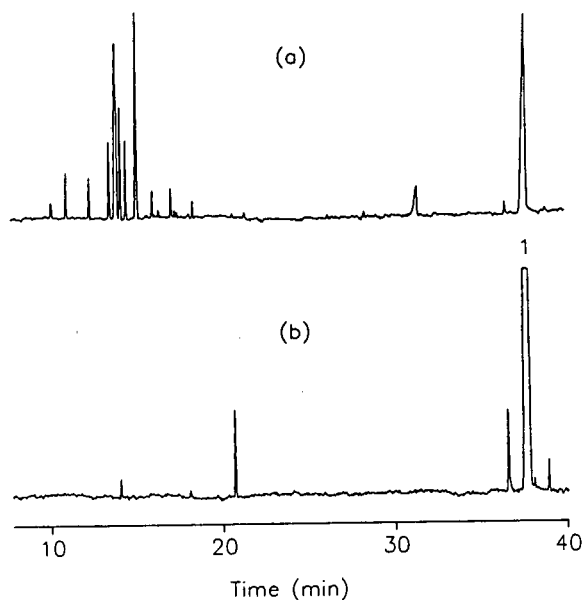


Fig. 12. Parallel chromatograms of a commercial Ortho malathion solution with (a) FID and (b) AFID. Peak 1 represents 75 ng P as malathion. GC conditions as in Fig. 11.

tion is comparable. In addition, modification to a FID is easily implemented by a simple pneumatic switching procedure. Moreover this detector offers several other advantages, which include no indication of fatigue and contamination with chlorinated solvents, and the ability to rapidly revert to the FID mode. In its present configuration, this detector offers considerable potential versatility, namely, by varying selectivity towards other heteratoms can be demonstrated.

ACKNOWLEDGEMENTS

E.D.C. wishes to acknowledge the Graduate School at University of Massachusetts Lowell for a research fellowship. The authors thank Galactic Industries for the gift of the LabCalc software and appreciate pesticide donations from Jetline Labs (Lowell, MA, USA), Revet Environmental and Analytical Laboratories (Worcester, MA, USA) and the Lawrence Experimental Station (Lawrence, MA, USA).

REFERENCES

- 1 A. Karmen and L. Giuffrida, *Nature*, 201 (1964) 1204.
- 2 L. Giuffrida, *J. Ass. Offic. Agr. Chem.*, 47 (1964) 293.
- 3 D.R. Coahran, *Bull. Environ. Contam. Toxicol.*, 1 (1966) 141.
- 4 K.P. Dimick, C.H. Hartmann, D.M. Oaks and E. Trone, *US Pat.*, 3 423 181 (1969).
- 5 H.C. Hartmann, *Bull. Environ. Contam. Toxicol.*, 1 (1966) 159.
- 6 H.C. Hartmann, *J. Chromatogr. Sci.*, 7 (1969) 163.
- 7 V.V. Brazhnikov and E.B. Shmidel, *J. Chromatogr.*, 122 (1976) 527.
- 8 G.R. Verga and F.J. Poy, *J. Chromatogr.*, 116 (1976) 17.
- 9 B. Kolb and J. Bischoff, *J. Chromatogr. Sci.*, 12 (1974) 625.
- 10 J.E. Baudean, *Can. Res. Dev.*, 8 (1975) 30.
- 11 C.A. Burgett and D.H. Smith, *J. Chromatogr.*, 134 (1977) 57.
- 12 P.L. Patterson, *J. Chromatogr.*, 167 (1978) 381.
- 13 P.L. Patterson and R.L. Howe, *J. Chromatogr. Sci.*, 16 (1978) 275.
- 14 P.L. Patterson, R.A. Gatten and C. Ontiveros, *J. Chromatogr. Sci.*, 20 (1982) 97.
- 15 J. Sevcik, *Chromatographia*, 6 (1973) 139.
- 16 V.V. Brazhnikov, M.V. Gur'ev and K.I. Sakodinskii, *Chromatographia*, 2 (1970) 53.
- 17 J. Carlson, *M.S. Thesis*, University of Lowell, Lowell, MA, 1981.
- 18 J.P. Foley and J.G. Dorsey, *Chromatographia*, 18 (1984) 503.

Determination of polar pesticides by phase-transfer catalysed derivatization and negative-ion chemical ionization gas chromatography-mass spectrometry

H.D. Meiring*, G. den Engelsman and A.P.J.M. de Jong

Laboratory of Organic Analytical Chemistry, National Institute of Public Health and Environmental Protection, P.O. Box 1, NL-3720 BA Bilthoven (Netherlands)

(Received February 18th, 1993)

ABSTRACT

A single-step procedure for the extraction and derivatization of carboxylic pesticides from aqueous samples is described. The acidic compounds, including phenoxy herbicides, were extracted from aqueous samples using tetrahexylammonium hydrogensulphate as a catalyst and were subsequently derivatized with pentafluorobenzyl bromide to volatile stable and electron-capturing derivatives. Analysis was performed by gas chromatography with electron-capture detection combined with negative-ion chemical ionization mass spectrometry. The recovery of the compounds was $108 \pm 8\%$. Detection limits were typically $0.05 \mu\text{g/l}$, using mass unit resolution. Highly contaminated samples required increased resolution ($1000 \leq R_f \leq 4000$) for reduced chemical background and enhanced selectivity for detection at low-ppb levels. The method was applied to the determination of some phenoxy-carboxylic pesticides in surface water and in blood samples.

INTRODUCTION

Sensitive methods are needed for the determination of a wide variety of pesticides in water in order to meet the present norms for drinking water as set by the US Environmental Protection Agency (EPA) and individual governments. In most methods chromatographic techniques are applied [1,2], but also immunoassays [3], *e.g.*, enzyme-linked immunosorbent assay, and electrochemical techniques, *e.g.*, polarography [4], are now being used for specific pesticides or special applications. The use of different detection techniques in conjunction with adequate isolation methods makes it possible to determine pesticides with a wide range of polarities and volatilities. The determination of polar pesticides, however, is complicated concerning both

their isolation and their chromatographic separation and detection.

For the determination of polar pesticides, high-performance liquid chromatography (HPLC) appears to be the most appropriate technique. In recent years, numerous methods for the determination of polar pesticides have been published [5,6]. In most methods clean-up and concentration are achieved by solid-phase extraction (SPE) or column-switching techniques [7]. In addition, the coupled technique of LC with mass spectrometry (MS) has been used for confirmation and identification purposes [8]. Several interfaces have been described for coupling these two techniques [9,10], but the thermospray and particle beam interfaces have become the most popular. However, it was found that the behaviour and sensitivity of these techniques for different pesticides may vary widely. The behaviour appears to be mainly determined by the chemical and physical prop-

* Corresponding author.

erties of the analytes, but may also be dependent on instrumental and analytical conditions. In addition, LC–MS interfaces have restrictions concerning flow-rate and eluent additives (buffers, salts, etc). Further, LC is less useful for screening purposes than gas chromatography (GC), mainly because of its relatively low separation efficiency. GC may be the preferred technique for screening. The determination of polar compounds by GC, however, often necessitates prior chemical modification in order to increase their extraction and/or enhance their GC properties.

For polar pesticides, numerous isolation and derivatization techniques have been published [11]. Particularly isolation and SPE clean-up are often used for a wide range of pesticides, also because of the good possibility of automation for routine analysis.

For acidic herbicides, isolation from aqueous samples can be performed by liquid–liquid extraction or on C_{18} SPE columns, followed by alkylation (e.g., methylation with diazomethane) and GC with flame ionization detection (FID) or electron-capture detection (ECD) [12]. The latter technique can only be used for the detection of compounds that have electron-capturing properties. Typical detection limits for such compounds are in the range 0.05–0.1 ppb in water, depending on the extent of concentration during sample preparation. However, the detection of non-electron-capturing compounds (e.g., bentazone) can only be achieved by ECD after derivatization with a reagent having an electro-negative function.

In this paper, we describe a method for the extraction and subsequent esterification of the acidic functional groups with pentafluorobenzyl bromide (PFB-Br). To ensure simplicity of the method for screening purposes (*i.e.*, rapid sam-

ple clean-up and the use of small, easy-to-handle sample sizes), we chose to extract and derivatize the compounds of interest simultaneously using phase-transfer catalysed (PTC) derivatization [13]. This technique has been applied previously in biochemical and pharmaceutical analysis, but has not been used frequently in environmental analysis [14,15].

PTC derivatization uses a complexing agent (commonly a tetraalkylammonium compound) which transports the compound of interest from the aqueous sample into the organic layer, where the derivatization occurs (Fig. 1). The derivatization of the compounds is based on the alkylation by an alkyl halide of the carboxylic moiety to the corresponding ester. To achieve maximum sensitivity, some constraints with respect to the derivatization reagent are necessary: (1) the reagent must be fairly stable towards hydrolysis because of the presence of a two-phase system; and (2) for sensitive measurements, compounds with electron-capturing groups are preferred to accomplish electron-capture negative ion chemical ionization MS (EC-NICI-MS) detection; consequently, a halogen-rich reagent has to be used to introduce the electron-capturing moiety into all of the derivatives. The use of perfluorobenzyl bromide satisfies these conditions and, in addition, yields stable and volatile derivatives.

In addition to the method development, the application of the method to the determination of some polar herbicides in different water samples and in human blood is described.

EXPERIMENTAL

Chemicals and reagents

Before use, demineralized water was passed through a Milli-Q reagent water system (Milli-

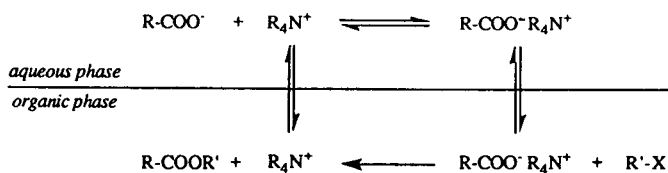


Fig. 1. Scheme of the phase-transfer alkylation of a carboxylic acid (RCOOH) with an alkyl halide (R'X) in the presence of a tetraalkylammonium catalyst (R₄N⁺X⁻).

pore, Milford, MA, USA), fitted with one Super-C carbon cartridge, two Ion-Ex cartridges and an Organex-Q cartridge.

The structures of the compounds studied are shown in Fig. 2. Dalapon-sodium (2,2-dichloropropionic acid, sodium salt) was obtained from Riedel-de Haën (Seelze, Germany), dicamba (3,6-dichloro-*o*-anisic acid), endothal-sodium (7-oxabicyclo[2.2.1]heptane-2,3-dicarboxylic acid, disodium salt), MCPA (4-chloro-*o*-tolylxyacetic acid), MCPB [4-(4-chloro-*o*-tolylxy)butyric acid], mecoprop [MCPP; (*R,S*)-2-(4-chloro-*o*-tolylxy)propionic acid], 2,4,5-T [(2,4,5-trichlorophenoxy)acetic acid] and bentazone [3-isopropyl-1*H*-2,1,3-benzothiadiazin-4(3*H*)-one 2,2-dioxide] from Dr. S. Ehrenstorfer (Augsburg, Germany), dikegulac-sodium (2,3:4,6-di-*O*-isopropylidene- α -*L*-xylo-2-hexulofuranosonic acid, sodium salt) from Schmidt (Amsterdam, Nether-

lands) and 2,3,6-TBA (2,3,6-trichlorobenzoic acid) from the National Physical Laboratory (Teddington, Middlesex, UK). Tetrahexylammonium hydrogensulphate was obtained from Fluka (Buchs, Switzerland), pentafluorobenzyl bromide and triethylamine from Pierce (Rockford, IL, USA), acetonitrile from Rathburn (Walkerburn, UK) and sodium dihydrogenphosphate monohydrate, anhydrous dipotassium hydrogenphosphate, orthophosphoric acid (85%), fuming hydrochloric acid (37%), dichloromethane and *n*-hexane from Merck (Darmstadt, Germany). Anhydrous sodium sulphate (Baker, Deventer, Netherlands) was heated at 450°C for at least 4 h before use.

A 10 mM solution of tetrahexylammonium hydrogensulphate in dichloromethane was prepared freshly each week. Phosphate buffer (pH 7.4) was made by dissolving 14.96 g of

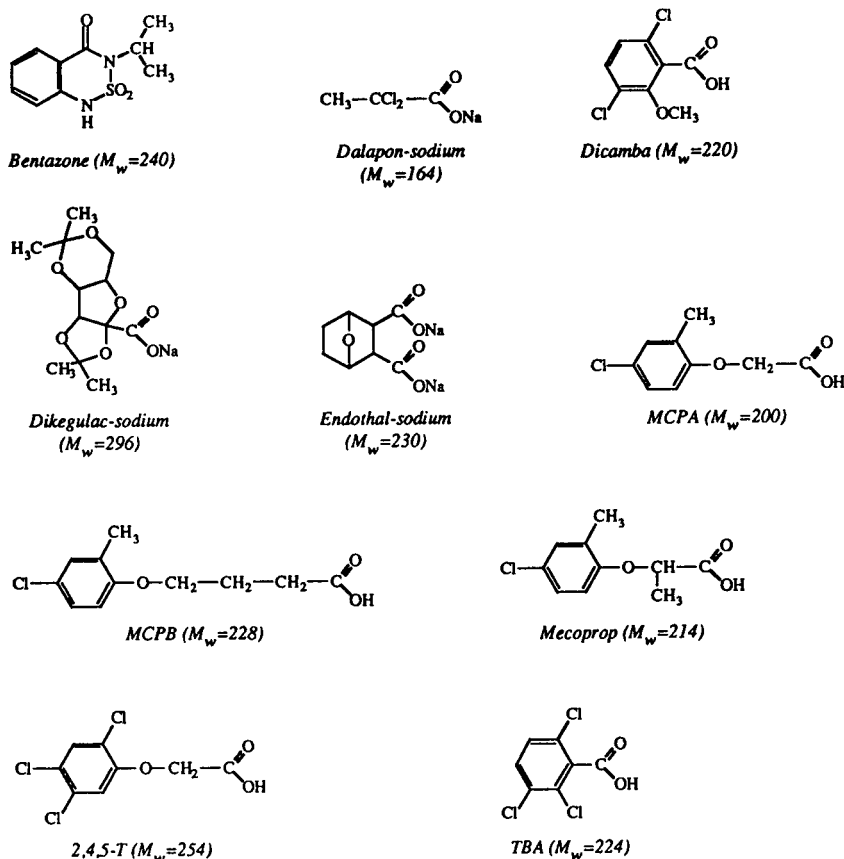


Fig. 2. Structures of model compounds studied. M_w = Molecular mass.

$\text{Na}_2\text{HPO}_4 \cdot 2\text{H}_2\text{O}$ and 2.16 g of KH_2PO_4 in 100 ml of demineralized water.

Standard solutions of the individual pesticides were prepared at a concentration of 1 mg/ml in demineralized water. A pesticide standard mixture with a final concentration of 0.5 ng/ml of each pesticide in demineralized water was prepared from the individual standard solutions and stored at 4°C.

Derivatization

Simultaneous extraction and derivatization of the compounds was carried out in test-tubes with PTFE-lined screw-caps. To the water sample or the pesticide standard mixture (9 ml) were added 1 ml of phosphate buffer (pH 7.4), 3 ml of tetrahexylammonium hydrogensulphate in dichloromethane (10 mM) and 20 μl of pentafluorobenzyl bromide. The mixture was shaken vigorously for 50 min in a horizontal position with *ca.* 250 strokes/min. The reaction was stopped by the addition of 350 μl of 6 M HCl. After phase separation, the organic layer was transferred into a clean tube, dried with anhydrous sodium sulphate and subsequently evaporated to dryness with a small flow of nitrogen at room temperature. Finally, the residue was dissolved in 200 μl of *n*-hexane and 2 μl of the extract was subjected to GC–MS analysis.

Recoveries were calculated by comparison of the yield of the aqueous derivatization with that

of a direct anhydrous derivatization. This direct derivatization was carried out on dry residues in 50 μl of acetonitrile, to which 10 μl of pentafluorobenzyl bromide and 10 μl of triethylamine were added. After incubation for 10 min at room temperature, the derivatives were isolated by adding 0.5 ml of 0.1 M HCl and 3 ml of ethyl acetate. After extraction, 2 μl of the organic layer were subjected to GC–MS analysis.

Gas chromatography–mass spectrometry

Experiments were performed on a Finnigan 4500 GC–MS system. GC separations were carried out on a CP Sil 19CB fused-silica column (25 m \times 0.25 mm I.D., 0.25 μm film thickness) (Chrompack, Middelburg, Netherlands), connected to a split–splitless capillary injector. The injector and transfer line temperatures were 260°C and 2 μl of the final extract were injected in the splitless mode. The oven temperature was programmed from 70°C (held for 1 min) to 220°C at 15°C/min, followed by an increase to 260°C at 5°C/min, the final temperature being maintained for 10 min.

The mass spectrometer was operated in the negative-ion chemical ionization mode with methane as moderator gas [source pressure 0.30 Torr (1 Torr = 133.3 Pa)] and an electron energy of 70 eV. The source and manifold temperatures were 140 and 90°C, respectively. Multiple ion detection (MID) was performed at the *m/z*

TABLE I

PESTICIDES INVESTIGATED AND THE PROMINENT FRAGMENTS OF THE CORRESPONDING PENTAFLUOROBENZYL ESTERS WITH THE RELATIVE INTENSITIES UNDER EC-NICI CONDITIONS

No.	Compound	Molecular mass as PFB derivative	Main ions (<i>m/z</i>) ^a
1	Bentazone	420	239.0490 (100), 241.0470 (5.8)
2	Dalapon	322	140.9510 (100), 142.9481 (64)
3	Dicamba	400	218.9616 (100), 220.9587 (65)
4	Dikegulac	454	273.0974 (100)
5	Endothal	546	199.0606 (100)
6	MCPA	380	199.0162 (100), 201.0135 (33)
7	MCPB	408	227.0475 (100), 229.0449 (33)
8	Mecoprop	394	213.0318 (100), 215.0292 (33)
9	2,4,5-T	434	252.9226 (100), 254.9197 (97)
10	TBA	404	222.9120 (100), 224.9091 (97)

^a Relative intensities (%) in parentheses.

values listed in Table I. For identification purposes, full-scan spectra were acquired in both electron impact and positive-ion CI modes (1 scan/s).

High-resolution EC-NICI experiments ($1000 \leq R_f \leq 4000$) were carried out on a Finnigan MAT-95 GC-MS system. The GC parameters were as described above. The mass spectrometer was operated in the MID mode with perfluorokerosene (PFK) as reference gas. Methane was used as moderator gas at a source pressure of 0.15 Torr.

RESULTS

Derivatization

The most important parameters affecting the reaction kinetics are the pH of the aqueous phase, the polarity and solvation ability of the organic layer and the concentration of the counter ion.

Fogelquist *et al.* [16] showed that at high pH (>9) a significant increase in the amount of by-products occurred, which could hamper the determination of the compounds of interest. At pH 7.4 the derivatization was complete within 50 min, without the formation of excess by-products interfering the EC-NICI-MS measurements at low levels. However, the extracts were not clean enough for direct GC-ECD measurements at

trace levels, owing to the lack of selectivity of this detection method. Allender [17] described a method for an additional SPE clean-up of PFB extracts on Florisil for analysis by GC-ECD of the PFB esters of some chlorophenoxy herbicides.

The PTC derivatization of the pesticides was quantitative when compared with the anhydrous derivatization. The overall recovery of the PTC derivatization was $108 \pm 8\%$ (Table II).

GC-MS analysis

As shown in Fig. 3, the PFB derivatives of acidic pesticides possess favourable GC properties. Although co-elution occurred for some compounds, no interference was found when MID was performed. EI- and positive-ion CI measurements were carried out to confirm the identity of the derivatives. Negative-ion CI mass spectra contained intense fragment ions at $[M - 181]^-$ for most of the derivatives investigated (Fig. 4). After ionization, the esters were subjected to a unique tailor-made fragmentation to yield the neutral 2,3,4,5,6-pentafluorobenzyl radicals and $[M - 181]^-$ as the highly specific and diagnostic carboxylate anions [18]. For the doubly derivatized (aliphatic) pesticide endothal, the fragmentation pattern was different: rearrangement of the substituents occurred on both carboxylic moieties, yielding a monomethyl ester

TABLE II

COMPARISON OF THE YIELD OF THE AQUEOUS PHASE-TRANSFER CATALYSED DERIVATIZATION WITH THAT OF THE DIRECT ANHYDROUS DERIVATIZATION METHOD

Compound	PTC ^a (n = 2)	Direct ^a (n = 3)	Recovery of PTC method (direct = 100%)
Bentazone	4.66	4.61	101
Dalapon	8.69	6.99	124
Dicamba	4.53	4.33	105
Dikegulac	1.73	1.71	101
Endothal	1.12	0.96	117
MCPA	4.11	4.01	102
MCPB	1.99	1.81	110
Mecoprop	5.11	4.94	103
2,4,5-T	1.44	1.34	108
TBA	3.29	3.12	105

Mean: 108 ± 8

^a Response of the derivatized compound *versus* that of an injection standard added to the final extract (*i.e.* tetrachloro-*p*-phthalic acid dimethylester in *n*-hexane).

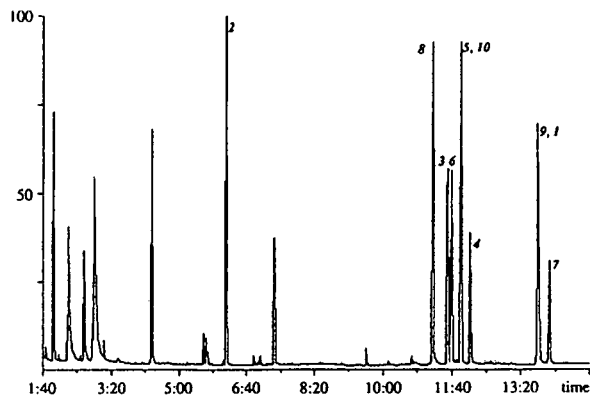


Fig. 3. Reconstructed ion chromatogram of a derivatized carboxylic pesticide mixture. Numbers on the peaks refer to Table I. Time in min:s.

(via proton transfer) in conjunction with a singly charged carboxylate anion $[M - 347]^-$.

In the absence of an additional clean-up, the detection limit was mainly determined by the chemical noise introduced from both the sample

and the derivatization procedure. In drinking water and relatively clean surface water samples, the selectivity of the method was high enough for detection and identification based on retention times and isotope ratios, permitting determinations at low- $\mu\text{g/l}$ levels ($\geq 0.05 \mu\text{g/l}$). The calibration graphs for the individual pesticides were straight and passed through the origin. An example is shown in Fig. 5 for dikegulac. Results of the determination of some polar acidic pesticides in samples from different origins are given in Table III. Groundwater, spiked at a level of *ca.* $0.2 \mu\text{g/l}$ of each pesticide, showed recoveries of *ca.* 106%. In polluted surface water, no significant difference was found in the results with or without removal of the solids by means of centrifugation prior to the PTC derivatization.

Further, the method was tested on whole blood samples from a subject suspected to have been exposed to mecoprop. After removal of the

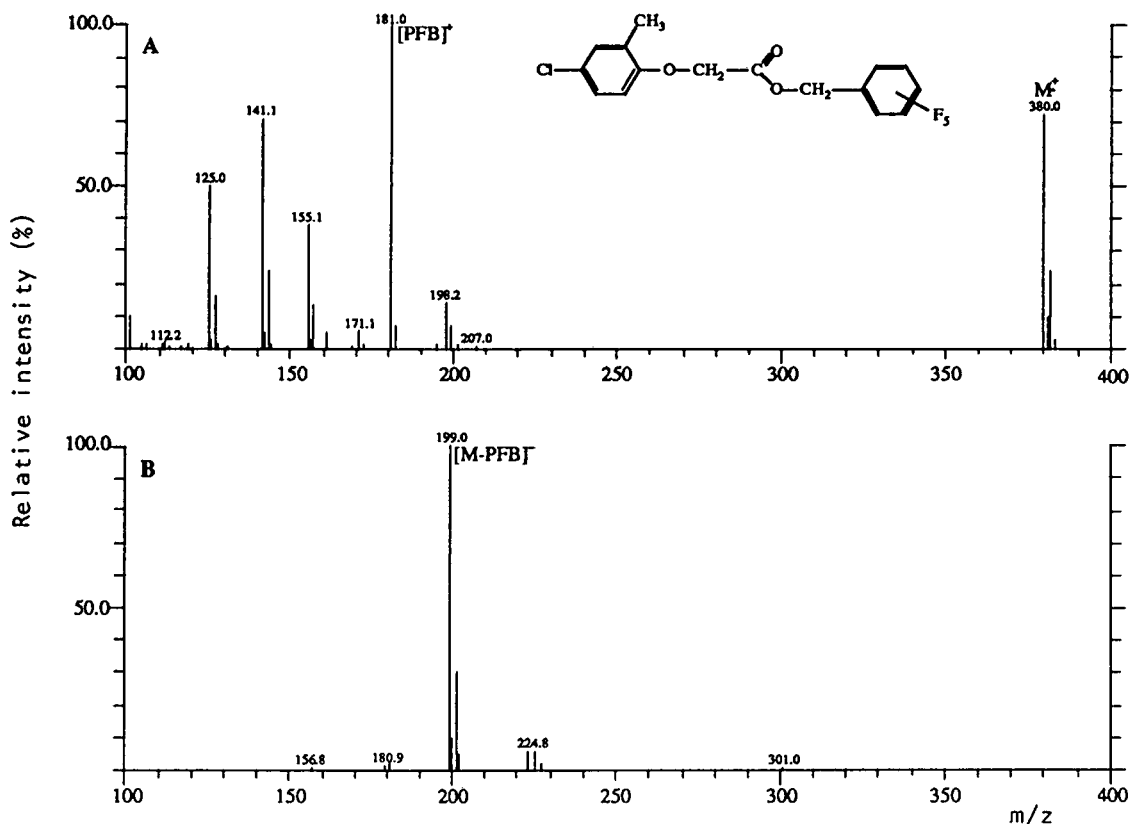


Fig. 4. (A) EI and (B) NICI mass spectra of the PFB derivative of MCPA.

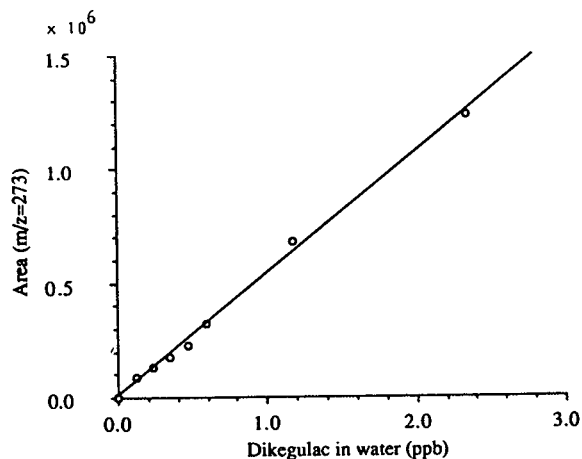


Fig. 5. Calibration graph for dikegulac in water using PTC derivatization with selected ion monitoring at m/z 273 (i.e., $[M - PFB]^-$). ppb = $\mu\text{g/l}$.

red blood cells by centrifugation, 400 μl of the clear supernatant were diluted with water and subjected to the PTC derivatization, followed by GC-MS on a quadrupole instrument. No mecoprop could be found in the sample, but the addition of mecoprop to the sample before the centrifugation step at a level of 1.2 mg/l resulted

in a high response for the mecoprop-PFB derivative. Under these conditions, the limit of detection for mecoprop in blood was found to be ca. 7 $\mu\text{g/l}$ at a signal-to-noise ratio of 10. Obviously, the PTC derivatization was suitable for the determination of acidic pesticides without further sample clean-up for difficult samples such as human blood.

Increased resolution MS analysis

Although mass unit resolution analysis on a quadrupole instrument gave sufficient selectivity for most samples, increased selectivity was required for low-level analyses of dirty samples. Addition of mecoprop at the 0.1 $\mu\text{g/l}$ level to such a sample (ground water), showed no identifiable peaks above the background at unit resolution (Fig. 6). At a resolution of 1000 the background was significantly reduced, but the measured isotope ratio from chlorine (theoretical ratio 33%, measured 5.4%) was indicative of a peak impurity. Elimination of the interfering chemical background was achieved at a resolving power of 4000, with a moderate decrease in sensitivity.

TABLE III

LEVELS OF SOME ACIDIC PESTICIDES IN SURFACE WATER

All measurements were performed at mass unit resolution.

Sample	Concentration ($\mu\text{g/l}$)						
	Bentazone	Dalapon	Dicamba	Dikegulac	MCPA	Mecoprop	2,4-D
Ground water 1		0.15	0.05		0.05	0.36	<0.05
Ground water 2		0.14	0.05		0.05	2.19	<0.05
Ground water 3		0.20	0.05		0.06	0.07	<0.03
Ground water 4		0.16	<0.05		0.08	0.06	0.06
Ground water (add.) ^a		0.22(0.21)	0.20(0.18)		0.21(0.19)	0.22(0.19)	0.19(0.20)
River water 1				0.31			
River water 2				0.36			
River water 3				<0.05			
Drinking water 1 ^b	688				790	523	853
Drinking water 2 ^b	793				87	<0.05	107
Drinking water 3 ^b	570				805	783	690
Drinking water 4 ^b	549				<0.05	<0.05	<0.05

^a Measured values of blank ground water with addition of ca. 0.2 $\mu\text{g/l}$ (in parentheses) of the pesticides.

^b Drinking water samples contained additions of several pesticides, used to investigate the behaviour of organic micropollutants during slow sand filtration.

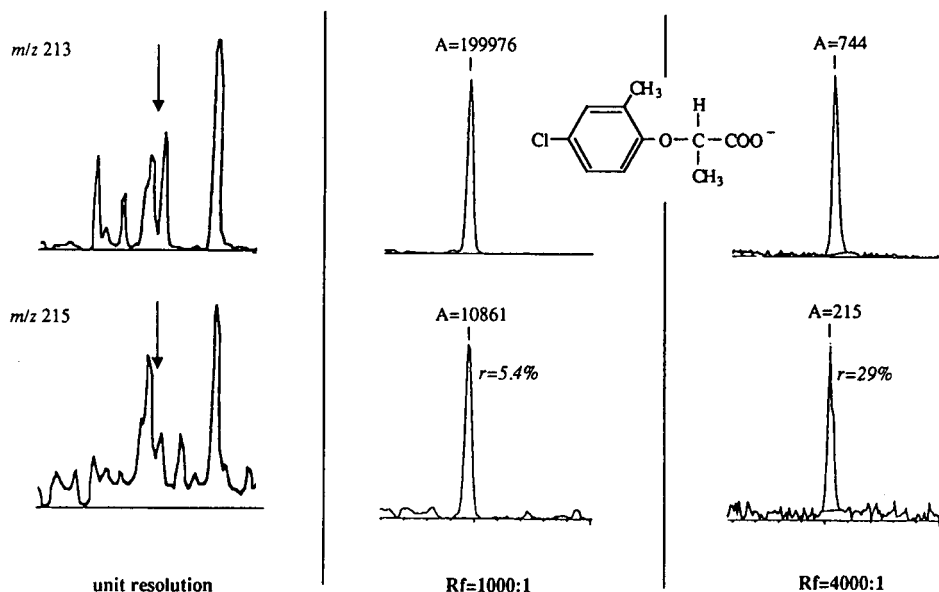


Fig. 6. Influence of increased mass resolution measurements of mecoprop at 0.1 $\mu\text{g/l}$ in a dirty ground water sample.

DISCUSSION

PTC derivatization was found to be a rapid and reliable method for the determination of polar acidic pesticides using GC techniques. For (phenoxy)-carboxylic pesticides, the PTC derivatization technique was found to be suitable for screening purposes. Although it is not possible to use this method with an ECD system without any further sample clean-up, MS detection provides sufficient selectivity and sensitivity in the negative-ion CI mode. An electron-capturing functionality is introduced into the compound by derivatization; hence the presence of an electron-capturing group in the original pesticide is not a prerequisite.

Confirmation and determination down to the 0.05 $\mu\text{g/l}$ level were easily achieved on a quadrupole instrument with mass unit resolution. However, increased resolution may be necessary when high chemical background levels are observed (e.g., with dirty samples).

Future research will be focused on the applicability of this screening method to other (phenoxy)-carboxylic pesticides and the application of the two-phase system derivatization technique to pesticides containing other classes of

functional groups (e.g., OH or NH/NH₂ groups).

REFERENCES

- H.J. Neu, *Fresenius' J. Anal. Chem.*, 337 (1990) 583.
- R.A. Baumann, G.F. Ernst, J.T.A. Jansen, A. Dekok, P.D.A. Olthof, L.G.M.T. Tuinstra, W. Verwaal, P. van Zoonen and F. Hernandez Hernandez, Working Group on "Development and Improvement of Residue-Analytical Methods", *Fresenius' J. Anal. Chem.*, 339 (1991) 357.
- F. Jung, S.J. Gee, R.O. Harrison, M.H. Goodrow, A.E. Karu, A.L. Braun, Q.X. Li and B.D. Hammock, *Pestic. Sci.*, 26 (1989) 303.
- P. Yáñez-Sedeño, J.M. Devillena, J.M. Pingarrón and L.M. Polo, *Anal. Chim. Acta*, 234 (1990) 309.
- D. Barceló, *Chromatographia*, 25 (1988) 928.
- P.A. Greve, *Gewässerschutz Wasser Abwasser*, 106 (1989) 427.
- E.A. Hogendoorn, C.E. Goewie and P. van Zoonen, *Fresenius' J. Anal. Chem.*, 339 (1991) 348.
- A. Farran, J.L. Cortina, J. Depablo and D. Barceló, *Anal. Chim. Acta*, 234 (1990) 119.
- T.R. Covey, E.D. Lee, A.P. Bruins and J.D. Henion, *Anal. Chem.*, 58 (1986) 1451A.
- P. Arpino, *Fresenius' J. Anal. Chem.*, 337 (1990) 667.
- J. Sherma, *Anal. Chem.*, 63 (1991) 118R.
- C.Z. Schlett, *Wasser Abwasser Forsch.*, 23 (1990) 32.
- D.R. Knapp, *Handbook of Analytical Derivatization Reactions*, Wiley, New York, 1979.
- K-E. Karlsson, *J. Chromatogr.*, 219 (1981) 373.

- 15 A. Arbin, H. Brink and J. Vessman, *J. Chromatogr.*, 196 (1980) 255.
- 16 E. Fogelquist, B. Josefsson and C. Roos, *J. High Resolut. Chromatogr. Chromatogr. Commun.*, 3 (1980) 568.

- 17 W.J. Allender, *J. Chromatogr. Sci.*, 27 (1989) 193.
- 18 U. Hofmann, S. Holzer and C.O. Meese, *J. Chromatogr.*, 508 (1990) 349.

CHROMSYMP. 2856

On-line combination of automated micro liquid–liquid extraction and capillary gas chromatography for the determination of pesticides in water

G. René van der Hoff and Robert A. Baumann

National Institute of Public Health and Environmental Protection (RIVM), P.O. Box 1, 3720 BA Bilthoven (Netherlands)

Udo A.Th. Brinkman

Department of Analytical Chemistry, Free University, De Boelelaan 1083, 1081 HV Amsterdam (Netherlands)

Piet van Zoonen*

National Institute of Public Health and Environmental Protection (RIVM), P.O. Box 1, 3720 BA Bilthoven (Netherlands)

(First received November 9th, 1992; revised manuscript received April 12th, 1993)

ABSTRACT

The determination of pesticides in water is often based on liquid–liquid extractions combined with concentration by evaporating the organic solvent followed by analysis with capillary GC. The use of selective detection such as thermionic detection (NPD) or flame photometric detection (FPD) makes the use of additional clean-up unnecessary in many instances. To obtain detection limits in the sub-ppb range with these detectors, typically the equivalent of approximately 1 ml of sample is injected. Hence, micro-extraction techniques, transferring the pesticide content of 1 ml of aqueous sample to a capillary GC are feasible. In this study, micro liquid–liquid extraction with methyl *tert.*-butyl ether was combined with GC–FPD in a fully automated set-up, using GC sample introduction volumes of 500 μ l, which were transferred via an on-column interface equipped with an early vapour exit. The organophosphorus pesticides diazinon, chlorpyrifos-methyl, malathion, chlorpyrifos-ethyl, chlorfenvinphos-*cis*, bromophos and azinphos-ethyl were determined in pond water spiked at the 0.5 μ g/l level. In most cases recoveries were over 70%, while the detection limit allowed quantification at the level of the EC maximum residue limits for water intended for human consumption (0.1 μ g/l). This communication demonstrates the practicality of an on-line micro liquid–liquid extraction procedure which eliminates the need to use a phase separator, resulting in a set-up robust also in the hands of relatively inexperienced personnel.

INTRODUCTION

Recent developments in LC–GC coupling open new ways for on-line sample handling in capillary GC. In particular, the solvent evaporation LC–GC interfaces equipped with an early

vapour exit developed by Grob and co-workers [1,2], which allow the introduction of almost any volume of solvent in a gas chromatograph, are extremely powerful.

The use of sample enrichment on non-polar solid phases coupled with LC–GC-type large-volume injections is described by Noroozian *et al.* [3] and more recently by Vreuls *et al.* [4]. Other approaches to automated sample enrichment coupled to gas chromatography are dis-

* Corresponding author.

cussed by Zlatkis [5] and Kaiser and Rieder [6], who described the extraction of analytes into the stationary phase film of the GC column. Major drawbacks of these approaches concerned low extraction efficiency (slow diffusion process) and poor reconcentration before on-line GC analysis (low phase ratio).

This paper deals with liquid–liquid extraction techniques coupled to capillary GC. Today, the gas chromatographic analysis of pesticides in aqueous environmental samples is focused on nitrogen- and phosphorus-containing pesticides, which are either deemed to reach the ground-water due to their mobility or found in surface water due to their extensive use. Detection with the readily available selective thermionic (NPD) and flame-photometric (FPD) detection systems is relatively simple. Owing to the selectivity of these detectors clean-up procedures by using, for example, adsorption chromatography can usually be omitted. In LC–GC this means that it is not necessary to use the LC part in a LC–GC system for clean-up. Standard procedures for the determination of nitrogen and phosphorus pesticides involve liquid–liquid extraction or solid-phase extraction of large sample volumes, typically 500–1000 ml, with appropriately volatile extraction solvents. In these procedures the extracts are concentrated down to a few millilitres, of which 1 or 2 μl are injected splitless or on-column into a capillary GC, thus introducing only about 0.1% of the original sample. LC–GC technology offers the possibility to inject larger samples, of the order of 1 ml, into a GC system. This gives the opportunity to combine the use of micro-extraction techniques and GC analysis. The comparison of conventional and micro-extraction techniques presented in Table I clearly illustrates the attractiveness of the latter approach.

Preference for either a liquid–liquid or a solid-phase extraction is primarily determined by the nature of the environmental problem under consideration. In wastewater and surface water analysis one is usually interested in the total sample, including pesticides adsorbed on particulate matter; the same is true for rain water if the total deposition is to be estimated. In ground-

TABLE I

COMPARISON OF CONVENTIONAL LIQUID–LIQUID EXTRACTION AND MICRO LIQUID–LIQUID EXTRACTION TECHNIQUES

<i>Conventional extraction</i>	<i>Micro extraction</i>
1000 ml water \rightarrow 1 ml extract	1 ml water \rightarrow 1 ml extract
1 $\mu\text{g/l}$ \rightarrow 1 $\mu\text{g/ml}$	1 ng/ml \rightarrow 1 ng/ml
1 μl injection \rightarrow 1 ng	1 ml injection \rightarrow 1 ng

water analysis, however, one is usually interested in the liquid phase of the sample only. If one is interested in the contents of the total sample, liquid–liquid extraction is to be preferred, since one can handle the total sample without filtration.

The disadvantages of conventional liquid–liquid extraction are: (i) the low sample throughput due to the laboriousness of first use, and then evaporating hundreds of millilitres of organic solvent and (ii) the waste problem created by the use of these amounts of organic solvent. If liquid–liquid extraction is preferred it is therefore highly attractive to use miniaturized extraction procedures which, in addition, are more easily automated.

Liquid–liquid extraction using segmented flow systems followed by flow injection-type phase separation coupled on-line with capillary GC has been utilized for chlorinated pesticides [7], aromatic hydrocarbons [8] and halocarbons [9], and for chlorinated anilines and carboxylic acids using a phase-transfer derivatization [10]. A similar approach was used for interfacing reversed-phase LC with capillary GC by on-line extraction of the analytes from the aqueous LC eluent into solvents of lower polarity [11].

Modern LC autosamplers are able to perform operations such as reagent addition, solvent mixing, collection and liquid–liquid extraction. This paper describes the application of such a sampler for micro liquid–liquid extraction coupled on-line with an LC–GC interface, thus providing the automated sample handling of aqueous environmental samples whilst eliminating the insertion of a phase separator.

EXPERIMENTAL

Chemicals

Pesticides with a purity of >99% were purchased from Promochem (Wesel, Germany). Stock solutions were prepared in acetone (Promochem, nanograde). Dilute solutions for direct LC–GC analysis were prepared in *n*-pentane (Baker resialysed grade), methyl *tert.*-butyl ether (MTBE) (Baker HPLC grade) or dichloromethane (Promochem, nanograde). MTBE used in the LC pump was degassed ultrasonically under light vacuum each day.

Equipment

In order to perform automated micro liquid–liquid extractions the original Dualchrom 3000 LC–GC system was modified. The LC–GC equipment consisted of a Dualchrom 3000 HPLC–HRGC system from Carlo Erba Strumentazione (Milan, Italy) equipped with a Model 232 Bio autosampler from Gilson (Villiers-le-Bel, France), in combination with a Model 401 dilutor from Gilson equipped with a 5.0-ml syringe and 3.0-ml PTFE transfer tubing for solvent delivery and sample manipulation (Fig. 1). Since it is not necessary to use an LC

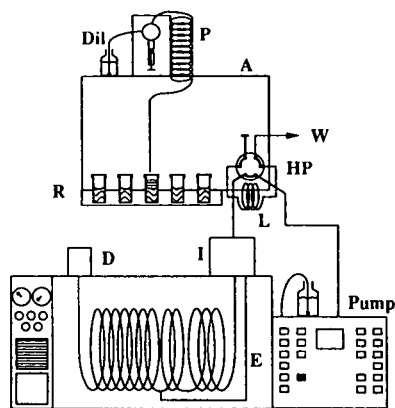


Fig. 1. Schematic representation of the equipment used for automated micro liquid–liquid extractions. A = Auto-sampler; Dil = dilutor; P = PTFE transfer tubing; R = rack with samples; HP = high-pressure six-way valve; L = 500- μ l storage loop; W = waste; I = on-column interface; E = early vapour exit; D = flame photometric detector.

column, the UV–Vis LC detector of the Dualchrom 3000 was also removed.

For sample introduction the on-column interface equipped with an early vapour exit using partially concurrent solvent evaporation of the Dualchrom was utilized.

Solvent evaporation was performed in a 6 m \times 0.53 mm I.D. phenyl-silyl deactivated retention gap obtained from Gimex (Düren, Germany) connected via a pressfit connection to a 3 m \times 0.32 mm I.D. DB-5 retaining precolumn with a film thickness of 0.25 μ m (J&W Scientific, Folsom, CA, USA). The GC separation was achieved on a 22 m \times 0.32 mm I.D. DB-5 capillary column with a film thickness of 0.25 μ m obtained from J&W Scientific, which was coupled to the retaining precolumn by means of a three-way pressfit. The third exit of the three-way pressfit was connected to a 0.4 m \times 0.32 I.D. fused-silica capillary connected to the early vapour exit. The oven temperature was programmed as follows: 65°C for 10 min, 20°C/min to 150°C, 5°C/min to 260°C, 30 min hold at 260°C. The helium inlet pressure was set at 100 kPa.

Detection was performed with a Model 700 flame photometric detector from Carlo Erba equipped with two photomultiplier tubes for phosphorus and sulphur detection, using filters of 526 nm and 394 nm, respectively. The detector body temperature was 180°C and the detector base temperature 300°C. The volumetric flow-rates of the flame gases hydrogen and air were set at 90 ml/min and 140 ml/min, respectively. A volumetric flow-rate of 22 ml/min helium was used as make-up gas.

Spiked samples were prepared from stock standard solutions in acetone, ensuring an acetone content of less than 1% in the final solution. All calibrations were performed by large-volume injections following essentially the same procedure as for the extracts of the samples.

RESULTS AND DISCUSSION

Instrumental set-up

The commercially available Dualchrom equipment provides two options for sample intro-

duction: the loop-type interface and the on-column interface. In this study the use of the on-column interface was preferred since this injection technique is more versatile with respect to the more volatile compounds, a group of compounds that is certainly relevant for the development of future applications.

Choice of extraction solvent

The selection of extractants used in micro-extraction techniques is based on the applicability of the solvent in the interface introduction in combination with its properties for the extraction of moderately polar pesticides from water. The GC introduction technique requires a low boiling solvent; the application of the technique to polar pesticides requires a relatively polar organic solvent. Technically a solvent with a density lower than water should be preferred in order to transfer the organic layer efficiently to the GC column. In early experiments diethyl ether was tested as extraction solvent. However, this resulted in difficulties with the handling of the liquid in the PTFE transfer coil of the autosampler (Fig. 1) due to evaporation of the solvent in the aspirator tubing. In order to prevent cross-contamination, an airplug is aspirated between diethyl ether and the solvent present in the remainder of the dilutor system. Apparently, the combination of the airplug with the evaporation of diethyl ether inside the transfer tubing causes overpressure in the PTFE transfer coil. Hence, diethylether is partially lost during the extraction procedure. MTBE was tested in the same procedure without the problems caused by undesired solvent loss during the manipulations performed by the autosampler. Apparently, the application of very volatile solvents in combination with solvent manipulation by an autosampler should be avoided due to solvent loss and solvent evaporation in the sample vial in which the extraction is performed. At this moment, the application of volatile solvents seems to be limited to closed on-line extraction systems in combination with a phase separator. With regard to automation, solvents with a density lower than water are manipulated by the autosampler more easily, without the risk of

aspirating water which is situated below the extraction solvent.

Micro liquid–liquid extraction

De Ruiter *et al.* [12] used autosamplers for their micro liquid–liquid extractions. They described an extraction of phenolic steroids that were derivatized by a phase transfer-catalysed dansylation in a two-phase system consisting of an aqueous solution and dichloromethane or chloroform. By aspirating the mixture repeatedly in the coiled PTFE transfer capillary of the sampler, they created a segmented flow in which efficient extraction took place. In the quoted paper, the introduction of the segmented aqueous/organic mixtures into the capillary caused cross-contamination; therefore rinsing with acetone and water was necessary. To prevent this problem we performed the extraction procedure by aspirating the organic phase only.

Micro liquid–liquid extraction was carried out using 4-ml autosampler vials closed with a cap containing a PTFE inlay to prevent solvent evaporation during the process. These vials contained 1.5 ml of the water sample, to which the dilutor added 1.5 ml of MTBE. Automated liquid–liquid extraction was carried out by letting the dilutor aspirate—at the correct needle depth—1.0 ml of solvent at a flow-rate of 100 $\mu\text{l/s}$. After raising the needle to a level of 4 ml, dispensing was performed at a flow-rate of 1600 $\mu\text{l/s}$, forcing the organic solvent into the water phase and thus extracting the pesticides. After 1 min—the time needed to separate the two immiscible phases—the procedure was repeated six times.

Optimization of GC introduction

After extraction, 1.0 ml of the organic fraction was injected through a 500- μl storage loop situated at the six-way valve of the autosampler (Fig. 1). The extract was transported from the loop to the on-column interface by means of the LC pump of the Dualchrom. In order to compensate for the volume of the transfer lines an additional 100 μl of MTBE were introduced, yielding a total injection volume of 600 μl of MTBE to be transferred into the GC column. Sample introduction took place over 3 min at a

flow-rate of 200 $\mu\text{l}/\text{min}$, using an oven temperature of 65°C and a helium pressure of 100 kPa. The required closure time of the early vapour exit was determined by igniting the solvent vapours leaving the exit tube.

Solvent vapours arrived after 14 s, counting from the moment the GC introduction commenced, which can be considered as the dead time of the retention gap and retaining pre-column. Flame extinction after GC introduction was observed after 267 s, closure of the early vapour exit was set at 282 s, a delay of 15 s after completion of solvent evaporation. Hence, the time needed for the evaporation of 600 μl of MTBE can be estimated correcting of the total sample introduction time (267 s) for the dead time of the retention gap/solvent vapour exit system (14 s), yielding an evaporation time of 253 s. The corresponding evaporation rate can be calculated by division of the volume introduced in GC (600 μl) by the evaporation time (253 s), which resulted in an evaporation rate of 142 $\mu\text{l}/\text{min}$ MTBE, which is in agreement with the evaporation rate for MTBE found by Schmarr *et al.* [2]. The introduction rate (200 $\mu\text{l}/\text{min}$) leaves approximately 175 μl to be evaporated after completion of the sample transfer. It can be concluded that the flooded zone is rather high in comparison with those reported by other authors [2]. Prediction of the allowable flooded zone is complicated, because it depends on the wettability of the retention gap surface. The relatively low surface tension of ethers in combination with the retention gap used in this study partially explains the large flooded zone that can be handled. It should be mentioned here that too large a flooded zone should result in irregular flames during the experiments for the determination of the evaporation rate. However, no such effect was observed.

Application of automated micro liquid–liquid extraction

After stabilization of the LC–GC–FPD system, 4-ml vials containing aliquots of the pond-water samples were placed into a rack of the autosampler. Automated micro liquid–liquid extraction was performed by the autosampler, which applied the extraction procedure discussed

above. Six-fold repetition of this procedure gave plateau conditions for the analyte recovery for all seven organophosphorus pesticides tested. Table II shows an event schedule of the whole procedure of automated micro liquid–liquid extraction coupled to GC–FPD.

Table III shows that the total on-line extraction–GC–FPD system showed good performance at the sub- $\mu\text{g}/\text{l}$ level, with bromophos being a notable exception. The reason for this anomalous behaviour is as yet unknown.

Fig. 2 shows a chromatogram obtained for a 1.5-ml pond-water sample using the procedure described above. Detection was performed by means of dual-FPD detection; that is, chromatographic traces in the P- and S-mode are recorded simultaneously. Unfortunately, however, even with the Model 700 FPD system, the S-mode is not sensitive enough to detect sub- $\mu\text{g}/\text{l}$ levels of the pesticides in the small sample volumes used.

Micro liquid–liquid extraction coupled on-line to a GC system is attractive for volatile pesticides, since losses due to evaporation can be minimized because one uses a closed system during the evaporation step. In order to test the applicability of this set-up to volatile pesticides, dichlorvos (DDVP), a volatile organophosphorus pesticide, was used as a model compound. The application of MTBE as solvent to introduce DDVP into GC turned out to be unsuitable: no peak appeared in the chromatogram, probably because of co-evaporation of the pesticide with the evaporating MTBE despite the use of an on-column interface.

As regards the selection of an alternative extractant, a distinctly polar solvent is required to extract the polar DDVP efficiently from water samples. Besides, because of GC introduction, the selected solvent should be low boiling. Dichloromethane appears to be the only sufficiently pure solvent available to meet these requirements. Unfortunately, the density of dichloromethane is higher than water, hence, the organic phase is situated below the aqueous sample phase. Therefore the organic phase has to be transferred through the aqueous phase, introducing a source of contamination, or even droplets of water.

Preliminary experiments applying liquid–liq-

TABLE II

EVENT SCHEDULE OF THE AUTOMATED LIQUID-LIQUID EXTRACTION OF WATER SAMPLES COUPLED ON-LINE TO GC-FPD

Step	Time (min:s)	Event(s) that take(s) place
1	0:00	LC autosampler starts extraction procedure, rinsing of the PTFE transfer tubing
2	0:30	Addition of 1.5 ml of MTBE to sample vial (first extraction), stabilization of two mixed phases
3	1:30	Aspiration of 1.0 ml of MTBE from sample vial
4	1:40	Dispensing of 1.0 ml of aspirated MTBE into sample vial (second extraction) and stabilization of two mixed phases
5	2:40	Aspiration of 1.0 ml of MTBE from sample vial
6	2:50	Dispension of 1.0 ml of aspirated MTBE into sample vial (third extraction) and stabilization of two mixed phases
7	3:50	Aspiration of 1.0 ml of MTBE from sample vial
8	4:00	Dispension of 1.0 ml of aspirated MTBE into sample vial (fourth extraction) and stabilization of two mixed phases
9	5:00	Aspiration of 1.0 ml of MTBE from sample vial
10	5:10	Dispension of 1.0 ml of aspirated MTBE into sample vial (fifth extraction) and stabilization of two mixed phases
11	6:10	Aspiration of 1.0 ml of MTBE from sample vial
12	6:20	Dispensing of 1.0 ml of aspirated MTBE into sample vial (sixth extraction) and stabilization of two mixed phases
13	7:20	Transfer of 1.0 ml of MTBE extract of the water sample to a 500- μ l storage loop
14	7:30	Start of GC introduction of the MTBE extract and start of temperature programme
15	10:30	End of GC transfer of the MTBE extract
16	11:57	End of solvent evaporation
17	12:12	Closure of the solvent vapour exit
18	61:23	End of temperature programme, GC oven starts cooling.
19	68:00	GC oven stabilizes on introduction temperature while LC autosampler starts extraction cycle from step 1

TABLE III

TRACE-LEVEL DETERMINATION OF ORGANOPHOSPORUS PESTICIDES IN POND WATER USING ON-LINE MICRO LIQUID-LIQUID EXTRACTION-GC-FPD

No.	Compound	Spiking level (μ g/l)	Recovery ^a					LOD ^b (μ g/l)
			Extr. 1	Extr. 2	Extr. 3	Mean (%)	R.S.D. (%)	
1	Diazinon	0.50	107	98	102	102	5	0.02
2	Chlorpyrifos-methyl	0.56	85	74	80	80	5	0.01
3	Malathion	0.44	75	72	76	74	2	0.03
4	Chlorpyrifos-ethyl	0.65	75	67	73	72	4	0.02
5	Chlorfenvinphos- <i>cis</i>	0.43	105	80	97	94	13	0.09
6	Bromophos	0.43	44	42	43	43	1	0.05
7	Azinphos-ethyl	0.53	113	92	109	105	11	0.02

^a Recovery values for the three separate extractions are given, as well as the mean recovery and the relative standard deviation (R.S.D.).

^b Limit of determination defined as a signal-to-noise ratio of 3.

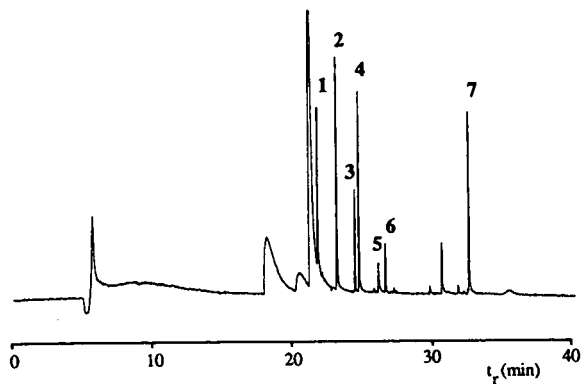


Fig. 2. Automated liquid–liquid extraction coupled on-line to GC–FPD analysis (P-mode; att. 16) of a pond-water sample spiked with seven organophosphorus pesticides at 0.5 $\mu\text{g/l}$, using MTBE as extraction solvent. For peak assignment, see Table II.

liquid extraction with dichloromethane were performed: 1.5 ml of water sample were transferred into a vial of 4 ml, after which 1.5 ml of dichloromethane were added. This vial was shaken for 30 s, and subsequently 600 μl of the organic extract were transferred into an auto-sampler vial, which was placed in the auto-sampler. The dichloromethane extract was introduced into the GC system by means of an on-column interface at an oven temperature of 50°C using a dichloromethane flow-rate of 150 $\mu\text{l/min}$.

Water spiked with DDVP at the 0.4 $\mu\text{g/l}$ level resulted in a chromatogram with a large solvent peak tailing up to a retention time of 20 min, probably caused by strong phase soaking of the stationary phase in the retaining precolumn, which resulted in a very broad DDVP peak.

Apparently, for the extraction of very volatile pesticides other extraction solvents are needed, because the use of dichloromethane can cause damage to the introduction system and the quartz windows of the FPD system. Also, soot formation inside the flame detector can occur. An additional drawback of dichloromethane is that its applicability for NPD is limited [11].

CONCLUSIONS

Micro-extraction techniques offer distinct advantages over conventional-size liquid–liquid ex-

tractions because of the ease of on-line coupling to LC–GC interfaces (and their automation), the increased sample throughput and the distinctly lower organic solvent consumption.

The present communication demonstrates the practicality of a simple micro liquid–liquid extraction procedure which eliminates the need to use a phase separator. This certainly makes the set-up robust even in the hands of relatively inexperienced personnel. As an example, a number of organophosphorus pesticides are determined in pond water at the 0.1–1 $\mu\text{g/l}$ level.

Problems are still encountered when highly volatile and polar analytes (and organic solvents) have to be used. Future research will involve a more detailed study of the compatibility of a wide range of organic solvents with the proposed technique.

REFERENCES

- 1 K. Grob, H.G. Schmarr and A. Mosandl, *J. High Resolut. Chromatogr.*, 12 (1989) 375.
- 2 H.G. Schmarr, A. Mosandl and K. Grob, *J. High Resolut. Chromatogr.*, 12 (1989) 721.
- 3 E. Noroozian, F.A. Maris, M.W.F. Nielen, R.W. Frei, G.J. de Jong and U.A.Th. Brinkman, *J. High Resolut. Chromatogr.*, 10 (1987) 17.
- 4 J.J. Vreuls, V.P. Goudriaan and U.A.Th. Brinkman, *J. High Resolut. Chromatogr.*, 14 (1991) 475.
- 5 A. Zlatkis, F.S. Wang and H. Shanfield, *Anal. Chem.*, 55 (1983) 1848.
- 6 R.E. Kaizer and R. Rieder, *J. Chromatogr.*, 477 (1989) 49.
- 7 E.C. Goosens, R.G. Bunschoten, V. Engelen, D. de Jong and J.M.H. van den Berg, *J. High Resolut. Chromatogr.*, 13 (1990) 438.
- 8 J. Roeraade, *J. Chromatogr.*, 330 (1985) 263.
- 9 E. Fogelquist, M. Krysell and L.G. Danielson, *Anal. Chem.*, 58 (1986) 1516.
- 10 E.C. Goosens, M.J. Broekman, M.H. Wolters, R.E. Strijker, D. de Jong, G.J. de Jong and U.A.Th. Brinkman, *J. High Resolut. Chromatogr.*, 15 (1992) 242.
- 11 P. van Zoonen, G.R. van der Hoff and E.A. Hogendoorn, *J. High Resolut. Chromatogr.*, 13 (1990) 483.
- 12 C. de Ruiter, J.N.L. Tai Tin Tsoi, U.A.Th. Brinkman and R.W. Frei, *Chromatographia*, 26 (1988) 267.

Gas chromatographic–mass spectrometric determination of halogenated acetic acids in water after direct derivatization

Hideaki Ozawa

Water and Soil Environment Division, National Institute for Environmental Studies, 16-2 Onogawa, Tsukuba-shi, Ibaraki 305 (Japan)

(First received November 19th, 1992; revised manuscript received April 19th, 1993)

ABSTRACT

A previously developed difluoroanilide derivatization method was used for the determination of trace levels of halogenated acetic acids (HAAs), including bromoacetic acids, in water. The derivatives formed by the reaction were separated with a gas chromatograph–mass spectrometer equipped with a fused-silica capillary column and detected by selected ion monitoring. Five acids (chloro- and bromoacetic acids) in water could be determined at $\mu\text{g l}^{-1}$ levels. The recoveries for $10 \mu\text{g l}^{-1}$ of analyte in natural waters (lake and sea waters) were greater than 85%. However, under the conditions used, tribromoacetic acid could be determined only at higher concentration levels. The proposed method was successfully used to determine concentrations of HAAs in a range of natural waters. HAA formation from raw river water was investigated by laboratory chlorination experiments.

INTRODUCTION

Dissolved organic compounds such as humic substances are known to form halogenated acetic acids (HAAs) in natural waters, especially chloroacetic acids (CAAs), by reaction with chlorine [1–4]. Among the chlorination products in drinking water, attention has been focused almost exclusively on volatile chlorinated organic compounds, particularly trihalomethanes (THMs) [1,5]. However, there has been an increased awareness that CAAs may represent potential hazards. CAAs seem to be the principal fraction of non-volatile chlorinated organic compounds in drinking water [2–4], with several researchers reporting concentrations of trichloroacetic acid (TCAA) and dichloroacetic acid (DCAA) up to $160 \mu\text{g l}^{-1}$ [6–11]. In Japan, both DCAA and TCAA have been found in drinking water at concentrations up to $35 \mu\text{g l}^{-1}$ [12]. Specific regulation may be needed to control the forma-

tion of these chlorination by-products formed during disinfection of drinking water [13].

Previously, a novel but simple difluoroanilide derivatization method was developed for trace amounts of CAAs in water [14]. The CAA derivatives formed by a reaction with dicyclohexylcarbodiimide (DCC) and 2,4-difluoroaniline (DFA) were separated and determined by gas chromatography with electron-capture detection (GC–ECD). This method permits the CAAs in water to be converted into the derivatives suitable for GC analysis and extracted into an organic phase in one step. In practice, this method is convenient for the detection and determination of CAAs in tap water and wastewater after disinfection. However, the use of packed GC columns has limitations with respect to the separation of the derivatives.

In this work, the direct derivatization method was applied to bromoacetic acids (BAAs), which are expected to be formed during water chlorina-

tion in the presence of bromide ion [7,11]. A gas chromatographic–mass spectrometric (GC–MS) system fitted with a capillary column was used to separate the difluoroanilide derivatives of HAAs (CAAs and BAAs) and detect them selectively. This method was employed for tap water analysis, and laboratory chlorination experiments were conducted to investigate the formation of HAAs in the surface water of rivers.

EXPERIMENTAL

Apparatus

The system and operating conditions were as follows: gas chromatograph–mass spectrometer, JEOL JMS-AX505W; fused-silica capillary columns (J & W Scientific), DB-17 (15 m × 0.53 mm I.D., film thickness 1.0 μm) and DB-5 (15 m × 0.53 mm I.D., film thickness 1.5 μm); temperature programme, initially 100°C for 2 min, then increased at 8°C min⁻¹ to a final temperature of 200°C; injection port temperature, 220°C; separator temperature, 230°C; ion source temperature, 260°C; ionization current, 0.3 mA; ionization voltage, 70 eV; and carrier gas, helium at a flow-rate of 20 ml min⁻¹. Aliquots of 2 μl of sample solution were introduced directly into the column.

A Shimadzu GC-6A gas chromatograph equipped with a ⁶³Ni electron-capture detector was used for the determination of THMs. A glass column (3 m × 3 mm I.D.) packed with 20% silicone DC-550 on Uniport HP was fitted. The column oven temperature was 90°C, the injection port temperature was 150°C and the carrier gas was nitrogen at a flow-rate of 30 ml min⁻¹. Aliquots of 5 μl of sample solution were introduced.

Reagents

DFA and DCC were used as 1 M solutions in ethyl acetate, as described previously [14]. Monochloroacetic acid (MCAA), DCAA and TCAA primary standards were prepared in distilled water at concentrations of 1000 μg ml⁻¹ and stored in a refrigerator prior to use after appropriate dilution. Monobromoacetic acid (MBAA) and tribromoacetic acid (TBAA) were obtained from Tokyo Kasei Kogyo (Tokyo,

Japan). Dibromoacetic acid (DBAA) was obtained from Aldrich (Milwaukee, WI, USA). MBAA and DBAA primary standards were prepared and used as aqueous solutions in the same manner as the CAAs. Aqueous TBAA standards (1000 μg ml⁻¹) were used immediately after dilution and were not stored. A mixed standard solution of six HAAs was prepared from each standard solution (1000 μg ml⁻¹). [²H₈]Naphthalene obtained from Cambridge Isotope Laboratories (Woburn, MA, USA) was dissolved in *n*-hexane. All organic solvents were of a suitable grade for pesticide residue analysis. Other reagents were of analytical-reagent grade.

Procedure

HAAs were derivatized as described previously [14]. Briefly, 1 g of sodium chloride and 0.4 ml of 10 M hydrochloric acid were added to a 50-ml water sample. After adding 0.4 ml of 1 M DFA solution and 0.4 ml of 1 M DCC solution, the mixture was vigorously shaken with 15 ml of ethyl acetate for 40 min. Following the addition of 5 g of sodium chloride, the aqueous layer was separated and then extracted with 5 ml of ethyl acetate. The combined organic layer was successively washed with 5 ml of 3 M hydrochloric acid, saturated sodium hydrogencarbonate solution and saturated sodium chloride solution and then dried over anhydrous sodium sulphate. The solution was concentrated to 10 ml and subjected to instrumental analysis.

A 50-μl volume of [²H₈]naphthalene solution (2 μg ml⁻¹) was added as an internal standard to 2 ml of the sample solution and aliquots of this solution were injected into the GC–MS system. Quantification was by comparison of the sample peak area with that of the internal standard. For calibration, 0.05–10-μg amounts of each halogenated acid were added to 50 ml of distilled water with the mixed standard solution of six HAAs and the samples were subjected to the derivatization procedure.

Laboratory chlorination experiment

Surface water samples were collected during January 1991 from five rivers (A, B, C, D and E) flowing through the city of Nagano. The samples were vacuum filtered through glass-fibre filter

paper (Whatman GF/C). The formation of HAAs and THMs in these filtrates following chlorination in the laboratory without pH adjustment was investigated.

Sodium hypochlorite solution was added to 1 l of each of two filtered river water samples (from A and B) at an initial free chlorine concentration of 10 mg l^{-1} and kept in sealed bottles in darkness at 20°C . Sodium sulphite (to quench the chlorine residue in samples) was added to 50-ml water samples taken periodically from the bottles to follow the kinetics of CAA formation.

The formation of these compounds was also studied in eight surface water samples collected from the five rivers (A, B1, B2, C1, C2, D, E1 and E2). There were two sampling stations in rivers B, C and E, as indicated by the numbers 1 (upper) and 2 (lower). In each instance, the lower sampling station was several kilometres downstream from the upper one. Sample waters were chlorinated for 24 h at an initial free chlorine concentration of 5 mg l^{-1} under the same conditions as described above. HAA concentrations were measured according to the procedure outlined above. THM concentrations were measured by *n*-hexane extraction and GC-ECD [15]. Residual chlorine in the treated water was measured by the *N,N*-diethyl-*p*-phenylenediamine (DPD) method with a comparator [16].

RESULTS AND DISCUSSION

Difluoroanilide derivatization of BAAs

The difluoroanilide derivatization method which was developed for CAA determination was tested here for its application to other HAAs. Aqueous solutions of BAAs produced derivatives when subjected to the same reaction conditions as applied to CAAs. Electron impact (EI) ionization mass spectra were measured for the products of the difluoroanilide derivatization of each of the BAAs (MBAA, DBAA and TBAA) (Fig. 1). Molecular ion peaks were observed at m/z 249, 327 and 405 for MBAA, DBAA and TBAA, respectively, which confirmed the formation of the difluoroanilide derivatives, 2,4-difluoromonobromoacetanilide (MBA-DFA), 2,4-difluorodibromoacetanilide

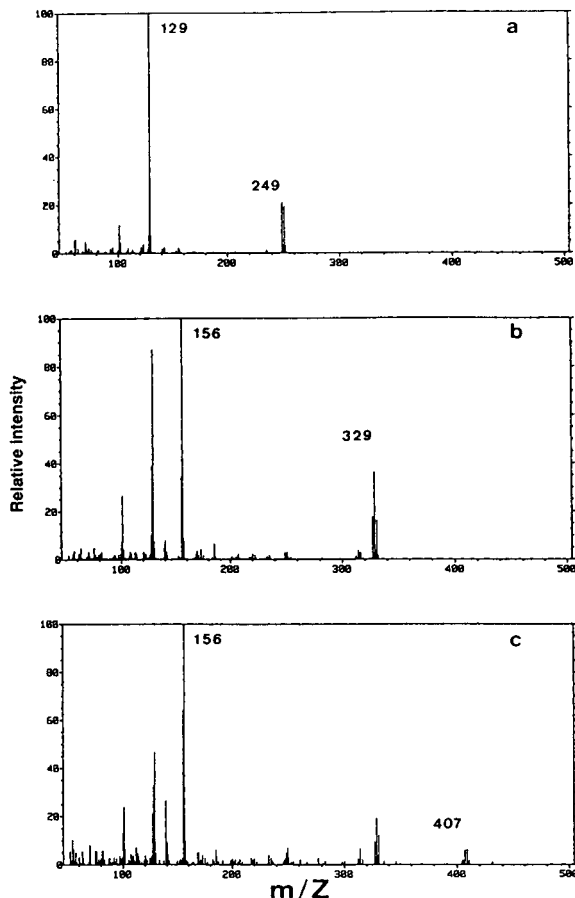


Fig. 1. EI mass spectra of the difluoroanilide derivatives of BAAs. (a) MBAA derivative (MBA-DFA); (b) DBAA derivative (DBA-DFA); (c) TBAA derivative (TBA-DFA).

(DBA-DFA) and 2,4-difluorotribromoacetanilide (TBA-DFA).

The MBAA derivative had a base peak at m/z 129, corresponding to a fragment ion $[M - 76]^+$, which can be explained by the elimination of ketene from the rearranged molecular ion M^+ . The derivatives of DBAA and TBAA, which possess two or more bromine atoms per molecule, exhibited base peaks at m/z 156, corresponding to a fragment ion $[\text{CONH} - \text{C}_6\text{H}_3\text{F}_2]^+$ which can be explained by cleavage of the carbon-carbon bond of the acetyl group. These base peaks for the derivatives of BAAs (from MBAA to TBAA) are similar to those observed for the CAA derivatives (from MCAA to TCAA). For the MCAA, DCAA and TCAA

derivatives, base peaks were observed at m/z 129, 156 and 156, respectively [14].

Separation and detection of HAA derivatives

In the previous study, difluoroanilide derivatives of CAAs were separated on packed columns with the stationary phases DEGS + H_3PO_4 and/or Apiezon grease L + H_3PO_4 [14]. In this study, fused-silica capillary columns with bonded stationary phases of slight polarity (5% diphenyl–95% dimethylpolysiloxane phase), DB-5, and of intermediate polarity (50% phenyl–50% methylpolysiloxane phase, equivalent to OV-17), DB-17, were tested for the separation of the HAA derivatives. Slight tailing of the chromatographic peaks was observed on both columns, especially for monohalogenated acetic acid derivatives. However, the intermediate polarity stationary phase yielded cleaner peak shapes.

With increasing number of chlorine and bromine atoms in an HAA molecule, the retention times of the corresponding CAA and BAA derivatives were prolonged (Table I). Monitoring ions for detection of the CAA [14] and BAA derivatives by selected ion monitoring (SIM) were chosen from the mass spectra (Fig. 2 is a typical SIM chromatogram obtained from a mixed standard solution of six HAAs at $200 \mu\text{g l}^{-1}$ each). The molecular ion peaks at m/z 205 and 249 or the fragment ion peak at m/z 129

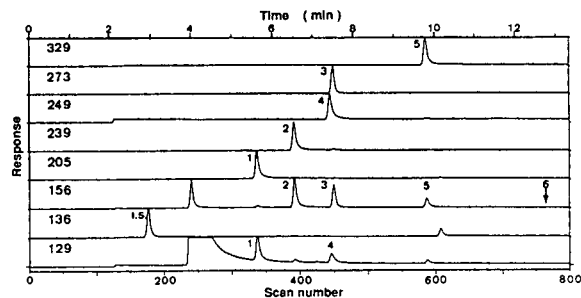


Fig. 2. SIM chromatogram of the difluoroanilide derivatives of HAAs obtained from a standard solution ($200 \mu\text{g l}^{-1}$ of each acid). Peaks: 1 = MCAA; 2 = DCAA; 3 = TCAA; 4 = MBAA; 5 = DBAA; 6 = TBAA; I.S. = $[^2H_8]$ naphthalene (internal standard).

were monitored for the MCAA and MBAA derivatives, respectively. The DCAA, TCAA, DBAA and TBAA derivatives were monitored by the fragment ion peak at m/z 156. HAA calibration graphs were prepared by normalizing the area of the ion peaks to the area of the molecular ion peak of the internal standard. Good linearity was shown by both the CAA derivatives over the range examined and by the MBAA and DBAA derivatives at concentrations of several $\mu\text{g l}^{-1}$. However, the TBAA derivative gave no peak at such low concentration levels. The detection limits of MCAA, DCAA, TCAA, MBAA and DBAA were 0.5, 0.5, 0.5, 2 and $1 \mu\text{g l}^{-1}$, respectively, in a 50-ml water sample. TBAA could be detected only at concentrations higher than *ca.* $100 \mu\text{g l}^{-1}$ under these conditions. Monitoring at m/z 156 was of interest for the detection of HAAs with two or more halogen atoms, as mentioned above. Five HAA derivatives eluted with retention times from 5.5 to 10 min and the TBAA derivative eluted at 12.8 min (Fig. 2).

Stability of derivatives

A mixed standard solution of six acids ($20 \mu\text{g l}^{-1}$ each) was derivatized and stored in a glass tube under various conditions to compare their stabilities (expressed as a percentage of the concentration remaining in an identical solution stored in darkness at 4°C) (Table II). TBAA could not be detected at the concentrations tested in this experiment and no data were obtained for it.

TABLE I

COLUMN RETENTION OF THE DIFLUOROANILIDE DERIVATIVES OF HAAs

Acid	Relative retention time ^a	
	DB-5	DB-17
MCAA	1.00	1.00
DCAA	1.19	1.16
TCAA	1.40	1.34
MBAA	1.26	1.32
DBAA	1.66	1.74
TBAA	2.13	2.28

^a Relative retention times were calculated on the basis of the retention time of the MCAA derivative on each column (15 m \times 0.53 mm I.D.).

TABLE II

STABILITY OF THE HAA DIFLUOROANILIDE DERIVATIVES

Percentage of the concentrations measured in a standard solution stored in darkness at 4°C.

Acid	Darkness ^a (48 h)	Fluorescent lamp ^a (24 h)	Sunlight ^c (3 h)
MCAA	105	104	91
DCAA	101	90	83
TCAA	97	82	68
MBAA	86	80	90
DBAA	93	69	54
TBAA	–	–	–

^a The derivatives were kept in darkness at 20°C for 48 h.

^b At 20°C under 2000 lx illumination provided by a white fluorescent lamp for 24 h.

^c Outdoors in direct sunlight for 3 h.

The other five HAA derivatives were stable in darkness at 20°C, but exposure to light diminished their peak area even at a constant temperature. When the analytical solution was allowed to stand for 1 day exposed to the light from a fluorescent lamp, most of the derivatives were reduced to 70–90% of the original concentrations. Exposure to direct sunlight reduced all the derivatives to 50–90% of the original concentrations after only 3 h.

The halogen atoms in HAAs appeared to affect the stability of the HAA derivatives. Acids with an increasing number of halogen atoms tended to form derivatives of lower stability. BAA derivatives were less stable than CAA derivatives in light. The analytical solution should be protected from light as much as practical and, if stored, it should be kept in a refrigerator.

Recovery experiments and tap water analysis

Six acids were added to lake and sea water samples at a concentration of 10 µg l⁻¹. The concentrations of these acids were then determined according to the procedures described above. In the analysis of sea water, the initial addition of sodium chloride to the sample water was omitted. Five HAAs showed recoveries of greater than 85% in both lake and sea water (Table III). Apparently inorganic salts other than sodium chloride in sea water exert hardly any influence on the derivatization reaction.

Drinking water was collected in winter in Nagano city at a water supply services tap. Residual chlorine in that sample was decomposed with sodium sulphite. DCAA and TCAA were detected in drinking water at concentrations of 4.5 and 7.5 µg l⁻¹, respectively (Fig. 3). MCAA was measured at 0.8 µg l⁻¹. However, no BAAs were detected.

TABLE III

RECOVERY OF HAAs FROM SPIKED NATURAL WATER

Lake water and sea water stored at 4°C were spiked with HAAs and analysed. (*n* = 3).

Acid	Concentration (µg l ⁻¹)	Lake water		Sea water		Monitored ion (<i>m/z</i>)
		Average recovery (%)	R.S.D. (%)	Average recovery (%)	R.S.D. (%)	
MCAA	10	95	1.5	97	4.1	129
DCAA	10	99	0.7	102	1.6	156
TCAA	10	96	1.9	103	2.5	156
MBAA	10	87	6.6	86	4.0	129
DBAA	10	104	1.8	92	1.5	156
TBAA	10	–	–	–	–	156

Laboratory chlorination experiments

The time course of CAA formation by chlorination was followed in river water from sampling sites A and B (Fig. 4). Immediately after sodium hypochlorite had been added to filtered river water, the CAA concentrations increased rapidly. The formation rate slowed after about 6 h. However, the concentrations of CAAs were still increasing even 1–2 days after chlorination. The two different river water samples showed similar time courses of CAA formation. The ratio of DCAA to TCAA was almost constant (*ca.* 1:2) and was independent of reaction time. This ratio (DCAA/TCAA) has been reported to be dependent on the chlorine-to-carbon ratio, that is, relatively large amounts of DCAA were formed in comparison with TCAA during chlorination under low chlorine-to-carbon ratio conditions [3]. For this experiment, the observed DCAA/TCAA ratio is consistent with a high chlorine-to-carbon ratio during chlorination.

The potential formation of HAAs in different river waters was compared by measuring the HAA concentrations after a given period following chlorination (Table IV). After 24 h, the residual chlorine concentrations were not less than 10% of the initial concentration (5 mg l^{-1}). CAA formation totalled $2.9\text{--}11 \text{ } \mu\text{g l}^{-1}$ for DCAA and $4.5\text{--}25 \text{ } \mu\text{g l}^{-1}$ for TCAA. MCAA formation was considerably less, below $1 \text{ } \mu\text{g l}^{-1}$. DBAA was undetected except for one river

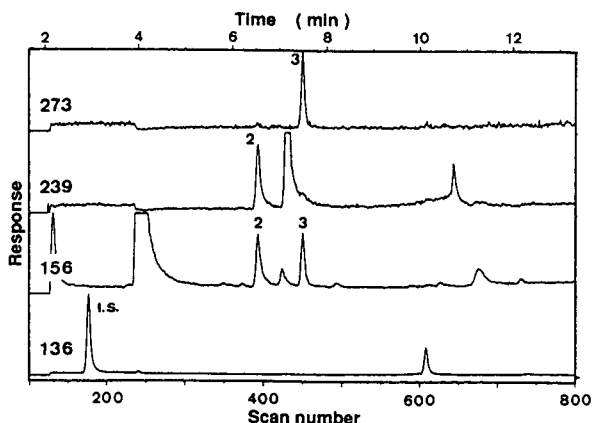


Fig. 3. SIM chromatogram for tap water. Peak numbers as in Fig. 2.

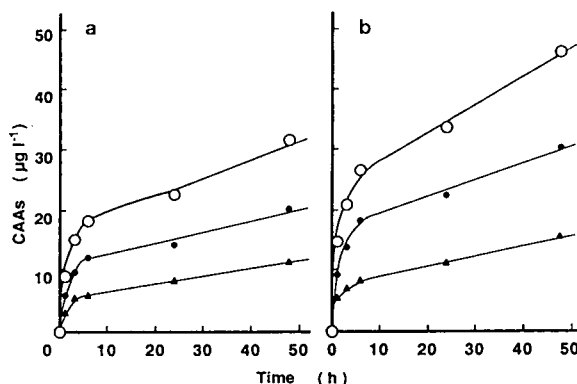


Fig. 4. Formation of CAAs as a function of reaction time from filtered river water samples collected at (a) site A and (b) site B. ● = TCAA; ▲ = DCAA; ○ = total CAAs. The pH values of the river samples were 7.3 and 7.4 at sites A and B, respectively. Reaction conditions: 10 mg l^{-1} chlorine dose; in darkness at 20°C . Residual free chlorine concentrations after treatment for 48 h were (a) 1.8 and (b) 2.8 mg l^{-1} .

water sample collected from site C2 (discussed below). In the rivers from which both upstream and downstream samples were collected, CAA formation tended to increase longitudinally downstream.

River water with high THM formation rates also had high HAA formation rates. There was a strong correlation between chloroform formation and total CAA formation (MCAA + DCAA + TCAA) represented by the equation [total CAAs] = $1.2[\text{chloroform}] - 1.1$ (units = $\mu\text{g l}^{-1}$, $r^2 = 0.949$; Fig. 5). The correlation between major components of total CAAs and chloroform was also high, *e.g.*, [TCAA] = $0.87[\text{chloroform}] - 2.4$ ($\mu\text{g l}^{-1}$, $r^2 = 0.936$) and [DCAA] = $0.31[\text{chloroform}] + 0.64$ ($\mu\text{g l}^{-1}$, $r^2 = 0.970$).

HAAs were not detected in the raw river water before treatment but were detected after treatment. Among BAAs, DBAA formation was found (at trace levels) only in the sample from station C2 (Fig. 6). Unlike all the other river samples, bromine-substituted THMs dominated total THM formation ($31 \text{ } \mu\text{g l}^{-1}$) at site C2. During water chlorination in the presence of bromide ions, chloroform formation is suppressed and there is a shift towards the forma-

TABLE IV
LABORATORY CHLORINATION OF RIVER WATER

Chlorination conditions: 5 mg l⁻¹ chlorine dose; in darkness at 20°C for 24 h.

Sampling station ^a	pH	Residual free chlorine (mg l ⁻¹)	HAAs (μg l ⁻¹)					THMs (μg l ⁻¹) ^b			
			MCAA	DCAA	TCAA	MBAA	DBAA	CHCl ₃	CHBrCl ₂	CHBr ₂ Cl	CHBr ₃
A	7.1	2.8	N.D. ^c	4.1	7.2	N.D.	N.D.	11	4.8	1.9	N.D.
B1	7.8	3.9	N.D.	9.6	24	N.D.	N.D.	30	4.0	0.4	N.D.
B2	8.4	3.3	N.D.	11	25	N.D.	N.D.	32	5.5	0.8	N.D.
C1	7.5	4.2	N.D.	2.9	4.5	N.D.	N.D.	8.8	5.7	3.3	N.D.
C2	7.4	2.4	0.7	3.3	6.5	N.D.	Trace	8.0	10	10	2.8
D	7.9	3.9	N.D.	8.2	21	N.D.	N.D.	25	6.8	1.4	N.D.
E1	8.9	3.2	0.9	5.6	7.7	N.D.	N.D.	17	7.5	3.4	N.D.
E2	8.1	0.6	0.7	7.0	14	N.D.	N.D.	17	8.6	3.9	N.D.

^a 1 and 2 indicate the upstream and downstream sampling stations in each river, respectively.

^b Detection limits of THMs: chloroform = 0.5 μg l⁻¹; bromodichloromethane = 0.1 μg l⁻¹; dibromochloromethane = 0.2 μg l⁻¹; bromoform = 1 μg l⁻¹.

^c N.D. = Not detected.

tion of brominated THMs [17–19]. Non-volatile brominated organic compounds are also produced under such conditions [20], and these might include BAAs. It can therefore be assumed that there was a comparatively high concentration of bromide ions in the river water

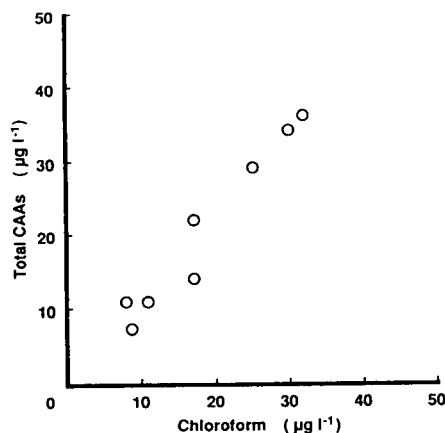


Fig. 5. Relationship between the formation of chloroform and total CAAs in filtered river water samples. Reaction conditions: 5 mg l⁻¹ chlorine dose; in darkness at 20°C for 24 h.

at site C2 before treatment. DBAA has been found to be the most prominent HAA in Dutch drinking waters prepared from surface waters [11].

In conclusion, the difluoroanilide derivatization method is applicable to BAAs. Five HAAs (except TBAA) were determined by GC–MS at the μg l⁻¹ level and good recoveries from natural waters were obtained in the recovery

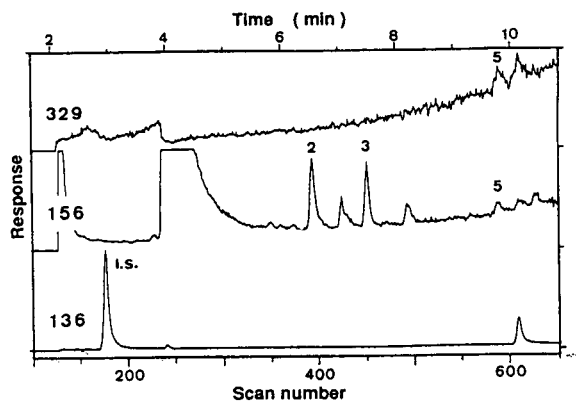


Fig. 6. SIM chromatogram obtained from the chlorinated surface water collected at site C2. Peak numbers as in Fig. 2.

experiments. The proposed method is useful for the simple determination of HAAs in water. However, the problem of the very high detection limit of TBAA remains to be solved.

ACKNOWLEDGEMENTS

The author is grateful to Professor A. Otsuki, Tokyo University of Fisheries, Dr. M. Kunugi, National Institute for Environmental Studies, and Dr. T. Tsukioka, Nagano Research Institute for Health and Pollution, for helpful advice. This study was partly supported by a Grant-in-Aid from the Nagano Prefectural Science Promotion Society.

REFERENCES

- 1 J.J. Rook, *Environ. Sci. Technol.*, 11 (1977) 478.
- 2 B.D. Quimby, M.F. Delaney, P.C. Uden and R.M. Barnes, *Anal. Chem.*, 52 (1980) 259.
- 3 J.W. Miller and P.C. Uden, *Environ. Sci. Technol.*, 17 (1983) 150.
- 4 R.F. Christman, D.L. Horwood, D.S. Millington, J.D. Johnson and A.A. Stevens, *Environ. Sci. Technol.*, 17 (1983) 625.
- 5 J.J. Rook, *Water Treat. Exam.*, 23 (1974) 234.
- 6 P.C. Uden and J.W. Miller, *J. Am. Water Works Assoc.*, 75 (1983) 524.
- 7 U. Lahl, B. Stachel, W. Schroer and B. Zeschmar, *Z. Wasser Abwasser Forsch.*, 17 (1984) 45.
- 8 D.L. Norwood, R.F. Christman, J.D. Johnson and J.R. Hass, *J. Am. Water Works Assoc.*, 78 (1986) 175.
- 9 E.E. Hargesheimer and T. Satchwill, *Aqua*, 38 (1989) 345.
- 10 S.W. Krasner, M.J. McGuire, J.G. Jacangelo, N.L. Patania, K.M. Reagan and E.M. Aieta, *J. Am. Water Works Assoc.*, 81 (1989) 41.
- 11 R.J.B. Peters, C. Erkelens, E.W.B. de Leer and L. de Galan, *Water Res.*, 25 (1991) 473.
- 12 K. Sugino, S. Nishi, R. Ohura and Y. Horimoto, *Suishitu Odaku Kenkyu*, 9 (1986) 87.
- 13 W.H. Glaze, *Environ. Sci. Technol.*, 25 (1991) 3.
- 14 H. Ozawa and T. Tsukioka, *Analyst*, 115 (1990) 1343.
- 15 *Testing Methods for Determination of Low Molecular Weight Halogenated Hydrocarbons in Industrial Water and Wastewater, Japanese Industrial Standard K 0125*, Japanese Standards Association, Tokyo, 1990, pp. 7–9.
- 16 *Standard Methods for the Examination of Water*, Japan Water Works Association, Tokyo, 1978, pp. 304–306.
- 17 J.J. Rook, A.A. Gras, B.G. van der Heijden and J.J. de Wee, *J. Environ. Sci. Health*, A13 (1978) 91.
- 18 T.V. Luong, C.J. Peters, and R. Perry, *Environ. Sci. Technol.*, 16 (1982) 473.
- 19 M.P. Italia and P.C. Uden, *J. Chromatogr.*, 605 (1992) 81.
- 20 J.M. Symons, P.L.K. Fu, R.C. Dressman and A.A. Stevens, *J. Am. Water Works Assoc.*, 79 (1987) 114.

Determination of furan-based amines in reaction mixtures by gas chromatography

Michael S. Holfinger[☆]

Department of Chemical Engineering, University of Wisconsin–Madison, 1415 Johnson Drive, Madison, WI 53706 (USA)

Anthony H. Conner

US Department of Agriculture–Forest Service, Forest Products Laboratory, 1 Gifford Pinchot Drive, Madison, WI 53705-2398 (USA)

Charles G. Hill, Jr.*

Department of Chemical Engineering, University of Wisconsin–Madison, 1415 Johnson Drive, Madison, WI 53706 (USA)

(Received March 4th, 1993)

ABSTRACT

A protocol which employs a methyl silicone gum capillary column for gas chromatographic analysis of the products of the acid-catalyzed reaction of furfurylamine with aldehydes is presented, and its efficacy is demonstrated.

INTRODUCTION

The synthesis of difurfuryl diamines (Fig. 1) via amido derivatives of furfurylamine has recently been reported [1]. Difurfuryl diamines are excellent curing agents for epoxy resins [2]. In addition, they are readily converted to the corresponding diisocyanates, which can be utilized in

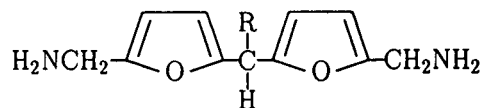


Fig. 1. Difurfuryl diamines.

the preparation of polyurethanes [3,4] and adhesive resins [5]. These compounds are of particular interest to the composite wood products industry because they can be derived from renewable resources (biomass), rather than petroleum.

The condensation reaction of furfurylamine with an aldehyde in the presence of hydrochloric acid offers a simpler route to difurfuryl diamines [6] than that previously reported [1]. Design and optimization of reactors for carrying out this reaction on a commercial scale necessitate the development of mathematical models which describe how reaction rates depend on temperature and on reactant and catalyst concentrations. To obtain the data on which such models are based, one requires a method for measuring the concentrations of amino species in sample aliquots from a reaction mixture. Although products of the

* Corresponding author.

[☆] Present address: The Upjohn Company, 7000 Portage Road, Kalamazoo, MI 49001, USA.

industrially important aniline–formaldehyde condensation reaction have been analyzed by TLC, HPLC, GC and gel permeation chromatography [7–9], chromatographic methods suitable for the analysis of the analogous reaction products of furfurylamine have not been previously reported in the literature. The purpose of this investigation was to develop a simple, reliable method for the analysis of mixtures of furfurylamino compounds by capillary column GC. The utility of the method that was developed is illustrated for the reaction of furfurylamine with formaldehyde to give 5,5'-methylene difurfurylamine via the intermediate 5-hydroxymethyl furfurylamine.

EXPERIMENTAL

Synthesis of standards

A pure sample of 5,5'-methylene difurfurylamine (Fig. 1; R = H) was prepared from furfurylamine (QO Chemicals; Memphis, TN, USA) by the method described in the literature [1]. 5-Hydroxymethyl furfurylamine was prepared by the reaction at 30°C in 6 M hydrochloric acid (Baker, Phillipsburg, NJ, USA) of 8.0 g of furfurylamine with 7.1 g of 35% (w/w) formaldehyde solution (Fisher, Fairlawn, NJ, USA). After 15 min, the reaction mixture was quenched with 104 ml of 6 M sodium hydroxide and 14.3 g of hydroxylamine hydrochloride. The mixture was then extracted with three 150-ml portions of chloroform. Crude 5-hydroxymethyl furfurylamine (2 g) was recovered from the second and third extracts. The crude compound was purified by vacuum distillation. A pure sample of furfurylamine (Aldrich, Milwaukee, WI, USA) was prepared by vacuum distillation. The identity and purity of all standards were verified by HPLC, by ^1H NMR, ^{13}C NMR and IR spectroscopies, and by GC–mass spectrometry.

Preparation of standard solutions

A series of 10 standard solutions was employed for the determination of relative response factors for furfurylamine, 5,5'-methylene difurfurylamine and 5-hydroxymethyl furfurylamine. The standard solutions were prepared by careful dilution of a chloroform stock solution of the compounds of interest in volumetric flasks con-

taining pre-weighed quantities of the internal standard (methyl stearate). Solute concentrations ranged from 0.20–20 mg/ml. The approximate concentration of the internal standard in all standard solutions was 2 mg/ml. If stored in a freezer, the standard solutions were stable for several months.

Instrumentation

Instrumentation consisted of a Hewlett-Packard Model 5890A gas chromatograph equipped with flame ionization detection (FID) and a Model 7670 automatic sample injector. Peak areas were measured with a Hewlett-Packard Model 3387 electronic integrator.

Column and conditions

An HP-1 (Hewlett-Packard) wide-bore capillary column (5 m \times 0.53 mm I.D., 2.65 μm film thickness) was employed for separations. The flow-rate of carrier gas (helium) was 17 ml/min, and the split ratio was approximately 9:1. No make-up gas was used. The initial column temperature was 40°C. After 1.5 min, the column temperature was increased to 200°C at a programmed rate of 30°C/min. A column temperature of 200°C was maintained for the remainder of the analysis. An injection volume of 1 μl was employed in all experiments. Samples were analyzed in triplicate.

Sample preparation and analysis

A 1-ml sample from the reaction mixture of furfurylamine and formaldehyde in hydrochloric acid was pipetted directly into a quench solution containing a slight stoichiometric excess of 6 M sodium hydroxide and 0.20 g of hydroxylamine hydrochloride. Then, the resultant mixture was extracted with chloroform (4 \times 3 ml). The extracts were combined with a known amount of internal standard. A sample of the resultant solution was injected into the gas chromatograph.

Recovery studies

The recovery of the chloroform extraction procedure was examined for the reaction of furfurylamine with formaldehyde. A 1-ml aliquot from a reaction of furfurylamine and formal-

dehyde in 6 M HCl at 30°C was withdrawn after 30 min. The sample was neutralized with 6 M NaOH and quenched with hydroxylamine hydrochloride. Then, the sample was extracted with chloroform (3 × 4 ml) by the standard procedure, but without combination of these extracts. A known amount of internal standard was added to each extract, and each was analyzed by gas chromatography.

Accuracy studies

To examine the accuracy of the method, six representative samples were prepared by mixing various amounts of the furfurylamine, 5-hydroxymethyl furfurylamine, and 5,5'-methylene difurfurylamine standards. The concentrations of furfurylamine (reactant) and 5,5'-methylene difurfurylamine (product) increased in reverse order in this set of samples, as would be expected for samples from an actual kinetics experiment. Each sample was diluted with 2.85 ml of a "reaction matrix" consisting of 6 M hydrochloric acid (8 ml), 6 M NaOH (12.4 ml), 34.7% (w/w) formaldehyde (0.47 ml), and hydroxylamine hydrochloride (1.52 g). Samples were worked up and analyzed by the standard procedure.

RESULTS AND DISCUSSION

The results obtained indicate that the products from the reaction of furfurylamine with aldehydes can be determined by a GC-FID method. A gas chromatogram obtained by the procedure utilized is depicted in Fig. 2. The chromatogram in Fig. 2 corresponds to a sample from the acid-catalyzed reaction of furfurylamine with formaldehyde. Chromatographic peaks for furfurylamine (reactant), 5-hydroxymethyl furfurylamine (intermediate) and 5,5'-methylene difurfurylamine (product) are well separated from one another and from peaks associated with the solvent and internal standard.

Data from the recovery studies are summarized in Table I. These data indicate that both furfurylamine and 5,5'-methylene difurfurylamine are quantitatively recovered from the aqueous reaction mixture by the standard extraction procedure. By contrast, the recovery of

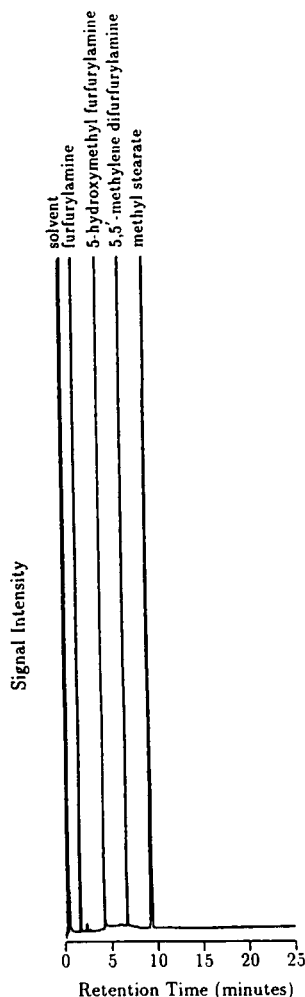


Fig. 2. Typical chromatogram for mixtures of furfurylamine, 5-hydroxymethyl furfurylamine, 5,5'-methylene difurfurylamine and the internal standard (methyl stearate).

5-hydroxymethyl furfurylamine was much less than 100%. Favorable interactions of the primary hydroxyl of 5-hydroxymethyl furfurylamine with the aqueous reaction matrix are believed to be primarily responsible for its preferential distribution into the aqueous phase.

Plots of measured vs. actual amounts of compounds based on data from the accuracy studies are depicted in Fig. 3. For both furfurylamine and 5,5'-methylene difurfurylamine, there is excellent agreement between measured and actual values, as indicated by the proximity of the data points to the line $y = x$ (see Fig. 3). The

TABLE I

ANALYSIS VIA GAS CHROMATOGRAPHY OF SUCCESSIVE CHLOROFORM EXTRACTS (3 ml) FROM A REACTION MIXTURE (1 ml) OF FURFURYLAMINE AND FORMALDEHYDE

Extract No.	Chromatographic peak area			
	Furfurylamine	5-Hydroxymethyl furfurylamine	5,5'-Methylene difurfurylamine	Internal standard
1	3 484 714	453 783	1 493 609	517 749
2	245 836	265 413	88 303	519 497
3	—	200 655	—	507 600
4	—	137 109	—	506 137

agreement between actual and measured amounts establishes the accuracy of the method for the analysis of these compounds. Due to incomplete recovery of 5-hydroxymethyl furfurylamine by the chloroform extraction procedure, the data for this compound fall close to the line $y = 0.68x$ (see Fig. 3). The slope of this line represents the overall recovery (68%) of 5-hydroxymethyl furfurylamine by the extraction procedure. In kinetics experiments, this value was employed for correction of the concentration data for this compound.

For analysis of amino compounds, derivatization is often employed to minimize the strong interactions of this functionality with surface sites in the GC column [10]. In initial work, both Schiff base (acetone) [11] and silyl ether [bis-

(trimethylsilyl)acetamide (BSA), Pierce, Rockford, IL, USA] [12] derivatives were evaluated. The Schiff base derivatives could not be formed quantitatively, whereas chromatographic peaks arising from the BSA derivatizing agent interfered with the determination of furfurylamine. Consequently, derivatization of the amino group is not employed in the present method.

The chromatographic method described above was used to determine concentration vs. time profiles for the reaction conditions of interest (see Fig. 4). These representative data are for reaction of furfurylamine and formaldehyde in 4.5 M hydrochloric acid at 50°C. The lack of appreciable scatter in the data, especially at long reaction times where the concentrations of the various species are approaching their asymptotic

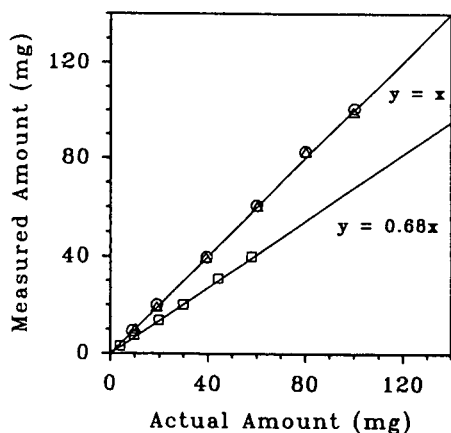


Fig. 3. Plots of measured vs. actual amounts of (○) furfurylamine, (△) 5,5'-methylene difurfurylamine and (□) 5-hydroxymethyl furfurylamine.

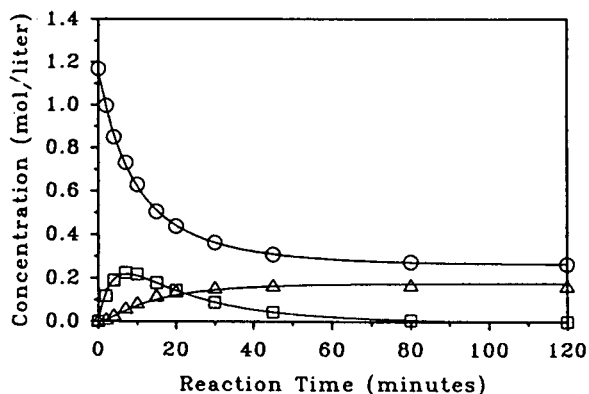


Fig. 4. Concentration profiles determined by gas chromatography for the reaction of furfurylamine and formaldehyde in 4.5 M HCl at 50°C. ○ = Furfurylamine; △ = 5,5'-methylene difurfurylamine; □ = 5-hydroxymethyl furfurylamine.

values is indicative of the good precision of the method.

CONCLUSIONS

A GC–FID method for the determination of products of the acid-catalyzed reaction of furfurylamine with aldehydes has been developed and demonstrated. The method involves the chloroform extraction of the compounds of interest from reaction mixtures followed by analysis on a methyl silicone gum (HP-1) capillary column. The method uses an internal standard (methyl stearate) for quantitation.

ACKNOWLEDGEMENTS

This article is based upon work supported under a National Science Foundation Graduate Fellowship. Additional financial support was provided by QO Chemicals Inc., Eureka Trading Ltd., and the USDA Forest Service Cost Share Program.

REFERENCES

1 J.L. Cawse, J.L. Stanford and R.H. Still, *Makromol. Chem.*, 185 (1984) 697.

- 2 X. He, A.H. Conner and J.A. Koutsky, *J. Polym. Sci., Polym. Chem. Ed.*, 30 (1992) 533.
- 3 J.L. Cawse, J.L. Stanford and R.H. Still, *Makromol. Chem.*, 185 (1984) 709.
- 4 J.L. Stanford, R.H. Still, J.L. Cawse and M.J. Donnelly, in R.W. Hemingway and A.H. Conner (Editors), *Adhesives from Renewable Resources*, American Chemical Society, Washington, DC, 1989, Ch. 30, p. 424.
- 5 M.S. Holfinger, A.H. Conner, L.F. Lorenz and C.G. Hill, Jr., in A.H. Conner, A.W. Christiansen, G.E. Myers, B.H. River, C.B. Vick and H.N. Spelter (Editors), *Wood Adhesives 1990*, Forest Products Research Society, Madison, WI, 1991, p. 61.
- 6 M.S. Holfinger, A.H. Conner and C.G. Hill, Jr., in preparation.
- 7 D.J. Francis, T.K. Radhakrishnan and M.R.G. Nayar, *J. Chromatogr.*, 103 (1975) 372.
- 8 M.R.G. Nayar and J.D. Francis, *Makromol. Chem.*, 179 (1978) 1783.
- 9 P. Falke, R. Tenner and H. Knopp, *J. Prakt. Chem.*, 328 (1986) 142.
- 10 M.W. Scoggins, L. Skurcenski and D.S. Weinberg, *J. Chromatogr. Sci.*, 10 (1972) 678.
- 11 W.J.A. Vanden Heuvel, W.L. Gardiner and E.C. Horning, *Anal. Chem.*, 36 (1964) 1550.
- 12 J.F. Klebe, H. Finkbeiner and D.M. White, *J. Am. Chem. Soc.*, 88 (1966) 3390.

Determination of ionic species formed during growth of *Escherichia coli* by capillary isotachopheresis

K. Futschik, M. Ammann and S. Bachmayer

Institute of Fundamentals and Theory of Electrotechnics, Bioelectricity and Magnetism Division, University of Technology, Gusshausstrasse 27, A-1040 Vienna (Austria)

E. Kenndler*

Institute of Analytical Chemistry, University of Vienna, Währingerstrasse 38, A-1090 Vienna (Austria)

(First received February 17th, 1993; revised manuscript received April 21st, 1993)

ABSTRACT

The ionic species that are formed during the microbial growth of *Escherichia coli* were determined by capillary isotachopheresis as a function of the time of cultivation. This formation was indicated by the change in a sum parameter, the impedance of the nutrient broth, measured by a special electrode system. Based on the determination of the individual ions formed under the given conditions (identified as acetate, lactate, α -ketoglutarate, fumarate, ammonium and probably a simple amine), the change in conductivity was calculated and compared with that obtained by the impedance measurement of the bulk medium. From the results it can be concluded that the change in the sum parameter as a function of time is originated by the ions determined.

INTRODUCTION

Examinations of bacterial contamination are routine procedures in the fields of food hygiene, cosmetics, pharmaceuticals and medicine. However, also in fields in which microorganisms are used for production processes, in biotechnology, methods of bacterial examination are of high relevance. As conventionally used standard methods are very time consuming, the development of automatic methods is of general interest. The so-called impedance method is one of these. With this method, microbial metabolic processes that produce electrically measurable changes in the nutrient broth are used to detect bacteria. There, nutrients are converted by the metabolism into smaller, charged components, which contribute additionally to the transport of cur-

rent. As a consequence, the electrical impedance of the nutrient medium will decrease.

At the Institute of Fundamentals and Theory of Electrotechnics a measuring system was developed, based on the so-called Impedance-splitting method (IS method [1]), which allows the separation of the impedance of the nutrient medium, Z_M , and that of the electrode system, Z_E . The latter is caused by ionic layers in the vicinity of the electrodes. Thus, two separate parameters are available for the determination and characterization of microbial growth. Which of them is used for routine examination, Z_M , Z_E or both, depends on the application and is discussed elsewhere [2–4].

A comparison of the registered time courses of the changes in Z_M and Z_E during microbial growth showed that both similar and contradictory time courses are observed. Large changes in Z_E with negligible changes in Z_M also occurred. To understand and interpret these different

* Corresponding author.

effects, it is necessary to know which nutrients are converted by the metabolism into which ionic substances.

Several metabolic pathways for the conversion of the different nutrients such as glucose, proteins, peptides, amino acids and lipids are possible. In addition, the bacteria are able to change the pathways during the growth depending on, e.g., the oxygen content or the composition of the nutrient broth. It is therefore virtually impossible to predict the amount and also sometimes the species of the secreted molecules. As a consequence, chemical analysis is necessary to solve first the question of which molecules contribute most to the changes in the electrical conductivity, κ , and second to provide a basis for investigations on the more difficult questions of what happens near the surface of the measuring electrodes and what causes the changes in Z_E .

The aim of this work was to solve the first question for the bacterium *Escherichia coli*, which was chosen because it is a very common and well known species. After identification and determination of at least the main components, that are formed in the nutrient broth by the metabolism, attempts were made to calculate the contributions to κ of the different ions, their sum being compared with the changes in Z_M recorded by the IS method.

It can be expected that the ionogenic components formed during such metabolism are relatively simple organic acids and bases. These have been described in general for the different metabolic pathways in the biochemical literature [5–7] and are summarized in Table I, but the individual species formed under the conditions applied in this investigation cannot be predicted in detail. Therefore, the analysis of the cultivation media must focus on the determination of such ionic species.

This attempt was carried out by capillary isotachopheresis (ITP) with conductivity detection, which has been favourably applied to the investigation of other aspects of bacterial metabolism [8–12]. This method combines separation by electromigration (based on effective mobilities, u_{eff}) with the principle of electrical conductivity detection (which is based on the same analyte property). In contrast to capillary

TABLE I

ANIONIC SUBSTANCES THAT MAY OCCUR IN THE NUTRIENT BROTH DURING THE GROWTH OF *E. COLI*, FORMED BY THE DIFFERENT METABOLIC PATHWAYS OR BY CELL LYSIS [5–7]

Monobasic	Dibasic	Tribasic
Formate	Oxalate	Citrate
Acetate	Fumarate	Phosphate
Propionate	Malate	
Butyrate	Tartrate	
Lactate	Malonate	
	α -Ketoglutarate	
	Adipate	
	Glutarate	

zone electrophoresis, this combination is favourable owing to the concentration adjustment in ITP, leading to relatively high concentrations of the sample components after separation, which are detected without the presence of a background electrolyte. Because this method is applied in a closed system without electroosmotic flow (EOF), the overall migration properties of the analytes, which are used for identification, are insensitive to wall adsorption effects compared with electrophoresis carried out in the presence of EOF (e.g., micellar electrokinetic chromatography or zone electrophoresis with EOF). This is a decisive advantage especially when the samples contain complex matrices at high concentration and are injected directly, without further pretreatment.

ITP can also be favourably applied in some instances rather than ion chromatography because, in contrast to the latter method, no stationary phase is present here to be contaminated and thus modified by the matrix. Solvent gradients for the elution of higher charged analytes are also unnecessary.

EXPERIMENTAL

Chemicals

The following chemicals were used for the preparation of the buffers: hydrochloric acid, butyric acid, acetic acid, morpholinoethane sul-

phonic acid (MES), β -alanine, tris(hydroxymethyl)aminomethane (Tris) and potassium hydroxide. All chemicals were of analytical-reagent grade (Merck, Darmstadt, Germany).

As nutrient broth for the bacteria, a mixture with the following common composition [13–16] was used (without sodium chloride): peptone from meat (tryptically digested, 7.8 g/l), peptone from casein (tryptically digested, 7.8 g/l), D-(+)-glucose monohydrate (1.0 g/l) and yeast extract (2.8 g/l).

In order to suppress electroosmosis, hydroxyethylcellulose (HEC) (Fluka, Buchs, Switzerland) was added to the leading electrolyte buffer solution. Water used for the preparation of the buffers was doubly distilled from a quartz apparatus.

Apparatus

For the measurement of the impedances, the BacTrac 4100 system (SY-LAB, Vienna, Austria), based on the impedance-splitting method, was used. It consists of an incubation block which allows temperature control from 4 to 65°C. The sample cells were made from glass (10 ml content) and were equipped with four stainless-steel electrodes for impedance measurement. A microprocessor-controlled electronic recorder registered data for the simultaneous determination of Z_M and Z_E on up to 40 sample cells. A personal computer was used to supervise up to six incubation blocks and showed on the screen the time courses of the relative decreases $-\Delta Z_M$ and $-\Delta Z_E$ (as a percentage) of the absolute values of Z_M and Z_E , respectively.

The concentration of bacteria (colony-forming units per ml; cfu/ml) was determined by the standard plate count method.

The pH of the nutrient broth was measured with a combined glass-calomel electrode (Portamess 654; Knick, Berlin, Germany) and absolute values of κ were additionally determined with a conductimeter (CG858; Schott, Hofheim, Germany).

Isotachophoretic measurements were carried out with a Trace 1 instrument (United Research, Vienna, Austria) equipped with a conductivity and a UV detector (at 254 nm) on-line. The separation capillary (20 cm \times 200 μ m I.D.) was made from a mixed polymer of polyethylene and polypropylene. Separation was carried out at a constant current of 50 μ A. The injector was made of ceramic and had a constant volume of 0.20 μ l. The control of the instrument and the data acquisition were done with a personal computer.

Procedure

The sample cells were filled with the described nutrient broth and inoculated with *E. coli* from an overnight culture, so that the initial bacterial concentration was about 10^6 cfu/ml. At the start and at 1-h intervals samples of the bacterial suspension were taken. One part of each sample was used for the determination of the number of bacteria (cfu/ml) and the other part was immediately sterilized by using a membrane filter technique (Minisart Plus, 0.2 μ m; Sartorius, Göttingen, Germany) to stop growth and metabolic activity. From this part the pH value, the absolute values of κ and the kind and concentration of the ions were determined, the latter by ITP (for the buffering electrolyte systems, see Table II).

TABLE II
BUFFERING ELECTROLYTE SYSTEMS USED FOR THE ISOTACHOPHORETIC MEASUREMENTS

System	Leading ion	Concentration (mol/l)	Counter ion	pH	HEC added (% w/w)	Terminating ion	Concentration (mol/l)	Counter ion	pH	Additive
Anionic, pH 7.5	Cl ⁻	0.01	Tris	7.5	0.05	MES	0.01	Tris	6.0	None
Anionic, pH 3.5	Cl ⁻	0.01	β -Alanine	3.5	0.05	Butyrate	0.01	β -Alanine	4.0	None
Cationic	K ⁺	0.01	Acetate	5.4	0.05	Tris	0.01	Acetate	5.0	None

RESULTS AND DISCUSSION

Identification of the ions formed by the metabolism of E. coli

In Figs. 1 and 2, typical isotachopherograms obtained from the nutrient broth at the beginning and end of the incubation time after 8 h are shown for the anionic and cationic modes. It can be seen that at the start of the growth a number of steps can be observed for the anions, but only

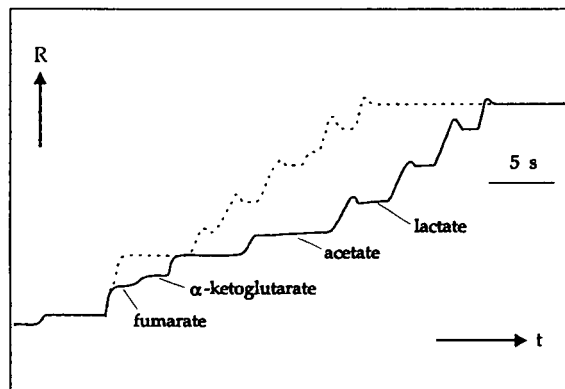


Fig. 1. Isotachopherograms of anions of the nutrient medium of *E. coli* at the beginning of the incubation period (dotted line) and after 8 h of growth (solid line). The electropherograms were measured at pH 7.5 of the leading electrolyte with a conductivity detector. The humps occurring at the front of the upper four zones are caused by substances migrating in the "enforced" mode. For conditions, see Experimental. R = Electrical resistance; t = time.

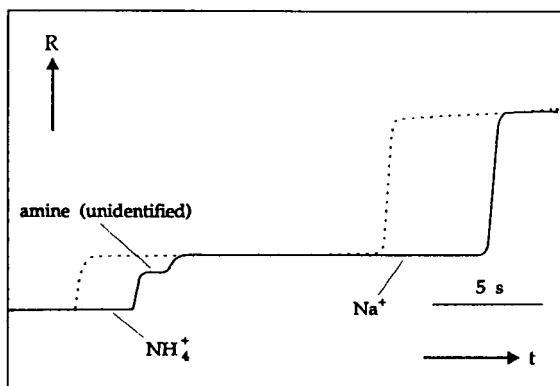


Fig. 2. Isotachopherograms of cations of the nutrient medium of *E. coli* at the beginning of the incubation period (dotted line) and after 8 h of growth (solid line). The electropherograms were measured at pH 5.4 of the leading electrolyte with a conductivity detector. R = Electrical resistance; t = time.

one step between the leading and terminating electrolytes occurs in the cationic mode. The occurrence of such steps is obvious, because the nutrient medium (see *Chemicals*) contains a variety of different ionic substances that may appear in the mobility region under consideration.

Identification of the components was attempted by comparison of the step heights of the zones in the isotachopherogram of the samples with those obtained from (pure) reference compounds according to Table I. The measured step heights were not used for a final identification, however, but they allowed a preselection of the analytes. Based on this selection, a closer identification was carried out by adding the corresponding reference ions to the samples.

It can be seen from Fig. 2 that prior to the incubation only one long zone for cations was observed, which was identified as sodium. This is surprising because, in contrast to the common recipes [13–16], no sodium chloride was added to the nutrient broth. The result of the isotachophoretic measurement was, however, confirmed by atomic emission spectrometry.

After the 8-h incubation period, a second zone occurred in the mobility range between sodium and potassium, the leading ion. As this ion has no UV absorbance at 254 nm (the wavelength of the detector), it must be a simple organic cation, probably an amine, but no further information about the nature of this substance was found in the literature. The formation of another cation can also be observed indirectly from the isotachopherogram, because the time of appearance of the first ion after the leading ion was shifted with high reproducibility to higher values for the samples taken after 8 h, compared with the initial solution. This must be the result of the migration of a (non-UV-absorbing) cation formed, which has about the same ionic mobility as potassium. This is most plausibly ammonium, which can be indirectly determined in this way. This assumption was supported by the expected increase in the length of the leading zone when NH_4^+ standard was added to the samples before injection.

It can be seen from Fig. 1 that after 8 h of cultivation the lengths of four zones of anions

increase remarkable. An approach to the identification of the ionic components of this solution will thus focus on these zones. According to the anions that can be expected (given in Table I), identification was carried out at two different pH values of the leading electrolyte, namely 3.5 (not shown) and 7.5. It was found that the same number of anions in about the same amount was observed in the isotachopherograms at both pH values. This result allows the conclusion that the substances detected are not amino acids, because these compounds would not migrate as anions at pH 3.5 owing to their zwitterionic character.

In both anionic electrolyte systems the relative step heights (with respect to acetate) were determined for the anions listed in Table I and were compared with the step heights of those zones which increased with incubation time. For final identification reference components were added to the samples, as already mentioned.

The results of this procedure allowed the identification of the compounds formed as fumarate, α -ketoglutarate, acetate and lactate. The most pronounced increase in zone length was observed for acetate and lactate.

Quantification

The determination of those components which showed an increase in concentration in the

nutrient broth during the growth of *E. coli* was carried out in the usual way using calibration graphs obtained from the solutions of the different pure reference compounds. These graphs relate the zone length in the isotachopherogram to the concentration of the analyte. Based on these graphs, the increase in concentration was determined over an 8-h period by taking samples at 1-h intervals as described under *Procedure*. The results of the measurements of the concentrations are given in Table III. The change within the first 3 h was too small for the anions to allow quantification. The maximum increase in the concentrations for both anions and cations is *ca.* 10^{-3} mol/l. It can be seen from Figs. 1 and 2 and Table III that the sum of the increase in concentration, Δc , relative to the initial concentration of ionic components at the beginning of growth ($t = 0$) is about 25%. The precision of the measurements (expressed by the relative standard deviation) was very high for subsequent injections, namely in the range of a few tenths of percent. The long-term precision was more than one order of magnitude lower (5–7%).

It can also be seen from Table III that the sum of the increase in cations is higher than that for anions. This is obvious because the different species stem from different metabolic pathways. Electroneutrality is established, however, as the

TABLE III

INCREASE IN CONCENTRATION, Δc , OF DIFFERENT IONIC COMPONENTS FORMED DURING AN 8-h CULTIVATION OF *E. coli* DETERMINED BY ITP

Time (h)	Δc (mol/l)					
	Cations		Anions			
	Ammonium	Unidentified amine	Fumarate	α -Ketoglutarate	Acetate	Lactate
0	0	0	0	0	0	0
1	$3.3 \cdot 10^{-4}$	— ^a	—	—	—	—
2	$5.2 \cdot 10^{-4}$	—	—	—	—	—
3	$8.8 \cdot 10^{-4}$	—	—	—	—	—
4	$2.4 \cdot 10^{-3}$	—	$1.7 \cdot 10^{-4}$	$2.4 \cdot 10^{-4}$	$1.0 \cdot 10^{-3}$	—
5	$2.9 \cdot 10^{-3}$	—	$7.0 \cdot 10^{-4}$	$9.6 \cdot 10^{-4}$	$2.8 \cdot 10^{-3}$	—
6	$3.2 \cdot 10^{-3}$	—	$1.1 \cdot 10^{-3}$	$1.3 \cdot 10^{-3}$	$5.3 \cdot 10^{-3}$	$3.6 \cdot 10^{-4}$
7	$3.2 \cdot 10^{-3}$	$8.4 \cdot 10^{-4}$	$1.3 \cdot 10^{-3}$	$2.1 \cdot 10^{-3}$	$6.5 \cdot 10^{-3}$	$1.1 \cdot 10^{-3}$
8	$3.7 \cdot 10^{-3}$	$1.7 \cdot 10^{-3}$	$1.3 \cdot 10^{-3}$	$2.2 \cdot 10^{-3}$	$7.8 \cdot 10^{-3}$	$1.5 \cdot 10^{-3}$

^a Dashes indicate concentrations too low to be determined.

free amines and acids released undergo protolysis reactions with the various buffering components in the broth (proteins, peptides, etc.).

Comparison of the measured and calculated conductivity changes

From the results of the ITP measurements given above, the corresponding changes in the conductivity, κ , can be calculated, based on the increase in concentration, c_i , as given in Table III, and the effective mobility, u_{ieff} , of the components of interest, i , at the pH of the nutrient broth, by $\kappa = \sum F c_i u_{ieff}$, F being the Faraday constant.

The time dependence of the pH of the nutrient medium is shown in Fig. 3: the pH remains constant at the first 3 h, but then decreases steeply from the initial value of 6.8 by more than one unit to 5.6 after 8 h, indicating the formation of acidic constituents.

A similar shape is observed for the dependence of the number of organisms as a function of time, as shown in Fig. 3: after an initial time

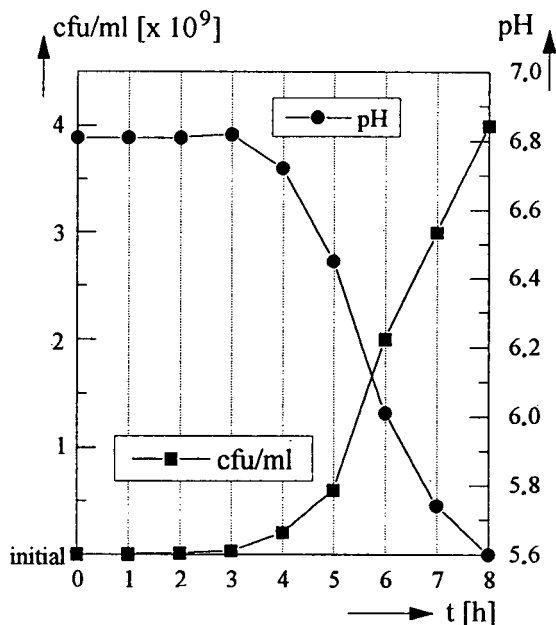


Fig. 3. Change in pH of the nutrient medium (●) and increase in the number (cfu/ml) of *E. coli* bacteria (initial concentration ca. 10^6 cfu/ml) (■) as a function of the time (t) of cultivation.

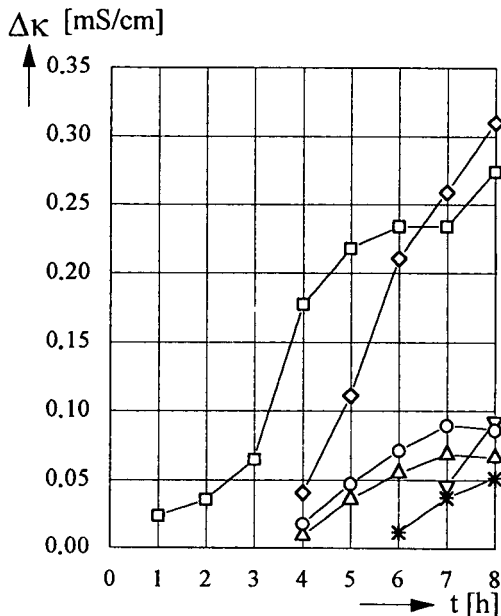


Fig. 4. Calculated increase in conductivity ($\Delta\kappa$) due to the formation of the individual ionic compounds during the cultivation of *E. coli*, based on the results of the isotachophoretic measurements. □ = Ammonium; ▽ = unidentified cation (plausibly a simple amine); ◇ = acetate; △ = fumarate; ○ = α -ketoglutarate; * = lactate. t = Time.

of about 3 h (where the number increases, however, by 2.5 orders of magnitude, a fact that is not visible from the bilinear plot in Fig. 3), a steep increase can be seen simultaneously with the decrease in pH.

TABLE IV

CHANGES IN CONDUCTIVITY, $\Delta\kappa$, OF THE NUTRIENT BROTH DURING THE BACTERIAL GROWTH AS CALCULATED FROM THE ITP RESULTS AND MEASURED WITH A CONDUCTIMETER

Time (h)	$\Delta\kappa$ (mS/cm)	
	Calculated	Measured
0	0	0
1	0.02	0.05
2	0.04	0.06
3	0.07	0.12
4	0.25	0.26
5	0.41	0.38
6	0.58	0.54
7	0.69	0.74
8	0.79	0.79

The result of the calculation of κ , which is based on the increase in the isotachophoretic zone lengths with time, considering the change in the pH of the nutrient broth, is shown for the different components in Fig. 4. It can be seen that in agreement with the pH and the cfu/ml versus time courses, $\Delta\kappa$ remains nearly zero during the first 3 h and then increases steeply, the most dominant increases stemming from acetate on the anionic side and from NH_4^+ at the cationic side, which finally contribute about 0.3 mS/cm each, compared with the initial conditions.

The values obtained for the calculated changes in κ by summing the individual contributions of the ions and the changes in κ obtained by conductimetric measurements are given in Table IV. The values exhibit a high linear correlation ($r = 0.996$).

For a comparison with the relative decrease $-\Delta Z_M$ (as percentage), measured by the impedance-splitting method, the relative decrease in the specific resistance was calculated for the two conductivities shown in Table IV. The results

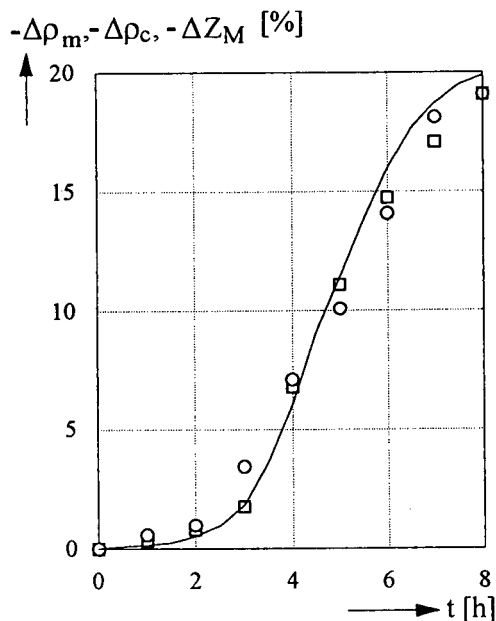


Fig. 5. Relative decreases in the measured and calculated specific resistances (○ = $-\Delta\rho_m$ and □ = $-\Delta\rho_c$, respectively) and the decrease $-\Delta Z_M$ of the impedance of the medium (solid line) as a function of time (t) of cultivation.

are shown in Fig. 5 and agree over the entire time period to within about 10%, which can be considered as an excellent correlation. From these findings it can be concluded that those species formed during the bacterial growth which are determined by ITP are in fact identical with those which cause the change $-\Delta Z_M$ during the incubation period. The change $-\Delta Z_M$ as a bulk property can indeed be interpreted by the changes in the concentration of the individual ions determined.

REFERENCES

- 1 K. Futschik, H. Pfützner, A. Doblender and H. Asperger, *Abstr. Int. Meet. Chem. Eng. Biotechnol., Achema* 88, 1988.
- 2 P. Pless, K. Futschik and E. Schopf, *J. Food Protect.*, in press.
- 3 B. Url, in *Proceedings, 32. Arbeitstagung des Arbeitsgebietes "Lebensmittelhygiene"*, Deutsche Veterinärmedizinische Gesellschaft, 1991, p. 313.
- 4 P. Pless, in *Proceedings of the 3rd World Congress on Foodborne Infections and Intoxications*, Federal Health Office, Berlin, 1992, p. 1194.
- 5 G. Gottschalk, *Bacterial Metabolism*, Springer, New York, Berlin, Heidelberg, Tokyo, 1985.
- 6 R.Y. Stanier, E.A. Adelberg and J.L. Ingraham, *General Microbiology*, Macmillan Press, Bristol, 4th ed., 1976.
- 7 B.D. Davis, R. Dulbeco, H.N. Eisen and H. Ginsberg, *Microbiology*, Harper International, Philadelphia, 3rd ed., 1980.
- 8 P. Boček, M. Deml and J. Janák, *J. Chromatogr.*, 106 (1975) 283.
- 9 P. Boček, K. Lekova, M. Deml and J. Janák, *J. Chromatogr.*, 117 (1976) 97.
- 10 J.S. van der Hoeven, H.C.M. Franken, P.J.M. Camp and C.W. Dellebarre, *Appl. Environ. Microbiol.*, 35 (1978) 17.
- 11 J.S. van der Hoeven and H.C.M. Franken, in A. Adam and C. Schots (Editors), *Biochemical and Biological Applications of Isotachophoresis — Proceedings of the First International Symposium, Baconfooy, May 4–5, 1979*, Elsevier, Amsterdam, 1980, p. 69.
- 12 P. Boček, S. Pavelka, K. Grigelová, M. Deml and J. Janák, *J. Chromatogr.*, 154 (1978) 356.
- 13 *Dehydrated Culture Media and Reagents for Microbiology, Manual*, Difco, Detroit, MI, 1984.
- 14 *Handbuch der "OXOID", Erzeugnisse für Mikrobiologische Zwecke*, OXOID Deutschland, Wesel, 1983.
- 15 *Präparate für die Mikrobiologie, Handbuch Nährböden*, Merck, Merck, Darmstadt, 1980.
- 16 *Proceedings of the 4th International Symposium on Quality Assurance and Quality Control of Microbiological Culture Media, Manchester, 1986; Int. J. Food Microbiol.*, 5 (1987) 195.

Short Communication

High-performance liquid chromatographic separation of fullerenes (C_{60} and C_{70}) using chemically bonded γ -cyclodextrin as stationary phase

K. Cabrera*, G. Wieland and M. Schäfer

E. Merck, R&D Chromatography, Frankfurter Strasse 250, 6100 Darmstadt (Germany)

(First received January 22nd, 1993; revised manuscript received April 22nd, 1993)

ABSTRACT

γ -Cyclodextrin chemically bonded to silica was used as a stationary phase for the HPLC separation of the two fullerenes, C_{60} and C_{70} . C_{70} is much more strongly retarded than C_{60} on this stationary phase. Chromatography on the corresponding unmodified silica showed no separation of the two fullerenes, indicating that the separation is due to the selective interaction with the γ -cyclodextrin moieties.

INTRODUCTION

The discovery of buckminsterfullerene (C_{60}) and the more recent development of methods to obtain fullerenes in larger amounts have opened up a highly active field of research [1,2]. Numerous scientists are now working on the synthesis and structural characterization of new fullerenes [3–5]. For all these investigations, chromatographic methods for the purification and analysis of fullerene mixtures are needed. So far, fullerenes have been successfully chromatographed on typical normal-phase systems using silica [3,6], alumina [7] or graphite [8] as the stationary phase and *n*-hexane as the mobile phase. Reversed-phase silica with C_{18} modification [9,10] and the Pirkle type of stationary phase (N-3,5-dinitrobenzoylphenylglycine bonded to amino-

propylsilica) [6,11] have also been used for the chromatographic separation of fullerenes. The latter shows high selectivity for the separation of the C_{60} and C_{70} compounds. Therefore, semi-preparative separations have also been performed on this type of phase. Recently, a synthetic polymer (polystyrene) has been used as a stationary phase for the gel permeation chromatography of fullerenes [12].

Cyclodextrins are cyclic oligosaccharides which are known for their ability to form inclusion complexes with different substrates [13]. As a result of this property, cyclodextrins can differentiate between structural, geometrical and optical isomers. This has been used for the chromatographic separation of compounds either by adding cyclodextrins to the mobile phase [14,15] or by their chemical bonding to the stationary phase [16,17]. Recently, γ -cyclodextrin has been used as a complexing reagent for C_{60} , resulting in a water-soluble fullerene [18].

* Corresponding author.

The incorporation of C_{60} in azacrown ethers which are oriented in a monolayer has also been reported [19]. It was therefore of interest to see whether γ -cyclodextrin chemically bonded to silica (ChiraDex-GAMMA) could be a specific stationary phase for the chromatographic separation of fullerenes.

In this paper, the efficient HPLC separation of C_{60} and C_{70} fullerenes on this stationary phase is described.

EXPERIMENTAL

Chemicals and reagents

A C_{60} – C_{70} fullerene mixture was obtained from Aldrich (Steinheim, Germany). Pure C_{60} was supplied by Fluka (Neu-Ulm, Germany). *n*-Hexane and toluene used for chromatography were of LiChrosolv grade (Merck, Darmstadt, Germany).

HPLC columns

LiChroCART LiChrospher Si 100, 5 μ m (250 mm \times 4 mm I.D.), and LiChroCART ChiraDex-GAMMA (γ -cyclodextrin chemically bonded to silica), 5 μ m (250 mm \times 4 mm I.D.), were obtained from Merck.

HPLC instrument

All chromatographic separations were carried out on a Merck–Hitachi HPLC system with a Rheodyne injection valve, an L-6200 intelligent pump, an L-4000 detector and a D-2500 integrator. Temperature experiments were performed with an Inlabo F 10-UC thermostat.

RESULTS AND DISCUSSION

γ -Cyclodextrin chemically bonded to silica (ChiraDex-GAMMA) was investigated as a stationary phase for the chromatographic separation of C_{60} and C_{70} with *n*-hexane as the mobile phase (Fig. 1a). A single injection of C_{60} onto ChiraDex-GAMMA showed that C_{70} is eluted after the C_{60} fullerene with a difference of almost 40 min in retention time. This indicates a much stronger interaction of C_{70} with the stationary phase. Attempts to separate the fullerene mixture on the corresponding unmodified

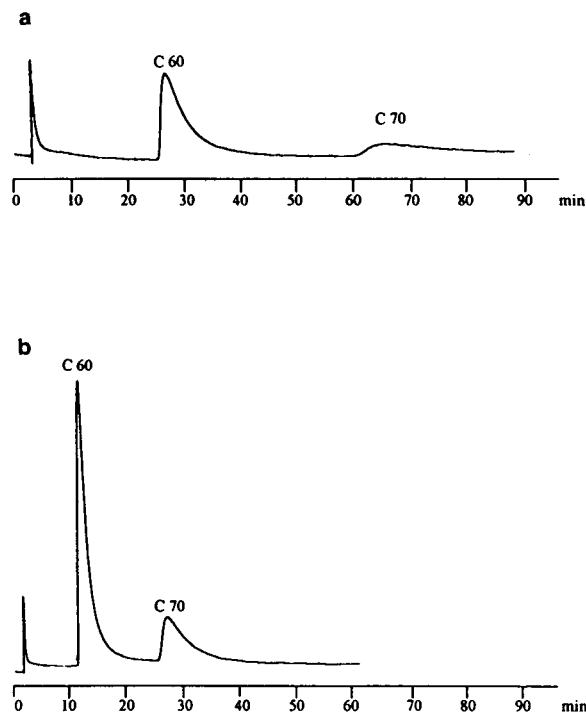


Fig. 1. Separation of C_{60} and C_{70} on ChiraDex-GAMMA. Chromatographic conditions: (a) mobile phase, *n*-hexane; flow-rate, 1 ml/min; temperature, room temperature; detection, UV at 298 nm; injection volume, 10 μ l; sample, 2 mg of C_{60} – C_{70} (ca. 10:1) dissolved in 10 ml of toluene; (b) as (a) except flow-rate, 2 ml/min and temperature, 30°C.

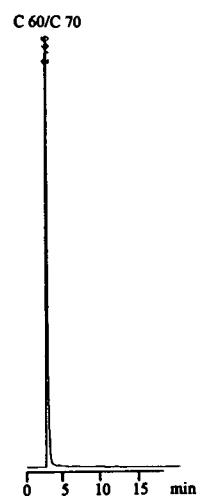


Fig. 2. Chromatography of C_{60} – C_{70} on LiChrospher Si 100. Chromatographic conditions: mobile phase, *n*-hexane; flow-rate, 1 ml/min; temperature, room temperature; detection, 334 nm; injection volume, 10 μ l; sample, 2 mg of C_{60} – C_{70} (ca. 10:1) dissolved in toluene.

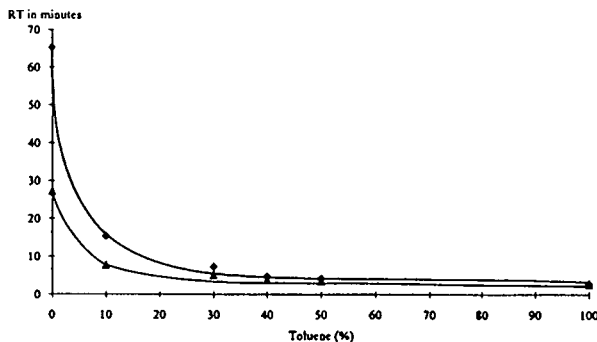


Fig. 3. Influence of the amount of toluene in the mobile phase on the separation of (\blacktriangle) C_{60} and (\blacklozenge) C_{70} on ChiraDex-GAMMA. Chromatographic conditions: mobile phase, *n*-hexane–toluene; flow-rate, 1 ml/min; temperature, room temperature; detection, 334 nm; injection volume, 10 μ l; sample, 2 mg of C_{60} – C_{70} (ca. 10:1) dissolved in toluene. RT = Retention time.

silica (LiChrospher Si 100) under comparable conditions failed (Fig. 2). Therefore, it is clear that the retention and separation of the two fullerenes is due to interactions with the γ -cyclodextrin moieties of the stationary phase. However, the previously described separation is not optimum for routine analyses, because of the long retention times and strong peak broadening. As expected, an increase of temperature (30°C) and flow-rate (2 ml/min) resulted in a considerable decrease in the retention times (Fig. 1b).

Despite the good separation of the two fullerenes under these conditions, the poor solubility of the compounds in *n*-hexane makes this separation useful only on an analytical scale. As toluene is one of the best solvents for fullerenes, the influence of toluene as a component of the

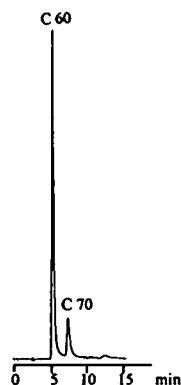


Fig. 4. Separation of C_{60} – C_{70} on ChiraDex-GAMMA. Chromatographic conditions: mobile phase, *n*-hexane–toluene (70:30, v/v); flow-rate, 1 ml/min; temperature, room temperature; detection, 334 nm; injection volume, 10 μ l; sample, 2 mg of C_{60} – C_{70} (ca. 10:1) dissolved in toluene.

mobile phase on the separation of ChiraDex-GAMMA was studied. An increase in toluene concentration in the mobile phase caused a strong decrease in the retention times and eventually resulted in a loss of separation (Fig. 3). These results indicate that there is competition between toluene and fullerene molecules for the interaction with the stationary phase. However, a mobile phase containing 30% (v/v) of toluene in *n*-hexane gave a sufficient difference in the retention times to allow a good separation of C_{60} and C_{70} (Fig. 4). Under these conditions it would be possible to perform separations on a preparative scale.

Concerning the mechanism leading to the separation of C_{60} and C_{70} on ChiraDex-GAMMA, at present we can only suggest the following interpretation. Chromatographic experiments have clearly shown that the γ -

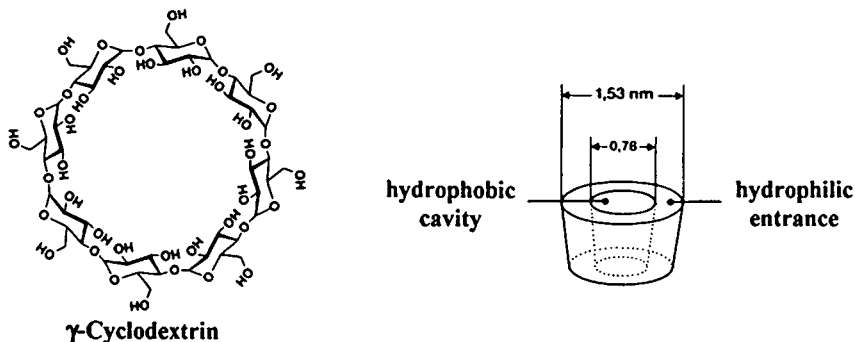


Fig. 5. Chemical and geometrical structures of γ -cyclodextrin.

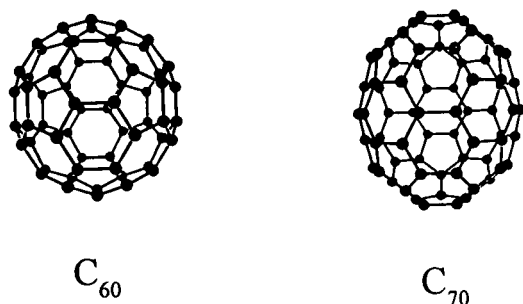


Fig. 6. Chemical and geometrical structures of C₆₀ (7.1 Å diameter [20]) and C₇₀ (6.9 Å diameter at centre, 7.8 Å longitudinal axis [21]).

cyclodextrin moieties of the stationary phase are responsible for the separation of C₆₀ and C₇₀ fullerenes. As γ -cyclodextrin is a cyclic oligosaccharide, formed by eight chiral D-glucose molecules (Fig. 5), it possesses a cavity, in which molecules of different structures can be included [13]. Therefore, it is possible that the fullerene molecules form at least partial inclusion complexes with γ -cyclodextrin. This would explain the retardation of C₆₀ and C₇₀ on ChiraDex-GAMMA in contrast to almost no retention and consequently no separation on the corresponding unmodified silica stationary phase. Moreover, the observed decrease in retention times caused by toluene, which was added to the mobile phase, can be explained by competitive interactions of toluene with the γ -cyclodextrin molecule, thereby occupying the cavity. These explanations, however, give no answer as to why C₇₀ is much more strongly retarded than C₆₀ in the presence of γ -cyclodextrin moieties. C₆₀ and C₇₀ are, however, different in size and shape (Fig. 6). It may therefore be that the geometry of C₇₀ is more favourable for the interaction with the γ -cyclodextrin molecules.

In conclusion, γ -cyclodextrin chemically bonded to silica (ChiraDex-GAMMA) is another highly selective stationary phase for the HPLC separation of C₆₀ and C₇₀ fullerenes. As the separation of these two fullerenes is probably due to the formation of at least partial inclusion complexes with γ -cyclodextrin, which is a chiral

moiety, it would be very interesting to try the separation of other fullerenes, especially chiral molecules [4].

REFERENCES

- 1 H.W. Kroto, J.R. Heath, S.C. O'Brien, R.F. Curl and R.E. Smalley, *Nature*, 318 (1985) 162.
- 2 W. Kraetschmer, K. Fostiropoulos and D.R. Huffman, *Chem. Phys. Lett.*, 170 (1990) 167.
- 3 F. Diederich, R. Ettl, Y. Rubin, R.L. Whetten, R. Beck, M. Alvarez, S. Anz, D. Sensharma, F. Wudl, K.C. Khemani and A. Koch, *Science*, 252 (1991) 548.
- 4 R. Ettl, I. Chao, F. Diederich and R. Whetten, *Nature*, 353 (1991) 149.
- 5 W.I.F. David, R.W. Ibberson, J.C. Matthewman, K. Prassides, T.J.S. Dennis, J.P. Hare, H.W. Kroto, R. Taylor and D.R.M. Walton, *Nature*, 353 (1991) 147.
- 6 J.M. Hawkins, T.A. Lewis, S.D. Loren, A. Meyer, J.R. Heath, Y. Shibato and R.J. Saykally, *J. Org. Chem.*, 55 (1990) 6250.
- 7 R. Taylor, J.P. Hare, A.K. Abdul-Sada and H.W. Kroto, *J. Chem. Soc., Chem. Commun.* (1990) 1423.
- 8 A.M. Vassallo, A.J. Palmisano, L.S.K. Pang and M.A. Wilson, *J. Chem. Soc., Chem. Commun.* (1992) 60.
- 9 F. Diederich, R.L. Whetten, C. Thilgen, R. Ettl, I. Chao and M.M. Alvarez, *Science*, 254 (1991) 1768.
- 10 A. Mittelbach, W. Hönl, H.G. von Schnering, J. Carlsson, R. Janiak and H. Quast, *Angew. Chem.*, 104 (1992) 1681.
- 11 W.H. Pirkle and C.J. Welch, *J. Org. Chem.*, 56 (1991) 6973.
- 12 A. Gügel, M. Becker, D. Hammel, L. Mindach, J. Räder, T. Simon, M. Wagner and K. Müllen, *Angew. Chem.*, 104 (1992) 666.
- 13 W. Saenger, *Angew. Chem.*, 92 (1980) 343.
- 14 K. Cabrera and G. Schwinn, *Kontakte*, 3 (1989) 3.
- 15 K. Cabrera and G. Schwinn, *Int. Lab.*, 7/8 (1990) 28.
- 16 T.Y. Ward and D.W. Armstrong, in M. Zief and L.J. Crane (Editors), *Chromatographic Chiral Separations (Chromatographic Science Series, Vol. 40)*, Marcel Dekker, New York, 1988, p. 131.
- 17 K. Cabrera and D. Lubda, *GIT Chromatogr.*, 2 (1991) 77.
- 18 Th. Andersson, K. Nilsson, M. Sundahl, G. Westman and O. Wennerström, *J. Chem. Soc., Chem. Commun.* (1992) 604.
- 19 F. Diederich, J. Effing, U. Jonas, L. Jullien, Th. Plesniviy, H. Ringsdorf, C. Thilgen and D. Weinstein, *Angew. Chem.*, 104 (1992) 1983.
- 20 D. Ugarte, *Nature*, 359 (1992) 707.
- 21 D.R. McKenzie, C.A. Davis, D.J.H. Cockayne, D.A. Muller and A.M. Vassallo, *Nature*, 355 (1992) 622.

Short Communication

Determination of isocyanuric acid and its chlorinated derivatives in swimming pool waters by ion chromatography

Janusz K. Debowski* and Frans A. Gerber

AECI Ltd., Research and Development Department, Modderfontein 1645 (South Africa)

(First received January 19th, 1993; revised manuscript received April 21st, 1993)

ABSTRACT

A reliable method is presented for the determination of the total isocyanuric acid, *i.e.* the sum of isocyanuric acid plus its chloro derivatives, in typical swimming pool waters. The method involves using ion chromatography with an Omnipac PAX-500 column, 28.8 mM sodium hydroxide solution with 3.5% methanol as mobile phase and UV detection at 213 nm. The analytical range was 20–240 mg/l and the detection limit was 0.5 mg/l. No interference by “free” chlorine or nitrate was observed.

INTRODUCTION

The N-chlorinated derivatives of 1,3,5-triazine-2,4,6-trione or isocyanuric acid (ICA) are products currently used as sources of chlorine in swimming pools, the most popular chemicals being trichloroisocyanuric acid (TCICA) and the sodium salt of dichloroisocyanuric acid (DCICA). Their action is attributed to the presence in solution of “free” chlorine, *i.e.* HOCl and OCl⁻ arising from various hydrolytic equilibria described in detail together with mathematical models in a paper by Solastiouk and Deglise [1]. Companies involved in pool chemical manufacture have sought for some time to find a reliable and quick method of determin-

ing the isocyanuric acid content in swimming pools.

Although there are a few analytical methods available in the literature, *e.g.* turbidimetric [2,3], gravimetric [4], UV absorbance [2,5], thin-layer chromatography [6] and high-performance liquid chromatography [2,7–9], the first four are not reliable enough or are time-consuming, and in all of them interference of ICA with “free” chlorine/nitrate or other pool contaminants (*e.g.* algicides) is likely to occur.

The HPLC–ion chromatography (IC) method developed by Downes *et al.* [2] is interesting because of the use of a Parlisisil SAX column and a tris(hydroxymethyl)methylamine sulphate buffer of pH 7.8, so an anion exchange/ion-pairing mechanism should be expected. Unfortunately, the relevant chromatogram was not reproduced, and according to the authors only a single peak was observed, although a small peak at the same

* Corresponding author.

retention time as ICA was present in a sample in which no ICA was used. This was explained as a carry-over phenomenon, although it seems that interference by “free” chlorine/nitrate is also a possibility. Therefore, the development of a reliable, precise, interference-free method was necessary.

Initially an HPLC method was developed in our laboratory based on the use of a Nucleosil diol column, 0.001 M ammonium hydrogen phosphate solution as mobile phase and UV detection at 213 nm. Although the method provided almost complete separation of ICA from “free” chlorine/nitrate, the chromatographic conditions deteriorated rapidly (loss of separation), so the method had to be abandoned.

This situation prompted us to develop a new ion chromatographic method based on a strong interaction between ICA and reversed-phase/anion exchanger stationary phase.

EXPERIMENTAL

Instrumentation

We used a Dionex 4500i ion chromatograph system equipped with a VDM-2 Dionex variable-wavelength detector at 213 nm, a Dionex 4270 integrator, a manual-pneumatic injector with 10- μ l sample loop, a Dionex Omnipac PAX-500 guard column (50 \times 4.0 mm I.D.), a Dionex Omnipac PAX-500 analytical column (250 \times 4.0 mm I.D.) and an Omnipac PAX-100 with guard column.

Chemicals and reagents

ICA, DCICA and TCICA were analytical-reagent grade. The mobile phase was prepared from analytical reagent-grade sodium hydroxide and HPLC-grade (Burdick & Jackson) methanol. Water was purified through a Milli-R04/Milli-Q plus Millipore water purification system. The mobile phase was 28.8 mM sodium hydroxide in 3.5% methanol with a flow-rate of 1.0 cm³/min.

Sample preparation

Samples were filtered through a 0.45- μ m nylon filter prior to injection.

RESULTS AND DISCUSSION

Typical chromatograms obtained from swimming pool water samples treated with TCICA are illustrated in Figs. 1A (PAX-500 column) and 2 (PAX-100 column).

Standards of ICA, DCICA and TCICA were injected separately using the same conditions as in Figs. 1 and 2, and all of them produced single peaks with retention times equal to peak No. 2 on both figures. The same situation occurred when using the HPLC method (developed previously and mentioned in the Introduction), except that the elution order was reversed and the

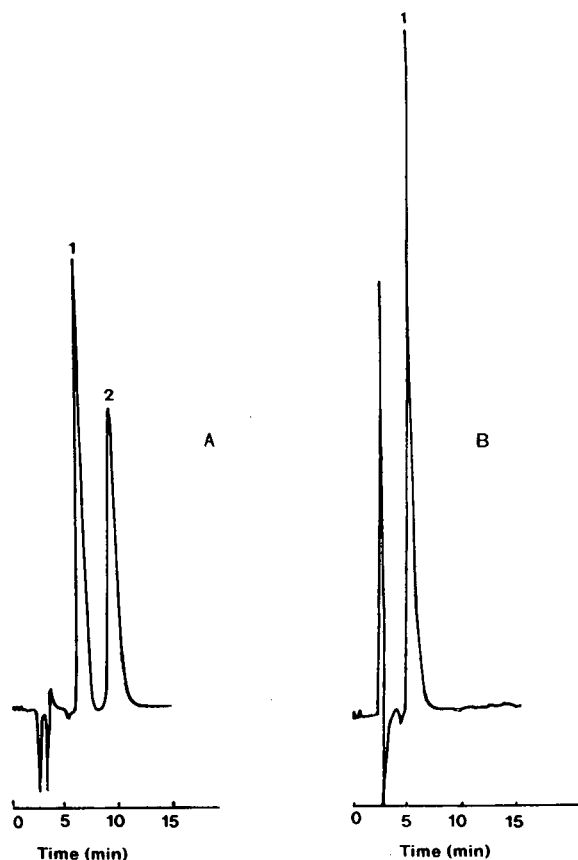


Fig. 1. Ion chromatogram of swimming pool samples. Conditions: column, Omnipac PAX-500; injection volume, 10 μ l; mobile phase, 28.8 mM sodium hydroxide–3.5% methanol; flow-rate, 1.0 cm³/min; detection, UV 213 nm. (A) Sample treated with TCICA. Peaks: 1 = OCl⁻/NO₃⁻; 2 = ICA. (B) Sample treated only by calcium hypochlorite. Peak 1 = OCl⁻/NO₃⁻.



Fig. 2. Ion chromatogram of swimming pool sample treated with TCICA. Conditions: column, Omnipac PAX-100; injection volume, 10 μ l; mobile phase, 28.8 mM sodium hydroxide-3.5% methanol; flow-rate, 1.0 cm^3/min ; detection, UV 213 nm. Peaks: 1 = $\text{OCl}^-/\text{NO}_3^-$; 2 = ICA.

peaks were not as well separated. Moreover, in the HPLC experiments ICA, DCICA and TCICA produced identical UV spectra when scanned by a diode-array detector. (Unfortunately the diode-array detector could not be used in the present ion chromatographic experiments because of the possibility of damage caused by the sodium hydroxide solution in the mobile phase.) The calculated response factors (peak area/ M) for each individually injected standard of ICA, DCICA and TCICA were the same.

To explain the above phenomena one should remember that ICA and its chloro derivatives are in dynamic equilibria in solution, which are fast enough to produce one single common peak for all of these compounds. The observed broadness of the second peaks on Figs. 1A and 2 may be explained by this effect. This is in agreement with observations made by Pinsky and Hu [10].

Therefore, all of the ICA-related components present in swimming pool waters are probably converted into ICA under the high pH conditions [1] and are contained in the one peak. Thus, it is not possible to measure the concentrations of the individual chloro derivatives. Attempts, however, were made to calculate them by Solastiouk and Deglise [1].

Fig. 1B shows a chromatogram of the sample taken from a swimming pool treated exclusively with calcium hypochlorite. The retention time of

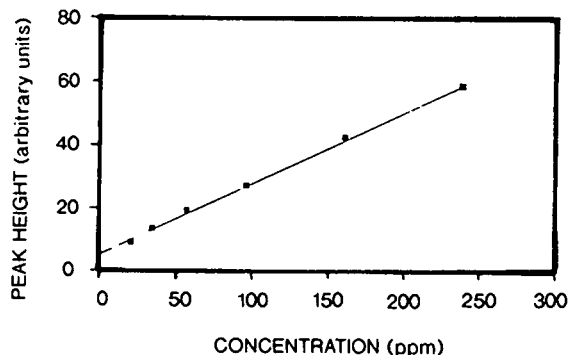


Fig. 3. Calibration graph for ICA. $y = 5.245 + 0.224x$; $R^2 = 0.998$. ppm = mg/l.

peak 1 in this figure should be identical to the retention time of peak No. 1 in Fig. 1A, so one can conclude that both represent "free" chlorine *i.e.* hypochlorite ion.

After further examination it was found that peak No. 1 in Figs. 1A and B and 2 are mixtures of hypochlorite and nitrate. Unfortunately, it was not possible to separate these two anions with this set of columns. By comparing Figs. 1

TABLE I

THE TOTAL MAXIMUM ICA CONTENT IN SWIMMING POOL SAMPLES DETERMINED BY THE TURBIDIMETRIC METHOD [3] AND ION CHROMATOGRAPHY

Omnipac PAX-500 column, 28.8 mM sodium hydroxide-3.5% methanol

Sample No.	Total maximum ICA concentration (mg/l)	
	Turbidimetric method	Ion chromatography method
1	97	96
2	107	104
3	130	113
4	125	118
5	75	72
6	48	50
7	37	42
8	49	41
9	85	75
10	60	67
11	0	0

and 2 one can conclude that retention of ICA is caused primarily by strong ion interaction (column PAX-100 does not possess the reversed-phase features of column PAX-500 and is a stronger anion exchanger than the latter).

The calibration graph of ICA peak height *versus* concentration is shown in Fig. 3. The detection limit was estimated to be 0.5 mg/l. The method was tested by adding known concentrations of ICA to a typical pool water sample and then determining the total amount present. The results expressed as percent recovery varied between 100.4 and 105.4. The variation based on five consecutive measurements of one of the typical samples was estimated to be $\pm 0.8\%$ as relative standard deviation.

The preliminary results of the total maximum ICA content in typical swimming pools by ion chromatography (PAX-500) and the turbidimetric method [3] are shown in Table I, which shows good agreement between two methods. The proposed ion chromatography method is a reli-

able analytical tool for monitoring the total maximum isocyanuric acid content in swimming pool waters.

REFERENCES

- 1 B. Solastiouk and X. Deglise, *Can. J. Chem.*, 66 (1988) 2188.
- 2 C.J. Downes, J.W. Mitchell, E.S. Viotto and N.J. Eggers, *Water Res.*, 18 (1984) 277.
- 3 P. Scotte, *Eau. Ind.*, 64 (1982) 36.
- 4 J. Saldick, *Appl. Microbiol.*, 28 (1974) 1004.
- 5 G. van de Haar, F.M. Pijper-Noordhoff, K. Strikwerda, *H₂O*, 12 (1979) 420.
- 6 E. Knappe and I. Rohdewald, *Z. Anal. Chem.*, 223 (1966) 174.
- 7 J.A. Jessee, C. Valerias, R.E. Benoit, A.C. Hendricks and H.M. McNair, *J. Chromatogr.*, 207 (1981) 454.
- 8 T.V. Briggie, L.M. Allen, R.C. Duncan and C.D. Pfaffenberger, *J. Assoc. Anal. Chem.*, 64 (1981) 1222.
- 9 L.M. Allen, T.V. Briggie and C.D. Pfaffenberger, *Drug Metab. Rev.*, 13 (1982) 499.
- 10 M.L. Pinsky and Hua-Ching Hu, *Environ. Sci. and Technol.*, 15 (1981) 423.

Short Communication

High-performance liquid chromatographic determination of the major saponin from *Opilia celtidifolia* Guill. Perr.

F. Crespin, E. Ollivier, R. Elias, C. Maillard and G. Balansard*

Laboratoire of Pharmacognosy, Faculty of Pharmacy, 27 Boulevard Jean Moulin, 13385 Marseille Cedex 5 (France)

(First received July 29th, 1992; revised manuscript received April 13th, 1993)

ABSTRACT

A reversed-phase high-performance liquid chromatographic method for the identification of four bidesmosidic saponins of *Opilia celtidifolia* Guill. Perr. leaves is produced. The determination of the major saponin was realized with an external standard. The method was validated and two samples of leaves were analysed.

INTRODUCTION

For many years, high-performance liquid chromatography (HPLC) has been used for qualitative and quantitative analyses for the constituents of crude drugs and extracts. Many papers concerning the separation of saponins by HPLC have been reported. The reversed-phase method is the most often described and the solvent generally used is a mixture of water and acetonitrile either in the isocratic mode or with an elution gradient [1–3]. Acids (orthophosphoric acid and trifluoroacetic acid) have been added to the mobile phase to improve the separation of monodesmosidic saponins or saponins including glucuronic acid [4,5].

This paper describes the separation and determination of bidesmosidic saponins of *Opilia celtidifolia* leaves. *Opilia celtidifolia* Guill. Perr. is an African medicinal plant known for its

traditional therapeutic applications. The bark is used as an anthelmintic and the leaves are employed in the treatment of oedema and dental abscesses [6–8]. Previously we reported the isolation of six saponins from barks and leaves [9]. Their structures were elucidated by mass and ^1H and ^{13}C NMR spectrometry (Fig. 1). Until now, no method has been described for assaying *opilia* raw materials. In this paper we propose the determination of the major bidesmosidic saponin (2) by HPLC using an external standard and identification of the other known bidesmosidic saponins (3–6).

EXPERIMENTAL

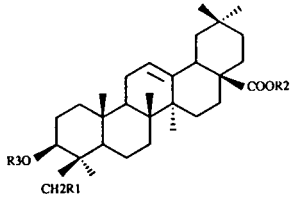
Plant material

Leaves of *Opilia celtidifolia* were collected from the Ivory Coast (Bouake) (sample 1) and Burkina Faso (sample 2).

Sample preparation

An extract of *Opilia celtidifolia* was prepared

* Corresponding author.



Saponins	R1	R2	R3
1	H	H	Aglu ³ — 1 Rham
2	H	Glu	-
3	OH	Glu	-
4	H	Glu	Aglu ³ — 1 Rham 2 — 1 Glu
5	H	Glu	Aglu ³
6	H	Glu	Aglu ³ — 1 Rham 2 — 1 Xyl
Arvensoside C (7)	H	Glu	2 — 1 Glu 3 — 1 Gal

Aglu : β-D-glucuronopyranoside ; Glu : β-D-glucopyranoside
 Xyl : β-D-xylopyranoside ; Rham : α-L-rhamnopyranoside
 Gal : β-D-galactopyranoside.

Fig. 1. Structures of saponins.

by extracting 10 g of leaves with 100 ml of 80% aqueous methanol after 12 h of maceration.

Saponin standards (Fig. 1) were obtained by extraction and purification from *Opilia celtidifolia* [9]. Samples were dissolved in methanol to give a concentration of 1 mg/ml.

Apparatus and conditions

The liquid chromatograph consisted of an automatic sample injector (Waters WISP 712), two solvent-delivery systems (Waters M510) and a variable-wavelength UV detector (Waters Model 490), connected to a computer to monitor chromatographic parameters and process data.

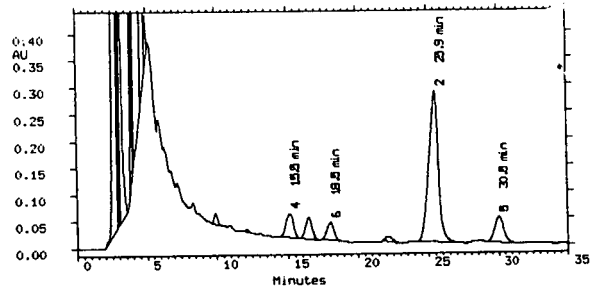
The column was Nucleosil C₁₈ (5 μm) (250 × 4.6 mm I.D.) from Interchim (Montlagon, France) and a μBondapak C₁₈ guard column (10 μm), Guard-Pak insert (Waters), was also used. The eluent was acetonitrile (HPLC grade; Carlo Erba, Milan, Italy)-water (pH adjusted to 2.65

with concentrated orthophosphoric acid) (33:67, v/v). Solvents were filtered through a Millipore filter (0.45 μm). The flow-rate was 1 ml/min, the injection volume was 20 μl and detection was at 210 nm.

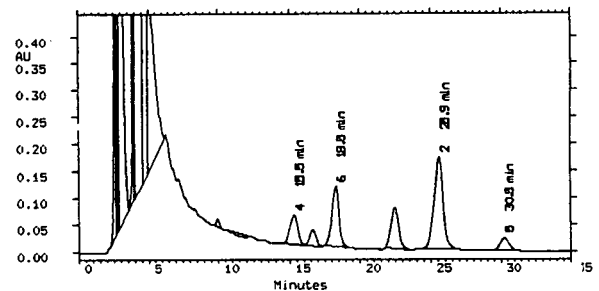
RESULTS AND DISCUSSION

Chromatograms of two extracts of *Opilia celtidifolia* leaves are shown in Fig. 2. Complete separation of four saponins was achieved in 35 min. All peaks were well resolved. Bidesmosidic saponins in the samples were identified by comparison with the retention times of standards (Table I). Saponin 1 is not eluted with this system. The same saponins were found in the two opilia leaf samples. Saponin 3 was not present in the leaves (Fig. 2).

Determination of saponin 2 in these extracts was achieved by the external standard method.



Sample 1: Ivory Coast



Sample 2: Burkina Faso

Fig. 2. Chromatograms of extracts of *Opilia celtidifolia* leaves. For identification of peaks, see Table I and Fig. 1

TABLE I
RETENTION TIMES OF SAPONINS

Saponin	t_R (min)
3	11.1
4	15.5
6	18.5
2	5.9
5	30.5

Method validation

The method was tested on saponin 2. The linearity of the response *versus* concentration curve was investigated in the range of 0.6–3 mg/ml. Data for least-squares regression analysis of the calibration graph were $y = 2.36 \cdot 10^{-7} x - 1.33 \cdot 10^{-2}$ ($r = 0.9992$), where y = concentration in mg/ml, x = peak area and r = correlation coefficient.

The reproducibility of the method was calculated by assaying ten replicates of the same sample at a concentration of 1 mg/ml. For saponin 2 the relative standard deviation was estimated to be 1.17%. The reproducibility of standard preparation was tested by assaying five preparations at a concentration of 1 mg/ml. The relative standard deviation was estimated to be 0.57%. The reproducibility of the extraction method was tested for saponin 2. Five extractions were tested. The relative standard deviation was 2.76%.

TABLE II
DETERMINATION OF SAPONIN 2 IN TWO *OPILIA*
CELTIDIFOLIA LEAF SAMPLES

Sample	Saponin 2 (g per 100 g)
1 (Ivory Coast)	3.86
2 (Burkina Faso)	3.32

The detection limit was calculated to be 3 $\mu\text{g/ml}$ for saponin 2 at a signal-to-noise ratio of 2:1.

These results indicate that the method is suitable for the determination of saponin 2 in *Opilia celtidifolia* leaves.

Determination of saponin 2

The determination of saponin 2 was carried out by external standardization in two *opilia* leaves samples. The results are given in Table II and Fig. 2.

CONCLUSIONS

The identification of bidesmosidic saponins in *Opilia celtidifolia* leaves and the determination of the major compound (saponin 2) is possible by the proposed method.

REFERENCES

- 1 H. Kanazawa, Y. Nagata, Y. Matsushima and M. Tomada, *J. Chromatogr.*, 507 (1990) 327.
- 2 I. Slacanin, A. Marston and K. Hostettmann, *J. Chromatogr.*, 448 (1988) 265.
- 3 B. Domo, A.C. Dorsaz and K. Hostettmann, *J. Chromatogr.*, 315 (1984) 441.
- 4 H. Wagner and N. Neger, *Dtsch. Apoth.-Ztg.*, 126 (1986) 2613.
- 5 M. Burnouf-Radosevich and N.E. Delfel, *J. Chromatogr.*, 368 (1986) 433.
- 6 E. Vidal-Ollivier, A. Babadjamian, C. Maillard, R. Elias and G. Balansard, *Pharm. Acta Helv.*, 64 (1989) 5.
- 7 E.J. Adjanohoun, *Médecine Traditionnelle et Pharmacopée. Contribution aux Études Ethnobotanique et Floristique au Mali*, ACCT, Paris, 1985.
- 8 E.J. Adjanohoun, *Médecine Traditionnelle et Pharmacopée. Contribution aux Études Ethnobotanique et Floristique au Bénin*, ACCT, Paris, 1989.
- 9 F. Crespin, E. Ollivier, C. Lavaud, A. Babadjamian, R. Faure, L. Debrauwer and G. Balansard, *Phytochemistry*, (1993) in press.

Short Communication

Isotachophoretic separation of polyols in boric acid solutions

S.P. Atamas* and G.V. Troitsky[☆]

Department of Biochemistry, the Crimean Medical Institute, bulv. Lenina 5/7, Simferopol 333 670 (Ukraine)

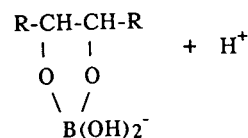
(First received May 21st, 1992; revised manuscript received February 16th, 1993)

ABSTRACT

This work deals with a new approach to fractionation of polyhydroxyl compounds and amphoteric ions. The new technique is based on isotachopheresis of borated polyols leading to pH gradient formation. The Theoretical section contains a number of equations to determine pH values for different borated polyol ion zones on the basis of their absolute electrophoretic mobilities or concentrations. The Experimental section gives a description of tentative experiments demonstrating the possibility of isotachopoietic separation of polyhydroxyl compounds.

INTRODUCTION

Boric acid can react with substances of polyhydroxyl nature to form borated polyols (BPs). This reaction is exploited to detect polyols and boric acid as well as to carry out electrophoresis of polyols [1]. Structurally, such complexes of boric acid and polyhydroxyl compounds are commonly presented as dissociable acid:



Compared with free boric acid, the complexes formed are stronger and more mobile in electric field acids.

It has previously been demonstrated that a borate–polyol system (BPS) can be used to produce pH gradients that can be applied to isoelectric focusing of proteins [2–4] and even cells [5]. BPS has some advantages over the widely used standard ampholine gradients, a disadvantage being their comparatively low temporal stability at alkaline pH. This is caused by appreciable BP electrophoresis in the alkaline region and has for a long time prevented BPS from becoming popular in research.

We have attempted to change BP electrophoresis from a destructive factor into the stabilizing one for both BP pH gradients and the electrophoretic system as a whole.

It has been reported [6] that boric acid may act as a complexing agent in the separation of substances by isotachopheresis. Provided ITP of complexes of boric acid and polyhydroxyl compounds is achieved, a discontinuous pH gradient will appear.

* Corresponding author.

[☆] Author deceased.

THEORETICAL

From the molecular structure of BPs it can be concluded that observed differences in the electrophoretic mobilities of various complexes must be explained by differences in the composition or space configuration of the polyols used. For example, mannitol and sorbitol, which are stereoisomers, under identical conditions move at different velocities in an electric field. It seems natural to expect Kohlrausch boundary formation in an electrophoretic system into which polyols have been placed according to their mobilities. As voltage steps are formed on the boundaries of different polyol zones, mixing in the electrophoresis is likely to disappear. In other words, if the order of placing polyols into electric field in the presence of boric acid is correct, ITP is sure to take place.

Equilibrium in an ITP system is generally described by the widely used Kohlrausch equation:

$$\frac{C_1}{C_2} = \frac{m_1}{m_1 + m_s} \cdot \frac{m_2 + m_s}{m_2} \quad (1)$$

where C_1 and C_2 are ion concentrations, m_1 and m_2 are their absolute electrophoretic mobilities and m_s is absolute mobility of the common positive ion. The same equation is appropriate for the determination of polyol concentrations by ITP. BP absolute mobilities are given in ref. 3. On the other hand, net mobility, U , in boric acid solution is dependent on polyol concentration, C , according to the equation cited in refs. 2 and 3:

$$U = m \frac{(1-g)C_s + 10^{-\text{pH}}}{C} \quad (2)$$

where m is the absolute mobility of the BP ion, C_s is borate salt concentration and g is its degree of hydrolysis.

The fraction on the right side of the equation is the degree of BP complex dissociation. Since the dissociation of free boric acid and its salts is negligible in comparison with BP complex dissociation, practically all hydrogen ions and cations of the salt not participating in hydrolysis will act as counterions towards BP anions.

We have expressed C by means of eqn. 2 and

substituted C_1 and C_2 in the Kohlrausch equation for the formula obtained. Taking into account the ITP condition, *i.e.* $U_1/U_2 = 1$, we get:

$$\frac{10^{-\text{pH}_1} + (1-g)C_s}{10^{-\text{pH}_2} + (1-g)C_s} = \frac{m_2 + m_s}{m_1 + m_s} \quad (3)$$

Such a complicated expression of pH zone correlation is not very convenient for practical application, although it allows pH values to be related to the ion mobilities given in refs. 2 and 3. That is why we have obtained another expression including empirical, easily determined constants.

According to refs. 2 and 3, boric acid solution pH is known to depend on polyol concentration C owing to:

$$\text{pH} = e + f \log C \quad (4)$$

where e and f are constants characteristic of a certain polyol in boric acid of the given concentration.

Many reports in the literature (especially ref. 1) contain data on the boric acid solution pH vs. polyol electrophoretic mobility dependence. This relation is known to be of a typically sigmoid nature. We attempted to deduce empirically an equation that would express satisfactorily the pH vs. net mobility sigmoid curve. Sufficient accuracy here, as it happens, may be obtained from:

$$\text{pH} = g + \log \frac{U}{h - U} \quad (5)$$

where g and h are polyol-characterizing constants (Fig. 1).

Provided that ITP of two different polyols (with concentrations C_1 and C_2 and acidities pH_1 and pH_2) is attained, *i.e.* $U_1 = U_2$, it becomes possible to describe the correlation between all parameters of the two zones by means of empirically obtained eqns. 4 and 5 with the help of simple transformations.

Because of this we have to take the anti-logarithm of both sides of eqn. 5 and express U through the obtained equality. We then apply this expression of velocity to polyol zones 1 and 2, equalize the right sides of velocity equations for the two zones as is conditioned by ITP, express $10^{\text{pH}_1}/10^{\text{pH}_2}$ and logarithmically obtain an expression for pH difference between the two

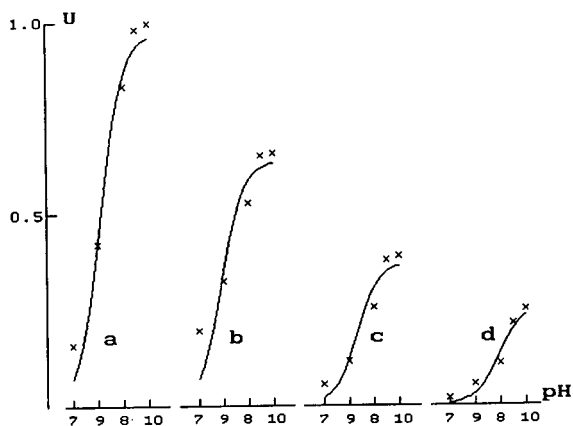


Fig. 1. Relative ionophoretic mobility (U) of various carbohydrates vs. pH (in the alkaline region) [1]. Glucose mobility ($< \text{pH } 10$) was chosen as a unit. Experimental data (\times) are approximated with the curves drawn on the basis of eqn. 5: (a) glucose, $g = 8.1$, $h = 14.6$; (b) mannose, $g = 7.9$, $h = 9.5$; (c) rhamnose, $g = 8.3$, $h = 5.5$; (d) cellobiose, $g = 8.9$, $h = 3.7$.

zones. Then we substitute 10^{pH} for $C \cdot 10^e$ in the right side of the equality for each of the zones. Such a substitution is possible as soon as the antilogarithm of eqn. 4 has been taken.

Since the "g" constant of different polyols varies very little and its value is close to 8.5, it could be considered to be a common constant for all compounds of this type. Under the condition of stable borate concentration, "e" values for different polyols are obviously also identical.

If 10^e , 10^g and $\log(h_2/h_1)$ are thus designated K_e , K_g and K_h , the expression for ITP of two polyol zones is as follows:

$$\text{pH}_1 - \text{pH}_2 = K_h + \log \frac{K_g + K_e C_1^{f_1}}{K_g + K_e C_2^{f_2}} \quad (6)$$

With this expression being applied, it becomes easy to describe the pH gradient that occurs when a polyol set is used in ITP.

EXPERIMENTAL

Chemicals

Polyhydroxyl compounds used included dulcitol, mannitol, sorbitol, galactose, glycerol, suc-

rose, maltose (in decreasing order of electrophoretic mobility in boric acid solution). Sodium hydroxide or tris(hydroxymethyl)aminomethane was added to obtain the required pH value of buffer solution with boric acid. All the chemicals were of analytical grade and were purchased from Serva (Heidelberg, Germany), including reagents for obtaining polyacrylamide gel. Of these, only galactose and dulcitol were from Sigma (St. Louis, MO, USA). The water used was twice distilled.

Instruments

The instruments used for vertical electrophoresis in tubes and horizontal electrophoresis in layers of polyacrylamide gel were manufactured by Hiju Kalur (Tallinn, Estonia). Ultrathin gel layers were obtained with a set of appliances from Serva. Voltage gradient in gels was measured with a platinum electrode, positioned with high precision by a device of our own design.

Preparation of solutions and gel

Below is given a concrete and simple example of a system in which one could observe Kohlrausch zone formation and ITP of polyols and proteins.

The basic buffer was 0.05 M boric acid and 0.0125 M tris(hydroxymethyl)aminomethane, pH 8.1. The anode solution was prepared by dissolving 0.05 M dulcitol in the buffer; the cathode solution was obtained by dissolving 0.05 M maltose in the buffer.

The following solution was prepared: 5 g of acrylamide, 140 mg of bisacrylamide and the anode solution mentioned above to a final volume of 50 ml. To 5 ml of that solution after deaeration was added 0.1 ml of mixture containing 200 mg of ammonium persulphate and 50 μg of N,N,N',N'-tetramethylethylenediamine (TEMED) in 1 ml of distilled water. Slab gel, 125 mm \times 50 mm \times 0.3 mm, was formed using the solution described. Electrode wicks were soaked with anode or cathode solution. The electric current density in cooled gel layers was about 0.12 mA/m².

RESULTS AND DISCUSSION

BP compounds are known to be unsteady complexes that exist in aqueous solutions. It is because of their unsteadiness that it has been impossible to isolate them. This explains the importance of showing the possibility of ITP separation of unsteady-in-time BP ions.

ITP of polyols was observed both in a free solution without a supporting medium and in tubes and layers of polyacrylamide gel. In the first case (ITP in free solution), one should take into account the phenomenon of the solution density change on the Kohlrausch zone boundaries as well as the possibility of a charge of polyol concentration during ITP. The resultant solution density gradient may have the opposite direction to the one of the gravitation field, which brings about a mixture of zones.

Boundaries of different polyol zones can be registered by measuring the electric potential or heat emission gradient, a striking change in optical refraction or pH indicator colour, etc.

The anode solution used in our experiments contained a high-mobility polyol, such as mannitol or dulcitol. The cathode solution contained, as a rule, such low-mobility polyols as glycerol or sucrose.

A mixture of polyols to be separated was placed directly onto gel, if the separation process was to be carried out in vertical tubes, or by sample applicator strips onto a horizontal gel layer.

After the electric field is applied, one can observe even visually the process of Kohlrausch boundary formation between the separating polyols as well as their motion as sharp steps of optical refraction. As in any ITP, the total electrical resistance of the system increases with time, which makes it necessary that the voltage is increased to maintain constant current.

Zone quantity and dimensions depended on the proportional composition of the sample mixture. If the mixture contained any proteins with distinct isoelectric points, their narrow bands divided by polyols were determined with Coomassie staining. BP bands were detected by means of voltage gradient measurement. One of the simplest cases is shown in Fig. 2.

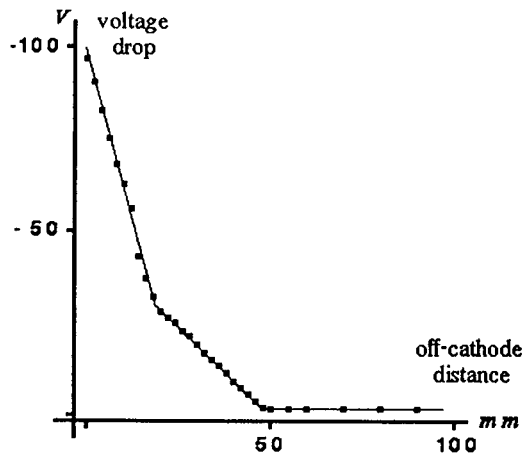


Fig. 2. Voltage gradient formed in a dulcitol-glycerol-maltose ITP system. The steepest part is associated with maltose, which is a carbohydrate of the lowest mobility; the almost horizontal part is associated with dulcitol, a polyol of the highest mobility and lowest specific electric resistance in this system.

In this very case a gel layer was prepared in the way described above, *i.e.* it contained dulcitol. A cathode paper wick was soaked with cathode solution containing 0.025 M maltose and 0.025 M glycerol. Fig. 2 shows that separation of maltose (the steepest part of the gradient) and glycerol (the mid-part of the gradient) occurred. This is evidence of how easily BP ITP in pH alkaline region can be performed.

CONCLUSIONS

The mobility of borated polyols is known to be inversely proportional to their dissociation constant in most cases [2,3]. Consequently, if polyols are gleaned correctly, the natural discrete pH gradient appears and becomes stable in the course of isotachopheresis. The acid part of this gradient belongs to the area of more mobile zones. There appears to be the possibility of using borate-polyol pH gradients not only for the traditional acid range but for the whole pH range. Such gradients can be applied to separation of amphoteric ion mixtures, in particular proteins. Moreover, this is an inexpensive method of purifying and separating substances of polyhydroxyl nature and non-amphoteric ions.

REFERENCES

- 1 E.M. Shwarts, *Kompleksnie soedinenia bora s polioxy-soedineniyami*, Zinatne, Riga, 1966, p. 237.
- 2 G.V. Troitsky and G.Y. Azhitsky, *J. Chromatogr.*, 324 (1985) 285–297.
- 3 G.V. Troitsky and G.Y. Azhitsky, *Isoelektricheskoe focusirovanie belkov v samoorganizuyuschihsia i iskusstvenih pH-gradientah*, Naukova Dumka, Kiev, 1984, p. 219.
- 4 P. Todd, *Electrophoresis*, 11 (1990) 947–952.
- 5 P. Todd. in D.S. Kompala and P. Todd (Editors), *Cell Separation Science and Technology*, American Chemical Society, Washington, DC, 1987, p. 216.
- 6 S. Tanaka, T. Kaneta and H. Yoshida, *J. Chromatogr.*, 498 (1990) 205–211.

Short Communication

Separation of D-galactonic and D-gluconic acids by capillary zone electrophoresis

Akio Bergholdt, Jan Overgaard and Arne Colding*

The Engineering Academy of Denmark, Department of Chemistry and Chemical Engineering, DIAK 376, DK-2800 Lyngby (Denmark).

Rune Buhl Frederiksen

Waters Chromatography Division, Millipore A/S, Baldersbuen 46, DK-2640 Hedehusene (Denmark)

(First received January 19th, 1993; revised manuscript received April 15th, 1993)

ABSTRACT

Capillary zone electrophoresis was used for the analysis of the aldonic acids, D-galactonic and D-gluconic acids. The dependence of the resolution on the pH of the running electrolyte was examined. Separation with the resolution 1.2 was achieved at both pH 4.1 and 5.0. The chiral mobile phase additive, β -cyclodextrin, showed no additional optimizing effect on the separation at the optimum pH.

INTRODUCTION

Capillary zone electrophoresis (CZE) is an efficient method for the separation of charged components. Since the aldonic acids are partly ionized in aqueous solution, they are suitable candidates for CZE investigations. In the study described here we successfully applied the CZE technique to separate the free D-galactonic and D-gluconic acids.

Previously, D-galactonic and D-gluconic acids have been analysed using liquid chromatographic (LC) systems based on strong basic anion-ex-

change resin [1–3]. Recently, however, separation of the aldonic acids by high-performance liquid chromatography (HPLC) was examined. The analysis was carried out on an anion-exchange column, but no separation was achieved [4]. In the same reference separation was achieved by applying pre-column derivatization followed by capillary gas chromatography (GC). The above-mentioned methods can only be applied to aldonic acids that have been altered by derivatization or complexation.

When the CZE technique is utilized to analyse the aldonic acids, detection is a challenging problem owing to the very low UV absorbance of the aldonic acids. A similar problem is encountered when investigating carbohydrates. This problem can be solved by derivatization [5,6], complexation [7] or by combination of both [8–

* Corresponding author.

10]. Alternatively, indirect photometric detection can be applied using sorbic acid as both carrier electrolyte anion and chromophore. Using this method various aldonic acids were examined at pH 12.1, but separation of D-galactonic and D-gluconic acids was not achieved [10,11].

By investigating the effect of pH on the resolution we separated and detected the free D-galactonic and D-gluconic acids applying the CZE technique and indirect photometric detection.

EXPERIMENTAL

Materials

Standard solutions of D-galactonic acid (Sigma, St. Louis, MO, USA) and D-gluconic acid (Merck, Darmstadt, Germany) were prepared in purified water obtained from a Milli-Q purification system (Millipore, Bedford, MA, USA) at concentrations of 0.4 mg/ml (pK_a values of the aldonic acids are approximately 3.6). The buffers employed were prepared by dissolving 0.67 g of sorbic acid (Merck) in 1000 ml of Milli-Q water to yield a final concentration of 6 mM (pK_a of value of sorbic acid is 4.8). When working with β -cyclodextrin (Sigma) 1.7 g of β -cyclodextrin were added to 100 ml of the buffer, resulting in concentrations of 15 mM. The pH was adjusted with 1 M sodium hydroxide. The final electrolytes were filtered through HV 0.45- μ m filters (Millipore) and degassed in a vacuum for 30 min.

Equipment

All the experiments were performed on a Quanta 4000 capillary electrophoresis system from Waters (Waters Chromatography Division, Millipore, Milford, MA, USA). The Quanta 4000 was equipped with an untreated fused-silica capillary (Waters) of total length 100 cm and internal diameter 50 μ m. The capillary was ventilated to ensure a uniform temperature. Hydrostatic injection was performed by raising the injection end 9.8 cm relative to the detector end for 10 s. Detection was carried out by on-column measurement of UV absorption at 254

nm at 7.6 cm from the detection end using a time constant of 0.1 s.

The electrophoretic data system was a Millennium 2010 chromatography manager (Millipore) operated on a PowerMate 386/33i computer (NEC Technologies, Boxborough, MA, USA). The data were collected at a rate of five data points per second.

Capillary conditioning

Every new fused-silica capillary was washed with 1 M sodium hydroxide for 1 h followed by 0.001 M sodium hydroxide for 20 min. In between runs the capillary was treated with 1 M sodium hydroxide for 2 min, and then with 0.001 M sodium hydroxide for 2 min, and finally it was equilibrated with the buffer for 8 min. When the capillary was stored for more than 24 h it was flushed with Milli-Q water.

All experiments was carried out at room temperature.

RESULTS AND DISCUSSION

The D-galactonic and D-gluconic acids shown in Fig. 1 are chiral 4-epimers, and therefore their electrophoretic mobilities differ only slightly. Since the components are acids, the difference between the electrophoretic mobilities depends on pH. Therefore, we examined how the resolution depends on pH from pH 3.8 to pH 11.0 using the conditions described in the Experimen-

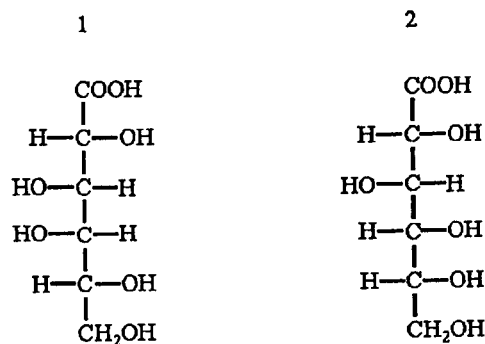


Fig. 1. Constitutional formulas of the 4-epimer aldonic acids. 1 = D-Galactonic acid; 2 = D-gluconic acid.

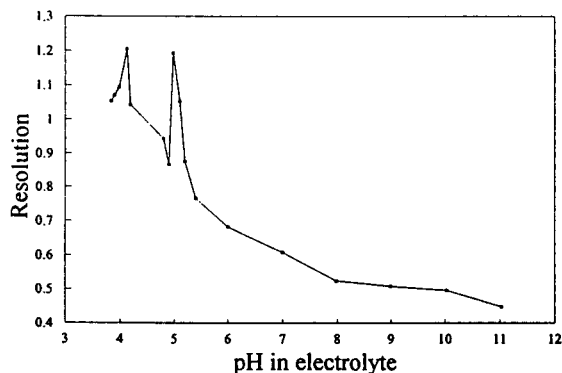


Fig. 2. Effect of pH on the resolution of D-galactonic and D-gluconic acids. Electrolyte: 6 mM sorbate at pH 3.8, 3.9, 4.0, 4.1, 4.2, 4.8, 4.9, 5.0, 5.1, 5.2, 5.4, 6.0, 7.0, 8.0, 9.0, 10.0 and 11.0. Current: 0.4–4.2 μ A. Temperature: room temperature. Capillary: fused silica of length 92.4 cm and internal diameter 50 μ m. Voltage: 20 kV. UV detection: indirect at 254 nm. Injection: hydrostatic in 10 s.

tal section. The results are depicted in Fig. 2 in terms of resolution *versus* pH of the buffer solution. The resolution, R_s , is calculated from the equation, $R_s = 2(t_{m2} - t_{m1}) / (W_2 + W_1)$, where t_m is the migration time and W is the peak width at baseline using tangent lines drawn through 50th percentile points until they intercept the baseline.

It was noted that the resolution is very sensitive to changes in pH around 4 and 5. Therefore the resolution in the pH range 3.8–5.2 was further investigated. The best resolutions were obtained at the pH values 4.1 and 5.0, and the

results at these pH values are reported in Table I.

In Fig. 3a we show the baseline separation of the 4-epimer aldonic acids at pH 4.1. The tailing is due to a higher mobility of the electrolyte compared with the mobility of the sample at this low pH. Fig. 3a and Table I show separation with resolution 1.2 was achieved at pH 4.1. The number of theoretical plates per metre is around 10^4 , and the migration times are more than 30 min. Correspondingly, Fig. 3b shows the separation of the aldonic acids at pH 5.0. By altering the pH from 4.1 to 5.0 it is noted from Fig. 3b and Table I that the number of theoretical plates is enhanced by an order of magnitude, and the separation of the aldonic acids is achieved with a migration time of approximately 25 min. The shorter migration time is due to an increase in the electro-osmotic flow, because the higher electrolyte pH enhances the ionization of the silanol groups on the surface of fused-silica capillaries.

Equal concentrations were analysed during all runs. At a signal-to-noise ratio of 3 the detection limit is 18 fmol at pH 4.1. Correspondingly, the detection limit is 18 fmol at pH 5.0 with a signal-to-noise ratio of 5.

The chiral mobile phase additive, β -cyclodextrin (β -CD) has yielded good results in the separation of chiral compounds by CZE [12]. In order to optimize the separation, 15 mM β -CD was added at various pH values ranging from 4.1

TABLE I

EFFECT OF pH ON NUMBER OF THEORETICAL PLATES AND MIGRATION TIMES

Conditions: electrolyte: 6 mM sorbate. Temperature: room temperature. Capillary: fused silica of length 92.4 cm and internal diameter 50 μ m. Voltage: 20 kV. Current: 0.8 μ A at pH 4.1 and 1.6 μ A at pH 5.0. UV detection: indirect at 254 nm. Injection: hydrostatic in 10 s.

pH in electrolyte	Standard amount (pmol)	Resolution	Number of theoretical plates per m ^a		Migration time (min)	
			Galactonic acid	Gluconic acid	Galactonic acid	Gluconic acid
4.1	3	1.2	8 000	12 000	33.1	34.8
5.0	3	1.2	75 000	100 000	24.8	25.3

^a Number of theoretical plates: $N = 16(t/W)^2$, where t = migration time, W = peak width at baseline using tangent lines drawn through 50th percentile points until they intercept the baseline.

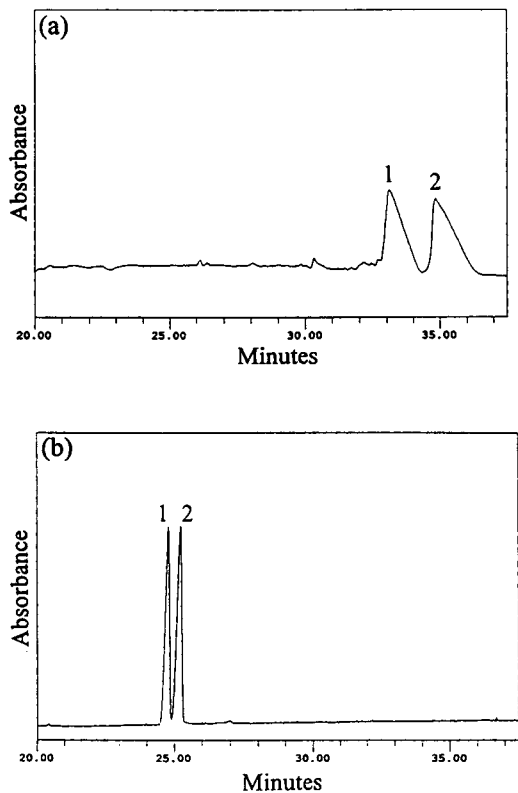


Fig. 3. CZE separation of the 4-epimer aldonic acids. (a) Electrolyte: 6 mM sorbate at pH 4.1. Current: 0.8 μ A. Temperature: room temperature. Capillary: fused silica of length 92.4 cm and internal diameter 50 μ m. Voltage: 20 kV. UV detection: indirect at 254 nm. Range: 7 mAu. Injection: hydrostatic in 10 s. (b) Electrolyte: 6 mM sorbate at pH 5.0. Current: 1.6 μ A. All other conditions as in (a). Identification: 1 = D-galactonic acid; 2 = D-gluconic acid.

to 7.9. The results are shown in Fig. 4 in terms of resolution *versus* pH of the electrolyte solution. The results show that the effect of β -CD depends on pH, but the separation is not further improved.

CONCLUSIONS

The potential of the CZE technique for separating the free aldonic acids, D-galactonic and D-gluconic acids, has been demonstrated. It is shown that the separation of the chiral compounds by the CZE technique is very sensitive to the pH value of the buffer. Addition of β -CD to the buffer did not improve the separation at the optimum pH.

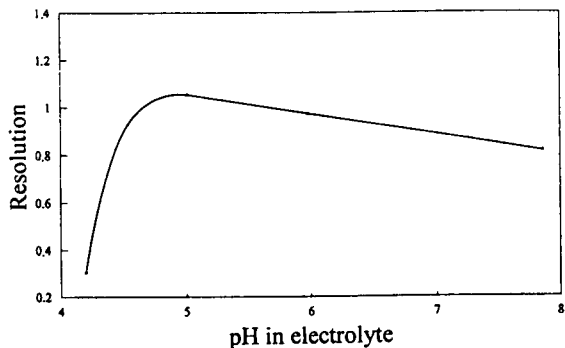


Fig. 4. The resolution of D-galactonic and D-gluconic acids as a function of pH with 15 mM β -cyclodextrin added to the 6 mM sorbate buffer. The experiment was performed at pH 4.1, 5.0, 6.0 and 7.9. Current: 0.2–2.1 μ A. Temperature: room temperature. Capillary: fused silica of length 92.4 cm and internal diameter 50 μ m. Voltage: 20 kV. UV detection: indirect at 254 nm. Injection: hydrostatic in 10 s.

ACKNOWLEDGEMENTS

We wish to thank G. Bondoux, Millipore, France, for helpful discussions, and I. Shim, The Engineering Academy of Denmark, and G. Mandrup, Novo Nordisk A/S, Denmark, for critical reading of the manuscript.

REFERENCES

- O. Samuelson and R. Simonson, *Svensk Papperstidn.*, 9 (1962) 363.
- O. Samuelson and L.O. Wallenius, *J. Chromatogr.*, 12 (1963) 236.
- B. Carlson and O. Samuelson, *Anal. Chim. Acta*, 49 (1970) 247.
- J.C. Motte, N. Van Huynh, M. Declaire, P. Wattiau, J. Walravens and X. Monseur, *J. Chromatogr.*, 507 (1990) 321.
- S. Hase, S. Hara and Y. Matsushima, *J. Biochem.*, 85 (1979) 217.
- W. Nashabeh and Z. El Rassi, *J. Chromatogr.*, 514 (1990) 57.
- S. Hoffstetter-Kuhn, A. Paulus, E. Gassmann and H.M. Widmer, *Anal. Chem.*, 63 (1991) 1541.
- S. Honda, S. Iwase, A. Makino and S. Fujiwara, *Anal. Biochem.*, 176 (1989) 72.
- A.E. Vorndarn, E. Grill, C. Huber, P.J. Oefner and G.K. Bonn, *Chromatographia*, 34 (1992) 109.
- P.J. Oefner, A.E. Vorndarn, E. Grill, C. Huber and G.K. Bonn, *Chromatographia*, 34 (1992) 308.
- A.E. Vorndarn, P.J. Oefner, H. Scherz and G.K. Bonn, *Chromatographia*, 33 (1992) 163.
- K.D. Altria, D.M. Goodall and M.M. Rogan, *Chromatographia*, 34 (1992) 19.

Book Review

Advances in Chromatography, Vol. 31, edited by J.C. Giddings, E. Grushka, J. Cazes and P.R. Brown, Marcel Dekker, New York, Basle, Hong Kong, 1992, XIX + 393 pp., price US\$ 150.00 (USA and Canada), US\$ 172.50 (rest of world), ISBN 0-8247-8568-1.

Volume 31 continues in the well established tradition of this series in presenting first-rate articles written by leading experts in various fields of chromatography. It contains six contributed chapters.

An excellent review of the fundamentals of non-linear chromatography, the theoretical background for preparative-scale HPLC overloaded separations, by Katti and Guiochon gives a comprehensive survey of recent progress in this exciting field. The authors have succeeded in presenting the topic to the full extent whilst limiting to absolute minimum the complex mathematical descriptions connected with the theoretical models discussed. The major part of this chapter deals with the predictive simulations of the band profiles in both the elution and displacement modes of non-linear chromatography, using various numerical approaches to the problem. The authors show that the theory of non-linear chromatography has been developed to the point that any concentration signal at the column outlet can be predicted, provided that the parameters of the distribution isotherms necessary in these calculations can be accurately determined. The methods for the determination of single- and multi-component (competitive) isotherms are presented in detail and strategies for optimization of the experimental conditions aimed at achieving the maximum production rate in preparative chromatography are surveyed. This chapter provides reading that will be extremely useful not only for those working in the field of preparative chromatography, but for everyone seriously interested in the theoretical fundamentals of chromatography.

The second chapter, written by Dubin, gives a

survey of commercially available packings for aqueous size-exclusion chromatography (SEC) and deals with solute–substrate interactions in “non-ideal” SEC, discusses pitfalls connected with using “universal calibration” in aqueous media and presents a brief outline of the applications in the field of chromatography of proteins and of surfactant micelles.

Gasparič surveys the principles and applications of partition thin-layer chromatography on layers impregnated with organic stationary liquids. A survey of recent publications demonstrates that this technique is still viable as it makes possible many chromatographic separations that are comparable in quality to but less expensive than those using more convenient thin-layer chromatography on chemically bonded materials. In addition to analytical applications, this chapter reports the use of partition TLC in studies on quantitative structure–activity relationships and, with 650 citations, provides a useful source of information for the selection of separation conditions for many pharmaceuticals, naturally occurring compounds and environmental pollutants.

The contribution by Knight describes the history and development of countercurrent chromatography and discusses future possibilities of this technique to meet the needs of peptide separations on analytical, preparative and industrial scales.

In the last two chapters, Singhal and De Silva present recent advances in the affinity chromatography of biomolecules based on the interactions with immobilized boronate ligands and Motohashi, Kamata and Meyer review chromatographic methods for determining car-

cinogenic benz[*c*]acridine, including column, paper chromatography, TLC, HPLC and GLC.

The volume is nicely produced and contains many useful tables, diagrams and references to the original literature. All the chapters are valuable for chromatographers working in the specific areas concerned, but because of the

specialized character of the individual contributions (with the exception of the first chapter and, possibly, the third), most workers are likely to be interested in reading only one or two of them.

Pardubice (Czech Republic) Pavel Jandera

Author Index

- Abraham, M.H.
Hydrogen bonding. XXVII. Solvation parameters for functionally substituted aromatic compounds and heterocyclic compounds, from gas-liquid chromatographic data 644(1993)95
- Akhlaq, M.S.
Rapid group-type analysis of crude oils using high-performance liquid chromatography and gas chromatography 644(1993)253
- Ammann, M., see Futschik, K. 644(1993)389
- Atamas, S.P. and Troitsky, G.V.
Isotachophoretic separation of polyols in boric acid solutions 644(1993)407
- Bachmayer, S., see Futschik, K. 644(1993)389
- Baiocchi, C., Marengo, E., Saini, G., Roggero, M.A. and Giacosa, D.
Reversed-phase high-performance liquid chromatography and chemometrics, a combined investigation tool for complex phytochemical problems 644(1993)259
- Balansard, G., see Crespin, F. 644(1993)404
- Bando, H., see Wada, K. 644(1993)43
- Barry, E.F., see Conte, E.D. 644(1993)349
- Baumann, R.A., see Van der Hoff, G.R. 644(1993)367
- Bergholdt, A., Overgaard, J., Colding, A. and Frederiksen, R.B.
Separation of D-galactonic and D-gluconic acids by capillary zone electrophoresis 644(1993)412
- Bignami, S., Daví, M.L., Milan, C., Moretti, M. and Navarra, F.
Evaluation of ion-exchange chromatography for nitrate determination in wastewaters 644(1993)341
- Bignami, S., see Daví, M.L. 644(1993)345
- Birkenmeier, G., see Otto, A. 644(1993)25
- Bouriotis, V., see Martinou, A. 644(1993)35
- Brinkman, U.A.Th., see Hogendoorn, E.A. 644(1993)307
- Brinkman, U.A.Th., see Van der Hoff, G.R. 644(1993)367
- Cabrera, K., Wieland, G. and Schäfer, M.
High-performance liquid chromatographic separation of fullerenes (C₆₀ and C₇₀) using chemically bonded γ -cyclodextrin as stationary phase 644(1993)396
- Calzaferri, G., see Herren, D. 644(1993)188
- Capri, S., see Marcomini, A. 644(1993)59
- Carabias Martínez, R., Rodríguez Gonzalo, E., Garay García, F. and Hernández Méndez, J.
Automated high-performance liquid chromatographic method for the determination of organophosphorus pesticides in waters with dual electrochemical (reductive-oxidative) detection 644(1993)49
- Chen, I.-C. and Whang, C.-W.
Capillary electrophoresis with amperometric detection using a porous cellulose acetate joint 644(1993)208
- Chen, N., Wang, L. and Zhang, Y.
Influence of column temperature and physico-chemical properties on the electrophoretic behaviour of polyglycine peptides in free-solution capillary electrophoresis 644(1993)175
- Cihlár, T. and Rosenberg, I.
Efficient separation of natural ribonucleotides by low-pressure anion-exchange chromatography 644(1993)299
- Colding, A., see Bergholdt, A. 644(1993)412
- Conner, A.H., see Holfinger, M.S. 644(1993)383
- Conte, E.D. and Barry, E.F.
Alkali flame ionization detector for gas chromatography using an alkali salt aerosol as the enhancement source 644(1993)349
- Crespin, F., Ollivier, E., Elias, R., Maillard, C. and Balansard, G.
High-performance liquid chromatographic determination of the major saponin from *Opilia celtidifolia* Guill. Perr. 644(1993)404
- Daví, M.L., Bignami, S., Milan, C., Liboni, M. and Malfatto, M.G.
Determination of nitrate in surface waters by ion-exchange chromatography after oxidation of total organic nitrogen to nitrate 644(1993)345
- Daví, M.L., see Bignami, S. 644(1993)341
- Debowski, J.K. and Gerber, F.A.
Determination of isocyanuric acid and its chlorinated derivatives in swimming pool waters by ion chromatography 644(1993)400
- De Jong, A.P.J.M., see Meiring, H.D. 644(1993)357
- Den Engelsman, G., see Meiring, H.D. 644(1993)357
- De Vries, J.X. and Schmitz-Kummer, E.
Direct column liquid chromatographic enantiomer separation of the coumarin anticoagulants phenprocoumon, warfarin, acenocoumarol and metabolites on an α_1 -acid glycoprotein chiral stationary phase 644(1993)315
- Di Corcia, A., see Marcomini, A. 644(1993)59
- Diederich, F., see Herren, D. 644(1993)188
- Dolan, J.W.
Savant computer-based instruction series in HPLC: Troubleshooting high performance liquid chromatography (by D. Saunders) (Software Review) 644(1993)213
- Dowling, T.M. and Uden, P.C.
Alkyltin speciation in sea water with on-line hydride conversion and gas chromatography-atomic emission detection 644(1993)153
- Elias, R., see Crespin, F. 644(1993)404
- Fales, H.M., see Shinomiya, K. 644(1993)215
- Fliniaux, M.-A., Manceau, F. and Jacquín-Dubreuil, A.
Simultaneous analysis of *l*-hyoscyamine, *l*-scopolamine and *dl*-tropic acid in plant material by reversed-phase high-performance liquid chromatography 644(1993)193
- Frederiksen, R.B., see Bergholdt, A. 644(1993)412
- Futschik, K., Ammann, M., Bachmayer, S. and Kenndler, E.
Determination of ionic species formed during growth of *Escherichia coli* by capillary isotachophoresis 644(1993)389
- Garay García, F., see Carabias Martínez, R. 644(1993)49

- Gaš, B.
Axial temperature effects in electromigration
644(1993)161
- Gerber, F.A., see Debowski, J.K. 644(1993)400
- Giacofei, R.A., see Martin, M.W. 644(1993)333
- Giacosa, D., see Baiocchi, C. 644(1993)259
- Haupt, K. and Vijayalakshmi, M.A.
Interaction of catechol-2,3-dioxygenase of
Pseudomonas putida with immobilized histidine and
histamine 644(1993)289
- Hayakawa, K., see Yamamoto, A. 644(1993)183
- Hernández Méndez, J., see Carabias Martínez, R.
644(1993)49
- Herren, D., Thilgen, C., Calzaferri, G. and Diederich, F.
Preparative separation of higher fullerenes by high-
performance liquid chromatography on a
tetrachlorophthalimidopropyl-modified silica column
644(1993)188
- Hill Jr., C.G., see Holfinger, M.S. 644(1993)383
- Hogendoorn, E.A., Brinkman, U.A.Th. and Van Zoonen, P.
Coupled-column reversed-phase liquid
chromatography-UV analyser for the determination of
polar pesticides in water 644(1993)307
- Holfinger, M.S., Conner, A.H. and Hill Jr, C.G.
Determination of furan-based amines in reaction
mixtures by gas chromatography 644(1993)383
- Hong, M., see Zou, H. 644(1993)269
- Ishimitsu, S., see Komatsu, H. 644(1993)17
- Ito, Y., see Menet, J.-M. 644(1993)231
- Ito, Y., see Menet, J.-M. 644(1993)239
- Ito, Y., see Shinomiya, K. 644(1993)215
- Jacquin-Dubreuil, A., see Fliniaux, M.-A. 644(1993)193
- Jandera, P.
Advances in Chromatography (by J.C. Giddings, E.
Grushka, J. Cazes and P.R. Brown) (Book Review)
644(1993)416
- Janeček, M., Quilliam, M.A. and Lawrence, J.F.
Analysis of paralytic shellfish poisoning toxins by
automated pre-column oxidation and microcolumn
liquid chromatography with fluorescence detection
644(1993)321
- Kafetzopoulos, D., see Martinou, A. 644(1993)35
- Kawahara, N., see Wada, K. 644(1993)43
- Kenndler, E., see Futschik, K. 644(1993)389
- Kok, W.Th., see Van Asten, A.C. 644(1993)83
- Komatsu, H., Yoshii, K., Ishimitsu, S., Okada, S. and
Takahata, T.
Molecular mass determination of low-molecular-mass
heparins. Application of wide collection angle
measurements of light scattering using a high-
performance gel permeation chromatographic system
equipped with a low-angle laser light-scattering
photometer 644(1993)17
- Kura, G.
Anion-exchange selectivity of cyclic phosphate
oligomers 644(1993)198
- Lawrence, J.F., see Janeček, M. 644(1993)321
- Lebl, M.
Observation of a conformational effect in peptide
molecule by reversed-phase high-performance liquid
chromatography 644(1993)285
- Liapis, A.I., see McCoy, M.A. 644(1993)1
- Liboni, M., see Daví, M.L. 644(1993)345
- Lin, J.-Y. and Yang, M.-H.
High-performance liquid chromatographic separation of
enantiomeric amino acids on bis[carbamoyl(alkyl)-
methylamino]-6-chloro-*s*-triazine- derived chiral
stationary phases 644(1993)277
- Liu, Y. and Wang, Q.
Rapid and continuous ion chromatographic
determination of trace heavy metal impurities in noble
metals 644(1993)73
- Lu, P., see Zou, H. 644(1993)269
- Maillard, C., see Crespin, F. 644(1993)404
- Malfatto, M.G., see Daví, M.L. 644(1993)345
- Manceau, F., see Fliniaux, M.-A. 644(1993)193
- Marcomini, A., Di Corcia, A., Samperi, R. and Capri, S.
Reversed-phase high-performance liquid
chromatographic determination of linear alkylbenzene
sulphonates, nonylphenol polyethoxylates and their
carboxylic biotransformation products 644(1993)59
- Marengo, E., see Baiocchi, C. 644(1993)259
- Martin, M.W. and Giacofei, R.A.
Ultratrace anion analysis of high-purity water. A
column comparison 644(1993)333
- Martinou, A., Kafetzopoulos, D. and Bouriotis, V.
Isolation of chitin deacetylase from *Mucor rouxii* by
immunoaffinity chromatography 644(1993)35
- Matsunaga, A., see Yamamoto, A. 644(1993)183
- McCoy, M.A., Liapis, A.I. and Unger, K.K.
Applications of mathematical modelling to the
simulation of binary perfusion chromatography
644(1993)1
- Meiring, H.D., Den Engelsman, G. and De Jong,
A.P.J.M.
Determination of polar pesticides by phase-transfer
catalysed derivatization and negative-ion chemical
ionization gas chromatography-mass spectrometry
644(1993)357
- Menet, J.-M. and Ito, Y.
Studies on a new cross-axis coil planet centrifuge for
performing counter-current chromatography. II. Path
and acceleration of coils and comparison with type J
coil planet centrifuge 644(1993)231
- Menet, J.-M., see Shinomiya, K. 644(1993)215
- Menet, J.-M., Shinomiya, K. and Ito, Y.
Studies on new cross-axis coil planet centrifuge for
performing counter-current chromatography. III.
Speculations on the hydrodynamic mechanism in
stationary phase retention 644(1993)239
- Milan, C., see Bignami, S. 644(1993)341
- Milan, C., see Daví, M.L. 644(1993)345
- Miyazaki, M., see Yamamoto, A. 644(1993)183
- Mizukami, E., see Yamamoto, A. 644(1993)183
- Moretti, M., see Bignami, S. 644(1993)341
- Navarra, F., see Bignami, S. 644(1993)341
- Okada, S., see Komatsu, H. 644(1993)17
- Ollivier, E., see Crespin, F. 644(1993)404
- Otto, A. and Birkenmeier, G.
Recognition and separation of isoenzymes by metal
chelates. Immobilized metal ion affinity partitioning of
lactate dehydrogenase isoenzymes 644(1993)25

- Ou, Q., see Wan, H. 644(1993)202
- Overgaard, J., see Bergholdt, A. 644(1993)412
- Ozawa, H.
Gas chromatographic-mass spectrometric determination of halogenated acetic acids in water after direct derivatization 644(1993)375
- Poppe, H., see Van Asten, A.C. 644(1993)83
- Quilliam, M.A., see Janeček, M. 644(1993)321
- Rodríguez Gonzalo, E., see Carabias Martínez, R. 644(1993)49
- Roggero, M.A., see Baiocchi, C. 644(1993)259
- Rosenberg, I., see Cihlák, T. 644(1993)299
- Saini, G., see Baiocchi, C. 644(1993)259
- Samperi, R., see Marcomini, A. 644(1993)59
- Schäfer, M., see Cabrera, K. 644(1993)396
- Schmidt, D.E., see Wheatley, J.B. 644(1993)11
- Schmitz-Kummer, E., see De Vries, J.X. 644(1993)315
- Shinomiya, K., see Menet, J.-M. 644(1993)239
- Shinomiya, K., Menet, J.-M., Fales, H.M. and Ito, Y.
Studies on a new cross-axis coil planet centrifuge for performing counter-current chromatography. I. Design of the apparatus, retention of the stationary phase, and efficiency in the separation of proteins with polymer phase systems 644(1993)215
- Stephanou, E.G. and Stratigakis, N.E.
Determination of anthropogenic and biogenic organic compounds on airborne particles: flash chromatographic fractionation and capillary gas chromatographic analysis 644(1993)141
- Stratigakis, N.E., see Stephanou, E.G. 644(1993)141
- Takahata, T., see Komatsu, H. 644(1993)17
- Thilgen, C., see Herren, D. 644(1993)188
- Troitsky, G.V., see Atamas, S.P. 644(1993)407
- Uden, P.C., see Dowling, T.M. 644(1993)153
- Unger, K.K., see McCoy, M.A. 644(1993)1
- Van Asten, A.C., Venema, E., Kok, W.Th. and Poppe, H.
Use of thermal field flow fractionation for the fractionation of polybutadiene in various organic solvents 644(1993)83
- Van der Hoff, G.R., Baumann, R.A., Brinkman, U.A.Th. and Van Zoonen, P.
On-line combination of automated micro liquid-liquid extraction and capillary gas chromatography for the determination of pesticides in water 644(1993)367
- Van Zoonen, P., see Hoogendoorn, E.A. 644(1993)307
- Van Zoonen, P., see Van der Hoff, G.R. 644(1993)367
- Venema, E., see Van Asten, A.C. 644(1993)83
- Vijayalakshmi, M.A., see Haupt, K. 644(1993)289
- Wada, K., Bando, H. and Kawahara, N.
Determination and quantitative analysis of *Aconitum* alkaloids in plants by liquid chromatography-atmospheric pressure chemical ionization mass spectrometry 644(1993)43
- Wang, L., see Chen, N. 644(1993)175
- Wang, Q., see Liu, Y. 644(1993)73
- Wang, Y., see Wan, H. 644(1993)202
- Wan, H., Wang, Y., Ou, Q. and Yu, W.
Improved enantiomeric separation with a 2,6-di-O-pentyl-3-O-trifluoroacetylated β -cyclodextrin and OV-7 mixed stationary phase chiral capillary column 644(1993)202
- Whang, C.-W., see Chen, I.-C. 644(1993)208
- Wheatley, J.B. and Schmidt, D.E.
Salt-induced immobilization of proteins on a high-performance liquid chromatographic epoxide affinity support 644(1993)11
- Wieland, G., see Cabrera, K. 644(1993)396
- Yamamoto, A., Matsunaga, A., Mizukami, E., Hayakawa, K. and Miyazaki, M.
Adsorption isotherm of undissociated eluent acid and its relation to the retention of system peaks in non-suppressed ion chromatography 644(1993)183
- Yang, M.-H., see Lin, J.-Y. 644(1993)277
- Yoshii, K., see Komatsu, H. 644(1993)17
- Yu, W., see Wan, H. 644(1993)202
- Zhang, Y., see Chen, N. 644(1993)175
- Zhang, Y., see Zou, H. 644(1993)269
- Zou, H., Zhang, Y., Hong, M. and Lu, P.
Retention behaviour of aromatic sulphonic acids in reversed-phase ion-pair liquid chromatography with methanol and acetonitrile as organic modifiers 644(1993)269

Erratum

J. Chromatogr., 637 (1993) 201–205

Pages 203 and 204, Figs. 2 and 3 should be interchanged (the captions are correct).

BIOAFFINITY CHROMATOGRAPHY

By **J. Turková**, Czechoslovak Academy of Sciences, Institute of Organic
Chemistry and Biochemistry, Prague, Czech Republic

Journal of Chromatography Library Volume 55

Bioaffinity chromatography is now the preferred choice for the purification, determination or removal of many biologically active substances. The book includes information on biologically active substances with their affinants, solid supports and methods of coupling, summarized in tables covering classical, high-performance liquid and large-scale bioaffinity chromatography.

Optimization of the preparation and the use of highly active and stable biospecific adsorbents is discussed in several chapters. Following a chapter dealing with the choice of affinity ligands, affinity-sorbent bonding is described in detail. Other chapters give information on solid supports, the most common coupling procedures and a general discussion of sorption and elution. Several applications of bioaffinity chromatography are described, e.g. quantitative evaluation of biospecific complexes and many applications in medicine and in the biotechnology industry.

Contents:

1. Introduction.
2. The principle, history and use of bioaffinity chromatography.
3. Choice of affinity ligands (affinants).
4. General considerations on affinant - sorbent bonding.
5. Solid matrix supports.
6. Survey of the most common coupling procedures.
7. Characterization of supports and immobilized affinity ligands.
8. General considerations on sorption, elution and non-specific binding.
9. Bioaffinity chromatography in the isolation, determination or removal of biologically active substances.
10. Immobilization of enzymes by biospecific adsorption to immobilized monoclonal or polyclonal antibodies.

11. Study of the modification, mechanism of action and structure of biologically active substances using bioaffinity chromatography.
 12. Solid-phase immunoassay and enzyme-linked lectin assay.
 13. Several examples of the application of biospecific adsorption in medicine.
 14. Application of bioaffinity chromatography to the quantitative evaluation of specific complexes.
 15. Theory of bioaffinity chromatography.
- Subject Index.

© 1993 819 pages Hardbound
Price: Dfl. 495.00 / US \$ 282.75
ISBN 0-444-89030-0

ORDER INFORMATION

For USA and Canada
ELSEVIER SCIENCE PUBLISHERS
Judy Weislogel, P.O. Box 945
Madison Square Station
New York, NY 10160-0757
Fax: (212) 633 3880

In all other countries
ELSEVIER SCIENCE PUBLISHERS
P.O. Box 330
1000 AH Amsterdam
The Netherlands
Fax: (+31-20) 5862 845

US\$ prices are valid only for the USA & Canada and are subject to exchange rate fluctuations; in all other countries the Dutch guilder price (Dfl.) is definitive. Customers in the European Community should add the appropriate VAT rate applicable in their country to the price(s). Books are sent postfree if prepaid.



ELSEVIER
SCIENCE PUBLISHERS

CATALOGUE 1993 ON CD-ROM

Elsevier Science Publishers - the world's largest scientific publisher - presents for the first time details of all its publications on CD-ROM

ADVANTAGES

- Easy to use.
- Get more comprehensive information than ever before.
- Make fast and effective searches.
- Find what you want even with incomplete information.
- Compile special lists of products without typing.
- Improve your control of scientific product information.
- Enhance service to clients.

PRODUCT DESCRIPTION

The CD-ROM contains descriptions of all Elsevier products.

- All the journals, with complete information about journal editors and editorial boards
- Listings of recently published papers for many journals
- Complete descriptions and contents lists of book titles
- Independent reviews of published books
- Forthcoming title information
- Book series
- All other products, e.g. software, CDs, dictionaries, wallcharts.

In addition, the CD-ROM features easy-to-use search tools, making the information

accessible and useful. For example, searches can be made by subject area, by year of publication, by author/editor or title and by "free text" search.

Full book and journal information can be printed to initiate your order.

If you do not find what you need, or wish to know more about Elsevier's publishing programme, the CD-ROM can supply you with the name, address and fax number of the correct person to contact.

AUDIENCE

Librarians, booksellers, researchers, agents and information specialists.

SYSTEM REQUIREMENTS

The CD-ROM has been designed to run under Microsoft® Windows™ 3.0, on IBM PC-ATs and compatibles. The CD-ROM is Microsoft® Windows™ 3.1 compatible.



ELSEVIER
SCIENCE PUBLISHERS

The minimum requirements are:

- IBM or IBM-compatible PC with a 80286 or higher processor
- 2 MB or more RAM
- MS-DOS® 3.3 or higher installed
- Microsoft® Windows™ 3.0 (or 3.1) installed
- Microsoft® Windows™ compatible mouse or other pointing device
- VGA graphics adapter (colour or monochrome)
- Hard disk with at least 2 MB free disk space
- CD-ROM drive which is accessible from Microsoft® Windows™
- For faster operation a 80386SX or higher processor is recommended, as well as a fast CD-ROM drive (access time less than 0.4 seconds).

The CD-ROM can be installed in a local area network.

For further information please contact

ELSEVIER SCIENCE PUBLISHERS
Attn. Vivian Wong Swie San
Marketing Services Department
P.O. Box 211
1000 AE Amsterdam
The Netherlands
FAX: (020) 5862 425
In the USA & Canada
Journal Information Center
P.O. Box 882
Madison Square Station
New York, NY 10159, USA
FAX: (212) 633 3764

PUBLICATION SCHEDULE FOR THE 1993 SUBSCRIPTION

Journal of Chromatography and Journal of Chromatography, Biomedical Applications

MONTH	1992	J-A	M	J	J	A	S	O	N	D	1994
Journal of Chromatography	Vols. 623-627	Vols. 628/636	637/1 637/2 638/1 638/2	639/1 639/2 640/1 + 2	641/1 641/2 642/1 + 2 643/1 + 2 644/1	644/2 645/1 645/2 646/1	646/2 647/1 647/2	648/1 648/2			
Cumulative Indexes, Vols. 601-650											651/1 + 2
Bibliography Section		649/1		649/2			650/1			650/2	
Biomedical Applications		Vols. 612, 613 and 614/1	614/2 615/1	615/2 616/1	616/2 617/1	617/2 618/1 + 2	619/1 619/2	620/1 620/2	621/1 621/2	622/1 622/2	

INFORMATION FOR AUTHORS

(Detailed *Instructions to Authors* were published in Vol. 609, pp. 437-443. A free reprint can be obtained by application to the publisher, Elsevier Science Publishers B.V., P.O. Box 330, 1000 AH Amsterdam, Netherlands.)

Types of Contributions. The following types of papers are published in the *Journal of Chromatography* and the section on *Biomedical Applications*: Regular research papers (Full-length papers), Review articles, Short Communications and Discussions. Short Communications are usually descriptions of short investigations, or they can report minor technical improvements of previously published procedures; they reflect the same quality of research as Full-length papers, but should preferably not exceed five printed pages. Discussions (one or two pages) should explain, amplify, correct or otherwise comment substantively upon an article recently published in the journal. For Review articles, see inside front cover under Submission of Papers.

Submission. Every paper must be accompanied by a letter from the senior author, stating that he/she is submitting the paper for publication in the *Journal of Chromatography*.

Manuscripts. Manuscripts should be typed in **double spacing** on consecutively numbered pages of uniform size. The manuscript should be preceded by a sheet of manuscript paper carrying the title of the paper and the name and full postal address of the person to whom the proofs are to be sent. As a rule, papers should be divided into sections, headed by a caption (e.g., Abstract, Introduction, Experimental, Results, Discussion, etc.) All illustrations, photographs, tables, etc., should be on separate sheets.

Abstract. All articles should have an abstract of 50-100 words which clearly and briefly indicates what is new, different and significant. No references should be given.

Introduction. Every paper must have a concise introduction mentioning what has been done before on the topic described, and stating clearly what is new in the paper now submitted.

Illustrations. The figures should be submitted in a form suitable for reproduction, drawn in Indian ink on drawing or tracing paper. Each illustration should have a legend, all the *legends* being typed (with double spacing) together on a *separate sheet*. If structures are given in the text, the original drawings should be supplied. Coloured illustrations are reproduced at the author's expense, the cost being determined by the number of pages and by the number of colours needed. The written permission of the author and publisher must be obtained for the use of any figure already published. Its source must be indicated in the legend.

References. References should be numbered in the order in which they are cited in the text, and listed in numerical sequence on a separate sheet at the end of the article. Please check a recent issue for the layout of the reference list. Abbreviations for the titles of journals should follow the system used by *Chemical Abstracts*. Articles not yet published should be given as "in press" (journal should be specified), "submitted for publication" (journal should be specified), "in preparation" or "personal communication".

Dispatch. Before sending the manuscript to the Editor please check that the envelope contains four copies of the paper complete with references, legends and figures. One of the sets of figures must be the originals suitable for direct reproduction. Please also ensure that permission to publish has been obtained from your institute.

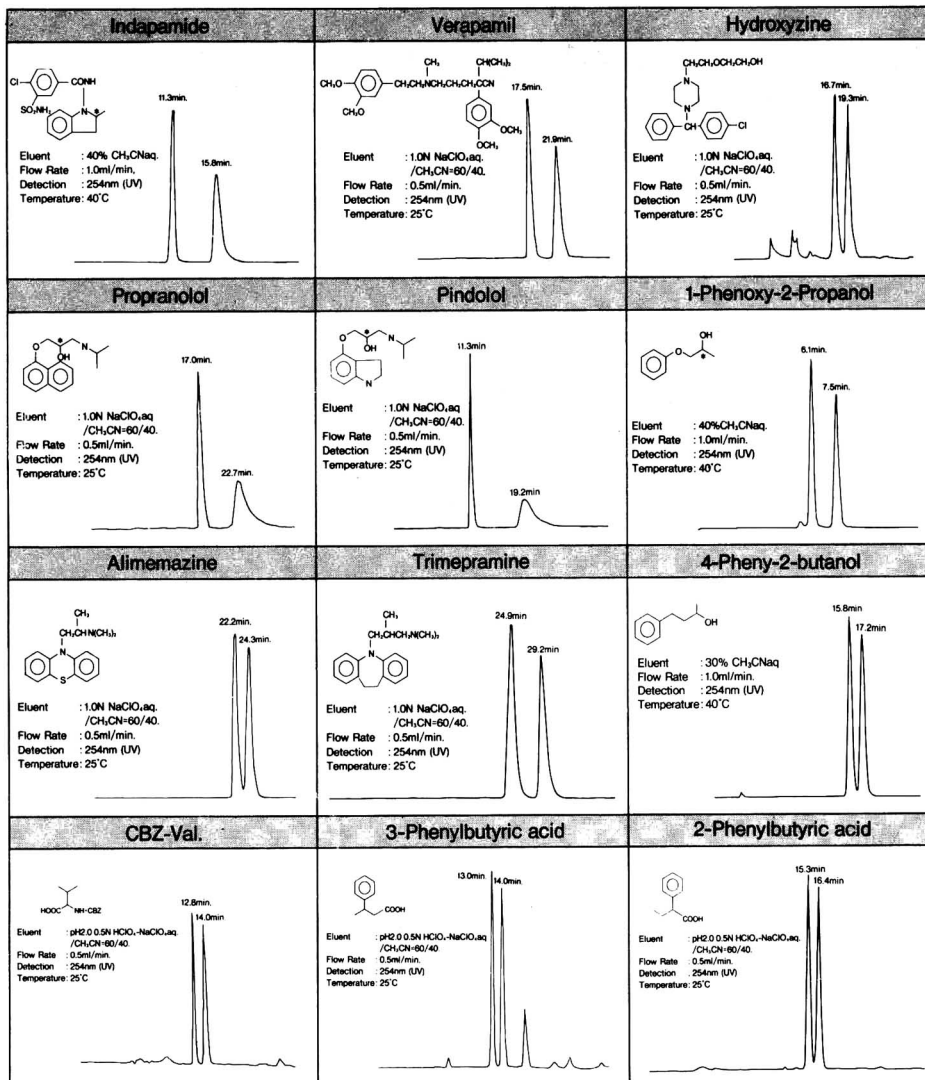
Proofs. One set of proofs will be sent to the author to be carefully checked for printer's errors. Corrections must be restricted to instances in which the proof is at variance with the manuscript. "Extra corrections" will be inserted at the author's expense.

Reprints. Fifty reprints will be supplied free of charge. Additional reprints can be ordered by the authors. An order form containing price quotations will be sent to the authors together with the proofs of their article.

Advertisements. The Editors of the journal accept no responsibility for the contents of the advertisements. Advertisement rates are available on request. Advertising orders and enquiries can be sent to the Advertising Manager, Elsevier Science Publishers B.V., Advertising Department, P.O. Box 211, 1000 AE Amsterdam, Netherlands; courier shipments to: Van de Sande Bakhuyzenstraat 4, 1061 AG Amsterdam, Netherlands; Tel. (+31-20) 515 3220/515 3222, Telefax (+31-20) 6833 041, Telex 16479 els vi nl. UK: T.G. Scott & Son Ltd., Tim Blake, Portland House, 21 Narborough Road, Cosby, Leics. LE9 5TA, UK; Tel. (+44-533) 753 333, Telefax (+44-533) 750 522. USA and Canada: Weston Media Associates, Daniel S. Lipner, P.O. Box 1110, Greens Farms, CT 06436-1110, USA; Tel. (+1-203) 261 2500, Telefax (+1-203) 261 0101.

Reversed Phase CHIRAL HPLC Column

NEW CHIRALCEL® OD-R



For more information about CHIRALCEL OD-R column, please give us a call.



DAICEL CHEMICAL INDUSTRIES, LTD.

CHIRAL CHEMICALS DIVISION 8-1, Kasumigaseki 3-chome, Chiyoda-ku, Tokyo 100, JAPAN
Phone: +81-3-3507-3151 Facsimile: +81-3-3507-3193

AMERICA
CHIRAL TECHNOLOGIES, INC.
730 SPRINGDALE DRIVE
DRAWER I EXTON, PA 19341
Phone: 215-594-2100
Facsimile: 215-594-2325

EUROPE
DAICEL (EUROPA) GmbH
Ost Street 22
4000 Düsseldorf 1, Germany
Phone: +49-211-369848
Facsimile: +49-211-364429

ASIA/OCEANIA
DAICEL CHEMICAL (ASIA) PTE. LTD.
65 Chulia Street #40-07
OCBC Centre, Singapore 0104.
Phone: +65-5332511
Facsimile: +65-5326454